



**Department of Electrical, Electronic and Computer Engineering**  
**MEng: Electrical Engineering**

**IEC61850 GOOSE message application for power transformer  
voltage control**

**Student Name : Joniff Wellen**

**Student Number : 205223567**

**Supervisor : Prof. Senthil Krishnamurthy**

**Date : December 2024**

# DECLARATION

I, Joniff Wellen, declare that the contents of this proposal represent my own work and have not been submitted for academic examination towards any qualification. Furthermore, it represents my opinions, not necessarily those of the Cape Peninsula University of Technology.



---

Signed

15/12/2024

---

Date

## **Acknowledgements**

I want to express my gratitude to the following:

1. My supervisor, Prof. S. Krishnamurthy for his guidance and advice.
2. The CSAEMS laboratory management and staff for granting me the opportunity to use the laboratory equipment.
3. The CPUT Library management and staff for their support and willingness to provide me with the information needed for this study.
4. My wife and kids, thank you for allocating the time and continued support needed for this study.

## Abstract

Voltage regulation of power transformers is critical to controlling and maintaining system voltage levels in the electrical transmission and distribution network system. It is vital to keep the transmission and distribution network's voltage levels within a specified range and avoid allowing voltage levels to fluctuate outside the predetermined range of allowed tolerance levels. As independent and renewable energy producers enter the transmission and distribution networks, generation hubs in modern electrical infrastructure networks are no longer centralized. The decentralization of electrical generating adds to the complexity of maintaining system voltage levels within acceptable limits. Traditional transformers utilized manual mechanical changing of the tap position of power transformers. Modern power grids require system voltages levels to be continually monitored and for automatic voltage regulation if voltage levels fluctuate outside the pre-set limits in order to maintain acceptable power quality. The power transformer's automatic tap changer executes this voltage-regulating function. The automatic tap changer is responsible for altering the tap position of the power transformer's windings in order to maintain the proper voltage levels. With the advent of the IEC61850 standard for communication for a standardized communication protocol between power system equipment, the industry embraced and adopted this standard, making their equipment IEC61850 compatible. The development of the IEC61850 GOOSE message application for voltage control of power transformers using automatic tap changer technology, the design and development of an algorithm, programming the IED, and the construction of a hardware-in-loop test bench setup to demonstrate the IED's working performance will be the focus of this study.

**Keywords:** Power transformer, Voltage regulation, Independent power producers, Renewable energy, IEC61850, GOOSE, Intelligent electronic device, Automatic tap changer



# Table of Contents:

Acknowledgements .....	iii
Abstract .....	iv
Definitions .....	xii
Nomenclature .....	xiii
List of Figures .....	xvi
List of Tables .....	xxv
CHAPTER 1 .....	1
1.1 Introduction .....	1
1.2 Awareness of the problem .....	3
1.3 Problem statement .....	3
1.4 Research aim and objectives .....	4
1.4.1 Aim .....	4
1.4.2 Research objectives .....	5
1.5 Hypothesis .....	6
1.6 Assumptions .....	6
1.7 Motivation of the research project .....	7
1.8 Delimitation .....	8
1.9 Research Methodology and Design .....	8
1.10 Literature Review .....	9
1.11 Simulation .....	9
1.12 Data collection .....	10
1.13 Control scheme .....	10
1.13.1 Lab-scale test bench setup for testing the Master- and Slave- Follower relays control algorithms and GOOSE configurations .....	13

1.13.2 Hardware-in-the-loop Simulation .....	13
1.14 Chapter Breakdown .....	15
1.14.1 Chapter One .....	15
1.14.3 Chapter Three .....	16
1.14.4 Chapter Four .....	16
1.14.5 Chapter Five .....	16
1.14.6 Chapter Six .....	16
1.15 Conclusion .....	16
CHAPTER 2 .....	17
2.1 Literature Review on IEC61850 Standard .....	17
2.1.1 Introduction .....	17
2.1.2 Literature Survey on IEC61850 .....	19
2.1.3 Discussion of literature survey on IEC61850 standard .....	29
2.1.4 Review summary on IEC61850 standard .....	31
2.2 Literature Review on Voltage regulation of transformers .....	40
2.2.1 Introduction .....	40
2.2.2 Literature survey on Voltage regulation of transformers .....	41
2.2.3 Discussion of literature survey on Voltage regulation of transformers .....	50
2.2.4 Review summary on Voltage regulation on transformers .....	51
2.3. Literature Review on transformer Tap changer controller algorithms .....	57
2.3.1 Introduction .....	57
2.3.2 Literature survey on Tap changer controller algorithms .....	58
2.3.3 Discussion of literature survey on Tap changer controller algorithms .....	70
2.3.4 Review summary on transformer Tap changer controller algorithms .....	72
2.4. Literature Review on Hardware-in-the-loop Simulations on OLTC .....	82
2.4.1 Introduction .....	82

2.4.2 Literature survey on Hardware-in-loop simulations .....	83
2.4.3 Literature review summary on Hardware-in-the-loop simulations .....	93
2.4.4 Discussion of literature survey on Protection and Hardware-in-loop simulation.....	103
2.5 Conclusion .....	103
CHAPTER THREE .....	104
OLTC THEORY AND MODELLING AND SIMULATION OF THE POWER SYSTEM NETWORK.....	104
3.1 Introduction .....	104
3.2 Transformers.....	105
3.3 Transformer Tap Changers.....	109
3.3.1 On-Load-Tap-Changers.....	109
3.4 Control methods for OLTCs of parallel transformers.....	111
3.4.1 Master-Follower Control Method.....	112
3.4.2 Circulating current method .....	113
3.4.3 Negative reactance method .....	114
3.4.4 Discussion of the Control methods for OLTCs on parallel transformers ....	114
3.5 Modelling and simulation of the modified IEEE 14 bus network.....	115
3.5.1 Data of the Modified version of the IEEE 14 bus network: .....	115
3.5.2 Implementation of DigSilent Power Factory model .....	119
3.5.3 Load Flow Analysis .....	121
3.5.4 Load Flow Analysis .....	123
3.5.4.1 Calculating Load Flow with base case values.....	123
3.5.4.2 Investigating the load flow for steady-state conditions .....	125
3.5.4.3 Investigating the Load Flow for over-voltage conditions.....	126
3.5.4.4 Investigating the Load Flow for under voltage conditions.....	129
3.5.4.5 Comparative study of the Load flow analysis for steady state, over voltage conditions, and under voltage conditions .....	132

3.5.4.5.1 Steady state load flow .....	132
3.5.4.5.2 Overvoltage load flow.....	133
3.5.4.5.3 Undervoltage load flow.....	133
3.6 Conclusion .....	134
CHAPTER FOUR.....	135
LAB SCALE SIMULATION AND TESTING OF THE POWER TRANSFORMER ON THE LOAD TAP CHANGER .....	135
4.1 Introduction .....	135
4.2 Transformer Relay Control Configuration Settings.....	135
.....	136
4.2.1 Engineering Configuration of Master Relay.....	137
4.2.3 Developed OLTC algorithm Raising Master tap.....	145
4.2.4 Engineering configuration of Slave-Follower relay .....	148
4.2.5 Developed OLTC algorithm Raising Slave-Follower tap .....	152
4.2.6 Developed OLTC algorithm Lowering Slave-Follower tap:.....	155
4.2.7 Developed OLTC algorithm for Tap synchronisation in Slave-Follower relay .....	157
4.2.8 Tap Position Monitoring .....	157
4.3 Transformer Relay IEC61850 GOOSE Configuration Settings: .....	160
4.3.1 GOOSE Configuration of Master relay .....	161
4.3.1.1 Enable GOOSE protocol on relay .....	162
4.3.1.2 Adding IED to project .....	163
4.3.1.3 Adding data items to dataset.....	163
4.3.1.4 Adding datasets to GOOSE transmit.....	168
4.3.1.5 Adding GOOSE subscriptions.....	168
4.3.1.5 Setting IED properties .....	168
4.3.1.6 Exporting CID file .....	169
4.3.2 GOOSE Configuration of Slave-Follower Relay .....	170

4.3.2.1 Adding data items to dataset.....	170
4.3.2.2 Adding datasets to GOOSE transmit.....	172
4.3.2.3 Adding GOOSE subscriptions.....	173
4.3.2.4 Setting IED properties.....	173
4.4 Configuring the Omicron CMC 356 test injection device to receive GOOSE messages.....	174
4.5 Configuring the Omicron CMC 356 .....	176
4.5.1 Configuring the Omicron CMC 356 to generate the 3-phase voltage ....	177
4.5.2 Configuring the Omicron CMC 356 to generate the 110VDC used for the tap indication on the relays .....	179
4.6 Lab-scale test bench setup for testing the Master- and Slave- Follower relays control algorithms and GOOSE configurations.....	179
4.6.1 Case Study 1: Steady-state condition .....	180
4.6.2 Case Study 2: Overvoltage conditions .....	182
4.6.3 Case Study 3: Under voltage conditions .....	186
4.7 Conclusion .....	190
CHAPTER FIVE .....	191
HARDWARE-IN-THE-LOOP SIMULATION AND TESTING OF THE POWER TRANSFORMER TAP-CHANGE CONTROLLER.....	191
5.1 Introduction .....	191
5.2 Modelling the Modified IEEE 14 Bus Network.....	194
5.2.1 Modelling of transformers in RSCAD FX.....	195
5.2.2 Modelling the Transformer T16 .....	197
5.2.3 Modelling the Transformer T15 .....	199
5.2.4 Modelling the Transformer T18 .....	200
5.2.5 Modelling the Transformer T17 .....	203
5.3 Modelling of Loads in RSCAD FX .....	207
5.3.1 Modelling the Loads of the Modified IEEE 14 Bus network:.....	207

5.4 Modelling the power sources in RSCAD FX:.....	208
5.5 Modelling the transmission lines in RSCAD FX .....	208
5.6 Configuring the RTDS Hardware Components .....	210
5.6.1 Gigabit Transceiver Analogue Output Card (GTAO).....	210
5.6.2 Front Panel Interface Card (GTFPI).....	211
5.7 IEC61850 GOOSE configuration of the RTDS equipment .....	214
5.8 Case Studies.....	222
5.8.1 Case Study 1: Steady-state condition: .....	222
5.8.2 Case Study 2: Overvoltage conditions .....	224
5.8.3 Case Study 3: Under voltage conditions .....	229
5.9 Comparison of DigSilent load flow results and RTDS real-time results.....	233
5.9.1 Steady state results comparison .....	233
5.9.2 Overvoltage Results Comparison .....	234
5.9.2.1 Overvoltage results comparison –before tap adjustments .....	235
5.9.3 Under voltage results comparison.....	236
5.9.3.1 Under voltage results comparison – before tap adjustments .....	236
5.9.3.2 Under voltage results comparison – after tap adjustments .....	237
5.9.4 Discussion of comparison between DIgSilent load flow results and RTDS real-time results .....	238
5.10 Conclusion .....	239
CHAPTER SIX .....	240
CONCLUSION .....	240
6.1 Introduction .....	240
6.2 Research Aim & Objectives .....	241
6.3 Deliverables .....	242
6.3.1 Literature review .....	243
6.3.2 Modelling and simulation of the network in DigSilent & RTDS and base caseload flow analysis .....	243

6.3.3 Lab-scale setup to validate the OLTC operation for different case scenarios.....	244
6.3.4 HIL lab-scale setup to validate the OLTC operation.....	244
6.3.5 Engineering configuration of the OLTC relay and OLTC control configurations.....	245
6.3.6 Simulation, validation, and results analysis of the OLTC operation for different case scenarios .....	245
6.3.7 IEC61850 GOOSE Engineering configuration of the OLTC relay .....	245
6.3.8 Simulation, validation, and results analysis of the IEC61850 GOOSE application for the OLTC operation for different use case scenarios.....	246
6.4 Application .....	246
6.5 Future work .....	246
6.6 Publications.....	246
6.7. Conclusion .....	247
Bibliography .....	248
APPENDIX A .....	<b>Error! Bookmark not defined.</b>
APPENDIX B .....	261

## Definitions:

**Algorithm:** A step-by-step procedure for solving a problem using a computer.

**Apparent Impedance:** The applied current and voltage determine the impedance to a fault as seen by a distance relay. It may differ from the actual impedance because of the current outfeed or current infeed at some point between the relay and the fault.

**Current Transformer:** A device that transforms current from one magnitude to another.

**Voltage Transformer:** A device that transforms voltage from one magnitude to another magnitude

**Interoperability:** It is the ability of two or more IEDs, regardless of the vendor, to exchange and interpret information and use that information for correct execution of specified functions

**Dead band range:** A range of values a system does not issue any response



## Nomenclature

<b>ADA</b>	Advanced Distribution Automation
<b>IED</b>	Intelligent Electronic Device
<b>SV</b>	Sampled Values
<b>GOOSE</b>	Generic Object Oriented Substation Event
<b>RTDS</b>	Real Time Digital Simulation
<b>HIL</b>	Hardware-in-loop
<b>CHIL</b>	Control-Hardware-in-loop
<b>PHIL</b>	Power-Hardware-in-loop
<b>IEC</b>	International Electrotechnical Commission
<b>CT</b>	Current Transformer
<b>VT</b>	Voltage Transformer
<b>OLTC</b>	On-Load Tap Changer
<b>MU</b>	Merging Unit
<b>R&amp;D</b>	Research & Development
<b>PHIL</b>	Power Hardware-In-the-Loop
<b>D/A</b>	Digital to Analogue
<b>A/D</b>	Analogue to digital
<b>GTAO</b>	GT Analogue Output
<b>GTAI</b>	GT Analogue Input Card
<b>HuT</b>	Hardware under test
<b>AC</b>	Alternating current
<b>DC</b>	Direct current

<b>PU</b>	Per unit
<b>kV</b>	Kilo Volt
<b>SEL</b>	Schweitzer Engineering Laboratories
<b>IDMT</b>	Inverse Definite Minimum Time
<b>FSMC</b>	Fuzzy Sliding Mode Controller
<b>GTFPI</b>	GT Front Panel Interface
<b>GTDI</b>	GT Digital Input Card
<b>DER</b>	Distributed Energy Resources
<b>LAN</b>	Local Area Network
<b>VT</b>	Voltage Transformer
<b>HV</b>	High Voltage
<b>SCADA</b>	Supervisory Control and Data Acquisition
<b>HV</b>	High Voltage
<b>CT</b>	Current Transformer
<b>SCL</b>	Substation Configuration Language
<b>EMT</b>	Electro-Magnetic Transient
<b>DSP</b>	Digital Signal Processor
<b>LN</b>	Logical Nodes
<b>FLA</b>	Full Load Amps
<b>GPS</b>	Global Positioning System
<b>EFTDR</b>	Empirical Fourier Transform-based Transformer Differential Relay
<b>SMV</b>	Samples Measured Values
<b>SCSM</b>	Specific Communication Service Mapping

<b>CDC</b>	Common Data Classes
<b>ACSI</b>	Abstract Communication Service Interfaces
<b>MPS</b>	Multifunction Protection Systems
<b>IPTP</b>	Improved Power Transformer Protection

## List of Figures

Figure 1: Modified IEEE 14 bus network with added transformer.....	11
Figure 2: The basic configurations of the on-load tap changer (Sangeerthana, Priyadharsini, 2020) .....	11
Figure 3: Basic structure of the lab-scale test bench setup.....	13
Figure 4: Hardware-in –the-loop Simulation setup .....	15
Figure 5: Literature Review Structure.....	18
Figure 6: IEC61850 documents reviewed per year .....	19
Figure 7: Functional hierarchy of the IEC61850 standard (Apostlov, Vandiver, 2010) .....	20
Figure 8: Communication structure between IEDs and between different levels of the automation topology (Brand, Brunner, Wimmer, 2011) .....	22
Figure 9: Comparison between hardwired communication cables and an Ethernet-based cable (Sichwart, 2012).....	23
Figure 10: Basic structure of the load tap controller overall structure (Sichwart, 2012) .....	24
Figure 11: Logical Nodes in Transformer Bay (Roostae, 2015) .....	25
Figure 12: Tap position monitoring system (Roostae, 2015).....	25
Figure 13: Linking GOOSE messages between IEDs (Hampson, 2018).....	26
Figure 14: Harmonic blocking scheme utilized for transformer protection with IEC 61850 GOOSE-based communication (Krishnamurthy, Baningobera, 2019).....	27
Figure 15: Microgrid protection scheme set up SEL-351 directional overcurrent relay with IEC 61850 GOOSE-based communication structure for improved coordination between protection relays (de Graaff Genis, Krishnamurthy, 2024).....	28
Figure 16: Interoperability assessment (Shangase, Ratshitanga, and Mnguni, 2024) .....	29
Figure 17: LAN network topology (Yepez-Nicola, Reyes-Lopez, 2024) .....	29
Figure 18: Voltage regulation of transformers documents reviewed per year .....	41
Figure 19: Flowchart of real-time voltage regulation (Xie, Shentu, Wu, Ding, Hua, Cui, et al., 2019).....	43
Figure 20: Operating principle of the line voltage regulator (Carlen et al., 2015) .....	44
Figure 21: Parallel operation of two transformers (Ferrero, Cimadevilla, Yarza, Solaun, 2014).....	45

Figure 22: The proposed tap changer system (Sangeerthana, Priyadharsini, 2020)	46
Figure 23: The proposed structure of the Flexible On-Load Voltage Regulation transformer (Han, Yin, Wu, Sun, Wei, 2022)	48
Figure 24: The proposed network modelled in MATLAB (Alkahdely, Alsammak, 2023)	48
Figure 25: Equivalent EHV System used in the study (Devi, Kumar, 2023)	49
Figure 26: Tap Changer Controller Algorithms reviewed per year	57
Figure 27: Daily generation variation of a PV DG system with cloud cover changes (Kabiri et al., 2014)	58
Figure 28: Tap changer control algorithm (Kabiri et al., 2014)	59
Figure 29: Voltage profile of feeder end bus with and without tap changing for advanced tap controller (Kabiri et al., 2014)	59
Figure 30: Parallel transformers on unequal tap positions (Okanik, Kurth, Harlow, 1999)	60
Figure 31: New LTC control diagram, including paralleling control (Okanik, Kurth, Harlow, 1999)	60
Figure 32: Distribution substation with mismatched paralleled transformers (Madzonga, et al., 2009)	61
Figure 33: AVR relay event recording on Auto (Madzonga, et al., 2009)	62
Figure 34: AVR relay event recording on Manual (Madzonga, et al., 2009)	62
Figure 35: The structure of OLTC controller based on PLC (Yongxing, Peng, Enyuan, Zhongwei, Jiyan, and Xuanshu, 2011)	63
Figure 36: The flow chart/algorithm for the control system (Yongxing, Peng, Enyuan, Zhongwei, Jiyan, and Xuanshu, 2011)	64
Figure 37: The test power system diagram with EOLTC (Hasan et al., 2018)	65
Figure 38: Left shows without EOLTC & right shows with EOLTC (Hasan et al., 2018)	65
Figure 39: Optimal tap selection framework (Xu et al., 2019)	66
Figure 40: Algorithm to control the OLTC derived from the internal game theory (Tasnim, Sarimuthu, Lan, Tan, 2022)	67
Figure 41: Flowchart of used genetic algorithm (Otchere, Ampofo, Dantuo, Frimpong, 2023)	69
Figure 42: The proposed algorithm to enhance system voltage profiles (Dung, 2023)	69

Figure 43: The algorithm proposed for OLTC control (Wróblewski, Kowalik, Januszewski, Kurek, 2024) .....	70
Figure 44: Hardware-in-the-loop reviewed per year .....	83
Figure 45: Hardware setup with RTDS and DSP (Murugan, et al., 2019) .....	85
Figure 46: The system diagram with AVR HIL (Nguyen, Yang, Nielsen, Jenson, 2020) .....	86
Figure 47: The simulated case to evaluate the energy and reactive power differential protection for the application in transformers (Dantas, Pellini, Junior, 2018).....	87
Figure 48: Buck converter simulation with external control (Cha et al., 2012).....	88
Figure 49: The proposed test system (Reda, Ray, Peidaee, Anwar, Mahmood, Kalam, Islam, 2021) .....	89
Figure 50: The HIL test setup structure (Nomandela et al., 2023).....	90
Figure 51: Network under study (Yadav et al., 2023) .....	91
Figure 52: IEEE 9 bus network used for the HIL testing (Shangase et al., 2024).....	92
Figure 53: Equivalent circuit of a transformer .....	105
Figure 54: Basic configuration of two parallel transformers.....	107
Figure 55: Basic principle of how a tap changer adjusts the transformer ratio .....	109
Figure 56: Basic rotational adjustments for selecting taps (Aung, Thike, 2019) .....	110
Figure 57: Basic control operation of OLTC to regulate the network voltage (Banakar, Muralidhara, Maheswara Rao, 2016) .....	112
Figure 58: Modified IEEE 14 Bus Network with parallel transformers .....	116
Figure 59: Parallel transformers between Bus 5 & Bus 6 .....	119
Figure 60: Transformer between Bus 5 & Bus 6 .....	120
Figure 61: Indication of two parallel transformers between Bus 5 & Bus 6.....	120
Figure 62: Configuring the OLTCs of the parallel transformers .....	121
Figure 63: Load Flow Analysis Diagram.....	121
Figure 64: Calculating load flow in DIgSilent software.....	123
Figure 65: Results for base case values of Bus 5 & Bus 6 from DIgSilent .....	124
Figure 66: Results for base case values of Bus 5 & Bus 6 from RSCAD .....	124
Figure 67: Results for steady-state condition loading of Bus 5 & Bus 6 from DIgSilent .....	125
Figure 68: Voltage magnitudes of Buses for stead-state conditions from DIgSilent.....	126
Figure 69: Initial load flow results for over-voltage loading conditions of Bus 5 and Bus 6 from DIgSilent before tap positions are adjusted.....	127

Figure 70: Voltage magnitudes of Buses for initial over voltage conditions from DlgSilent - before tap position is adjusted .....	127
Figure 71: Load flow results for the over-voltage loading condition values of Bus 5 and Bus 6 from DlgSilent after the tap positions are adjusted.....	128
Figure 72: Voltage magnitudes of Buses for over-voltage conditions from DlgSilent - after tap position is adjusted.....	129
Figure 73: Initial load flow results for under voltage loading conditions of Bus 5 & Bus 6 from DlgSilent - before tap positions is adjusted. ....	130
Figure 74: Voltage magnitudes of Buses for initial under voltage conditions from DlgSilent - before tap position is adjusted .....	130
Figure 75: Load flow results for over voltage loading condition values of Bus 5 & Bus 6 from DlgSilent - after tap positions is adjusted .....	131
Figure 76: Voltage magnitudes of Buses for under voltage conditions from DlgSilent - after tap position is adjusted.....	132
Figure 77: Structure of the Lab-scale test bench setup for testing the Master- and Slave-Follower relays control algorithms and GOOSE configurations .....	136
Figure 78: Relay engineering configuration sequence followed .....	136
Figure 79: Connecting to the relay, powering the relay .....	137
Figure 80: Establishing communication with Master relay.....	138
Figure 81: Part Number of Master relay .....	139
Figure 82: Algorithm to control the tap-lowering function of the Master transformer .....	144
Figure 83: Algorithm to control the tap-raising function of the Master transformer .	147
Figure 84: Establishing communication with Slave-Follower relay .....	148
Figure 85: Part Number of Slave-Follower relay .....	149
Figure 86: Algorithm to control the tap-raising function of the Slave-Follower transformer.....	154
Figure 87: Algorithm to control the tap-lowering function of the Slave-Follower transformer.....	156
Figure 88: Algorithm to verify Tap positions of the Master transformer and the Slave-Follower Transformer is synchronised.....	157
Figure 89: LTPC Monitoring Block Diagram (SEL, 2017. SEL-2414 Relay Instruction Manual) .....	158

Figure 90: High Voltage Digital Interface Panel generating binary code for relay to calculate OLTC tap position .....	160
Figure 91: GOOSE configuration sequence .....	162
Figure 92: Enabling IEC 61850 GOOSE functionality on the relay.....	163
Figure 93: Added IEDs to an AcSELerator Architect project .....	164
Figure 94: LTC_RSE mapped to OUT101 and LTC_LWR mapped to OUT102 of Master relay .....	164
Figure 95: Tap the position of the Master relay mapped to Math Variable MV01...	165
Figure 96: Adding the data item to the dataset of the Master relay Lower signal...	166
Figure 97: Adding the data item to the dataset of the Master relay Raise signal....	167
Figure 98: Adding the data item to the dataset of the Master Tap Position .....	167
Figure 99: The datasets of the Master relay that are published to the external devices .....	168
Figure 100: The GOOSE datasets the Master relay receives from Slave-Follower relay .....	168
Figure 101: The IED Properties of the Master relay .....	169
Figure 102: Sending the CID file of the Master relay.....	169
Figure 103: Confirming the network settings of the Master relay before sending the CID file .....	170
Figure 104: Adding the data item to the dataset of the Slave-Follower relay lower signal.....	171
Figure 105: Adding the data item to the dataset of the Slave-Follower relay raise signal.....	172
Figure 106: Adding the data item to the dataset of the Slave-Follower relay for Tap synchronisation signal .....	172
Figure 107: The datasets of the Slave-Follower relay that are published to the external devices .....	173
Figure 108: The GOOSE datasets Slave-Follower relay receives for Master relay	173
Figure 109: The IED Properties of the Slave-Follower relay .....	174
Figure 110: Importing the SCL file into the Omicron CMC 356 device .....	175
Figure 111: Choosing the GOOSE Datasets for which you wish to create subscriptions .....	175
Figure 112: Subscribing the GOOSE datasets to binary inputs on the.....	176
Figure 113: Configuring the hardware setup of the Omicron CMC 356.....	177



Figure 114: Selecting the inputs on the Omicron CMC 356 to monitor .....	178
Figure 115: Test template created in Quick CMC to inject 3-phase voltage into the Master relay .....	179
Figure 116: Selecting the Aux DC voltage.....	179
Figure 117: Structure of the Lab-scale test bench setup for testing the Master- and Slave-Follower relays control algorithms and GOOSE configurations .....	180
Figure 118: Quick CMC test template indicating the 3 phase 69 VAC generated with no binary inputs.....	181
Figure 119: HMI of the Master relay showing the measured values.....	182
Figure 120: Quick CMC test template indicating the 3 phase 74 VAC generated with binary inputs from Master- and Slave-Follower relays. ....	183
Figure 121: Master relay event report for over voltage conditions.....	183
Figure 122: Slave-Follower relay event report for over-voltage conditions.....	184
Figure 123: Voltage measured by the Master relay during over voltage conditions being published to the Slave-Follower relay via analog GOOSE .....	184
Figure 124: The Master relay publishes a tap Raise control signal to the network.	185
Figure 125: The Slave-Follower relay publishing a tap Raise control signal to the network.....	185
Figure 126: Shown in Figure # is the Tap position of the Master relay being published to the Slave-Follower relay via analog GOOSE .....	186
Figure 127: Quick CMC test template indicating the 3-phase 64 VAC generated with binary inputs received from Master- and Slave-Follower relays .....	187
Figure 128: Master relay event report for under voltage conditions .....	187
Figure 129: Slave-Follower relay event report for under-voltage conditions.....	188
Figure 130: Voltage measured by the Master relay during under voltage conditions being published to the Slave-Follower relay via analog GOOSE .....	188
Figure 131: The Master relay publishes a tap Lower control signal to the network	189
Figure 132: The Slave-Follower relay publishing a tap Lower control signal to the network.....	189
Figure 133: Modified IEEE 14 Bus network with an added transformer in RSCAD FX 2.1.1 environment .....	193
Figure 134: Standard IEEE 14 Bus network.....	194
Figure 135: Voltage levels before transformer tap change of IEEE 14 Bus network .....	195

Figure 136: Transformer voltage levels from the power system simulation tool .....	195
Figure 137: Configuration tab of transformer T16 .....	197
Figure 138: Winding 1 voltage magnitude of transformer T16.....	198
Figure 139: Winding 2 voltage magnitude of transformer T16.....	198
Figure 140: Winding 3 voltage magnitude of transformer T16.....	198
Figure 141: Configuration tab of transformer T15 .....	199
Figure 142: Winding 1 voltage magnitude of transformer T15.....	199
Figure 143: Winding two configuration of transformer T15.....	200
Figure 144: Configuration tab of transformer T18 .....	200
Figure 145: Winding one configuration of transformer T18 .....	201
Figure 146: Winding 2 configuration of transformer T18 .....	201
Figure 147: Tap changer configuration of transformer T18 .....	202
Figure 148: Tap settings (1-10) for transformer T18 .....	202
Figure 149: Tap settings (11-20) for transformer T18.....	203
Figure 150: Configuration tab of transformer T17 .....	204
Figure 151: Winding one configuration of transformer T17 .....	204
Figure 152: Winding 2 configuration of transformer T17 .....	205
Figure 153: Tap changer configuration of transformer T17 .....	205
Figure 154: Tap settings (1-10) for transformer T17 .....	206
Figure 155: Tap settings (11-20) for transformer T17.....	206
Figure 156: Configuration tab for a transmission line between Bus 2 and Bus 5 ...	209
Figure 157: Parameters for a transmission line between Bus 2 and Bus 5 in DigSilent environment .....	209
Figure 158: Configuration of the GTA0 card.....	211
Figure 159: Configure the GTFPI card for this project.....	212
Figure 160: Parallel transformers T18 & T17 controlled by two SEL-2414 relays ..	212
Figure 161: GTA0, GTFPI & GTFPIv2 and Out101, Out102, Out201 and Out202 and GTNETx2 .....	213
Figure 162: Configuration tab for GTNETx2.....	214
Figure 163: Selecting the GTNET GOOSE version.....	215
Figure 164: Process of creating the IED model.....	216
Figure 165: Importing the external publishers into RSCAD .....	217
Figure 166: Adding Logical Node subscriptions .....	218

Figure 167: Creating RSCAD IED subscriptions from external Master relay to raise tap .....	218
Figure 168: Creating IED subscription from external Master relay to lower tap.....	219
Figure 169: Creating IED subscription from external Slave relay to raise tap .....	220
Figure 170: Creating IED subscription from external Slave relay to lower tap.....	220
Figure 171: Binding the GOOSE data model in the RSCAD FX draft model for receiving the IEC61850-7-4 GOOSE messages from the SEL-2414 IEDs.....	221
Figure 172: Access Points Configuration of the GTNETx2.....	222
Figure 173: Dashboard with steady state voltage conditions – no voltage regulation needed .....	223
Figure 174: Measured voltage at Bus 6 and the tap positions at steady state loading conditions - no voltage regulation needed.....	223
Figure 175: HMI from Master relay with measured voltages and an indication of binary inputs for tap position .....	224
Figure 176: Dashboard with initial under voltage conditions before voltage correction .....	225
Figure 177: Measured voltage at Bus 6 and the tap raise operation in progress during over voltage conditions.....	225
Figure 178: GOOSE message for raising tap signals being issued by the Master relay .....	226
Figure 179: GOOSE message for raising tap signals being issued by the Slave relay .....	227
Figure 180: HMI from Slave relay with indicating the Master relay tap position sent via GOOSE .....	227
Figure 181: Dashboard with results after under voltage conditions is corrected ....	228
Figure 182: Measured voltage at Bus 6 and the tap positions after overvoltage conditions are corrected .....	228
Figure 183: Dashboard with initial under voltage conditions before voltage correction .....	229
Figure 184: Measured voltage at Bus 6 and the tap lowering operation in progress under voltage conditions. ....	230
Figure 185: GOOSE message for lowering tap signals being issued by the Master relay .....	231

Figure 186: GOOSE message for raising tap signals being issued by the Slave relay .....	231
Figure 187: Dashboard with results after under voltage conditions is corrected ....	232
Figure 188: Measured voltage at Bus 6 and the tap positions after under voltage conditions is corrected.....	233

## List of Tables:

Table 1: The datasets that will be included in the Master relay GOOSE configuration .....	12
Table 2: The datasets that will be included in the Master relay GOOSE configuration .....	12
Table 3: Review summary on IEC 61850 .....	31
Table 4: Comparison of different OLTC voltage control schemes (Zhou, et al., 2018) .....	42
Table 5: comparison between modern OLTCs and mechanical OLTCs (Sangeerthana, Priyadharsini, 2020).....	46
Table 6: Comparison between the proposed strategy and existing strategies (Han, Yin, Wu, Sun, Wei, 2022) .....	47
Table 7: Review summary on Voltage regulation of transformers .....	51
Table 8: Review summary on transformer Tap changer controller algorithms .....	72
Table 9: Power transformer failure rates (Qasmi, 2014).....	83
Table 10: Review the summary on Hardware-in-the-loop simulation .....	93
Table 11: Advantages and disadvantages of placing power transformers in parallel (Trebolle, Valecillos, 2008).....	108
Table 12: Requirements for connecting power transformers in parallel (Trebolle, Valecillos, 2008).....	108
Table 13: Common procedures for testing OLTCs (Erbrink, Galski, Smit, Leich, 2009).....	110
Table 14: Load demand of network.....	117
Table 15: Generator controller settings .....	117
Table 16: Data of lines in the model.....	117
Table 17: Data of transformers given on a base of 100MVA, included is rated voltages.....	118
Table 18: Numerical techniques for calculating load flow in the power system in DlgSilent software (Dubey, 2016) .....	122
Table 19: Load flow results from Bus 5 & Bus 6 for the base case .....	125
Table 20: Steady state load conditions for Bus 5 and Bus 6 voltage, with voltage magnitudes obtained from DlgSilent - no corrections needed.....	126

Table 21: Over voltage load conditions for Bus 5 and Bus 6 voltage, with voltage magnitudes obtained from DIgSilent – before tap position is adjusted.....	128
Table 22: Over voltage load conditions for Bus 5 and Bus 6 voltage, with voltage magnitudes obtained from DIgSilent – after tap position is adjusted.....	129
Table 23: Under voltage load conditions for Bus 5 and Bus 6 voltage, with voltage magnitudes obtained from DIgSilent – before tap position is adjusted.....	131
Table 24: Under voltage load conditions for Bus 5 and Bus 6 voltage, with voltage magnitudes obtained from DIgSilent – after tap position is adjusted.....	132
Table 25: Load flow results of steady-state loading conditions .....	133
Table 26: Load flow results of overvoltage loading conditions .....	133
Table 27: Load flow results of under voltage loading conditions .....	134
Table 28: Load Tap Position and Control Monitoring Settings of Master relay.....	139
Table 29: Load Tap Position and Control Monitoring Inputs of Mater relay.....	140
Table 30: SELogic Variable/Timer Settings of Master relay .....	141
Table 31: The SEL-2414_A Master relay was configured according to the following settings.....	142
Table 32: Load Tap Position and Control Monitoring Settings of Slave-Follower relay .....	149
Table 33: Load Tap Position and Control Monitoring Input of Slave-follower relay	150
Table 34: SELogic Variable/Timer Settings is summarised of Slave-Follower relay .....	151
Table 35: The SEL-2414_B Slave-Follower relay was configured according to the following settings.....	151
Table 36: TAP_POS Calculation when ETPM_MDE = BIN.....	159
Table 37: Key requirements for IEC61850 Standard (Mackiewicz, 2004) .....	161
Table 38: The datasets that is included in the Master relay GOOSE configuration	165
Table 39: The datasets that is included in the Slave-Follower relay GOOSE configuration.....	170
Table 40: Most Frequently used transformers from the RSCAD library (RTDS Technologies, 2018).....	196
Table 41: Parameters considered when including transformer models from the RSCAD library (RTDS Technologies, 2018).....	196
Table 42: Types of loads and controllers in RSCAD library.....	207
Table 43: Characteristics of Loads .....	207

Table 44: Details of Voltage Sources .....	208
Table 45: Calculated Transmission Line data .....	210
Table 46: Steady state voltage conditions - no corrections needed .....	222
Table 47: Initial loading condition values - overvoltage .....	224
Table 48: Bus 6 voltage magnitude now within the acceptable range – after overvoltage condition is corrected.....	229
Table 5-49: Initial loading condition values – under voltage .....	229
Table 50: Bus 6 voltage magnitude now within the acceptable range – after under voltage condition is corrected.....	232
Table 51: Steady state load conditions for Bus 5 and Bus 6 voltage, with voltage magnitudes obtained from DIgSilent - no corrections needed.....	234
Table 52: Steady state load conditions for Bus 6 voltage, with voltage magnitudes obtained from RTDS - no corrections needed.....	234
Table 53: Over voltage load conditions for Bus 5 and Bus 6 voltage, with voltage magnitudes obtained from DIgSilent – before tap position is adjusted.....	235
Table 54: Over voltage load conditions for Bus 6 voltage, with voltage magnitudes obtained from RTDS – before tap position is adjusted .....	235
Table 55: Over voltage load conditions for Bus 5 and Bus 6 voltage, with voltage magnitudes obtained from DIgSilent – after tap position is adjusted.....	236
Table 56: Over voltage load conditions for Bus 6 voltage, with voltage magnitudes obtained from RTDS – after tap position is adjusted .....	236
Table 57: Under voltage load conditions for Bus 5 and Bus 6 voltage, with voltage magnitudes obtained from DIgSilent – before tap position is adjusted.....	237
Table 58: Under voltage load conditions for Bus 6 voltage, with voltage magnitudes obtained from RTDS – before tap position is adjusted .....	237
Table 59: Under voltage load conditions for Bus 5 and Bus 6 voltage, with voltage magnitudes obtained from DIgSilent – after tap position is adjusted.....	238
Table 60: Under voltage load conditions for Bus 6 voltage, with voltage magnitudes obtained from RTDS – after the tap position is adjusted .....	238

## CHAPTER 1:

### 1.1 Introduction:

The voltage level of the electrical supply system needs to be maintained at the desired levels and be within the predetermined specification level and acceptable tolerance levels. Line impedances cause a drop in voltage magnitude (Sen, 2015). The grid voltage magnitude levels must be supplied within the desired supply quality levels to meet the quality levels expected from the grid customers (Yuvaraja, Vigneshwaran, 2015). The primary equipment used to keep the voltage levels and voltage profiles within the desirable tolerated levels on the electrical supply system is the automatic voltage regulators found on the power transformers (Tu, Mi, 2019). This voltage regulation is achieved using automatic tap changing on power transformers to adjust the secondary side voltage on the power transformers by changing tap position to alter the transformer windings ratios (Gajic, Aganovic, Benovic, Leci, Gazzari, 2010). The introduction of independent power producers and renewable energy suppliers poses more problems to electrical quality because of multiple entry points where these supplies are tied into the electrical grid (Małkowski, Izdebski, Miller, 2020). Due to this decentralizing of the electrical generation units with many entry points onto the grid, voltage regulation would need to be done at more points on the electrical grid. The introduction of the IEC61850 standard for communication for a standardized communication protocol between power system equipment in the substation, transmission, and distribution networks was greatly accepted by the industry. The interoperability of equipment from different vendors is one of the driving forces behind the mass adoption of the IEC61850 standard (Mahoney, Coyne, Waldron, 2019). This IEC61850 standard for communication further took the need for substation and grid automation to the next level. Control, monitoring, and protection functions of the grid network could now be centralized to a central SCADA system, and data could be shared amongst the different equipment subscribed in the control and protection network (Li, Nair, Nguang, 2010). In the future, power generation topologies will shift from central generation systems to decentralised generation systems, injecting power into the grid at various junctions (Jurisic, Havelka, Capuder, Sucic, 2018). This study



focuses on developing an algorithm to efficiently perform the voltage regulation control of the power transformer using a tap change function. The operation of the OLTC function is controlled by IEC61850 GOOSE messages. The operation of the OLTC function is based on the Master-Follower control scheme. Two SEL-2414 Transformer Monitor IEDs are employed to control the automatic tap-changing function of the two parallel power transformers. The engineering configuration settings of the two SEL-2414 IEDs are configured for voltage control of the parallel power transformers using the tap change function. A lab-scale hardware-in-the-loop test bench setup is constructed to perform the voltage regulation of the power transformers in parallel operation and to analyse the performance results of the voltage regulation controller algorithm. Conventional voltage regulation systems use hardwired configurations, which have proved expensive and time-consuming to install. These hardwired configurations were also not very flexible if changes were to be made; it meant that physical infrastructure needed to be changed to enable changes to be made to the control network. The control system in this study incorporates the IEC61850 standard for communication for real-time control logging and analysis. Making use of the IEC61850 standard for communication function means that changes can be made to the control system without the need to alter any physical wiring, cutting down on commissioning costs in the process (Hakala-Ranta, Rintamäki, Starck, 2009). Including the IEC61850 GOOSE message application for control purposes makes the control system reconfigurable and flexible for future additions or changes (Mnguni, Tzoneva, 2015). System performance data can be stored and analyzed later and kept for record-keeping. The power system network under study is a modified version of the IEEE 14 Bus power system network. The IEEE 14 Bus power system network is modelled in the DIgSilent software, and OLTC performance is scrutinized under different loading conditions. Hardware-in-the-loop simulations are conducted in a closed-loop using RTDS equipment with the two SEL-2414 IEDs, each controlling the OLTCs of the parallel transformers incorporating IEC 61850 GOOSE messages for control signal transmission. The results obtained from the DIgSilent simulation are compared to those obtained from the hardware-in-the-loop simulations.

This section describes the importance of maintaining a stable and reliable grid voltage profile across the entire power system network. It suggests new ways of

achieving this goal by employing modern technology-based Intelligent electronic Devices coupled with IEC61850-based communication structures for control and protection signal transmission.

This section also includes awareness of the problem, Problem statement, Research aim and objectives, Hypothesis, Motivation of the research project, and Assumptions.

## **1.2 Awareness of the problem**

Traditional tap changers on power transformers are still widely utilized for voltage adjustment in transmission and distribution networks throughout South Africa and the world. Mechanical switches are used in traditional tap changers to modify the position of the taps on power transformers. These mechanical tap changers have several disadvantages, including the requirement for ongoing maintenance, a more extended operating period, associated arcing while switching between taps, and mechanical losses. In some circumstances, mechanical tap changes become caught between taps, rendering the associated transformers inoperable, resulting in system damage, power quality and reliability concerns, and grid outages.

Because these traditional control systems lack a monitoring function, these traditional voltage regulation mechanisms do not allow for proper fault investigations. Voltage regulation of power transformers must be brought into the twenty-first century; the process must be automated to be a part of the modern smart grid movement. This study aims to develop and implement a voltage controller algorithm to regulate the automatic tap changer. IEC61850 GOOSE would serve as the communication medium for controlling and monitoring the operation of the automatic tap changer setup. A hardware-in-the-loop test bench is built to replicate the functioning of the algorithm that controls the automatic tap changer. Two SEL-2414 Transformer Monitor IED parameters are customized for the control operation of the on-load tap changer.

## **1.3 Problem statement**

Traditional voltage regulation devices use mechanical equipment to change the tap positions of the power transformer. Compared to automatic tap changers, these conventional tap changers have numerous disadvantages.

***The research problem is to investigate the proper coordination of tap changers with other elements of the electrical grid, which is crucial for maintaining voltage stability and power quality. Automatic tap-changing control systems need to be efficient, fast, and reliable.***

With power systems evolving toward integrated smart grid networks, the project's problem statement investigates whether it is worthwhile to transition from traditional voltage regulation methods to newer technologies for voltage control on power transformers using the IEC 61850 standard.

Voltage regulation devices that use the IEC 61850 communication protocol can be easily incorporated into a smart grid network and thus controlled and monitored from a centralized SCADA system. They can also exchange and receive data from other IED devices on the smart grid network. Power transformers with automatic voltage regulation incorporating the IEC 61850 standard can rapidly adapt to changes and requirements in the power system network and make the appropriate tap changes to ensure that supply quality complies with industry standards for allowed tolerances in voltage supply levels.

## **1.4 Research aim and objectives**

### **1.4.1 Aim**

***To control and maintain power system voltages within predefined voltage levels using automatic voltage regulation by tap changer technology on power transformers and IEC 61850 GOOSE messages for control signal transmission.***

Explore the integration of tap changers into transformers with built-in sensors and communication capabilities, enabling remote monitoring and control. Research could involve communication protocols, and data analytics for optimized transformer management and voltage regulation.

The automatic voltage regulator will use the IEC61850 GOOSE communication standard. The tap changers must be controlled by the SEL-2414 IEDs' publication of GOOSE messages. The relay settings and configurations would need to be researched and configured to meet network criteria. An algorithm must be developed to regulate and operate the power transformers' automated tap changers.

The RSCAD software suite is used to model the modified version of the IEEE 14 Bus network. To analyze the performance of the automatic voltage control function under various grid operating situations, a hardware-in-the-loop simulation and testing of the automatic voltage control function will be performed using RTDS equipment and the two SEL-2414 IEDs. During the testing of the automatic voltage controller, the Omicron CMS156 device will be used to inject various operating circumstances into the appropriate IED. During the testing of the automatic voltage controller to confirm that the automatic tap changer maintains the network at the required voltage levels, the IEC61850 GOOSE application and the algorithm will also be tested.

### 1.4.2 Research objectives

- i) Conduct a literature review on transformer voltage control, IEC61850-7-4, automatic transformers, tap changers, tap changer controller algorithms, and hardware-in-the-loop simulations in a closed-loop simulation environment.
- ii) Investigate and comprehend the transformer tap change controller and its automatic operation, parallel transformer operation, and IEC61850 GOOSE message applications for transformer tap changer application.
- iii) Modelling and simulating the proposed power system network with the DigSilent and RTDS software suites RSCAD.
- iv) Using the IEC61850 accessible logical nodes, create a novel algorithm for voltage control of transformers. a) Tap changer (YLTC), b) Automatic tap change control (ATCC), and c) Voltage control (AVCO) OR design custom IEC61850-7-4 based logical nodes for a) to c).
- v) Perform the relay engineering configuration to set up for online transformer-tap change control (OLTC).
- vi) Perform the engineering configuration to the IEC61850 GOOSE message for OLTC operation.
- vii) Perform the engineering configuration to use a transformer tap changer and its controller to modulate the system voltage on a lab scale.

- viii) Implement hardware-in-the-loop simulation in a closed-loop simulation environment using RTDS and relay and validate simulation results

## 1.5 Hypothesis

- The use of IEC 61850 GOOSE (Generic Object-Oriented Substation Event) communication in transformer tap change control improves the responsiveness, accuracy, and coordination of voltage regulation in power distribution systems. It reduces response times and increases the reliability and fault detection capabilities of tap changer operations.
- Various operational situations, including load changes and fault circumstances, would be simulated to see how the tap changer system responded under GOOSE management. The system's performance, such as reaction time and tap change accuracy, would be compared to a baseline system controlled using traditional techniques.
- The suggested research can benefit the power systems industry and add to South Africa's knowledge base.

## 1.6 Assumptions

- The following software and hardware: RTDS equipment, RSCAD FX, Omicron CMS 156, Omicron CMC 356, SEL-2414 relay, DIgSilent Power Factory 2023, Wireshark Network Analyzer, OMICRON IEDScout, SEL-2725 Five-Port Ethernet Switch, AcSELERator Architect Software, AcSELERator QuickSet, to complete this research document is available from the Centre for Substation Automation and Energy Management Systems at the Cape Peninsula University of Technology, Bellville Campus.
- The proposed SEL-2414 IEDs can fulfil the required voltage regulation function to control the OLTC of the parallel transformers.
- When configured with the proprietary algorithm to regulate the voltage of the power transformer, the suggested SEL-2414 IEDs can perform the OLTC control function.
- In this study, the proposed IEC 61850 GOOSE-based communication topologies may be successfully implemented for the OLTC system.

- The SEL-2414 relay accommodates a customizable number of taps, in order to correspond to the specific requirements in this study
- The RTDS equipment has the computational capacity to simulate the network chosen for this study
- The DIgSilent software advanced computational abilities is able to calculate accurate load flow results when different network loading is simulated
- Traditional copper wiring in safety and control systems can be effectively replaced with modernized digital communications protocols inside a power system network using the IEC61850 standard-based communication.
- IEC 61850-based communications and data transfer services are as dependable as traditional hardwired cabling while lowering installation, commissioning, and operational costs.

## 1.7 Motivation of the research project

Network voltage fluctuations would not exist in an ideal working condition of a power system network. However, real-world power system operating circumstances are far from ideal, and system voltage deviations are standard in regular operations. Voltage control systems regulate system voltages within acceptable values to make the power system network stable and reliable and to keep consumers satisfied with the network's power quality.

With the development and deployment of new technologies in power system networks in recent years, new technologies for controlling automatic tap changers on power transformers have also become available. These technologies seek to improve the efficiency with which automatic tap changers operate, hence assisting in the more effective maintenance of system voltage. This study's research will be based on deploying intelligent electrical gadgets supported by custom-created algorithms for maximum performance. Reducing the reliance on expensive copper control cables between components. Including IEC61850-based communication protocols as communication between controllers and operating equipment will minimize the overall cost of the proposed application.

## 1.8 Delimitation

- The study uses the IEC 61850 GOOSE messaging protocol for communication among control devices in transformer tap change systems. It will primarily investigate the use of GOOSE for event-driven control and real-time communication in voltage regulation and tap changer operation. However, the research will exclude other communication protocols (e.g., Modbus, DNP3, or proprietary). It will not investigate the usage of IEC 61850 MMS (Manufacturing Message Specification) or other IEC 61850-based communication techniques that are not event-driven.
- The study will concentrate on controlling on-load tap changers (OLTCs), which are actively altered while operating without removing the transformer from the load. The research will not include off-loading tap changers (OLTCs), which need the transformer detached from the load for adjustment because GOOSE messaging's real-time capabilities are more relevant to on-load applications.
- The study will assess the tap changer control system's reaction time, accuracy, coordination efficiency, and dependability utilizing GOOSE messaging. However, the research will not assess the economic viability of adopting IEC 61850 GOOSE messaging for tap changer control or the system's long-term maintenance costs.

## 1.9 Research Methodology and Design

The study's goal is to analyze and test the operation of a power transformer OLTC under various operating situations. Various system situations will be simulated under various system loading conditions to assess whether the OLTC effectively regulates the system supply voltage by varying the tap winding positions on the parallel operational power transformers. The modified version of the IEEE 14 Bus power system network will be modeled in the DigSilent Powerfactory 2023 software suit to determine the simulated results in the digital environment with the predicted consequences.

The OLTC function will also be built and evaluated in the DigSilent Powerfactory 2023 digital environment to evaluate its performance in regulating the magnitude of

the system voltage. The power system network would next be modeled in the RSCAD FX 2.1.1 software suite, and the OLTCs function would be evaluated and scrutinized for efficient operation using hardware-in-the-loop simulations performed in the RTDS environment.

A test bench was built, as shown in Figures 1-3 and 1-4, to include the two physical SEL-2414 IEDs in a hardware-in-the-loop circuit. The AcSElerator Quickset environment will be used to configure the SEL-2414 IED and build the OLTC algorithm. The Omicron CMS 156 amplifier device will enhance signals generated by the RTDS signal generator before they are fed into the SEL-2414 IED. The control OLTC signals received from the SEL-2414 IED devices would be transmitted back to the RTDS equipment to be observed. The IEC 61850 GOOSE application will also be implemented and tested during the hardware-in-the-loop simulation. The IEC61850 GOOSE application would send the control signals from the SEL-2414 IEDs.

The SEL-2414 IED will perform the OLTC control functions and send the control signals back to the RTDS equipment via IEC61850 GOOSE messages.

The research methods that are employed in achieving the research aim are as follows:

### **1.10 Literature Review**

The literature review identified various approaches for voltage regulation of the power transformer and operation of the OLTC control using IEC61850 GOOSE communication. The literature review covered transformer control techniques, including RTDS and hardware-in-the-loop features. The OLTC control testing literature review was completed by reading books on voltage control of power transformers, relay manuals, online journals, published articles, and conducting web searches.

### **1.11 Simulation**

The power system network will be modeled in the DigSilent software suite, with the necessary network information entered and the SEL-2414 configured. The network to be evaluated will be modeled in the RSCAD software package using a hardware-in-the-loop technique that incorporates all the required network data to depict real-



world situations accurately. The information from the transformer's datasheet under test will mimic the transformer in the software environment. For the IEC 61850 GOOSE configuration of the relay, AcSELeator Architect will be used. The transformer monitor relay will be configured, and the OLTC control algorithms will be created in the AcSELeator Quickset environment. Omicron test universe software will be utilized for the signal amplifier Omicron CMS 156 & CMC 356 device configuration. Omicron IEDScout and Wireshark Network Analyzer software will be used for IEC 61850 GOOSE traffic monitoring in the network during simulations.

### **1.12 Data collection**

The findings from the RTDS environment and the event report files from the SEL-2414 IEDs will be utilized to analyze the OLTC's control function. Different network loading conditions would be simulated using the RSCAD software suit and the RTDS system. The IEC 61850 scheme will be deployed, and its performance characteristics and operating times will be monitored and analyzed. Results obtained from the DIgSilent simulations will be compared with those from the RTDS simulations.

### **1.13 Control scheme**

The RSCAD software suite will be used to model the circuit. To imitate the real-world scenario, the required network parameters will be entered. The circuit would be a modified version of the IEEE 14 Bus power system network. The transformers which will be controlled in circled as can be seen in [Figure 1](#).

The dynamic load connected to the 33 kV Bus 6 in the network will be varied to simulate different loading scenarios to cause unstable voltage conditions on Bus 6.

The two SEL-2414 IEDs monitor Bus 6's voltage profile. Suppose the profile deviates outside the control dead band. In that case, the SEL-2414 IEDs employ their internally programmed control algorithm to operate the OLTCs of the parallel transformer to bring the profile back to acceptable levels. [Figure 1](#) depicts the Modified IEEE 14 bus network with added transformer under study.

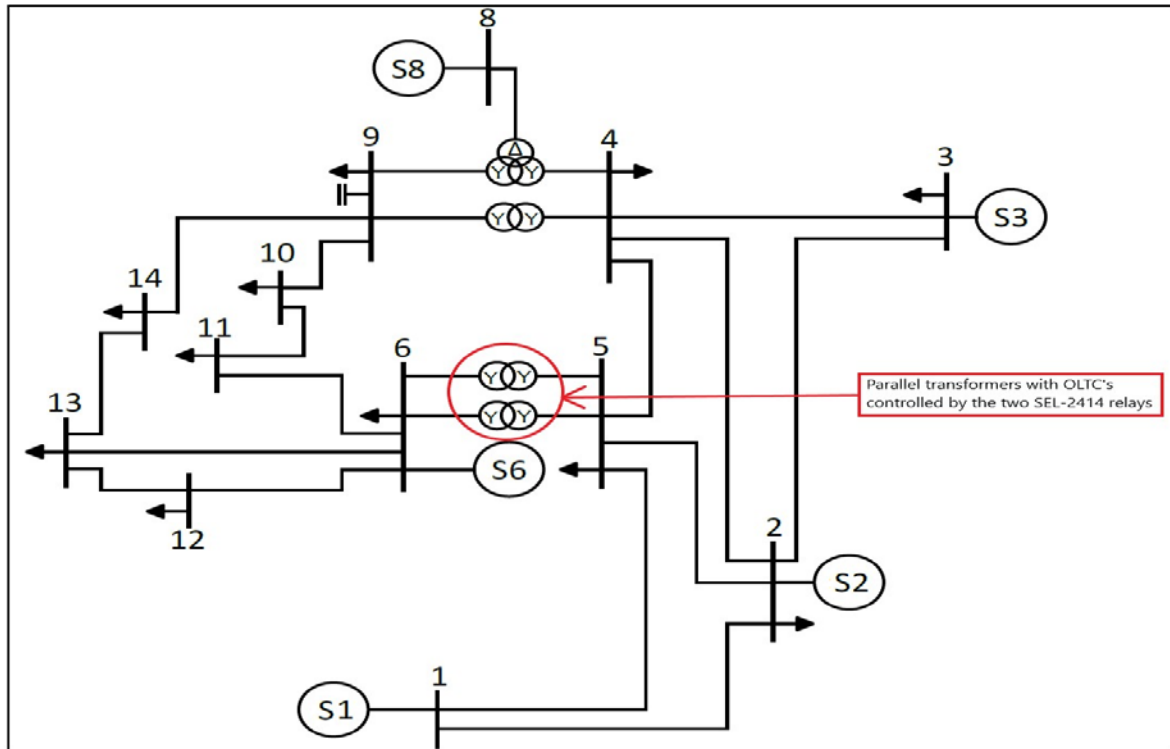


**Figure 1: Modified IEEE 14 bus network with added transformer**

The on-load tap changers need to vary the windings ratios of the power transformers to maintain a stable voltage supply to the associated loads. The SEL-2414 IEDs are configured and programmed using a custom-built algorithm to regulate the on-load-tap-changer operations. The basic configuration of the on-load tap changer is shown in Figure 2.

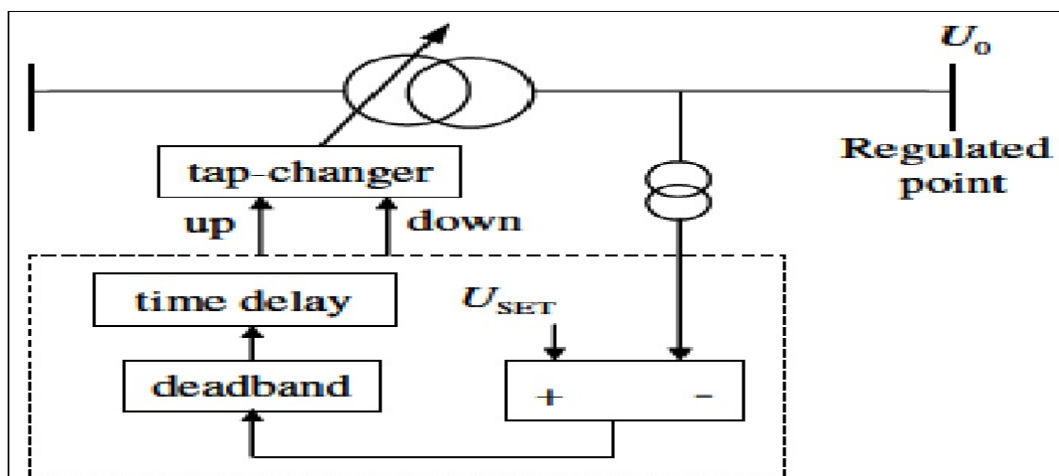


**Figure 2: The basic configurations of the on-load tap changer (Sangeerthana, Priyadharsini, 2020)**

The on-load tap change control function uses IEC 61850 GOOSE messages to send control and operating signals. The SEL-2414 transformer monitor relay will function as a real-world IED. The AcSELeator Quickset software package will be used to configure the SEL-2414 IED device and design the customized algorithm for the tap changer function. A test bench will be built with an IEC61850 GOOSE configuration. The relay datasets for the OLTC control elements of the SEL-2414 IEDs and their accompanying Logical Nodes in the IEC61850 GOOSE configuration are shown in **Table 1** for the Master relay and in **Table 2** for the Slave-Follower relay.

**Table 1: The datasets that will be included in the Master relay GOOSE configuration**

Logical Device: ANN (Annunciation)		
Logical Nodes	Status or Measurand	Device Word Bits or Analog Quantities
Analog Quantities		
MVGGIO12	AnIn01.mag to AnIn32.mag	Math Variables (MV01 to MV32)
Device Word Bits		
OUTAGGIO2	Ind01.stVal	Digital Output (OUT101)—Slot A
OUTAGGIO2	Ind02.stVal	Digital Output (OUT102)—Slot A
Logical Nodes	Measurand	Comment
METMMXU1	PhV.phsA.instCVal.mag	Instantaneous, Voltage Magnitude, Phase A
METMMXU1	PhV.phsB.instCVal.mag	Instantaneous, Voltage Magnitude, Phase B
METMMXU1	PhV.phsC.instCVal.mag	Instantaneous, Voltage Magnitude, Phase C

**Table 2: The datasets that will be included in the Master relay GOOSE configuration**

Logical Device: ANN (Annunciation)		
Logical Nodes	Status or Measurand	Device Word Bits or Analog Quantities
Device Word Bits		
OUTAGGIO2	Ind01.stVal	Digital Output (OUT101)—Slot A
OUTAGGIO2	Ind02.stVal	Digital Output (OUT102)—Slot A
OUTAGGIO2	Ind03.stVal	Digital Output (OUT103)—Slot A

The OLTC's function and operation time will also be evaluated during the implementation of the test bench configuration.

### 1.13.1 Lab-scale test bench setup for testing the Master- and Slave-Follower relays control algorithms and GOOSE configurations

A Lab-scale test bench setup is constructed for testing the Master- and Slave-Follower relays control algorithms and GOOSE configurations. This test bench setup is created to verify the performance of the developed voltage control algorithms and the successful implementation of the GOOSE communication protocol for transmitting data between the relays and to transmit control signals to the CMC356 device. Following the successful lab scale test bench setup, the SEL-2414 relays will be implemented into the hardware-in-the-loop test setup for real-world simulated testing. Figure 3 depicts the basic structure of the lab-scale test bench setup.

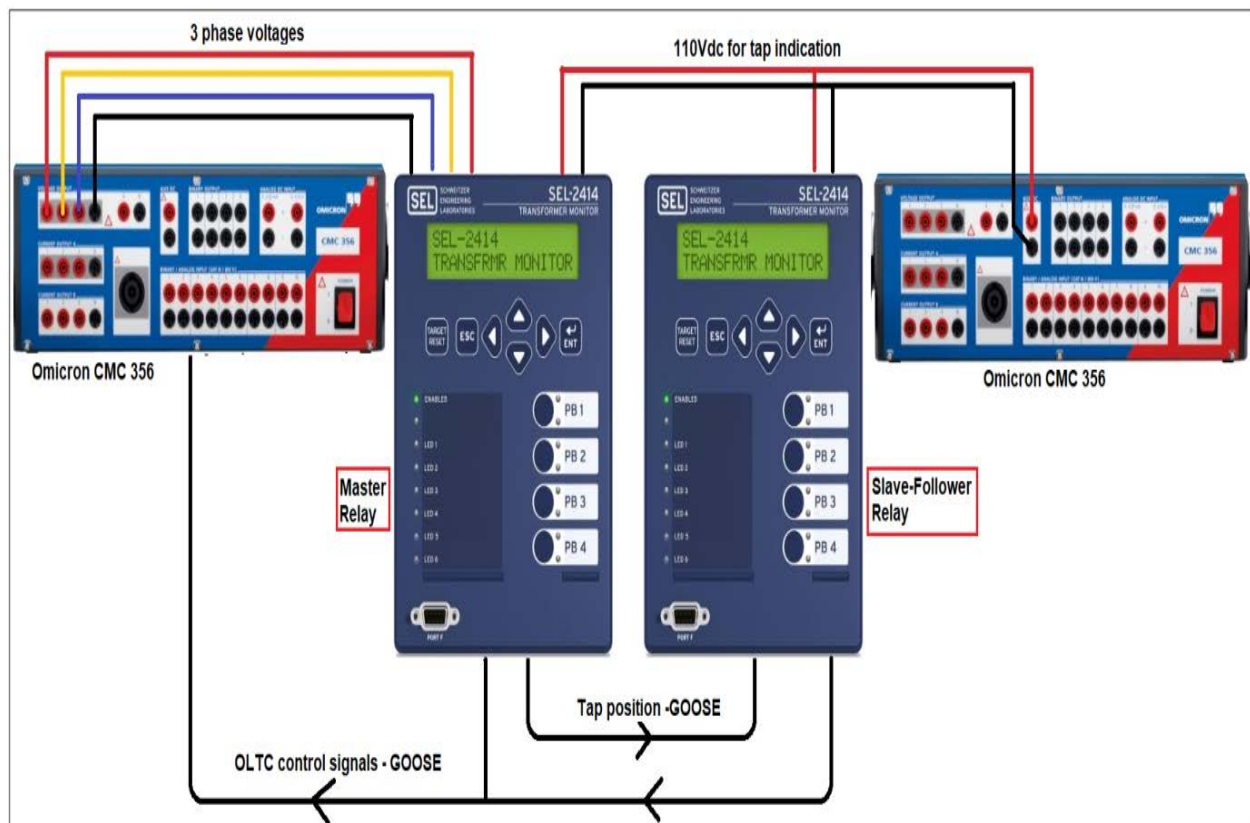


Figure 3: Basic structure of the lab-scale test bench setup

### 1.13.2 Hardware-in-the-loop Simulation

The hardware-in-the-loop simulation setup is shown in Figure 4. It represents the test bench setup arranged in a closed-loop testing configuration to test the power

transformer for the selected control schemes. Because the transformer to be controlled is digitally represented in the RSCAD software package and the actual SEL-2414 protection IEDs would be part of the circuit, this configuration would be in the form of control hardware-in-the-loop simulation (CHIL). The network under study is modeled in the RSCAD software package, and all necessary system characteristics will be entered to create a true-to-life simulation environment. The 100 MVA parallel power transformers that is controlled is constructed per its transformer data characteristics from the standard IEEE 14 Bus network found in the library of the RSCAD software. In the Quickset AcSELeator environment, the Master and Slave-Follower relays are configured. An Ethernet cable will connect the RSCAD software PC to the RTDS simulation equipment.

The RSCAD software suite would be used to replicate testing scenarios digitally, and the RTDS equipment's GT Analogue Output card (GTAO) would be utilized to generate an analogue output signal. Because the analog output signal of the RTDS has a maximum voltage of 10 V on its pins and a maximum current of 25 mA, some interface is required to boost the analog output values to usable values for the protection IED. The Omicron CMS 156 is used to amplify the RTDS equipment's output voltage signals. The SEL-2414 relay receives these enhanced voltage signals. An Omicron CMC 356 test injection device is used to generate a 110Vdc signal supplied to the high-voltage interface Panel of the RTDS equipment. The high voltage interface panel of the RTDS equipment used this 110Vdc to generate a binary code supplied to the SEL-2414 relays for tap indication of the OLTCs of the parallel transformers. Omicron Test Universe Software will be used to configure the CMC 356 test injection device. The SEL-2414 relay's capacity to regulate system voltage by adjusting the transformer tap positions will be analyzed in the RTDS environment. To complete the closed loop test environment, the SEL-2414 Master and Slave-Follower relay publishes IEC 61850 GOOSE control messages subscribed to by the RTDS equipment. The SEL-2414 relays will continuously monitor the voltage profile of Bus 6 and regulate the tap positions of the digital equipment in the RTDS environment if the measured voltage deviates from the dead band control setting. The data from the RTDS environment is analyzed to determine whether the operational performance tap change control algorithm is sufficient, as

well as the SEL-2414 IED's capacity to keep the system voltage within allowed voltage magnitude limits.

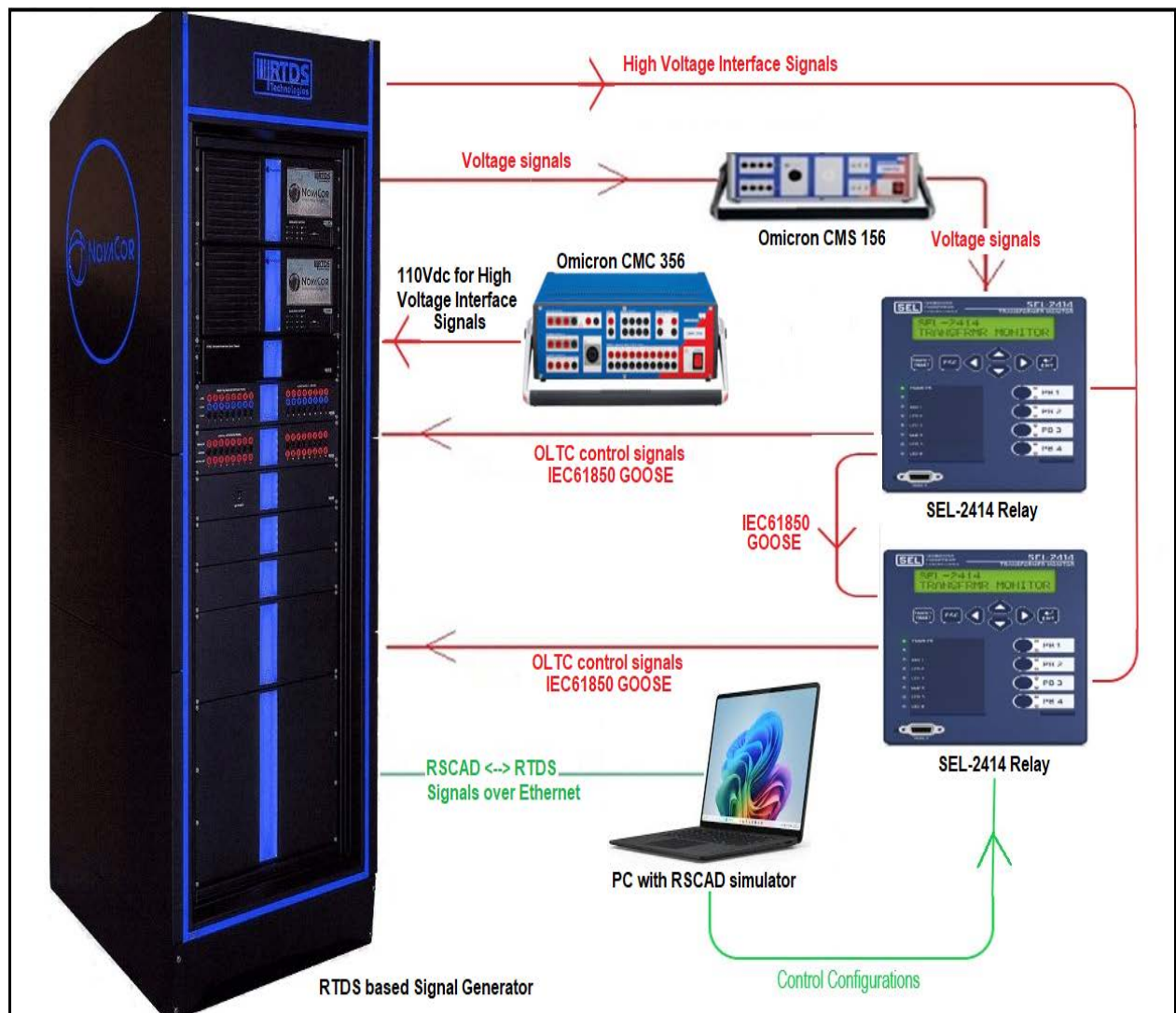


**Figure 4: Hardware-in –the-loop Simulation setup**

## 1.14 Chapter Breakdown

This thesis consists of six chapters and one appendix as follows:

### 1.14.1 Chapter One

This chapter describes the awareness of the research problem, the research aim and objectives, the Motivation of the research project, the project deliverables, and the research methodology.

### 1.14.2 Chapter Two

This chapter provides an overview of the literature reviewed when compiling this study. Literature was reviewed on the IEC61850 standard, voltage regulation of transformers, Tap changer controller algorithms, and hardware-in-the-loop simulations for transformer tap changers schemes.

### **1.14.3 Chapter Three**

This chapter presents the OLTC Theory & DIgSilent Implementation. OLTC operational principles were reviewed. Implementing the modified version of the IEEE 14 Bus network in the DIgSilent software.

### **1.14.4 Chapter Four**

This chapter showcases the lab-scale testing and implementation of OLTC. It presents the process of configuring the relays' control function and testing in a lab-scale environment.

### **1.14.5 Chapter Five**

This chapter presents the hardware-in-the-loop simulations. It describes the process of configuring the RTDS equipment. HIL simulations incorporating the two SEL-2414 relays and IEC61850 GOOSE communication are conducted, and the operational performance of the OLTC control algorithm is analysed.

### **1.14.6 Chapter Six**

This chapter summarises the research's key findings and conclusions and discusses the study's deliverables. It also presents future recommended work and applications of research.

## **1.15 Conclusion**

This chapter outlines the awareness of the research problem, research aim and objectives, motivation of the research project, project deliverables, and research methodology.

Chapter Two showcases the literature reviewed in compiling the project. The literature was divided into sections: 1) Literature review on IEC61850 standard 2) Voltage regulation of transformers 3) Tap changer controller algorithms 4) Hardware-in-the-loop simulations for transformer tap changer schemes.



## CHAPTER 2

### 2.1 Literature Review on IEC61850 Standard

#### 2.1.1 Introduction

Before developing the IEC communication standard, different equipment manufacturers developed and equipped their equipment with a unique communication structure. Only equipment from the same equipment manufacturers could communicate with each other. It meant substations were not flexible when it came to equipment procurement and that they had to stick to single vendors. The modern-day substation and development of intelligent electronic devices gave rise to communication problems between devices from different vendors. The need to establish a communication language understood by other components from different vendors was urgently needed to integrate devices harmoniously in substations. The IEC61850 standard was brought to life because there was a significant need in the industry for a standard communication platform between components and equipment in the substation. The IEC61850 standard is the accepted global communication standard in substations (Ivanova et al., 2016). The IEC61850 is much more than just a communication protocol. The abstract data models defined in IEC61850 can be mapped to many protocols, including MMS, GOOSE, and SMV (Montez et al., 2016).

MMS ensures that substation status information used for monitoring purposes is sent using the manufacturing messaging-specific protocol GOOSE is concerned with; critical data such as control signals and warnings are sent using the GOOSE protocol. SMV deals with power line current and voltage measurements, ensuring that these are sent using the SMV protocol (Tlali, 2017). The levels of the hierarchy are defined as:

- Station level
- Bay/unit level
- Process level

This section covers the literature review conducted for the research project on the IEC61850 GOOSE message application for power transformer voltage control. The



literature review was completed by reading books on voltage control of transformers and transformer protection systems, relay manuals, online journals, published articles, and web searches.

**Chapter 2 is organized into four sections on literature review: 2.1) Literature review on IEC61850 standard 2.2) Voltage regulation of transformers 2.3) Tap changer controller algorithms 2.4) Hardware-in-the-loop simulations for transformer tap changers and transformer tap changer protection schemes.**

The Literature Review structure shown in [Figure 5](#).

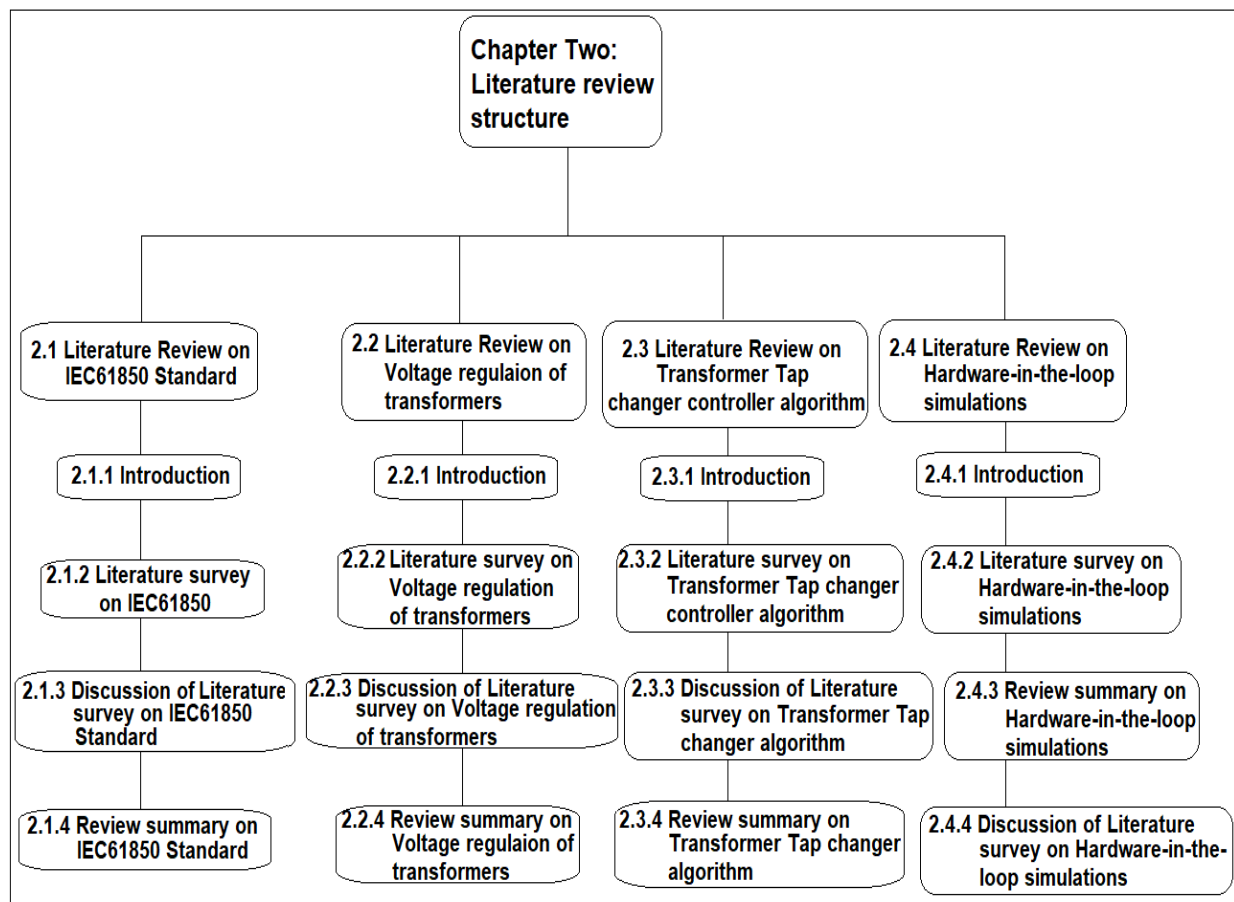


**Figure 5: Literature Review Structure**

The literature documents reviewed per year under the subsection IEC61850 are shown in [Figure 6](#).

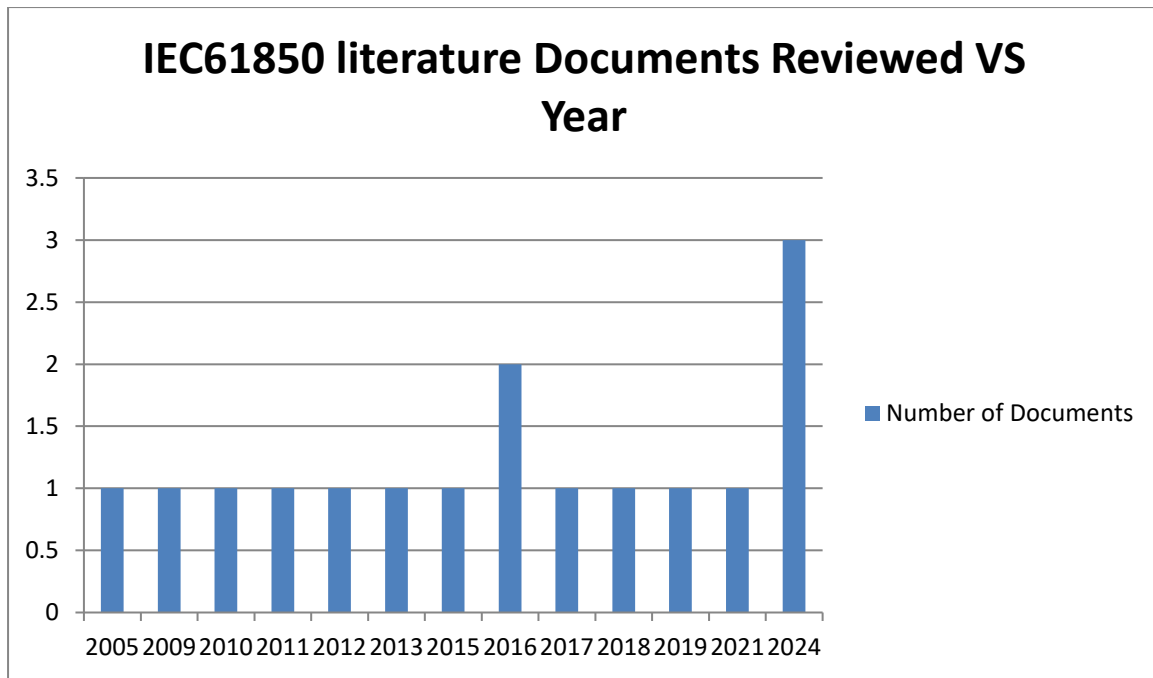


**Figure 6: IEC61850 documents reviewed per year**

### 2.1.2 Literature Survey on IEC61850

The authors (Apostlov, Vandiver, 2010) researched the impact of the IEC 61850 standard and its GOOSE application on wide-area protection schemes. They said IEC61850 and GOOSE can reduce the fault-clearing time in distributed protection schemes. According to the IEC61850 standard, it is possible to divide the substation into a function hierarchy, as can be seen in [Figure 7](#).

The three levels that the substation hierarchy is divided into can be defined as follow:

- Station level
- Bay/unit level
- Process level

The physical metering devices are found at the standard's process level. The process level sends measure values to the bay level, which consists of the IED devices. Control and monitoring are done at the station level.

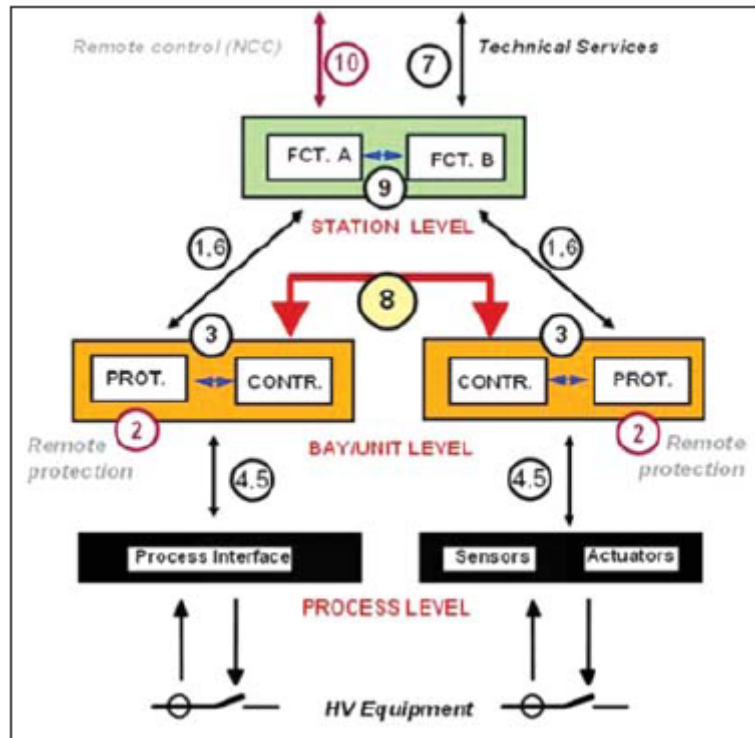


**Figure 7: Functional hierarchy of the IEC61850 standard (Apostlov, Vandiver, 2010)**

According to (Coffele, Blair, Booth, Kirkwood, and Fordyce, 2013), the benefits of incorporating the IEC61850 standard in adaptive protection include the fact that the IEC61850 has a standard language for data representation across all IEDs that is IEC61850 standard compliant. It allows for the interoperability of IEDs from different vendors. It makes it possible for a single substation to use IEDs from different vendors incorporated into a single protection system. The system configuration process complexity is greatly reduced due to IED standardized XML-based language. Limitations, however, still exist when dealing with IEDs from different vendors. IEDs from different vendors make use of different software platforms to configure and set the IED parameters. Vendors also have different name tags for logical nodes; parameters and setting values might also be in different units, and increments for setting values can also differ.

In a paper by the author (Schwarz, 2005) did a study on the application of the IEC61850 standard outside of the substation. Industries such as wind generation and power transmission realized the benefits of using the IEC61850 for standardized communication protocols for substation automation. They began to apply the standard in the entire electrical energy supply chain for communication between

IEDs. The IEC61850 standard was extended for the standardising of communication for applications outside the substation. Some of the applications of the standard was as follows:

- substation and feeder equipment (IEC61850-7-x)
- monitoring and control of wind power plants (IEC61400-25)
- monitoring and control of distributed energy resources (IEC61850)
- monitoring and control of hydropower plants (IEC61850)
- power quality monitoring (IEC61850)
- power system as seen from a control center viewpoint (IE 61970 CIM – common information model)

According to (Bhamare, 2009) IEC61850 offers major benefits for the control and protection industry with fast and supervised peer-to-peer communication protocol using GOOSE. Implementing GOOSE communication when designing substations enables the reduction of physical hardwiring between components of the substation. This expensive and heavy hardwiring can be replaced by a single Ethernet cable between components, which results in cost and time savings during the installation process and allows for a quicker and less time-consuming commissioning process. Changes to the control and protection process can also be implemented without physically having to change wiring between components. Changes can be implemented on the digital platform.

The authors (Brand, Brunner, Wimmer, 2011) wrote a paper about designing an IEC61850-based control system for substation automation according to the specifications provided by a customer. They said the IEC61850 standard will allow for the much-needed interoperability between IEDs in a substation automation system to perform functions such as:

- protection
- monitoring
- metering
- control
- automation

Communication between different components forms the backbone for a substation automation system; therefore IEC61850 plays an integral part of the substation

automation design process. The customer should provide the three areas of requirements for the design specifications:

- functionality
- performance needed
- applicable constraints

Logical nodes are the name given to the function of the IEC61850 standard. Each logical node is given a unique and standard name to identify a specific function. According to the IEC61850 standard, communication takes place between logical nodes of different IEDs (peer-to-peer) and between the different levels in the automation topology. See [Figure 8](#) for IEC61850-based communication structure between IEDs and between different levels of the automation topology.

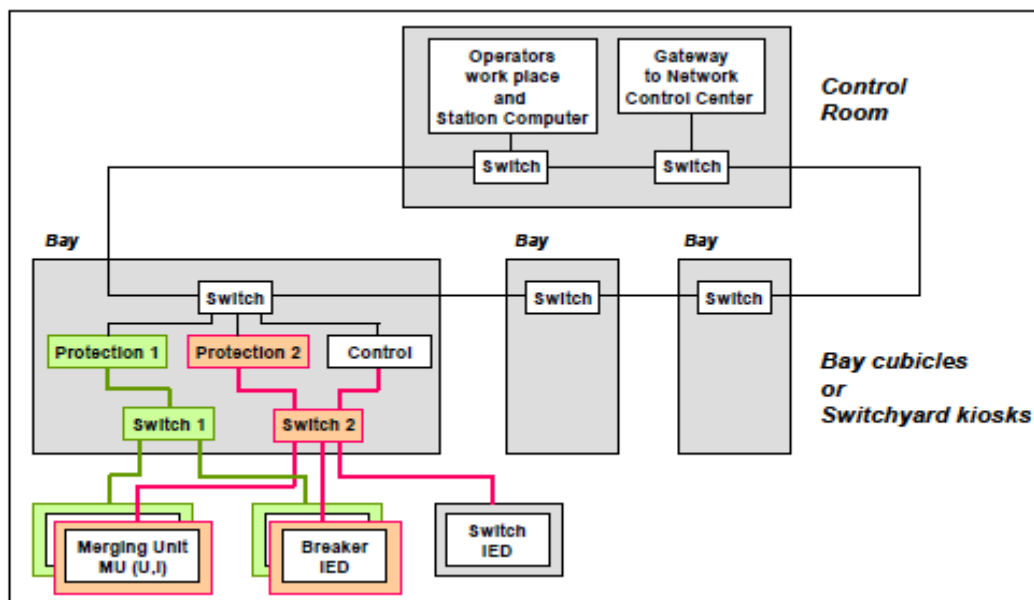


**Figure 8: Communication structure between IEDs and between different levels of the automation topology (Brand, Brunner, Wimmer, 2011)**

Data from the logical nodes is sent and received communication structures via Ethernet cable. Substation automation systems based on the IEC61850 standard are future-proof in design, flexible in terms of functions, inexpensive to install, and fairly cost-effective to maintain.

(Sichwart, 2012) did a study on the implementation of the IEC61850 GOOSE message for transformer load tap changing. GOOSE messages are used for peer-to-peer communications between the IEDs and communication protocol between

IEDs and the substation mainframe. GOOSE message statuses are published on a continuous basis for status indication and not just when an event changes. Sample values are used to communicate measured values between the actual devices (IEDs) and substation equipment. Sample values are also used to communicate status information and to publish updated statuses at regular intervals. It is believed by many people that in the future, the entire substations will be controlled by a central control computer, which is fed by an IEC61850-based communication structure to inform the central computer of the statuses of all the IEDs in the control system. Ethernet cable would replace hardwired copper wiring between IEDs. See [Figure 9](#) for comparison between hardwired communication cables and an Ethernet-based cable.



**Figure 9: Comparison between hardwired communication cables and an Ethernet-based cable (Sichwart, 2012)**

Using GOOSE messages makes it possible to communicate an entire set of data attributes grouped as a dataset. GOOSE messages are published to the entire connected network and other IEDs can read and interpret the messages published. The principle of the design of this tap changer is based on measured values communicated to a merging unit in the form of sample values. The merging unit will send the applicable data to the control unit via IEC61850 GOOSE messages. The actuator module received instructional data communication via GOOSE messages from the control unit to operate the transformer tap changer motor. See [Figure 10](#) for the basic structure of the load tap controller overall structure.

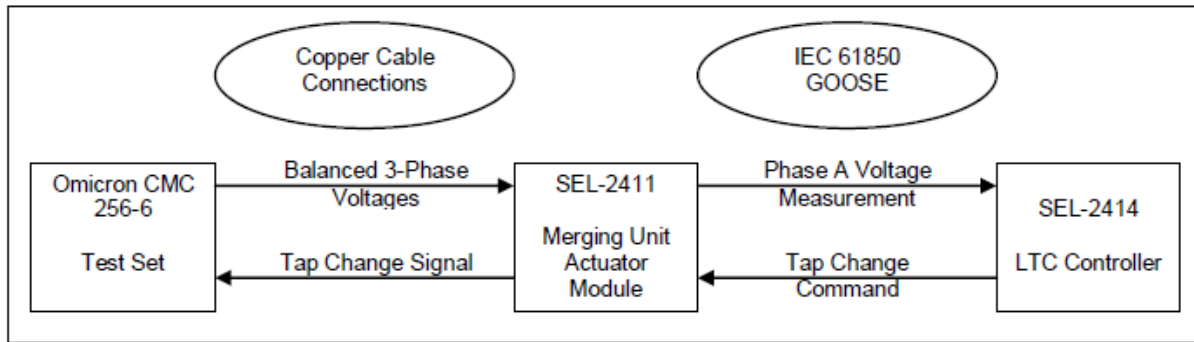


**Figure 10: Basic structure of the load tap controller overall structure (Sichwart, 2012)**

(Roostaei, 2015) said protection and control can be integrated into an IED. The rapid development in communication technology in recent years led to the establishment of more centralized control systems in automation systems. Data now needs to be sent to the centralised control system from a very broad network of smart devices. The IEC61850 satisfies most of the communication needs of such a centralized control system. He applied the IEC61850 standard for voltage regulation of a transformer with an automatic tap changer. To maintain constant voltage magnitude in a network with fluctuating load conditions, the transformer needs to alter its winding ratio in respect to its output voltage. The two IEC61850 standard communication protocols used:

- Generic Object Oriented Substation Event (GOOSE)
- Sample Values (SV)

These communication protocols allow for real-time communication between smart devices in a control and protection system. The building block for gathering system information in the IED is the Logical Node. The control system operates and makes decisions on the data received from the logical nodes. See [Figure 11](#) for logical nodes in the transformer bay.

Data gathered from the logical nodes in the transformer would communicate with the control system. The control system monitors the operational conditions of the transformer and issues instructional communications to the load tap changer if the transformer's winding ratio needs to be altered to rectify operational conditions. See [Figure 12](#) for the system that monitors the position of the tap in the control room.



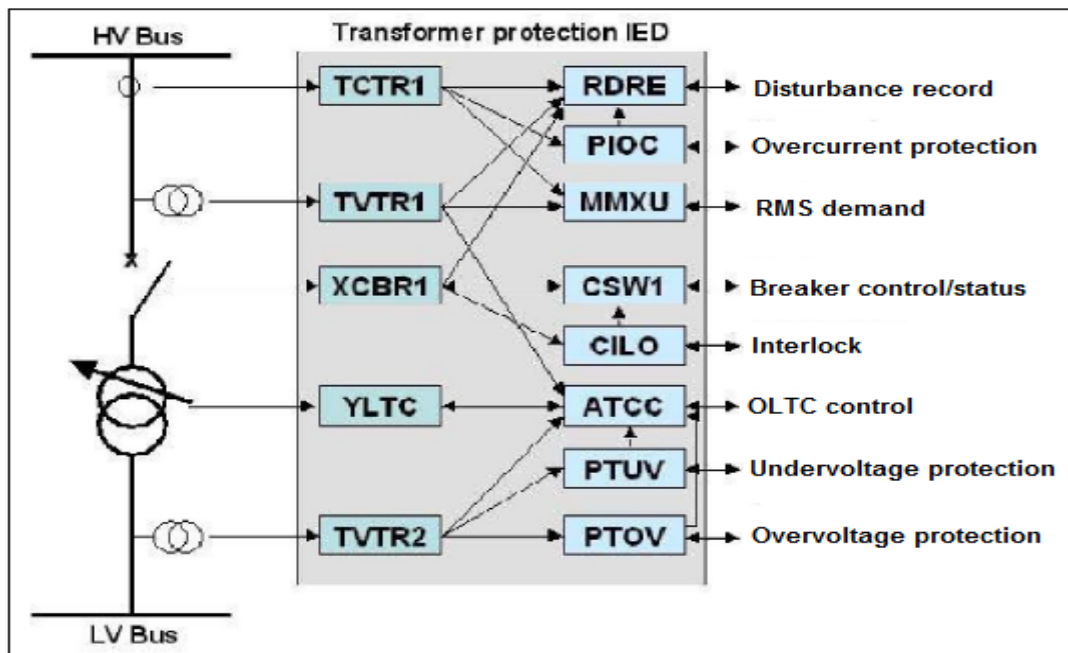


Figure 11: Logical Nodes in Transformer Bay (Roostae, 2015)

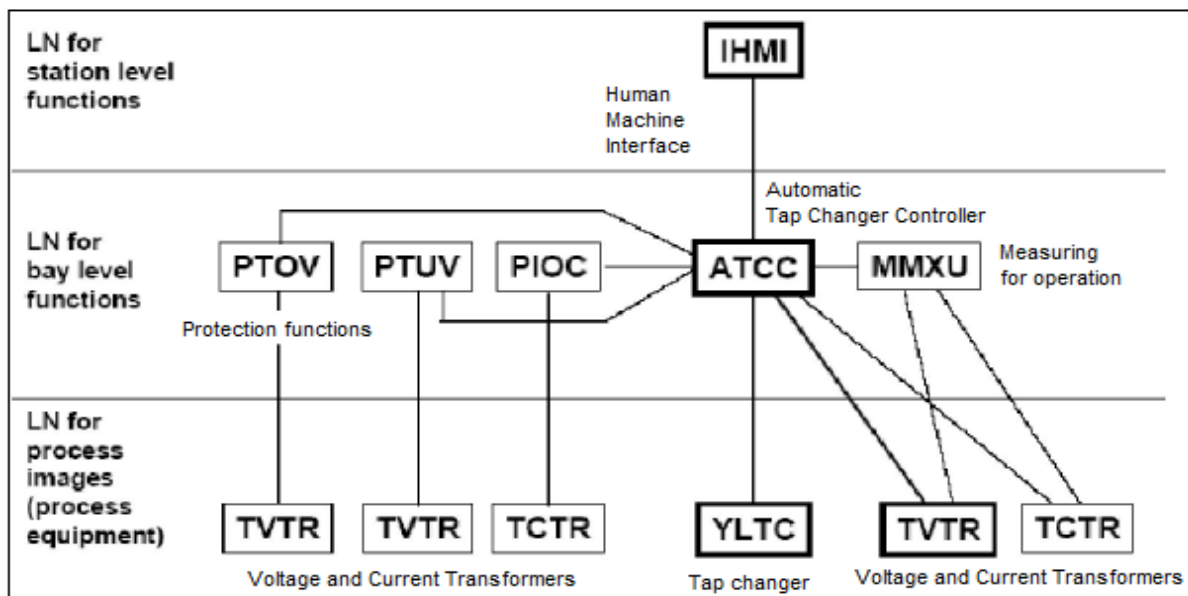
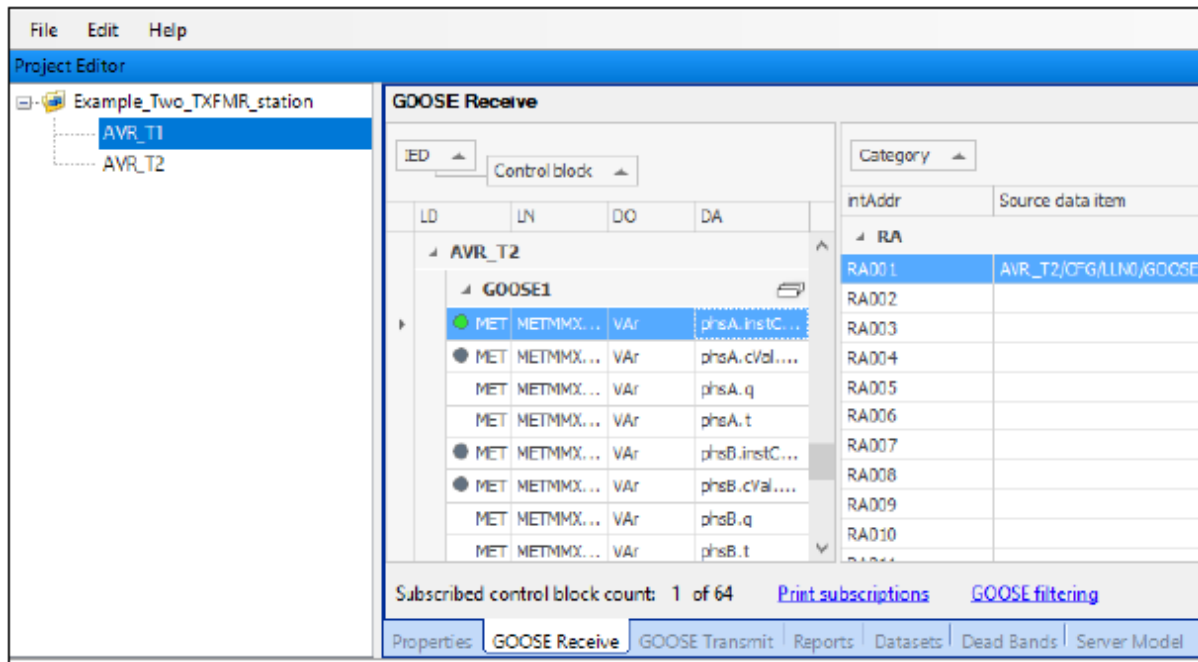


Figure 12: Tap position monitoring system (Roostae, 2015)

(Hampson, 2018) said the IEC61850 standard need not be applied to the entire substation. He believed that many operational, monitoring, and control issues could be addressed by only using could be addressed by using only parts of the technology of the IEC61850 standard. He applied the IEC61850 standard in a current circulating scheme to control the automatic tap changer of up to four parallel transformers. With logic created to control the paralleled transformer in place, the control data had to be communicated between the IEDs. In the case of two parallel



transformer configurations, each tap changer on each transformer will be controlled by an individual IED. In this application, a Configured IED Description (CID) file containing the GOOSE message must be sent to every IED that will be communicated with each tap changer. See Figure 13 for linking GOOSE messages between devices.



**Figure 13: Linking GOOSE messages between IEDs (Hampson, 2018)**

(Krishnamurthy, Balingobera, 2019) established a harmonic blocking scheme utilized for transformer protection schemes. The scheme incorporated an SEL-487E differential protection relay and an SEL-751A overcurrent relay as backup protection. The stumbling block they encountered was that inrush conditions would trip the backup protection because the SEL-751A relay does not have a harmonic restraint element. To mitigate this false tripping scenario, they developed a protection that uses the harmonic restraint element from the SEL-87E relay to send this information to the SEL-751A relay to block the backup relay from issuing trip signals during inrush current conditions of the power transformer. The protection signals were transmitted using IEC 61850 GOOSE-based communication. They found that compared to the simulation for an identical scheme configured using a hardwired configuration, the IEC 61850 GOOSE-based scheme proved superior in speed and reliability. Shown in Figure 14 is the harmonic blocking scheme utilized for transformer protection with IEC 61850 GOOSE-based communication?

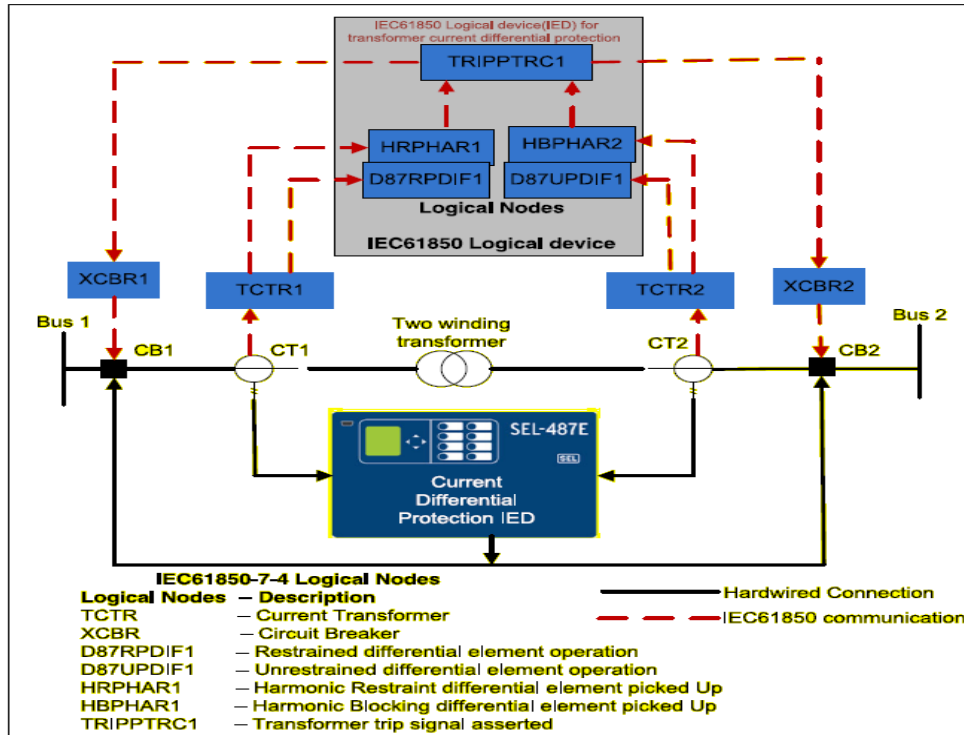


**Figure 14: Harmonic blocking scheme utilized for transformer protection with IEC 61850 GOOSE-based communication (Krishnamurthy, Baningobera, 2019)**

(De Graaff Genis, Krishnamurthy, 2024) did a study to address difficulties experienced due to the introduction of distributed generation to power grids. Distributed generation connected at various entry points on the grid creates bidirectional load flow. These conditions are not ideal for the conventional protection schemes employed on power system networks and lead to false operation of protection equipment. They developed an IEC 61850 GOOSE-based protection scheme for improved coordination between the directional overcurrent relays employed to protect transmission lines. Shown in Figure 15 is the test bench setup with the SEL-351 directional overcurrent relay and an IEC 61850 GOOSE-based communication structure for improved coordination between protection relays.

(Bonetti, Zhu, Ignatovski, 2021) Did a study about implementing the IEC61850 GOOSE protocols in power system protection. They found that the use of accurately defined GOOSE messages bolsters the protection security of a network without sacrificing dependability. They applied the concept in an overcurrent blocking protection scheme for testing purposes. Wireshark network analyzer monitors the IEC 61850 GOOSE messages published to the network.

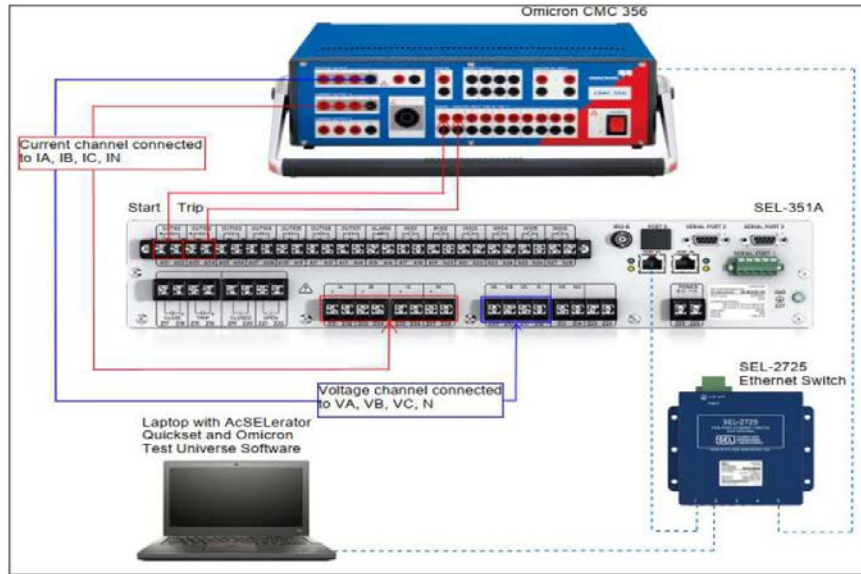


**Figure 15: Microgrid protection scheme set up SEL-351 directional overcurrent relay with IEC 61850 GOOSE-based communication structure for improved coordination between protection relays (de Graaff Genis, Krishnamurthy, 2024)**

In a paper authored by (Shangase, Ratshitanga, and Mnguni, 2024), the interoperability barriers experienced when employing IEC 61850 GOOSE-based communication in networks that consist of equipment from different vendors are discussed. Although IED conformance to the IEC 61850 standard is verified, it does not guarantee interoperability between devices from different manufacturers. A differential protection scheme is constructed for a network with a parallel transformer pair. A HIL simulation is done by incorporating a SEL-487E, and a MiCOM-P645 relay is used to demonstrate the interoperability capabilities of the protection function. Shown in Figure 16 is interoperability assessment they proposed.

(Yepez-Nicola, Reyes-Lopez, 2024) Developed a methodology based on IEC 61850 communication structures for improved coordination between transformer differential and overcurrent protection schemes. The SEL-751 IED is utilized for main feeder protection, and the SEL-387E is used for the transformer differential protection function. The IEC 61850 communication structure is improved coordination between transformer differential and overcurrent protection schemes. Incorporating this communication structure ensures the network is expansion-ready and GOOSE-compliant equipment from different vendors can be used in the network. Shown in Figure 17 is the LAN network topology they proposed.

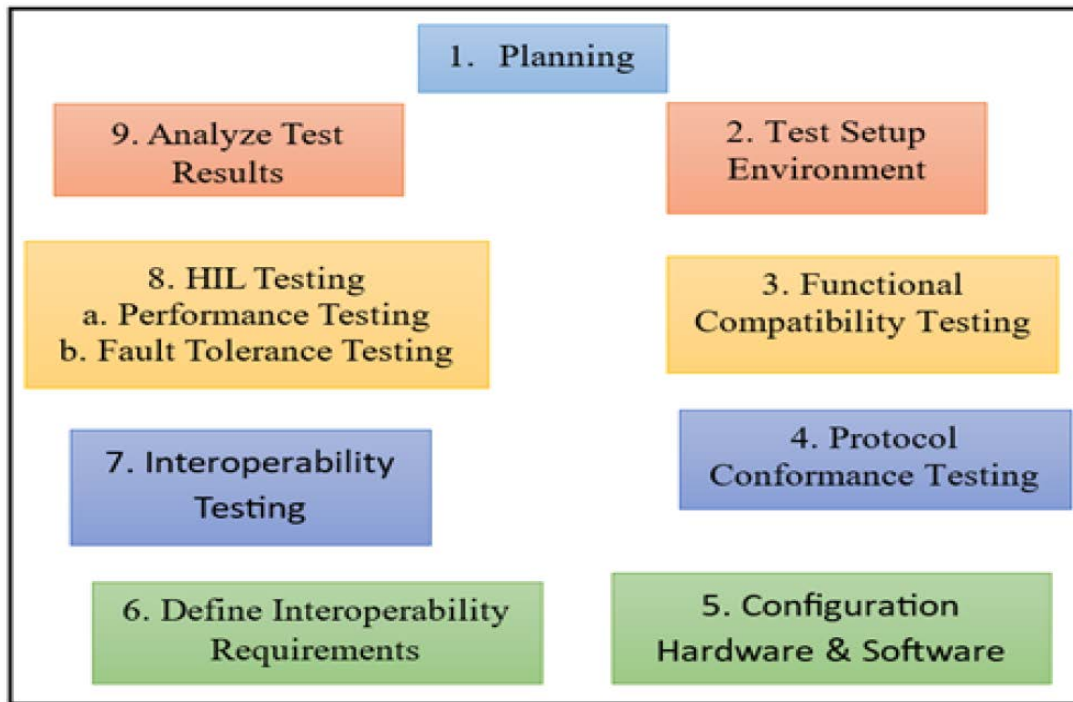


Figure 16: Interoperability assessment (Shangase, Ratshitanga, and Mnguni, 2024)

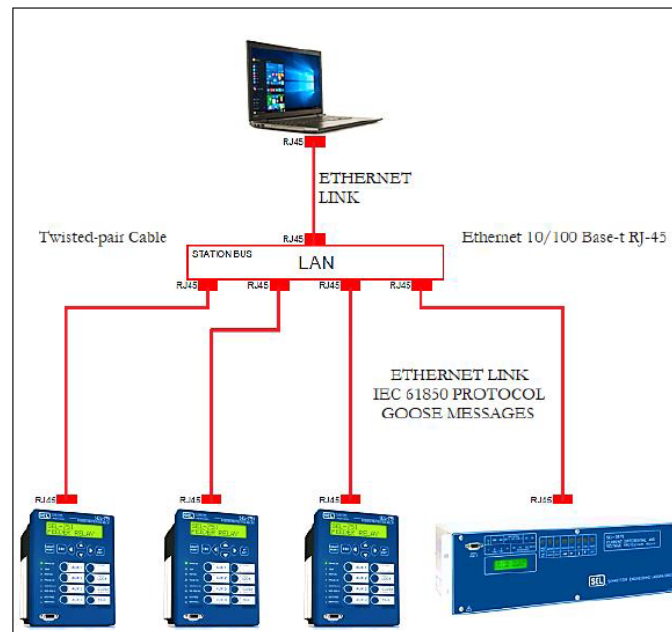


Figure 17: LAN network topology (Yepez-Nicola, Reyes-Lopez, 2024)

### 2.1.3 Discussion of literature survey on IEC61850 standard

With the increased demand for intelligent systems and gadgets in every aspect of modern life, the demand for intelligent devices has also increased in substations where energy is generated and throughout the transmission and distribution systems. Introducing these sophisticated electronic devices into electrical supply systems

dramatically increased the requirement for data sharing and communication within the electrical supply system. With the establishment of the IEC61850 communication standard, a standardized communication protocol widely accepted throughout the electrical generation and supply industries was made possible. Because of the use of a standardized communication platform, IED made by different suppliers were able to connect with one another within the same network effortlessly. This meant that IEDs could send and receive digital data from any other IED in a network.

The IEC61850 standard is much more than a communication protocol; the abstract data models provided in IEC61850 can be mapped to various protocols such as MMS, GOOSE, and SMV. The GOOSE protocol sends critical data such as control signals and alerts. Utilizing IEC61850 GOOSE messages, it is possible to communicate a whole collection of data attributes grouped as a dataset and provide another significant benefit to the control and protection business with a quick and supervised peer-to-peer communication protocol using GOOSE. The IEC61850 standard also divides the substation structure into three levels: the process level, the bay level, and the station level. Each level of the structure provides a distinct function.

The physical instruments, such as CTs and VTs, are found at the process level. The physical IEDs on the bay level are capable of sending and receiving data and communication from other IEDs on the same level. The signals collected from the instruments at the process level are analyzed at this level. The bay acts as the structure's control and monitoring center. In most cases, this is where the SCADA system is placed. One of the numerous advantages of the IEC61850 standard was eliminating the necessity for physical connections between network components. Ethernet connections, which send digital control and monitoring signals between devices in the digital hierarchy, have replaced heavy copper cables between terminals.

#### 2.1.4 Review summary on IEC61850 standard

**Table 3** comprehensively summarizes IEC61850 standard applications for voltage regulation on power transformers. Potential review papers are chosen from the literature to provide the comparison study based on their research work goal, techniques, simulation and hardware tools, and project benefits, as stated in **Table 3** below.

**Table 3: Review summary on IEC 61850**

<b>Paper</b>	<b>Aim</b>	<b>Method used</b>	<b>Simulation/ implementation Hardware/software</b>	<b>Benefits</b>
Ivanova, Rangelov, Nikolaev, 2016	To present the IEC61850 standard from the electrical engineer's point of observation, since the engineer is responsible for the electrical substations' design, construction, operation, and maintenance.	The general IEC61850 standard and variants of the standard were investigated.	The general IEC61850 standard was investigated. Other variants of the standard include: IEC61850-7-1, IEC61850-7-2, IEC61850-7-3, IEC61850-7-4.	The IEC61850 standard provides detailed and precise instructions and directions on achieving and implementing intense automation and protection functions in substations, utilities, and power plants.
Montez, Stemmer, Vasques, 2016	To demonstrate the functions of the IEC61850 standard communication by applying GOOSE messages and Sampled	IEC61850 Standard, GOOSE message application, and Sampled Measured Values.	The IEC61850 models were simulated through the OMNeT++/INETMANET framework and the OMNeT++/ framework.	The engineer can assess the scalability of the relevant network, it enables the engineer to analyze large and complex networks and it

	Measured Values.			also allows to obtain accessible end-to-end delays easily
Tlali, 2017	To analyze the impact that IEC61850 has on substation design.	The IEC61850 standard was investigated.	No simulations were conducted in this analysis.	It eliminates procurement ambiguity, lowers installation costs, transducer costs, commissioning costs, simplifies architecture, provides greater reliability and future-proof design, lowers integration costs, implements new capabilities, and lowers extension costs.
Apostlov, Vandiver, 2010	To investigate the impact that IEC61850 GOOSE has on distribution protection schemes.	The IEC 61850-8-1 and IEC 61850-9-2 were investigated.	IEC 61850-8-1 and IEC 61850-9-2 were used for high-speed peer-to-peer communication during simulations. The details of IED types and real-time simulation equipment should	In distribution protection schemes that employ the application of IEC 61850 GOOSE messages, this reduces fault clearing times and minimizes the effect of

			be mentioned.	short circuit faults on sensitive loads.
Coffee, Blair, Booth, Kirkwood, Fordyce, 2013	Describe and implement an adaptive overcurrent protection scheme using the IEC61850 communication structure.	The overcurrent protection scheme making use of the IEC61850 communication structure was demonstrated with the hardware-in-the-loop setup.	The overcurrent protection relays used are the Alstom MiCOM P145 and the ABB REF615. RTDS was used for hardware-in-the-loop simulations, and IEC61850 was used for the communication protocol. The substation computer used was an ABB COM615.	The HIL simulation has demonstrated that adaptive protection can be implemented with commercially available hardware and that the scheme improves the protection system's performance.
Schwarz, 2005	To study the application of the IEC61850 standard outside the substation in almost all electrical generation, transmission, and distribution systems.	The IEC61850 standard and IEC61850-based standards were investigated and analyzed to determine their compatibility for implementation in applications beyond the substation.	Substation and feeder equipment (IEC61850-7-x). Monitoring and control of wind power plants (IEC61400-25). Monitoring and control of distributed energy resources (IEC61850). Monitoring and control of hydropower plants (IEC61850).	Applying the IEC61850 and IEC61850-based standards in the electrical supply system achieves a standardized communication and information system. Standardized communication protocols and information are easily



			Power quality monitoring (IEC61850). The power system as seen from a control center viewpoint (IE 61970 CIM – standard information model).	shared between different levels of the digital hierarchy.
Bhamare, 2009	The research aimed to determine and investigate how GOOSE communication can improve system reliability and performance.	A Factory Acceptance test (FAT) was conducted at ABB Works to analyze the performance of the GOOSE communication.	Relion® 615 series IEDs were employed for the Feeder Protection function and as Control IEDs. IEC61850 GOOSE was used for the communication protocol.	IEC61850 offers major benefits for the control and protection industry. It uses a fast and supervised peer-to-peer communication protocol called GOOSE, which also enables simplified substation wiring. Although the IEC61850 standard is still in its infancy, many future developments will be based on it, which in turn will promise the longevity of its usage.
Brand, Brunner, Wimmer,	The research aimed to	A distributed substation	A distributed substation	Substation automation

2011	investigate how IEC61850 can be employed to satisfy customer needs and requirements in the design of substation automation systems.	automation system for a high- and medium-voltage substation was designed based on the IEC61850 standard and its IEC61850-9-x variant.	automation system for high- and medium-voltage substations was designed. The type of IEDs used and the simulation platform are not mentioned.	systems based on the IEC61850 standard are future-proof in design, flexible in functions, inexpensive to install, and relatively cost-effective to maintain.
Sichwart, 2012	The implementation of IEC61850 GOOSE message for transformer load taps changing.	The principle of the design of this tap changer is based on measured values communicated to a merging unit in the form of sample values. The merging unit sends the applicable data to the control unit via IEC61850 GOOSE messages. The actuator module received instructional data communication via GOOSE messages from the control unit to operate the transformer tap	The Omicron CMC 256-6 test set is used as the voltage-generating device. The SEL-2411 is used as the merging device. Sampled Values are sent via GOOSE messages to the SEL-2414 IED. The SEL-2414 IED serves as the load tap controller.	Ethernet cable would replace hardwired copper wiring between IEDs, saving both costs and reducing installation and commissioning costs. GOOSE messages can communicate an entire set of data attributes grouped as a dataset. GOOSE messages are published to the entire connected network, and other IEDs can read and interpret the

		changer motor.		messages published.
Roostaei, 2015	This research paper analyses the conventional tap changer and also the development of a transformer tap changer control with the implementation of IEC61850 standard.	The IEC61850 standard is applied in a current circulating scheme to control the automatic tap changer of up to four parallel transformers.	An Automatic Tap Changer Controller is modeled using the IEC61850 standard as a communication platform between the controller and the tap changer. The types of IEDs used in this experiment and the platform on which simulations were performed are not mentioned.	Using the IEC61850 standard as a communication medium enables the virtualization of all information from the transformer bay, which becomes accessible anywhere within the substation by various components in the virtual network. Based on this standard, new methods for control and protection functions are now possible.
Hampson, 2018	Implement a circulating current scheme employing IEC61850 GOOSE messages to control the automatic voltage regulator of	Based on the IEC61850 GOOSE for control, protection, and monitoring purposes.	A circulating current scheme is implemented for the operation of an automatic voltage regulator. The scheme uses IEC61850 GOOSE as a communication	Implementing the IEC61850 standard has enabled peer-to-peer communication topologies to evolve into peer-to-many

	parallel operating transformers.		medium. The specific control IEDs and simulation platforms are not mentioned.	communication topologies. Adding new protection protocols to an existing network is possible without adding or modifying the existing hardware setup.
Krishnamurthy, Elenga Baringobera, 2019	Implement a harmonic blocking scheme for transformer protection with IEC 61850 GOOSE-based communication.	The harmonic restraint element from the SEL-87E relay is sent to the SEL-751A relay to block the backup relay from issuing trip signals during the power transformer's inrush current conditions.	The CMC356 test injection device simulates inrush conditions. The SEL-487E relay monitors these conditions and sends the harmonic restraint element to the SEL-751A relay to prevent it from tripping during inrush conditions. IEC61850 GOOSE-based communication is used for signal transmission.	The IEC 61850 GOOSE-based scheme proved superior in speed and reliability to a scheme using a hardwired configuration for signal transfer.
Bonetti, Zhu, Ignatovski, 2021	To demonstrate that utilizing accurately defined GOOSE messages bolsters the	The concept is applied in an overcurrent blocking protection scheme for testing purposes.	No specific IEDs were used to implement the overcurrent blocking scheme. A Wireshark network analyzer	Accurately defined IEC 61850 GOOSE messages enhanced the protection security

	protection security without sacrificing dependability.		monitors the IEC 61850 GOOSE messages published to the network.	of a network without sacrificing dependability.
de Graaff Genis, Krishnamurthy, 2024	Addressing difficulties experienced by network protection coordination due to introducing distributed generation to power grids.	IEC61850 GOOSE communication is employed for better coordination of directional Overcurrent relays when distributed generation is introduced on power system networks.	The protection scheme was modelled in the DIgSilent software before test bench implementation. Directional currents are simulated using the CMC356 test injection device. The SEL-351 relays monitor these currents, and with the implementation of IEC 61850 GOOSE, GOOSE-based communication is better coordinated for unnecessary issuing trip signals.	The IEC 61850 GOOSE-based communication protocol improves coordination between directional Overcurrent relays. GOOSE communication improved the signal transmission speed and reliability of the protection scheme.
Shangase, Ratshitanga, Mnguni, 2024	Address the interoperability barriers experienced when employing IEC 61850 GOOSE-based communication in	A differential protection scheme is constructed for a network with a parallel transformer pair with IEDs from different vendors used for the protection	. An RTDS-based HIL simulation is done by incorporating a SEL-487E, and MiCOM-P645 relay is used to demonstrate the interoperability capabilities of	By incorporating IEC 61850 GOOSE communication into a protection function, interoperability between IECs manufactured by

	networks that consist of equipment from different vendors is discussed	functions. IEC 61850 GOOSE-based communication is used to achieve interoperability between the IEDs from different vendors.	the protection function to demonstrate protection function interoperability capabilities. RTDS. IEC 61850 GOOSE-based communication is used to achieve interoperability between the IEDs from different vendors.	different vendors can be achieved.
Yepez-Nicola, Reyes-Lopez, 2024	The methodology proposed is based on IEC 61850 communication structures for improved coordination between transformer differential and overcurrent protection schemes.	A coordinated protection scheme is developed incorporating IEC 61850 GOOSE communication for overcurrent and differential protection of a transformer.	The SEL-751 IED is used for main feeder protection, and the SEL-387E is used for transformer differential protection. The IEC 61850 communication structure is incorporated to improve coordination between transformer differential and overcurrent protection schemes.	The primary benefit of employing this methodology is that it can be applied to any substation employing IEC 61850-compliant IEDs and LAN networks. The network is expansion-ready, and GOOSE-compliant equipment from different vendors can be used in it.

## 2.2 Literature Review on Voltage regulation of transformers

### 2.2.1 Introduction

Customers connecting to the electrical supply system expect a certain grid voltage level to be maintained. Maintaining a stable voltage level throughout the electrical supply system is essential for a stable and reliable grid and maintaining power quality within certain acceptable limits along the grid. The power transformer maintains a stable voltage along the entire electrical supply system. Conventional on-load tap changers have been in operation for many years to compensate for voltage fluctuations along the grid. Conventional on-load tap changers employ mechanical switches to perform the tap change function on transformers (Bugade et al., 2018). Conventional on-load tap changers have many drawbacks, which include slow operation time and arcs when switching is done. With the modernization of the electrical supply system and customer demands for ever-improving power quality from power producers, maintaining a stable grid voltage profile came into the spotlight again. To perform the protection functions of the power transformer and the on-load tap change function, utilities have started to move away from electromechanical relays and static relays towards the new and improved digital microprocessor-based protection and control relays (Constantin ,Iliescu, 2012). Intelligent electronic devices are programmable to perform various protection, control, and monitoring functions. Custom algorithms can be created and programmed to the devices to perform certain functions.

The documents reviewed per year under the subsection Voltage regulation of transformers are shown in [Figure 18](#).

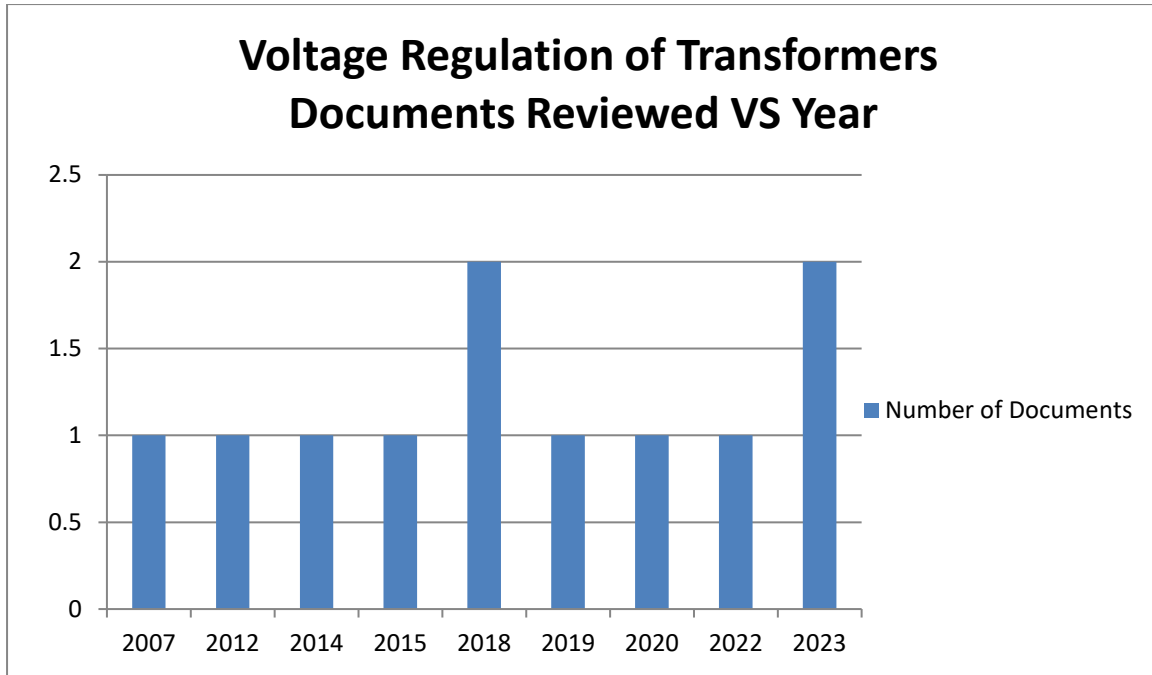


**Figure 18: Voltage regulation of transformers documents reviewed per year**

### 2.2.2 Literature survey on Voltage regulation of transformers

The authors (Zhou, et al., 2018) did a review paper on voltage control using an on-load voltage transformer for the power grid. They said that transformer voltage control is important for regulating feeder voltages throughout the power grid. They said the mechanical on-load tapping changer that is available presently is widely employed in power grid networks. However, these mechanical on-load tapping changers have many drawbacks and shortcomings relating to their complex mechanisms, slow response time, arcing when switching, etc. To improve the working characteristics of the mechanical on-load tap changer to adhere to new working requirements from grids specifications, manufacturers had to employ rapidly developing power electronics technology to improve the on-load tap changers. The authors researched several standard OLTC technology routes and analyzed trends for these technologies. From the research conducted they tabulated their findings as in [Table 4](#) .



**Table 4: Comparison of different OLTC voltage control schemes (Zhou, et al., 2018)**

<b>Type</b>	<b>Speed</b>	<b>Arc</b>	<b>Switch Loss</b>	<b>Impact after thyristor failure</b>	<b>System fault detection</b>	<b>Cost</b>
<b>Traditional mechanical</b>	Slow	Large	Yes	No	No	Higher
<b>Mechanical improved</b>	Slow	Smaller	Yes	No	No	Higher
<b>Power electronic switch</b>	Fast	Low	Little	Serious	Yes	Could be reduced

The research was conducted by the authors (Xie, Shentu, Wu, Ding, Hua, Cui, et al., 2019) to determine the effect of the increasing penetration of photovoltaic (PV) systems that may lead to a voltage increase in the distribution network. Conversely, with the increase and popularity of electric vehicles, the charging of these vehicles can lead to a voltage drop in the distribution network. In this study, they proposed an intelligent search algorithm called voltage ranking search algorithm (VRSA) to solve the optimization of flexible resource scheduling for voltage regulation. [Figure 19](#) shows the flowchart of real-time voltage regulation.

The algorithm they proposed is based on the radial power features of the distribution network. They experimented with the numerical simulations of power distribution grids and compared VRSA with genetic algorithm and voltage sensitivity method. From the results they obtained from testing the three methods, they observed that the best optimization results were from the VRSA. The reduction of tap operation time was achieved of on-load tap changers by using flexible resources through demand response.

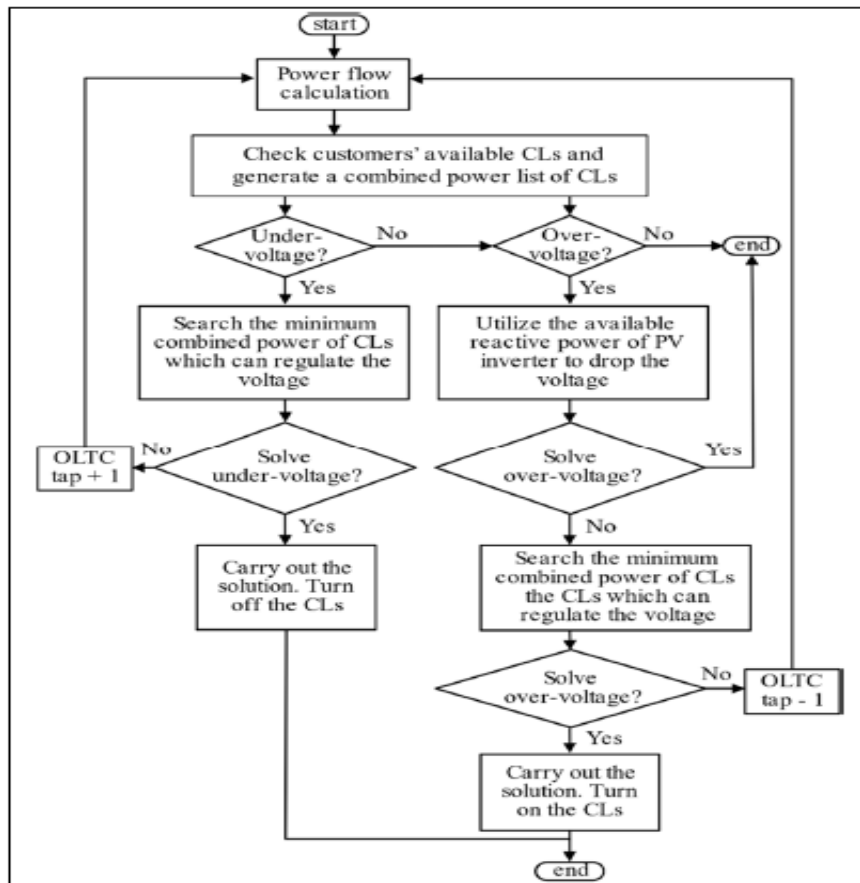


**Figure 19: Flowchart of real-time voltage regulation (Xie, Shentu, Wu, Ding, Hua, Cui, et al., 2019)**

According to the authors (Monroy et al., 2007), sophisticated electromechanical mechanisms that control the tap changing on power transformers achieve voltage regulation of transmission and distribution networks. According to their research, this type of system is prone to wearing out prematurely, and its operation time is slow. They researched the possibility of replacing these mechanical devices with electronic switching devices. The research utilized two types of configurations: electronic tap-changing devices. With 4 and 9 voltage steps, they are described as readily replacing existing 5-step mechanical changers at MV/LV transformers. The results they obtained from simulations showed an essential improvement in customers' voltage profiles, both at usual standards and in emergency emergencies.

In a paper by the authors (Carlen et al., 2015), they said the unprecedented increase in renewable energy being introduced into the distribution grids results in voltage increases in some regions. They came up with an innovative line voltage regulator (LVR) to remedy these over-voltage conditions. In Germany, renewable energy will

supply 50% of electricity consumed in the next 15 years. To allow for distributed generation devices to penetrate the grid at the distribution level and to decouple the MV side of the grid from the HV/MV transformer, an LVR is needed. An LVR would only alter the line where a voltage level problem is detected, where changing the taps of the HV/MV transformer would alter all the voltage levels of all the lines fed from this transformer. See Figure 20 for the operating principle of the LVR.

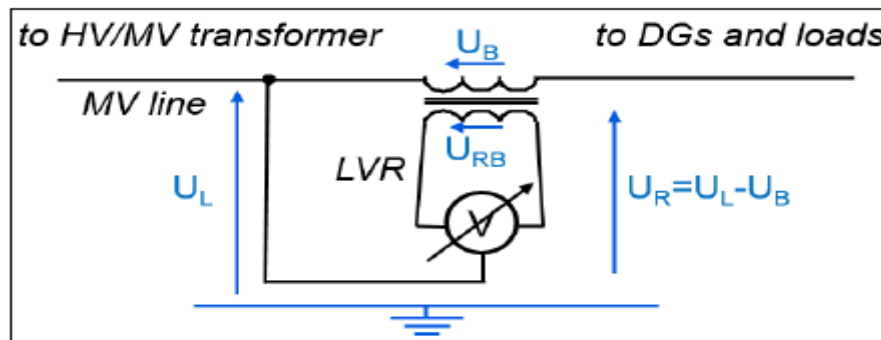


**Figure 20: Operating principle of the line voltage regulator (Carlen et al., 2015)**

(Ferrero, Cimadevilla, Yarza, Solaun, 2014) did a study of on-load tap changer (OLTC) control for a network configuration that operates with up to five transformers in parallel. The automatism control methods they considered for the OLTC control were:

- Reverse reactance method,
- Master-follower method
- Circulating current method

They modeled the different circuit constructions with hardware in the loop setup in the RTDS environment to evaluate network simulations. IEC 61850 GOOSE message communication was implemented to share data between the IEDs used in the simulations. Automatic voltage regulators (AVR) operating OLTC in customarily used to maintain constant voltage levels along a network. AVR also has to work with other devices such as capacitor banks to maintain continuous voltage levels and regulate reactive power flow in a network. See Figure 21 for the circuit modeled in RSCAD with two transformers operating in parallel with the single source.

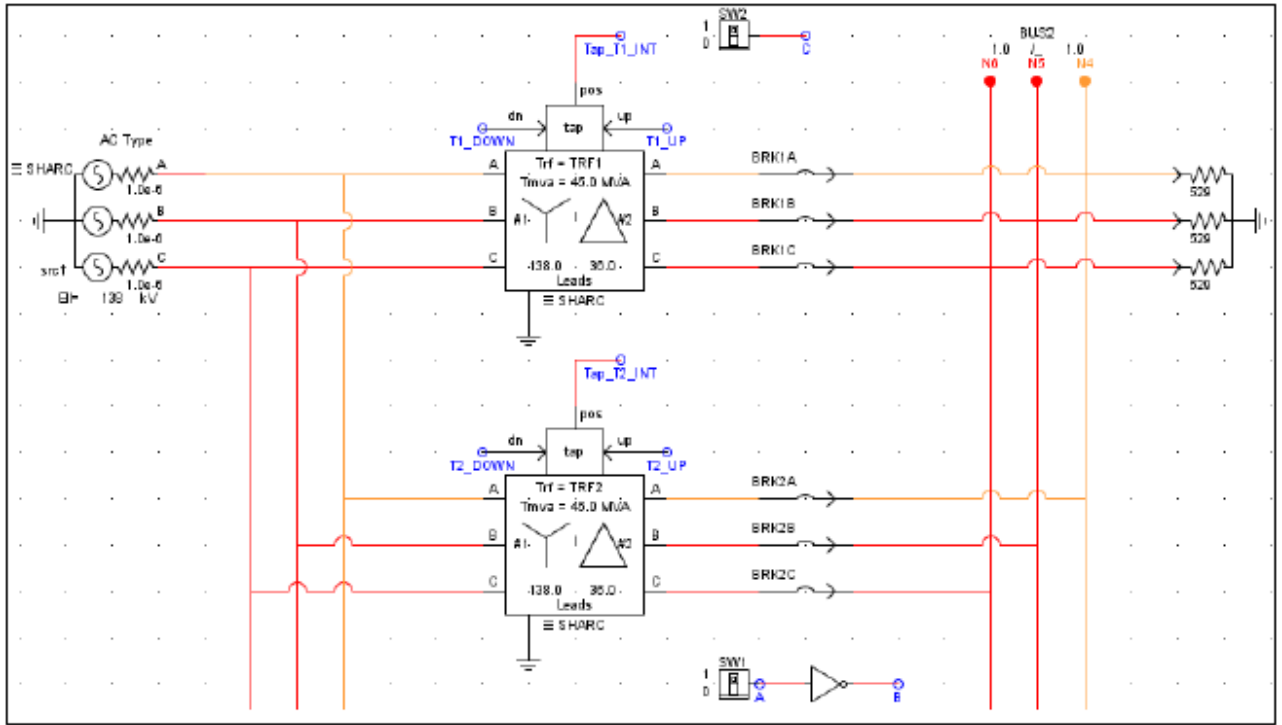


**Figure 21: Parallel operation of two transformers (Ferrero, Cimadevilla, Yarza, Solaun, 2014)**

From the simulation, they found that IEC61850 GOOSE allowed them to design a decentralized control structure without the need for any copper wiring, which has many benefits. Using this communication structure meant logical changes could be implemented without physical changes, making future additions more cost-effective and easier to implement. GOOSE messages also provide a high level of reliability due to the built-in repetition mechanism that detects communication faults. They found that using a master follower method, a complex feedback structure is required to ensure that the operations followed by each AVR are correct. With the current circulating process's implementation, the reactive power is shared between the AVRs.

(Sangeerthana, Priyadharsini, 2020) investigated the utilization of mechanical OLTCs and discussed the drawbacks of employing these tap changers. Mechanical OLTCs were replaced with modern power electronics-based and solid-state OLTCs to cope with the modernization of power grids. These modern OLTCs allowed for faster operating times as well as the reduction of sags and flickering. Shown in **Table 5** is the comparison they made between conventional mechanical and modern power electronics based and solid state OLTCs.

**Table 5: comparison between modern OLTCs and mechanical OLTCs (Sangeerthana, Priyadharsini, 2020)**

Modern OLTC	Mechanical OLTC
Reduced arcing	Arc present during tap switching
Power electronic-based tap switching	Mechanical tap switching
Low maintenance cost	High maintenance cost
Improved response and enhanced stability	Low stability
Quick tap change operation	Slow operation time

By incorporating FACTS devices for voltage regulation, network voltage stability is increased, and the controllability of OLTCs is greatly enhanced. Shown in Figure 22 is the tap changer system they proposed.

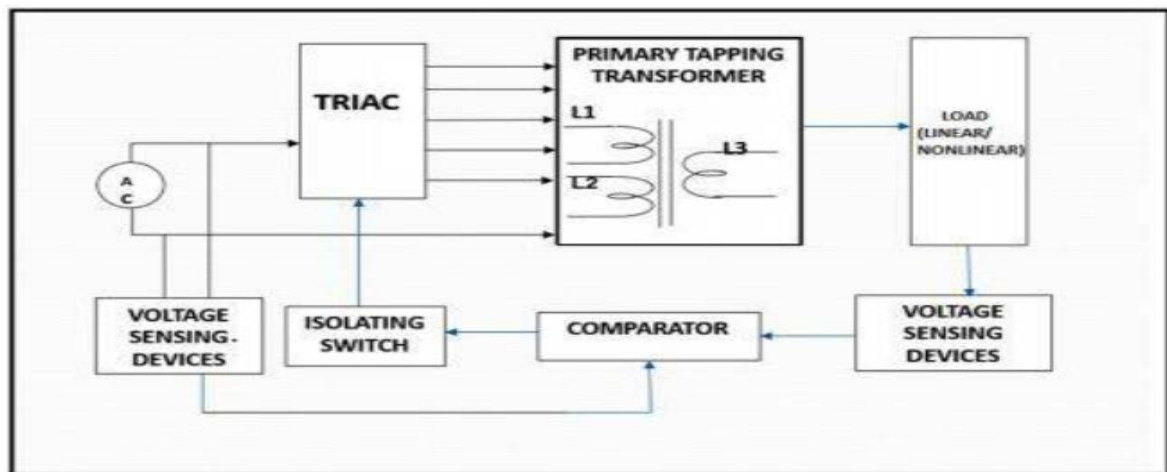


**Figure 22: The proposed tap changer system (Sangeerthana, Priyadharsini, 2020)**

(Han, Yin, Wu, Sun, Wei, 2022) researched to establish the relationship between heavy loads in a network and network voltage stability. They found that under heavy loading conditions in distribution networks, negative voltage regulation is caused by OLTC tap adjustments. The negative voltage regulation might even lead to network voltage instabilities and voltage collapse in the worst-case scenario. To address this concern, they proposed a Flexible On-Load Voltage Regulation. A step-less power electronics-based system is proposed for voltage and reactive power regulation. Shown in Table 6 A comparison is drawn between the proposed strategy and existing strategies.

**Table 6: Comparison between the proposed strategy and existing strategies (Han, Yin, Wu, Sun, Wei, 2022)**

<b>Topology</b>	<b>Voltage Regulation</b>	<b>Cost</b>	<b>Control Strategy</b>
<b>OLTC Transformer</b>	Step	Low	Simple
<b>Solid State Transformer</b>	Step-less	Highest	Complex
<b>Hybrid Transformer</b>	Step-less	Higher	Complex
<b>Flexible OLVR</b>	Step-less	Medium	Medium
<b>Topology</b>	<b>Response Time</b>	<b>Loss</b>	<b>Reactive Compensation</b>
<b>OLTC Transformer</b>	Slow	Low	Incapacity
<b>Solid State Transformer</b>	Fast	Highest	Full Capacity
<b>Hybrid Transformer</b>	Medium	Higher	Part of Capacity
<b>Flexible OLVR</b>	Medium	Medium	Part of Capacity

By constructing equivalent circuits of their proposed solution of a step-less power electronics-based electrophilic-based system controlling a flexible on-load voltage regulation transformer, they could mitigate the negative voltage regulation caused by OLTC tap adjustments. The overall network voltage stability is considerably stabilized, and the risk of voltage collapse is reduced. Shown in [Figure 23](#) is the proposed structure of the Flexible On-Load Voltage Regulation transformer.

(Alkاهدely, Alsammak, 2023) did research to investigate the impact of regular and reverse action operation of OLTCs on voltage stability on power transformers. With the increased load demand on power system networks, temporary voltage sags in some grid regions became a norm. OLTCs were employed to regulate the voltage across the grid better to address this reduced voltage concern. They found that the incorrect placement of OLTCs can contribute to network voltage instabilities. They called this the reverse action phenomenon. They examined in a MATLAB simulated study the improvement of OLTCs to enhance voltage stability and reduce the risk of network voltage collapse. Shown in [Figure 24](#) is the proposed network modeled in MATLAB.

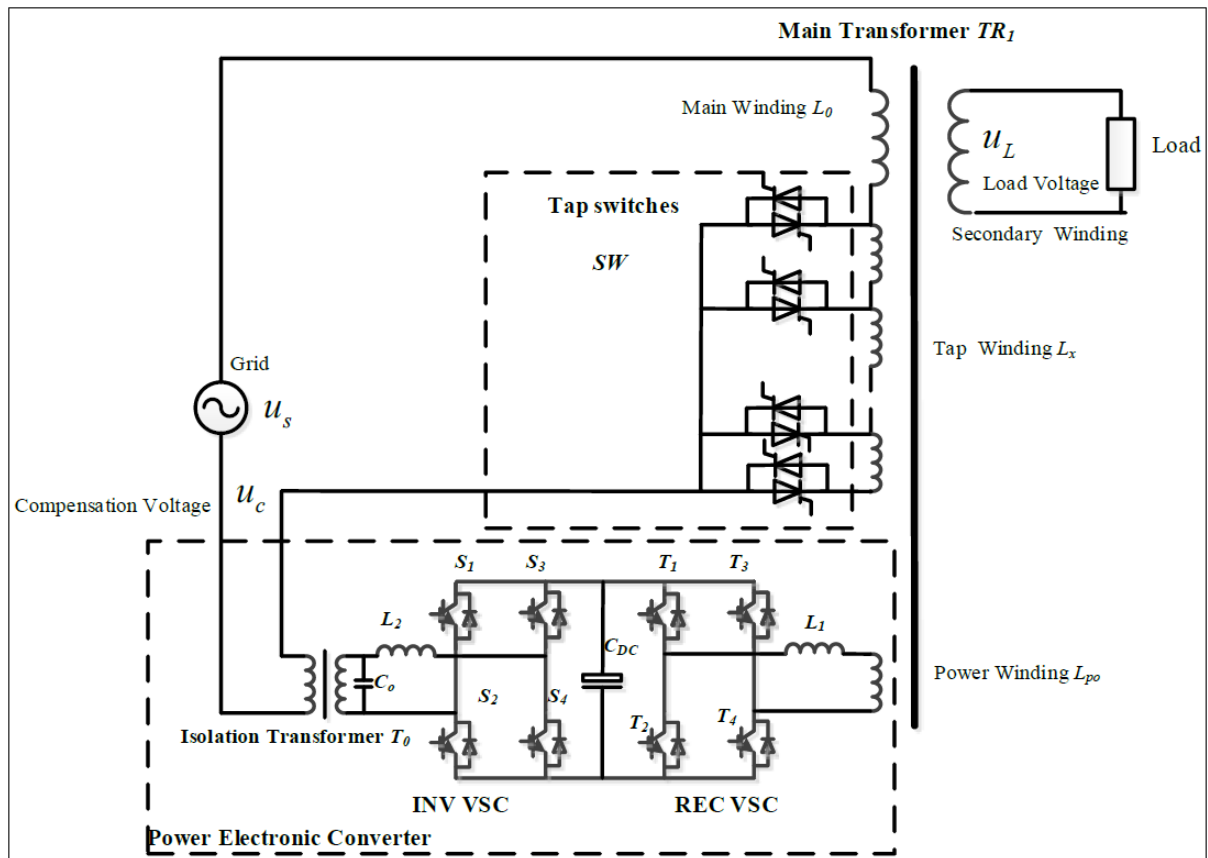


**Figure 23: The proposed structure of the Flexible On-Load Voltage Regulation transformer (Han, Yin, Wu, Sun, Wei, 2022)**

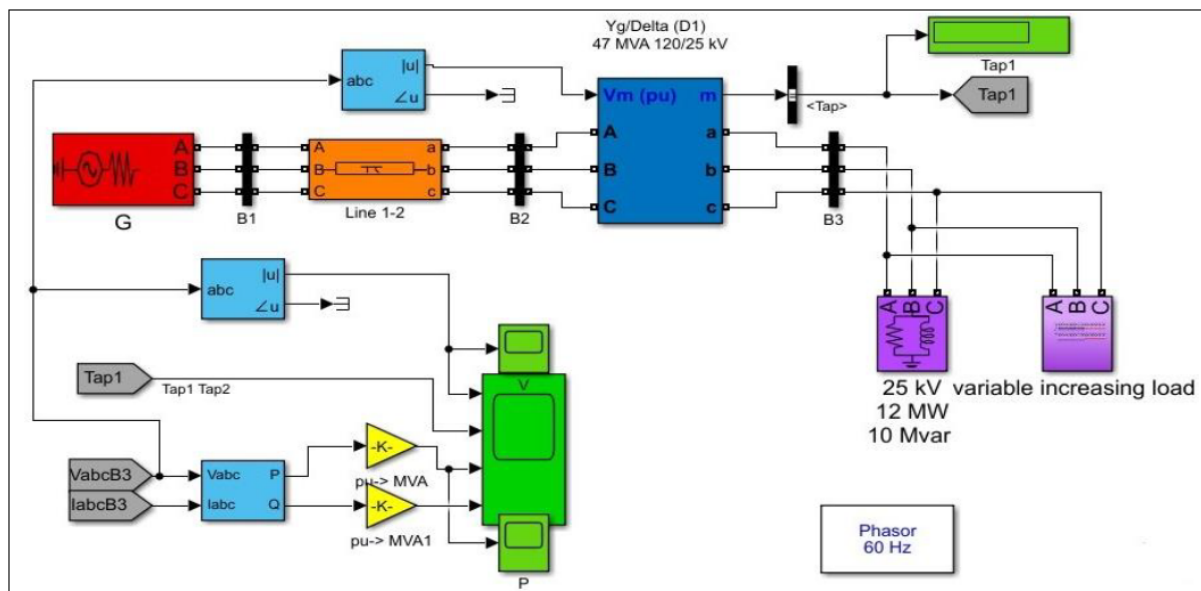


**Figure 24: The proposed network modelled in MATLAB (Alkاهدely, Alsammak, 2023)**

The research found that some OLTC parameters should be aligned to the type of load connected to the network. Aligning the OLTC parameters to the load type provides better network voltage regulation from the power transformer OLTCs.

(Devi, Kumar, 2023) did a study into preventing voltage collapse during OLTC switching for certain network conditions. They found that in conditions of network contingencies, OLTC operations can increase the risk of voltage collapse in a transmission line. From the investigation, they proposed an index that the critical OLTC responsible for the voltage collapse under contingencies needs to be identified. They also discussed the stabilizing effects of incorporating FACTS devices with Static VAR Compensators (SVC) placed at critical points in the network. With the incorporation of the devices, the OLTC reversal action effect is significantly reduced under network contingencies. Shown in [Figure 25](#) is the equivalent EHV System.

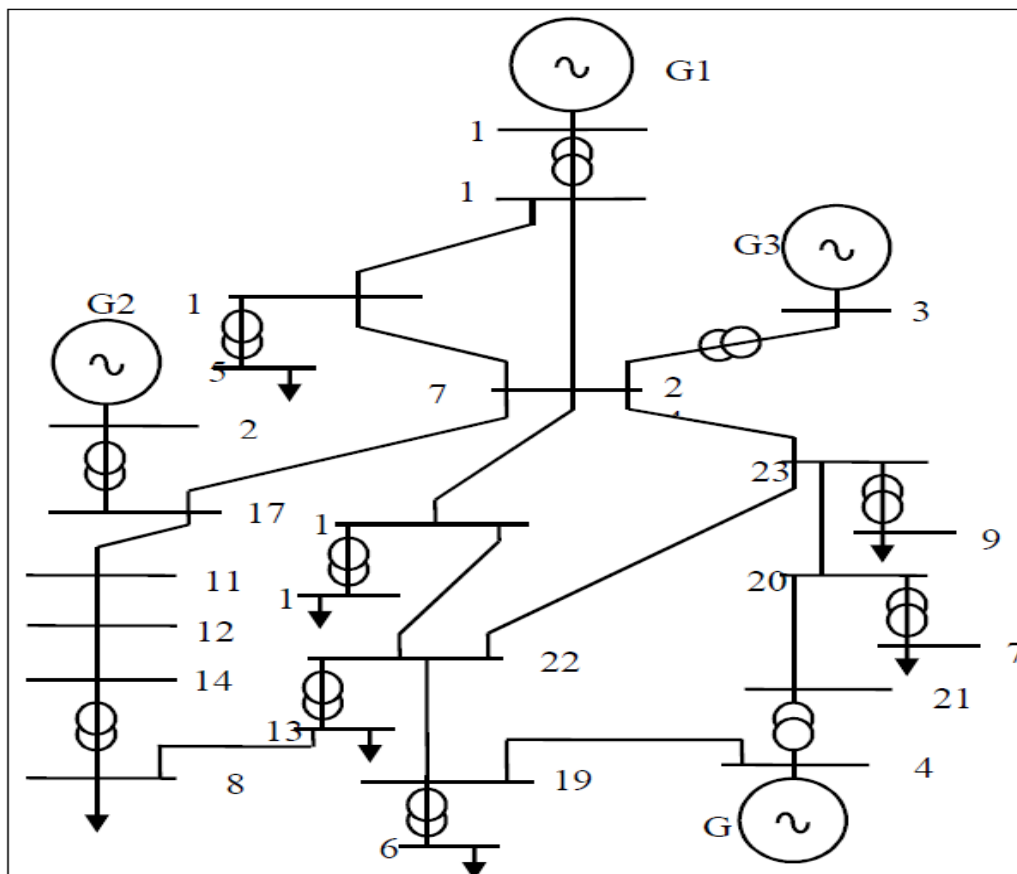


**Figure 25: Equivalent EHV System used in the study (Devi, Kumar, 2023)**



### **2.2.3 Discussion of literature survey on Voltage regulation of transformers**

The power system industry is concerned with maintaining a stable and reliable voltage profile throughout the network. The tap changers on the power transformers in a specific network primarily control voltage levels along the power system network. Tap changers on power transformers work by changing the transformer's windings ratio to either increase or reduce the voltage on the secondary side of the power transformer. Tap changers are typically found on the power transformer's primary windings. Traditional mechanical tap changers are still frequently used in power grids; however, they still need to improve in switching performance compared to newer tap changers.

According to the research, mechanical tap changers have slow switching speeds and more significant arcs while switching. Power electronics-based tap changers provide higher switching speeds and lower arcs during switching. Many countries' power-producing facilities incorporate renewable energy into their energy generation mix. Introducing renewable energy at distribution levels into the electrical grid causes the voltage profile and reactive power flow in the system to become unstable. These fluctuations must be adjusted by continuously monitoring grid conditions and commanding tap changers to operate if grid conditions exceed acceptable parameters. The use of IEDs to monitor grid conditions and manage the functioning of the power transformer's tap changer is proposed for the modernization of the power system network. IEDs are configurable for various operating situations and can be programmed with bespoke user-created algorithms to regulate tap change operations and conduct protective tasks.

Most current IEDs use the IEC 61850 standard for communication. Being IEC61850 compliant provides many advantages for developing dependable and modernized communication structures and grid automation opportunities. One of the numerous advantages of the IEC61850 standard was eliminating the necessity for physical connections between network components. Physical hard-wired copper connections between components can now be replaced with digital connections.

## 2.2.4 Review summary on Voltage regulation on transformers

**Table 7** comprehensively summarizes voltage regulation on power transformers. Potential review papers are chosen from the literature to provide the comparison study based on their research work goal, techniques, simulation and hardware tools, and project benefits, as stated in **Table 7** below.

**Table 7: Review summary on Voltage regulation of transformers**

<b>Paper</b>	<b>Aim</b>	<b>Method used</b>	<b>Simulation/ implementation Hardware/software</b>	<b>Benefits</b>
Bugade, Mishra, Jayebhaye, Joshi, Patil, Kale, 2018	Controlling the voltage profile at the load through an automatic on-load tap changer.	An automatic on-load tap changer is used with a TRIAC PE switch.	An ATMEGA-328P microcontroller is used. An Opto-coupler MOC 3021 was utilised. A TRIAC (BT136, 4A, 500V) is used for voltage detection. The simulation platform is not mentioned.	The system's benefits include maintaining a constant voltage profile, fast operation time, reduced maintenance cost, and a reduced size of the control circuit.
Constantin ,Iliescu, 2012	Demonstrating the features of an automatic voltage regulation controller	Controlling the voltage profile 400/220 kV and 400 MVA power	A 400/220 kV and 400 MVA power transformer. The automatic voltage	High quality, increased stability and compelling voltage profile—short operation time.

	on the secondary side of a transformer.	transformer. A protection system is also embedded in the design.	control function uses the step-by-step principle for its operation. Details of the IEDs used and simulation platform are not given.	
Zhou, Yan, Liu, 2018	Reviewing voltage control function using on-load voltage transformer.	The different types of OLTC technology are investigated and compared.	Theoretical assumptions are made based on the research papers available. The different types of OLTC technology are investigated and compared. No simulations were performed in this review.	Using power electronic technology for OLTC reduces the cost of the system. Using power electronic technology for OLTC achieves good arching results during tap switching.
Xie, Shentu, Wu, Ding, Hua, Cui, 2019	Using Voltage Ranking Search Algorithm to control	Using the intelligent search algorithm called voltage ranking	A simulation was performed in the IEEE 33-node distribution	The number of tap change operations by the OLTC can be significantly reduced.

	the OLTC operation.	search algorithm (VRSA) to solve the optimization of flexible resource scheduling for voltage regulation.	system, implementing the Voltage Ranking Search Algorithm to control the OLTC operation. Details of the IEDs used and simulation platform are not given.	
Monroy, Gomez-Exposito, Romero-Ramos, 2007	The application of Solid-State Tap Changers to improve voltage regulation of MV/LV transformers.	A solid-state under-load tap changer device replaced the off-load mechanical tap changer.	Two electronic tap changers' operations were analysed. They had 4 steps and 9 steps, respectively. The details of the IEDs used and the simulation platform are not mentioned.	Customers experienced an improvement in voltage profile in both standard and emergency operating situations.
Carlen, Jakobs, Slupinski, Cornelius, Schneider, Buschmann, Tepper,	Controlling the voltage profile MV grids with the introduction of a Line	An 8 MVA Line Voltage Regulator was installed into a 20 kV grid to counter	An 8 MVA Line Voltage Regulator was installed into a 20 kV grid. The line length is 26 km.	Investing in a Line Voltage Regulator (LVR) is more cost-effective than grid reinforcement.

Wiesler, 2015	Voltage Regulator.	the rising voltage levels caused by introducing renewable sources at various points along the grid.	The connected load consumes 3 MVA, and the feeder capacity is close to 5 MVA. The details of the IEDs used and the simulation platform are not given.	
Ferrero, Cimadevilla, Yarza, Solaun, 2014	Controlling the automatic voltage regulator of a system with up to 5 parallel transformers.	This is based on the current circulating method. In this study, IEC 61850 GOOSE was used as a communication medium.	The detail of power transformers is as follows: 45MVA, 138±13x5%/36 kV, YNd11. Simulations were conducted on the RTDS Platforms. Detail of the IEDs is not given.	The IEC 61850 GOOSE message application provides a high level of reliability to the overall system. This study utilizes the circulating current method to balance the reactive power.
Sangeerthana, Priyadharsini, 2020	Adding FACTS devices to power system networks enhances the control of transformer OLTCs.	FACTS devices are added to power system networks for voltage regulation, network voltage stability is increased,	The proposed network with FACTS devices is simulated in the MATLAB software. Adjusting the transformer winding	By incorporating FACTS devices for voltage regulation, network voltage stability is increased, and the controllability of OLTCs is greatly enhanced. Flickering and sags are significantly reduced.

		and the controllability of OLTCs is greatly enhanced.	ratios achieves voltage regulation.	
Han, Yin, Wu, Sun, Wei, 2022	Research is conducted to establish the relationship between heavy loads in a network and network voltage stability.	They implemented a Flexible On-Load Voltage Regulation transformer. For voltage and reactive power regulation, a step-less power electronics-based system is modelled.	The Flexible On-Load Voltage Regulation transformer is modelled in the Psim software. It has an HV rating of 10 kV and an LV rating of 0.4 kV, 8 steps with 5% voltage increments.	Implementing a step-less power electronics-based system controlling a Flexible On-Load Voltage Regulation transformer could mitigate the negative voltage regulation caused by OLTC tap adjustments. This would greatly stabilize the overall network voltage stability and reduce the risk of voltage collapse. Better voltage accuracy would be achieved at a reduced cost.
Alkاهدely, Alsammak, 2023	Assessing the impact caused on voltage stability by regular and reverse action operation of OLTCs on power	In a MATLAB-simulated study, they examined improving OLTCs to enhance voltage stability and reduce the risk of	A radial power distribution system is constructed in a MATLAB-simulated study. OLTC improvement is	Aligning the OLTC parameters to the load type provides better network voltage regulation from the power transformer OLTCs.

	transformers.	network voltage collapse.	investigated to enhance voltage stability and reduce the risk of network voltage collapse.	
Devi, Kumar, 2023	A study was conducted on preventing voltage collapse during OLTC switching for certain network conditions.	They proposed an index for identifying the critical OLTC responsible for the voltage collapse under contingencies. They also discussed the stabilizing effects of incorporating FACTS devices with SVC at critical network points.	The Equivalent EHV that forms part of the Indian power system network was modeled. The details of the applicable software should be mentioned.	Incorporating FACTS devices with SVC at critical points in the network dramatically reduces the OLTC reversal action effect under network contingencies.

## 2.3. Literature Review on transformer Tap changer controller algorithms

### 2.3.1 Introduction

More clarity is needed around the exclusive definition of the word algorithm. In engineering, an algorithm can be defined as a step of logical or mathematical procedures or a sequence followed to solve a problem. Microprocessor-based IEDs are broadly utilized to execute power system protection and control functions. (Ibrahim, 2012) Mathematical algorithms are used by IEDs to monitor the power system conditions and to issue protection and control functions if faulty conditions are detected. (Malkowski, Izdebski, Miller, 2020) As the power generation supplied to the grid becomes increasingly decentralized, the demand for voltage monitoring and correction procedures increases. Voltage profiles become increasingly volatile due to changes in load profiles and network load profiles. To address the increased volatility of voltage profiles, many utilities need to alter the existing transformer voltage control algorithms of the IEDs to compensate for the changed conditions.

The documents reviewed per year under the subsection Tap Changer Controller Algorithms are shown in [Figure 26](#).

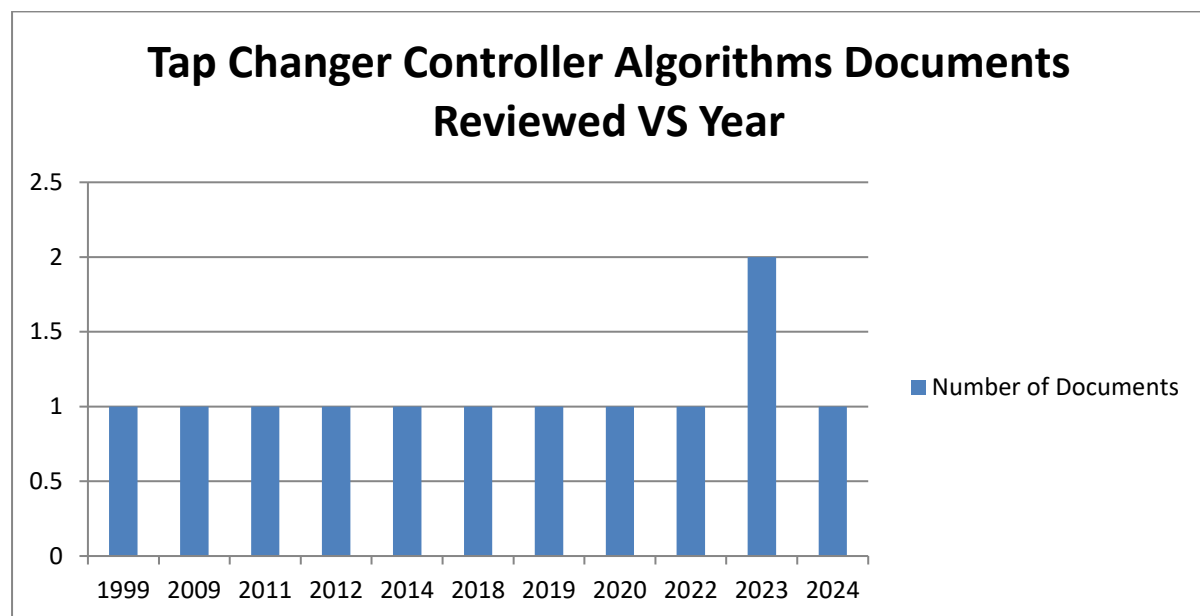


**Figure 26: Tap Changer Controller Algorithms reviewed per year**



### 2.3.2 Literature survey on Tap changer controller algorithms

In a conference paper titled “Voltage Regulation of LV Feeders with High Penetration of PV Distributed Generation Using Electronic Tap Changing Transformers,” authored by (Kabiri et al., 2014) said that utilities are struggling to maintain voltage profiles along low voltage feeders within acceptable magnitudes as the rising levels of penetration of distributed Photovoltaic generation into Low Voltage feeders. They said conventional voltage regulation along a low-voltage feeder was primarily achieved according to its design. The magnitude of PV penetration levels on low voltage feeders, power consumption, and demand from consumers and households varies throughout the days. See Figure 27 for the different levels of PV penetration during the day. These changing patterns can cause overvoltage conditions during the day when PV penetration levels are high and demand is low; the opposite happens at night.

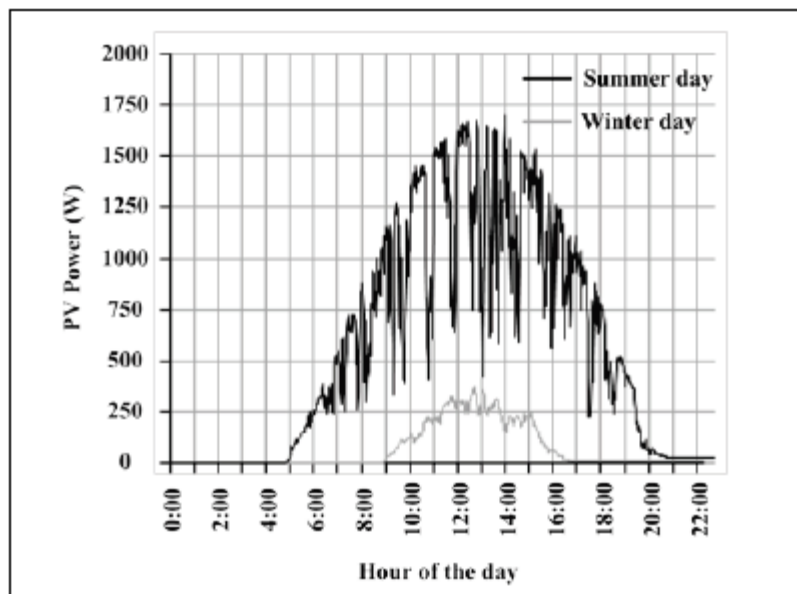


**Figure 27: Daily generation variation of a PV DG system with cloud cover changes (Kabiri et al., 2014)**

They proposed an alternative approach for voltage regulation; they said it's not the slope of the feeder voltage profile that is so important but rather the absolute magnitude position. They developed an algorithm that controls an electronic tap changer that varies the tap position on a cycle-by-cycle basis on the low-voltage feeder transformer. The algorithm they developed made the following decisions in determining the appropriate tap position as in Figure 28.

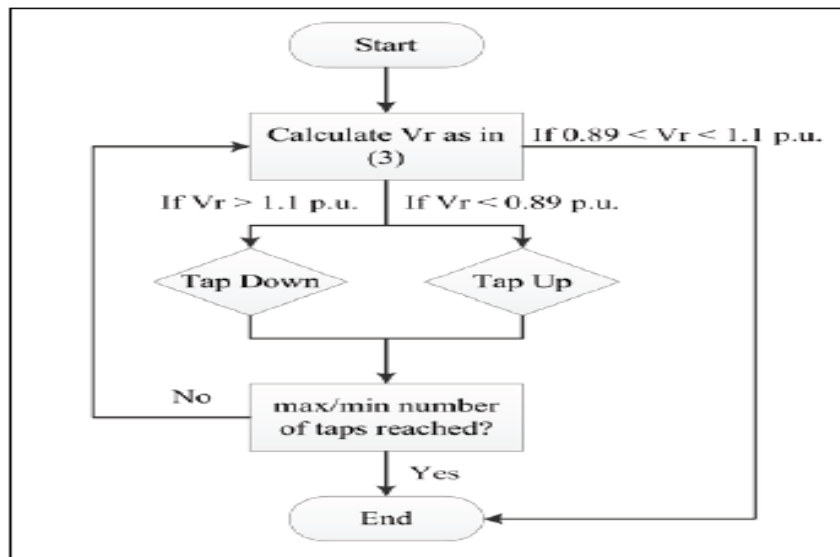


**Figure 28: Tap changer control algorithm (Kabiri et al., 2014)**

By doing this, they could continuously compensate for voltage profile magnitude fluctuations as the level of penetration from the PV system fluctuates. They investigated the algorithm's effectiveness for the rapid tap-changing configuration across various operating regions. Their developed system effectively maintained stable voltage profiles under different level of PV penetration fluctuations and varying grid impedance conditions. See Figure 29 for comparison of results with and without rapid tap-changing implementation.

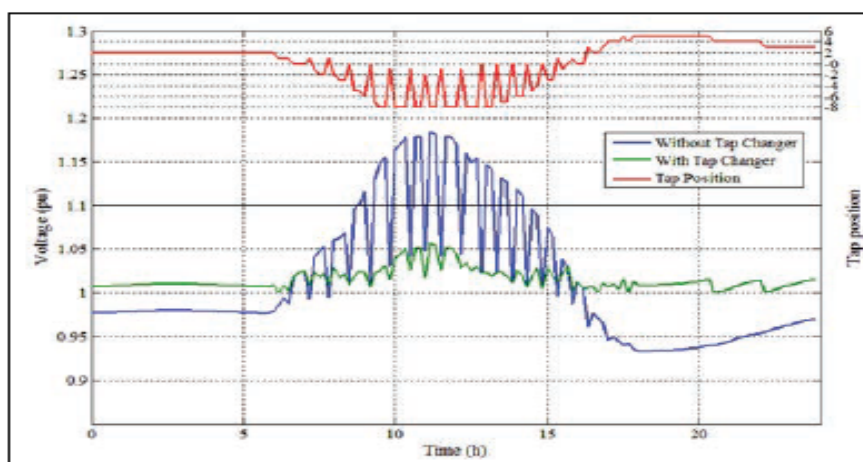


**Figure 29: Voltage profile of feeder end bus with and without tap changing for advanced tap controller (Kabiri et al., 2014)**

According to the authors (Okanik, Kurth, Harlow, 1999) of a conference paper, how the control of the on-load tap changers of power transformers in parallel has not changed significantly over the years. The minimum current circulating and master

follower methods for power transformer on-load tap changers are still widely used and have proven reliable and effective. See [Figure 30](#) for an illustration, when two parallel transformers on unequal tap positions would cause a circulating current to flow.

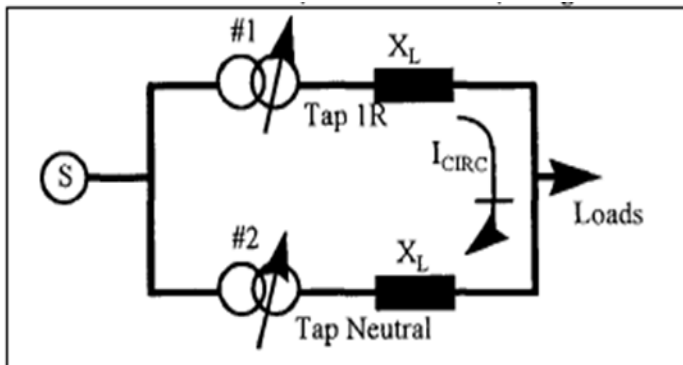


**Figure 30: Parallel transformers on unequal tap positions (Okanik, Kurth, Harlow, 1999)**

These methods are, however, still utilized in the traditional approach. These conventional approaches involve using discrete analog circuitry to employ current transformers to isolate particular aspects of the load circuit. With the global power industry moving toward digitizing equipment, digital electronics pave the way for modernizing the technology of paralleling transformers. By employing serial communication between the respective on-load tap changer controls, the copper, and the analog circuitry of paralleling balancers can effectively be eliminated. See [Figure 31](#) for the new LTC control diagram to simplify the transformer paralleling operation.

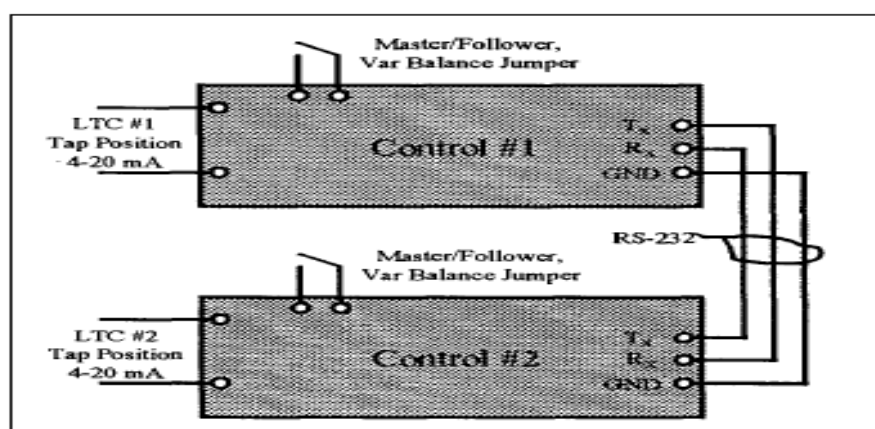


**Figure 31: New LTC control diagram, including paralleling control (Okanik, Kurth, Harlow, 1999)**

According to research conducted by the authors (Madzonga, et al., 2009), they analyzed the voltage regulation of the bus when the master-follower or master-slave tap change control method is utilized when two mismatched transformers are used that is operating in parallel. According to them, an automatic voltage regulating (AVR) relay is responsible for the operation of an on-load tap changer that regulates the bus voltage in a distribution substation. They said that when using a standard set-point of 103% and a master-follower/slave method, the customer supplied at the end of the feeder experienced low voltage conditions. The simulations conducted made use of a circuit with the following parameters. See Figure 32 for circuit construction with mismatched transformers and various types of loads it supplies.

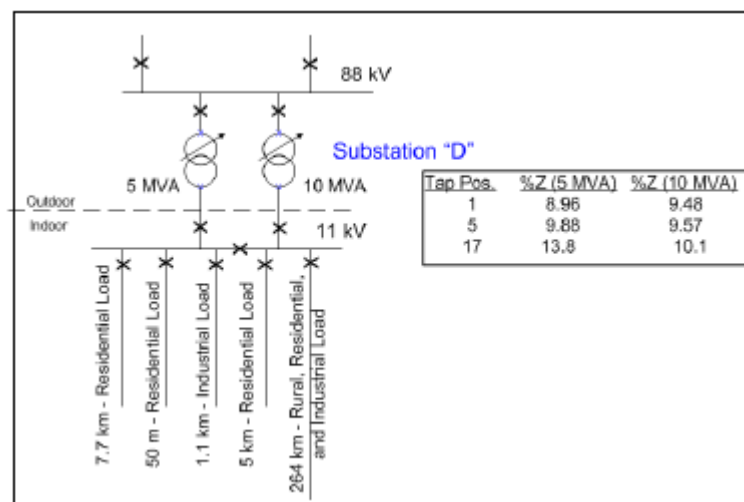


**Figure 32: Distribution substation with mismatched paralleled transformers (Madzonga, et al., 2009)**

For simulation purposes, they used the traditional Master-Follower and Master-Slave on-load tap changer control methods. They of the microprocessor-based REG-D AVR relay to record the event of the operation during the day to determine the average fluctuation of the voltage profile experienced by downstream consumers. The AVR relay recorded the following event when it was set to auto mode. See Figure 33 for the results obtained.

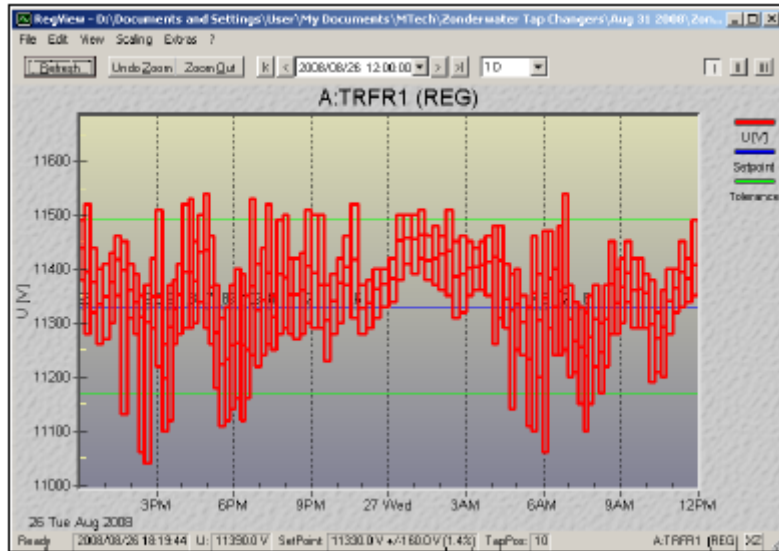


**Figure 33: AVR relay event recording on Auto (Madzonga, et al., 2009)**

As can be seen in Figure 33 when the relay was operating in auto mode, the average voltage was maintained in the expected dead band. The following results were obtained with the AVR relay operating in manual mode, meaning that the tap position was fixed. The Figure 34 shows that the average secondary voltage outside the deadband.

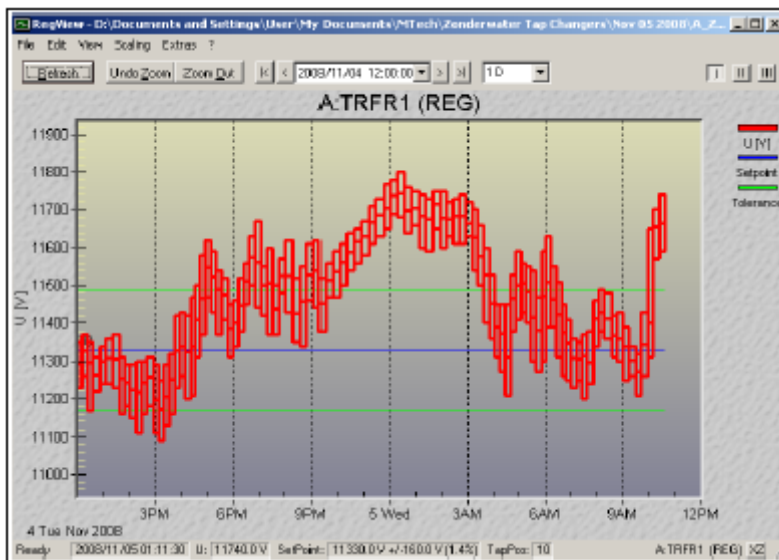


**Figure 34: AVR relay event recording on Manual (Madzonga, et al., 2009)**

The authors simulated the network with various parameters. They concluded from the results obtained that more aggressive AVR relay settings closer to the source were able to improve the resulting voltage profile. They found that utilizing an

increased set-point for voltage values together with increased bandwidth, the results obtained maintained the voltage profiles downstream more effectively.

The authors (Yongxing, Peng, Enyuan, Zhongwei, Jiyan, and Xuanshu, 2011) wrote a conference paper about creating an intelligent controller for an OLTC for a power transformer to maintain voltage levels within acceptable margins. They said that changing the tap position of the winding on the primary side of the transformer enables the desired voltage levels to be maintained under various loading or operating conditions. Due to the complexities and maintenance requirements of the traditional on-load tap changer, they opted to utilize a vacuum on-load tap changer for this project. The vacuum on-load tap changer they used is driven by a permanent magnetic actuator, increasing this on-load tap changer's capacity and switching reliability. They applied a programmable logic controller (PLC) to the intelligent controller of the on-load tap changer. They used the programmable logic controller to make the on-load tap changer control system less complicated thus improving the reliability and efficiency of the vacuum on-load tap changer. They applied a Siemens S7 series of CPU226 and its matching text display TD400 to the control system of the on-load tap changer. The structure of the on-load tap changer with the applied Siemens S7 can be seen in [Figure 35](#).

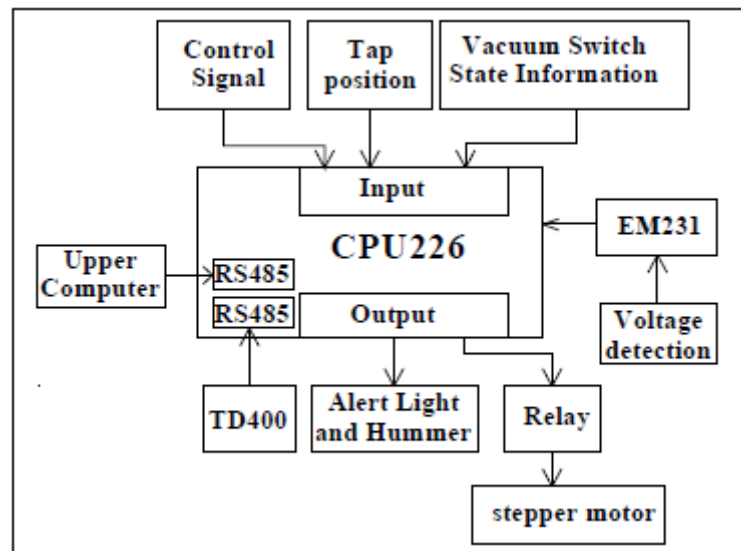


**Figure 35: The structure of OLTC controller based on PLC (Yongxing, Peng, Enyuan, Zhongwei, Jiyan, and Xuanshu, 2011)**

The programmable logic controller will compare variable inputs obtained and compare them with the predetermined voltage reference set-point to instruct the on-

load tap changer to either make tap adjustments or not. The algorithm used to determine the on-load tap changer course of action can be seen in Figure 36. The research conducted by the authors determined that the vacuum on-load tap changer has many advantages over the traditional oil on-load tap changer. These advantages include reduced maintenance, increased switching frequency, high breaking capacity, etc. The incorporation of the programmable logic controller decreases the complexity of the on-load tap changer control system. The reliability and stability of the vacuum on-load tap changer have significantly been improved.

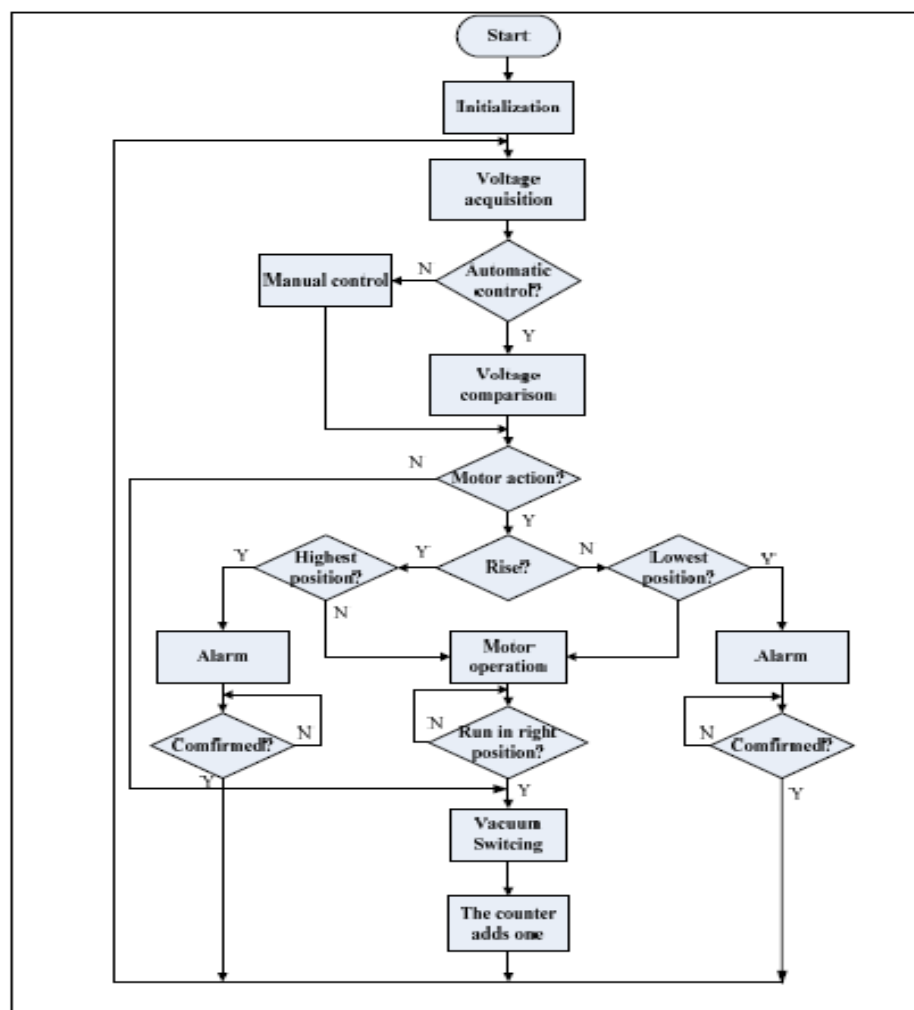


**Figure 36: The flow chart/algorithm for the control system (Yongxing, Peng, Enyuan, Zhongwei, Jiyang, and Xuanshu, 2011)**

In a research paper by (Hasan et al., 2018) they said that maintaining acceptable voltage profiles at load terminals is a serious challenge in electric distribution networks. In electric distribution networks, the most widely used mechanism for



voltage regulation is the on-load tap changer. These traditional on-load tap changers, however, have many drawbacks and limitations. Electronic on-load tap changer (EOLTC) was developed to overcome the limitations and disadvantages that traditional mechanical on-load tap changers have. In Figure 37 it shows the test power system diagram with EOLTC. Figure 38 shows on the left when grid and load voltages is decreased and EOLTC is not used. The right side shows with EOLTC implemented.

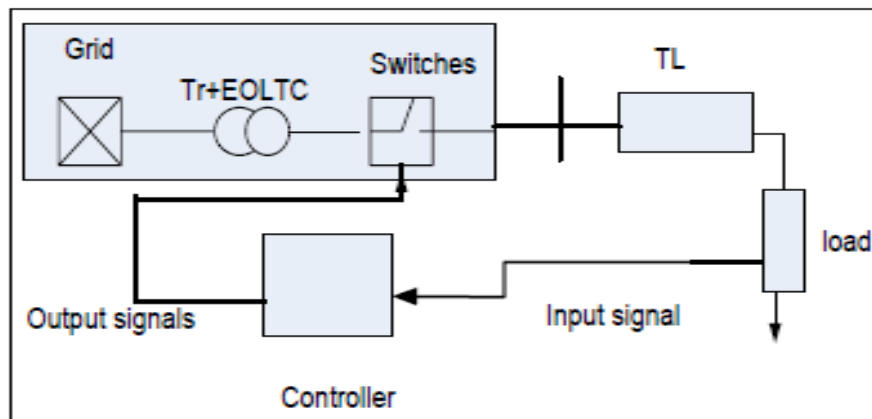


**Figure 37: The test power system diagram with EOLTC (Hasan et al., 2018)**

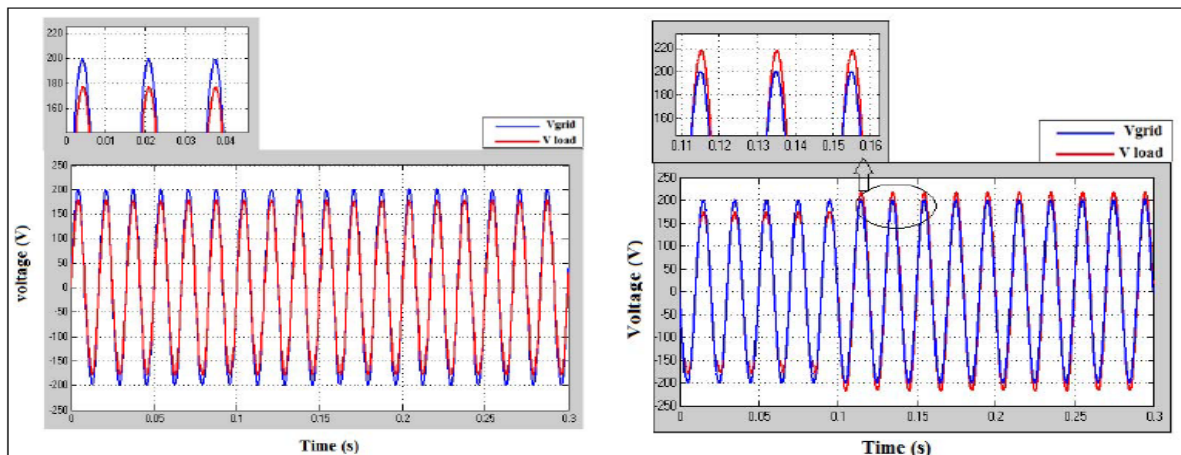


**Figure 38: Left shows without EOLTC & right shows with EOLTC (Hasan et al., 2018)**

As can be seen in Figure 38 they simulated how the load voltage is maintained when the grid voltage experiences a sudden reduction and found that the EOLTC effectively maintains a constant load voltage when the grid voltage experiences a sudden fluctuation.



The authors (Xu et al., 2019) did research to address the problem of optimal tap setting selection to maintain permissible voltage regulation in radial power distribution systems when the load profile is not constant. They developed a system that selects tap position by only considering voltage magnitude measurements and topology to keep the voltage fluctuation across the grid to a minimum. They used a linearized power flow model to develop an effective algorithm to determine the voltage regulation when different tap selections are in operation. Figure 39 shows their framework for optimal tap selection. To estimate the magnitude of the voltage if different tap settings were selected, they developed a virtual transition generator.

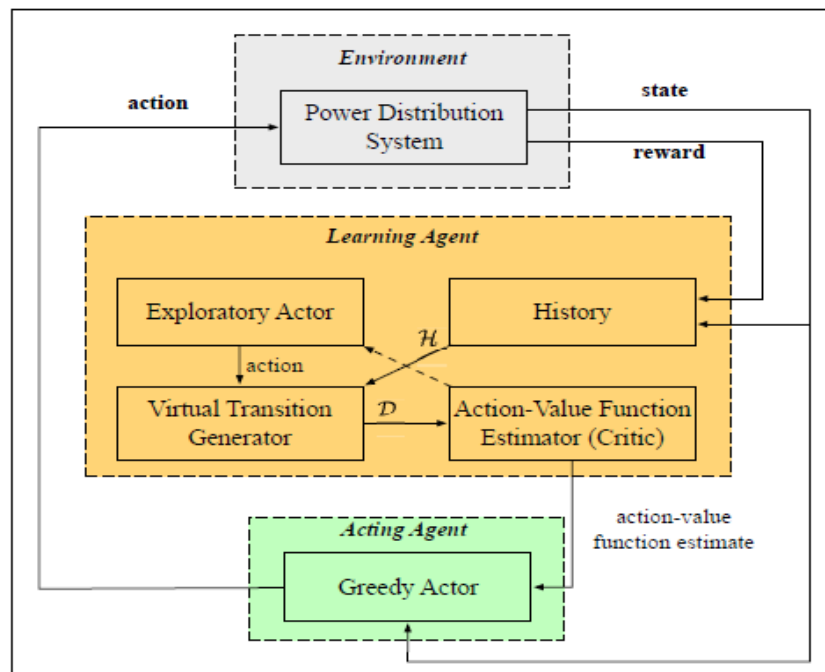


**Figure 39: Optimal tap selection framework (Xu et al., 2019)**

(Tasnim, Sarimuthu, Lan, Tan, 2022) Solar power generation is integrated into the power system network to supply the increased demand for energy. During high energy consumption and peak sun hours, grid voltages become increasingly unstable. Under these conditions, voltage fluctuations tend to creep out of the maximum allowed tolerable levels. Traditionally, power transformers equipped with OLTCs are responsible for keeping the network voltage profile in check by adjusting the transformer's winding ratio.

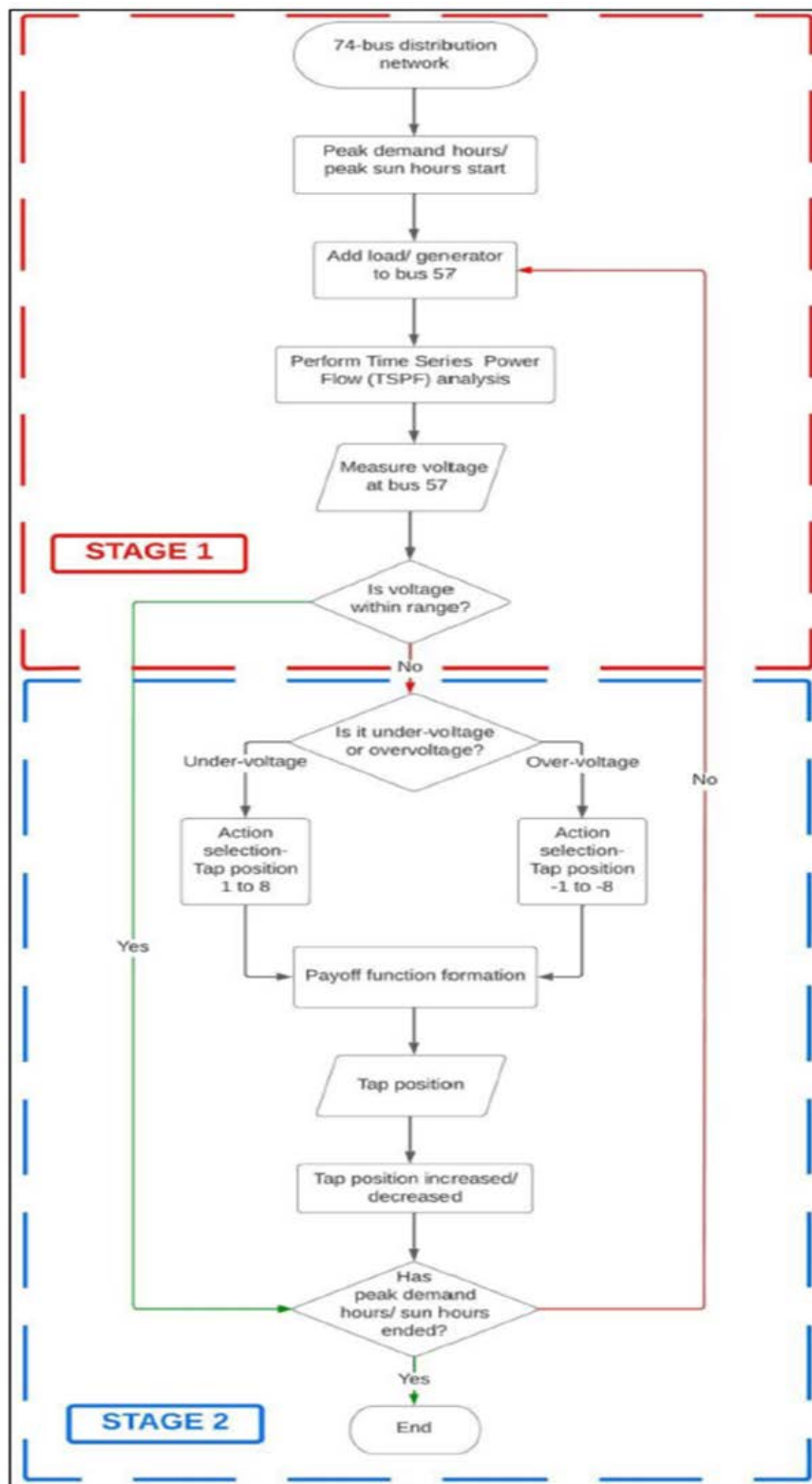


Figure 40: Algorithm to control the OLTC derived from the internal game theory (Tasnim, Sarimuthu, Lan, Tan, 2022)

They found that OLTC response time was too slow to mitigate the rapid voltage fluctuations. The internal game theory forms the basis for creating an algorithm to control the OLTC of the power transformer. The control algorithm is modeled in MATLAB software to verify its ability to enhance network voltage during periods of poor voltage quality conditions. From the test conducted, they concluded that the game theory-based algorithm managed to reduce voltage instability from 69.4% to 61.6% during high energy consumption coupled with peak sun hours. OLTC response increased by 50% during high energy consumption and 62.2% during peak sun hours. Shown in [Figure 40](#) is the Algorithm to control the OLTC derived from the internal game theory.

(Otchere, Ampofo, Dantuo, Frimpong, 2023) mentioned that the ever-increasing amount of distributed generation (DG) connected to the power system network causes the network voltage to rise above acceptable levels. The operational performance of devices traditionally used to control network voltages, such as capacitor banks and power transformers with OLTCs, is negatively influenced by these high levels of DG penetration. A genetic algorithm was proposed to perform an impact assessment of the capacitor banks and OLTCs. Shown in [Figure 41](#) is the genetic algorithm used for this study.

The study results concluded that the location of the capacitor banks is not influenced by DG penetration. An improvement in the voltage profile of the power system is observed when the DG introduced has a reactive power capability. Losses are at their minimum when DG is connected at the load center. DG also has minimal influence on OLTCs at the substation level. DG influence increases on OLTCs located in distribution feeders. From the results, it pointed out that when DG is situated at remote and isolated entry points, it tends to influence the voltage profile and losses adversely.

(Dung, 2023) investigated the OLTCs of power transformers to enhance the voltage profile in power system networks. An algorithm structure was created to control OLTC tap positions from a local or remote mode to improve the system voltage quality of the power transformers' primary and secondary sides. Theoretical modeling verified the formulas used for the OLTC control schemes. Results from the theoretical case study served as a benchmark for configuring the parameters used

for actual system implementation. Figure 42 shows the proposed algorithm to enhance system voltage profiles.

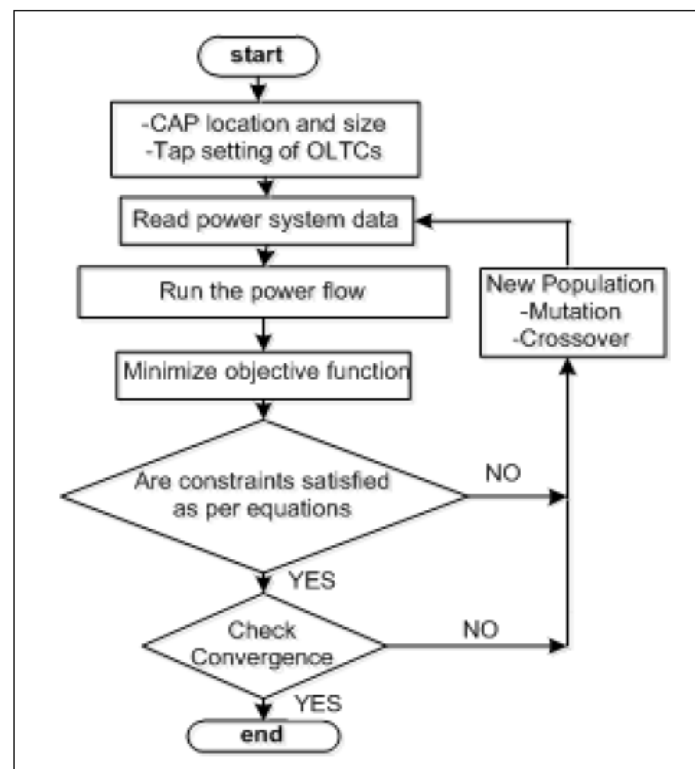


Figure 41: Flowchart of used genetic algorithm (Otchere, Ampofo, Dantuo, Frimpong, 2023)

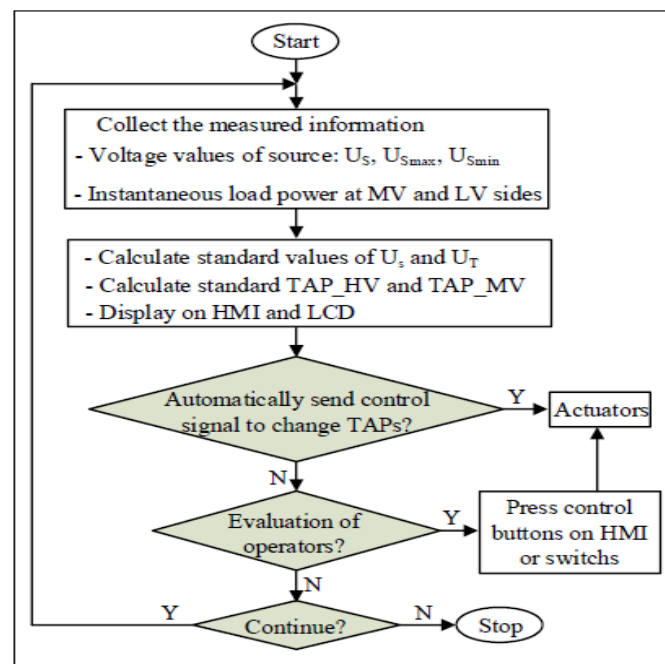
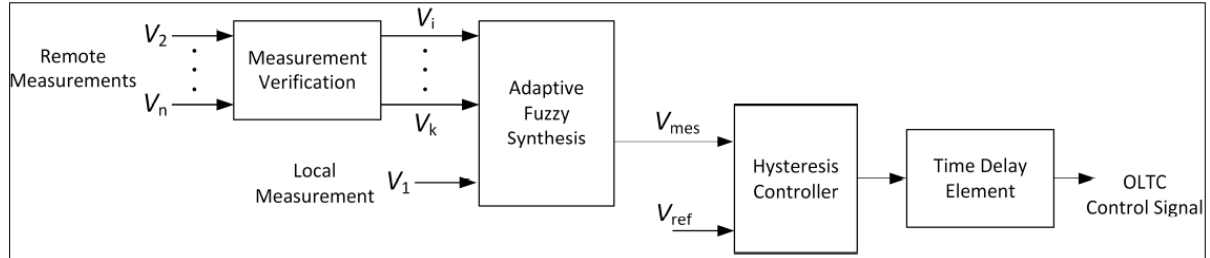


Figure 42: The proposed algorithm to enhance system voltage profiles (Dung, 2023)

(Wróblewski, Kowalik, Januszewski, Kurek, 2024) Proposed development of a Fuzzy Logic Controller control scheme for power transformer OLTC control to be introduced into networks with a high level of Distributed Generation (DG) penetration. Shown in Figure 43 is the algorithm proposed for OLTC control.



**Figure 43: The algorithm proposed for OLTC control (Wróblewski, Kowalik, Januszewski, Kurek, 2024)**

OLTCs are a highly preferred method of voltage control in MV distribution networks. They conducted software-in-the-loop experiments on a CIGRE Medium Voltage power system network. An OLTC control algorithm code was created in the Python 3.12 software, and tests were conducted in a closed-loop system. The results from the closed-loop testing revealed that with the implementation of the proposed algorithm, overvoltage conditions in the network were reduced from 1.072 to 1.0485 per-unit. They concluded that the proposed algorithm could enhance the network's overall power system voltage profile, and it could theoretically be implemented in field testing in real-world environments.

### 2.3.3 Discussion of literature survey on Tap changer controller algorithms

Maintaining stable and consistent voltage profiles over the whole power system network is critical to power quality and system reliability. Tap change controllers on power transformers are mainly responsible for sustaining voltage levels in a given network by adjusting the power transformer's winding ratios. Thanks to the development of Intelligent Electronic Devices, the tap change function can now be controlled by varying input from the power system network. The IED can measure voltage and current levels and provide control signals to the tap changer to rectify the conditions by changing the winding ratio of the power transformer to stabilize the power system based on the grid voltage and power flow profiles present in the power system. The IEDs used to regulate the on-load tap changer can be paired with

protective functions to separate the given power transformer from the grid in situations that present a danger of transformer damage or significantly impact the grid's integrity.

Traditional mechanical tap changers are still frequently used by power utilities; however, they have significant disadvantages in switching performance compared to newer tap changers available. According to the research, mechanical tap changers have slow switching speeds and bigger arcs while switching. Power electronics-based tap changers provide higher switching speeds and lower arcs during switching. Introducing highly configurable IEDs gives the protection and control engineer more options to make the protection and control function more efficient for the specific situation in which it will be used. These IEDs have undergone extensive research and development, and they are also programmable using bespoke user-created algorithms, allowing them to be tailored to specific settings.

Custom-created algorithms make IEDs' protection and control functions more efficient if properly built. Engineers can custom program IEDs with their algorithms and submit them to rigorous lab testing, which usually includes some Hardware-in-the-loop testing before field testing. While this testing is going on, the engineer can tweak and edit the algorithm until the results are good enough for field testing. Under various operating situations, remarkable system reactions to variable voltage profiles have been achieved using algorithms to control the power transformer's tap changer. As more decentralized producing units are added at scattered points throughout the grid, this has resulted in significant voltage profiles and power flow issues for associated customers. IEDs with specific algorithms have been used successfully in grids to combat this issue.

### 2.3.4 Review summary on transformer Tap changer controller algorithms

**Table 8** Provides a comprehensive summary of transformer Tap changer controller algorithms. Potential review papers are chosen from the literature to provide the comparison study based on their research work goal, techniques, simulation and hardware tools, and project benefits, as stated in **Table 8** below.

**Table 8: Review summary on transformer Tap changer controller algorithms**

<b>Paper</b>	<b>Aim</b>	<b>Method used</b>	<b>Simulation/ implementation Hardware/software</b>	<b>Benefits</b>
Kabiri, Holmes, McGrath, 2014	Using Electronic Tap Changing Transformers to maintain the voltage profile of LV feeders disturbed with the introduction of distributed generation.	The feeder voltage profiles are altered with varying PV power generated and introduced to the grid at distributed points. The algorithm programmed into the IED is able to alter the tap position of the Using Electronic Tap	The control algorithm was programmed to the IED in the DIgSILENT software. Simulations were conducted in the DIgSILENT software to analyse the algorithm's performance in maintaining a stable voltage profile under varying levels of PV	Good voltage profiles are maintained under varies operating scenarios.

		Changing Transformers to the most efficient positions within the shortest time to maintain the best possible voltage profile.	power injected into the grid.	
Okanik, Kurth, Harlow, 1999	Investigating the effect of the introduction of modern communication and control technology on the operation of the OLTC of power transformers in industry.	The research paper was compiled using a theoretical method. The Master/Follower and Circulating Current methods were investigated, and phasor relationships were visualised for the operation of transformers operating in parallel.	The research paper used a theoretical approach. Using theoretical data, phasor relationships were visualised for the operation of transformers operating in parallel. No simulations were performed.	With the introduction of modern communication and control technology, a control was developed that can perform all the basic operations of the traditional LTC. These control units are configurable and can be programmed with special control algorithms.



Xu, Dominguez-Garcia, Sauer, 2019	The aim of the paper is to address the problem of optimal tap setting selection and maintain permissible voltage regulation in radial power distribution networks when load profiles are not constant.	They developed a system that selects tap position by only considering voltage magnitude measurements and topology to keep the voltage fluctuation across the grid to a minimum. They used a linearized power flow model to develop an effective algorithm to determine the voltage regulation when different tap selections are in operation.	The researchers conducted theoretical simulations on the IEEE 13-bus and 123-bus distribution to determine the effectiveness of their proposed algorithm for voltage regulation. A virtual transition generator was developed to estimate the expected voltage profile under varying tap positions under fluctuating operating conditions.	The control algorithm they propose helps select the most appropriate tap position, keeping voltage fluctuations across the system to a minimum under various system operation conditions.
Hasan, Hatata, Badran, Yossef, 2018	Employing electronic OLTCs to address the issue of maintaining	The electronic OLTC was simulated in the MATLAB/Simulink	The electronic OLTC was simulated in the MATLAB/Simulink	When varying load conditions experience sudden fluctuations in

	acceptable voltage profiles at load terminals in electric distribution networks	software suite. Simulations were conducted to compare the results using and without the EOLTC. The simulation results verify that using the proposed EOLTC algorithm does, in fact, maintain a stable voltage profile and operating conditions in the electric distribution network.	software suite and tested to ensure effective operation under varying load conditions that experience sudden fluctuations in voltage profile.	voltage profile, the proposed algorithm is able to timeously and effectively control the electronic OLTC to maintain a stable voltage profile and operating conditions in the electric distribution network.
Yongxing, Peng, Enyuan, Zhongwei, Jiyan, Xuanshu, 2011	Creating an intelligent controller for an OLTC for a power transformer to maintain voltage level within acceptable margins.	The authors opted to use a vacuum on-load tap changer for this project. The vacuum on-load tap changer they used is	The authors applied a Siemens S7 series of CPU226 and its matching text display TD400 to the control system of the on-load	By utilising the proposed OLTC, they said it has an increased switching frequency, longer intervals between

		driven by a permanent magnetic actuator, increasing its capacity and switching reliability. They applied a programmable logic controller to the intelligent controller of the on-load tap changer.	tap changer.	maintenance is required, and an increased breaking capacity. The design of the OLTC is simplified with the addition of the intelligent controller and its operation is more reliable and stable.
Madzonga, Munda, Jimoh, 2009	Analysing the voltage regulation of the bus when the master-follower or master-slave tap change control method is utilised when two mismatched transformers operating in parallel are used.	For the simulation purposes, they used the traditional Master-Follower and Master-Slave on-load tap changer control methods. They also used the microprocessor-based REG-D AVR	They used the microprocessor-based REG-D AVR relay to control the OLTC. For simulation purposes, they used the traditional Master-Follower and Master-Slave on-load tap changer control methods. They used	The authors simulated the network with various parameters and concluded from the results obtained that more aggressive AVR relay settings closer to the source were able to improve the resulting voltage

		relay to record the operation during the day to determine the average fluctuation of the voltage profile experienced by downstream consumers.	RegView-D software to visualize graphs and data obtained from the AVR relay.	profile. They found that utilizing an increased set-point for voltage values together with increased bandwidth, the results obtained maintained the voltage profiles downstream more effectively.
Ibrahim, 2012	To determine the performance of measurement algorithms utilised by Intelligent Electronic Devices.	A system to monitor the performance of measurement algorithms utilised by Intelligent Electronic Devices in a steady state is designed. The algorithms' performance was evaluated by	SIMLAB software was used to perform the sensitivity study. The ATP/EMTP program was used for program interfacing, and MATLAB was used for script development. The tests were conducted using a SEL-421 relay,	The proposed solution can be used for performance measurement on different platforms. It can be implemented in a computer-based simulation and also in a practical testing platform. The

		performing uncertainty and sensitivity analyses.	SEL-5401, and the SEL-AMS devices.	proposed solution can be used to test several commercially available IEDs to evaluate the performance of their algorithms.
Malkowski, Izdebski, Miller, 2020	Reducing the risk of total voltage collapse of a transformer by using an adaptive algorithm for OLTC.	The algorithm they created proposed that a change in the preset voltage setting made at a specific time during the operation reduced the reactive power present at low voltages.	DigSilent PowerFactory was used for network simulations of the algorithm that would be implemented. Further testing, which included real physical hardware devices, was then conducted.	Test results showed an increase in the amount of node voltage stability reserves available. Implementing the proposed algorithm is very simple and does not require costly, complex technical resources.
Tasnim, Sarimuthu, Lan, Tan, 2022	Improving power transformer OLTC response time to	Algorithm to control the OLTC derived from the internal	The control algorithm is modelled in the MATLAB software and	From the test conducted the concluded that the

	regulate the power system networks voltage profile due to introducing solar generated energy to the grid. OLTC response is adversely affected during high energy consumption and peak sun hours.	game theory and incorporated into a 74-bus power system network to verify its ability to enhance network voltage during high energy consumption coupled with peak sun hours.	incorporated into a 74-bus power system network to verify its ability to enhance network voltage during poor voltage quality conditions.	game theory based algorithm managed to reduce voltage instability from 69.4% to 61.6% during periods of high energy consumption coupled with peak sun hours. OLTC response increased by 50% during periods of high energy consumption and 62.2% during periods of peak sun hours.
Otchere, Ampofo, Dantuo, Frimpong, 2023	The effects of distributed generations have on the operational performance of capacitors banks and	They proposed a genetic algorithm to perform an impact assessment of the capacitor banks	The MATPOWER software modelled a 16-bus United Kingdom power system network and obtained results and graphs.	Losses are at their minimum when DG is connected at the load centre. DG also has minimal influence on OLTCs at the

	OLTCs.			substation level. DG's influence increases on OLTCs located in distribution feeders. The results pointed out that when DG is located at remote and isolated entry points, it tends to adversely influence the voltage profile and losses.
Dung, 2023	Investigate and create a control algorithm OLTCs for power transformers to enhance the voltage profile in power system networks.	An algorithm structure was created to control OLTC tap positions from either a local or remote mode, improving the system voltage quality of the power transformers' primary and secondary sides.	Theoretical experiments were conducted and verified using the Arduino Mega 2560 microprocessor and actuating equipment for real system simulation.	Results from the theoretical modelling proved highly successful in calculating the parameters at an increased rate of computation.

		Theoretical modelling verified the formulas used for the OLTC control schemes.		
Wróblewski, Kowalik, Januszewski, Kurek, 2024	The development of a Fuzzy Logic Controller based control scheme for power transformer OLTC control to be introduced into networks with a high level of Distributed Generation penetration.	We conducted software-in-the-loop experiments on a CIGRE Medium-Voltage power system network. The OLTC control algorithm code was written in Python 3.12.	They conducted software-in-the-loop experiments on a CIGRE Medium-Voltage power system network. They wrote OLTC control algorithm code in Python 3.12 and conducted the tests in a closed-loop system.	The results from the closed-loop testing revealed with the implementation of the proposed algorithm, overvoltage conditions in the network was reduced from 1.072 p.u to 1.0485 p.u



## 2.4. Literature Review on Hardware-in-the-loop Simulations on OLTC

### 2.4.1 Introduction

A protective relay is a device designed to monitor and control by disconnecting faulted sections from an electrical system. It monitors a given system, compares monitored values against pre-set values, and issues a trip signal to the disconnecting device to remove the faulted section from a given network. In power system networks, many protective relays work together to protect the power transformer (Rahmati, Sanaye-Pasand, 2015). In the event of failure of one of these relays the overall protection functions and the total reliability of the protection function is severely diminished. For power transformers with a rating more excellent than 10 MVA, the differential protection function usually is employed to serve as the primary protection function (Alencar et al., 2014). More than a hundred years ago the electrical protection relay devices was first introduced. Since introducing protective relaying equipment, it has developed from highly mechanical mechanisms into highly sophisticated intelligent electronic devices. In hardware-in-the-loop simulations, actual physical hardware devices, i.e., protection relays, are interfaced into simulated power systems that represent their real-world counterparts to test and evaluate the performance of protective equipment in a simulated environment. Hardware-in-the-loop is a means of testing control and protection devices in a realistic simulated controlled environment. This way of testing protection and control devices offers a cost-efficient way of testing protection equipment in a safe and controlled environment before subjecting these devices to real-world conditions. By doing hardware-in-the-loop simulations first it is possible to configure protection relays and control devices and then test the adjustments made to the settings of the protection and control devices and its effects on the subsequent protection and control performance. By making use of hardware-in-the-loop simulations, these tests and configurations can be done in real-time, and feedback and results from tests conducted can also be observed and monitored in a real-time environment.

The documents reviewed per year under the subsection Hardware-in-the-loop are shown in [Figure 44](#).

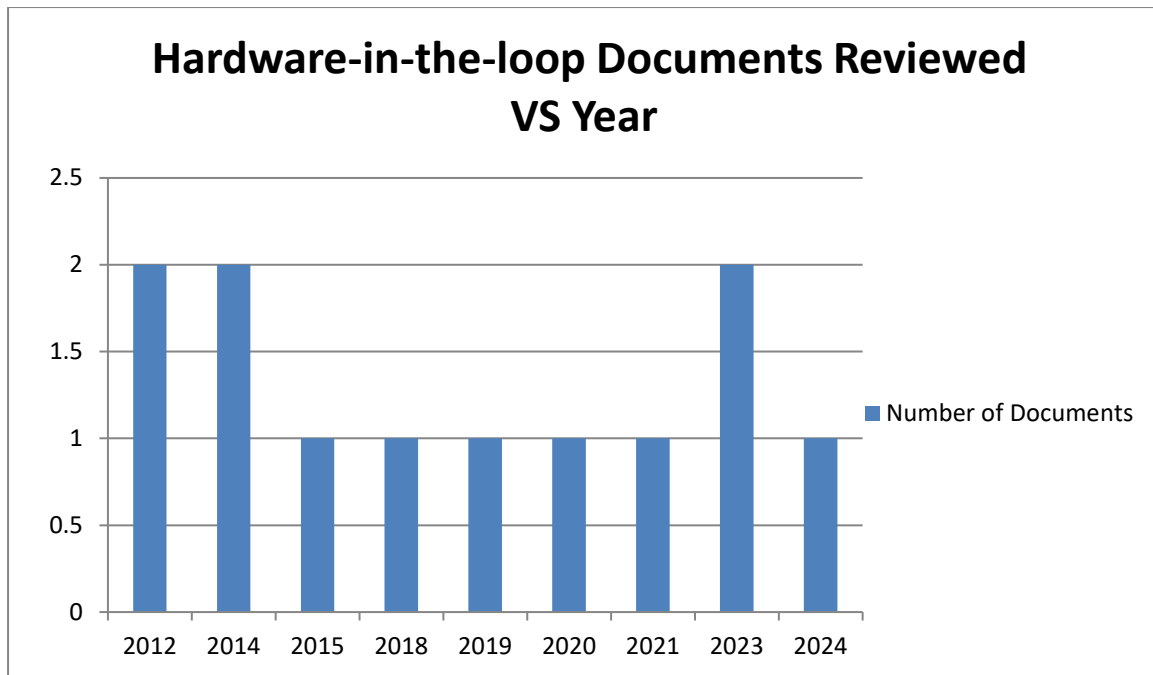


**Figure 44: Hardware-in-the-loop reviewed per year**

## 2.4.2 Literature survey on Hardware-in-loop simulations

According to (Qasmi, 2014), power transformers used in high-voltage applications have an increased vulnerability to damage. Taking this high risk of damage into account, power transformers need to be adequately protected with different types of protection schemes to enable these power transformers to deliver reliable and safe service to customers. High voltage transformers need to be protected by a primary protection system as some kind of backup protection function. The damage caused to transformers during fault conditions is directly proportional to the time the transformer is exposed to the fault conditions. Therefore, it is essential that power transformers be isolated from faulted conditions in the absolute minimum possible time to avoid severe damage. According to (IEEE C37.90, Guide for Protective Relay Applications to Power Transformers, Ref. 1), 70% of power transformer failures are caused by tap changer and winding failures. See [Table 9](#) for power transformer failure rates.

**Table 9: Power transformer failure rates (Qasmi, 2014)**

	1955-1965		1975-1982		1983-1988	
	Number	Percent of total	Number	Percent of total	Number	Percent of total

Winding failures	134	51	615	55	144	37
Tap changer failures	49	19	231	21	85	22
Bushing failures	41	15	114	10	42	11
Terminal board failures	19	7	71	6	13	3
Core failures	7	3	24	2	4	1
Miscellaneous failures	12	5	72	6	101	26
Total	262	100	1127	100	389	100

The authors (Rudez, et al., 2012) presented the paper on the testing of an overcurrent relay by incorporating special simulation hardware for a real-time digital simulation in a closed loop configuration. The protective relay they used in the experiment was the ABB protection relay REF 630. They used the RSCAD software suite to digitally simulate the testing conditions and the GT Analogue Output card (GTAO) of RTDS equipment to create an analog output signal. They determined because the maximum range of the voltage on the GTAO pins is  $\pm 10$  V, where the maximum current cannot exceed 25 mA they had to use some sort of interface between the RTDS equipment and the protection relay. They used an amplifier to scale the signals to real-world levels in order to test the protection relay under realistic real-world scenarios. The CMC 356 device manufactured by OMICRON device was used as an amplifier between output of the RTDS output card and the ABB protection relay REF 630. Feeding signal back from the protection relay to the RTDS environment can be done via three channels. It can be done via the GT Analogue Input Card (GTAI), GT Digital Input Card (GTDI) or GT Front Panel Interface (GTFPI). The main aim of their paper was to demonstrate the use of the RTDS equipment in a closed-loop configuration in the protection arena. They also

found that with the incorporation of the CMC 356 device in the loop, the time delay in the protection relay operation was approximately 150 milliseconds. They concluded that another alternative must be found in the future to reduce this time delay.

The authors (Murugan et al., 2019) tested a differential relay for the protection of a power transformer, using RTDS and DSP. They tested the operation of this Empirical Fourier Transform-based transformer differential relay (EFTDR) under various operating conditions of the power transformer. They modelled the EFTDR in the DSP environment - TMS320F28335. of using the analog and digital hardware circuit, the DSP circuit was interfaced with the RTDS system. See Figure 45 for the interfacing was achieved.

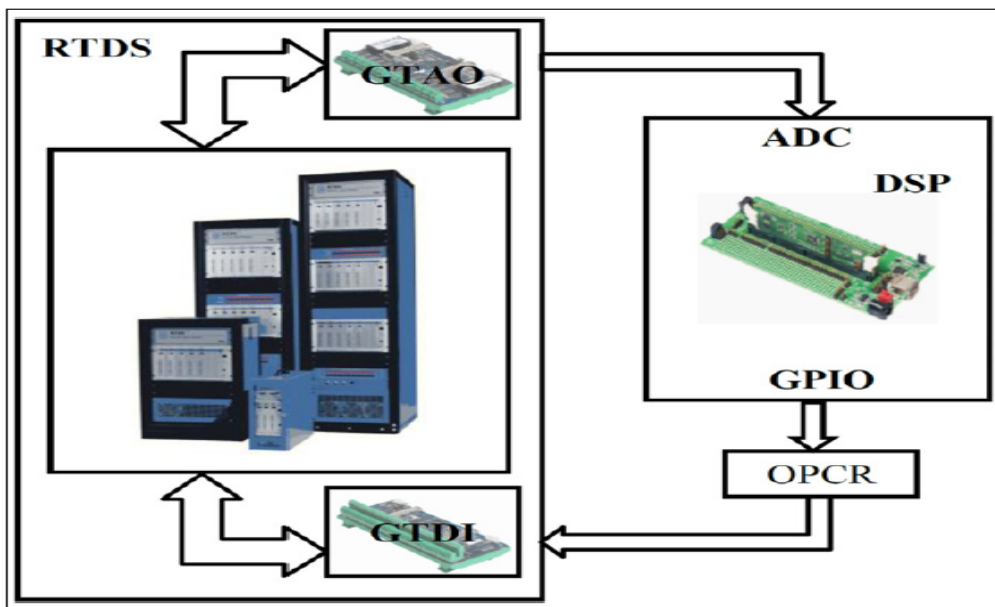


**Figure 45: Hardware setup with RTDS and DSP (Murugan, et al., 2019)**

They evaluated the EFTDR for the following conditions:

- Internal fault
- Inrush current
- CT saturation

After conducting HIL tests for various operating conditions and fault conditions, they found that the EFTDR is superior in terms of operating performance to the DFTDR. The results were scrutinized to accuracy and operating time. They believe that HIL testing of protection systems has proven its effectiveness in validating and assessing protection systems in real-time.

(Nguyen, Yang, Nielsen, Jenson, 2020) conducted HIL testing of the automatic voltage regulator of the synchronous condenser. They conducted tests to determine AVR's steady-state and dynamic performance under various operating scenarios.

The system was evaluated for the following conditions:

- Over excitation
- Under excitation
- AVR set point loss

The grid and the SC were constructed in the RTDS software suite, and the AVR was implemented using an HIL structure. The grid they constructed would generate via RTDS three-phase voltage, and current signals from the generator, which is fed to the HIL circuit. The AVR would send the AVR set point back to the RTDS equipment in the HIL circuit. The system diagram is shown in [Figure 46](#).

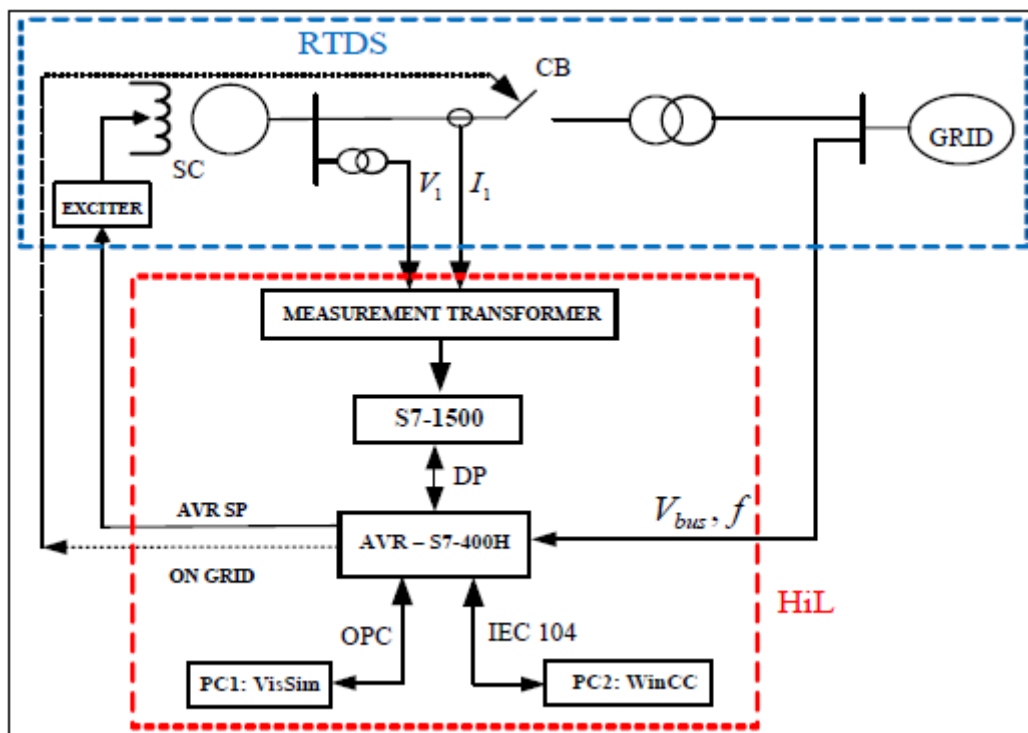


**Figure 46: The system diagram with AVR HIL (Nguyen, Yang, Nielsen, Jenson, 2020)**

Different tests were conducted to verify the AVR's performance. From the tests conducted, they were able to receive comparable results to scrutinise

the AVR's performance for the different operating scenarios. They said that with the inclusion of HIL in this study, they demonstrated that they were able to validate and modify the control function. This makes HIL useful handy tool that enables the protection engineer to test the performance of control and protection functions before final construction and commissioning.

The authors (Dantas, Pellini, Junior, 2018) did a study involving hardware-in-the-loop to validate and evaluate the energy and reactive power differential protection for the application in transformers. The protection solutions for the study are based on two time-domain protection algorithms. The algorithms they used were the 87E for the energy differential protection and the 87Q for the reactive power differential. A prototype relay was programmed with the relevant protection algorithms used for the study. The network was configured in the RSCAD software suite and applied to the prototype relay via the RTDS signal generators. For the simulation studies, the scenario was created to protect a 100 MW generator step-up transformer bank. See [Figure 47](#) for the simulated case.

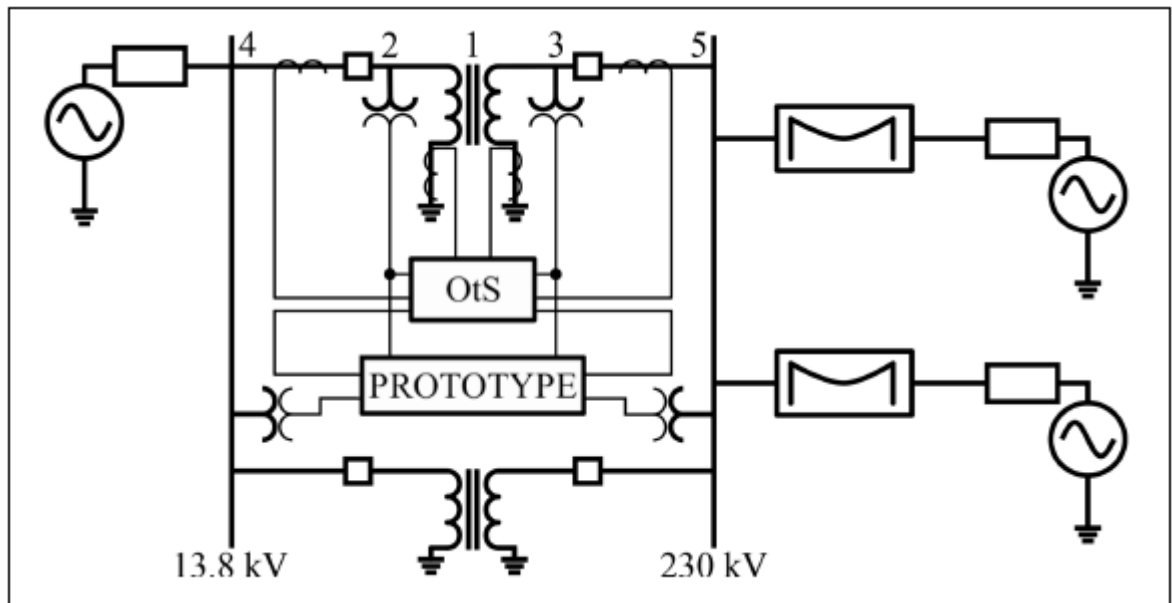


**Figure 47: The simulated case to evaluate the energy and reactive power differential protection for the application in transformers (Dantas, Pellini, Junior, 2018)**

The results obtained from the test were benchmarked against commercially available IED devices. From the tests conducted, it was found that the prototype relay created presented excellent fault-clearing characteristics. With the help of hardware-in-the-loop systems like RTDS, engineers can create and test custom prototype relays and test their performance and fault-clearing capabilities and characteristics.

The authors (Cha et al., 2012) did a research paper to discuss hardware-in-the-loop testing of power electronic controllers. For the research they conducted, the relevant power system was modelled in the RTDS environment. For test purposes, the control algorithms were programmed using the C language on a TI TMS320C28x DSP microcontroller. These C-programmed microcontrollers were tested using the real-time hardware-in-the-loop method. The TI TMS320C28x DSP microcontroller was programmed to perform the function of a buck converter and a DC-to-AC inverter. See Figure 48 for buck converter simulation with external control used in this study.

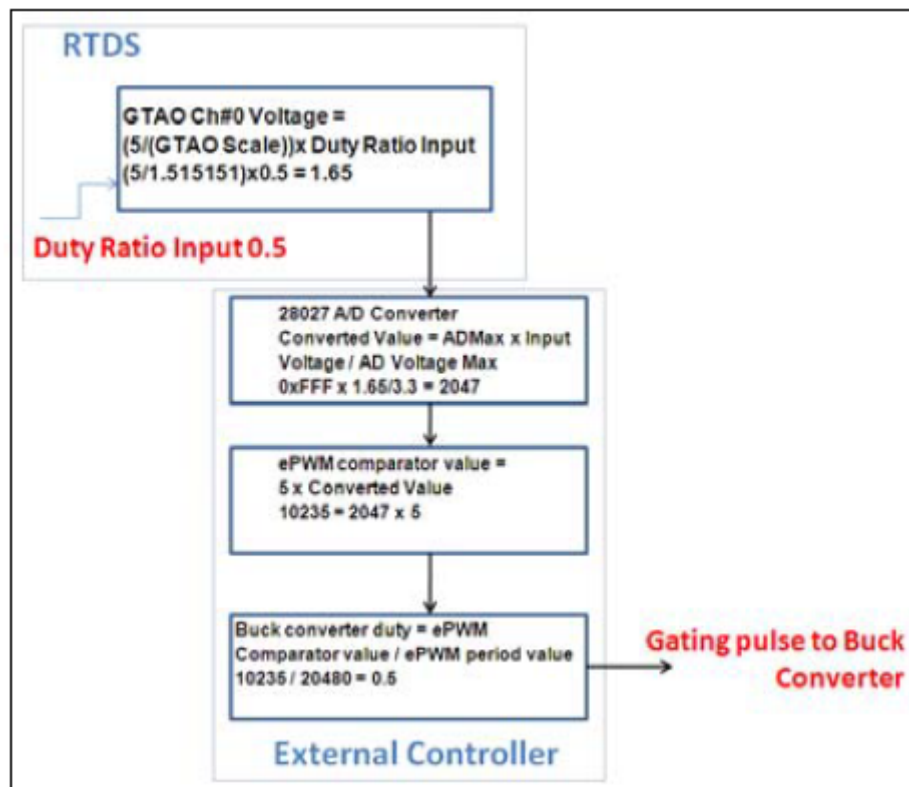


**Figure 48: Buck converter simulation with external control (Cha et al., 2012)**

Results obtained from the tests prove that the microcontrollers behave satisfactorily, as observed from the RTDS equipment. The control algorithms effectively regulate

the power converters during hardware-in-the-loop simulations. They said that employing hardware-in-the-loop simulations would potentially reduce the development cost involved and experimental risk during product development projects.

(Reda, Ray, Peidaee, Anwar, Mahmood, Kalam, Islam, 2021) conducted a HIL-based study to investigate and assess the security of the smart grid infrastructure due to the IEC 61850 GOOSE application. IEC 61850 is adopted by many IED manufacturers due to interoperability with equipment from other vendors and its scalability. They aim to analyze and expose the IEC 61850 communication protocol vulnerabilities by creating simulated attacks on the smart grid. They of the HIL simulation concept by using the OP5600 chassis of the OPAL-RT platform, which supports the IEC 61850 protocol. The IED from ABB, the REF615, served as a dedicated feeder protection and control IED in the study. Communication between IEDs and HIL simulation equipment was a LAN-based network. The proposed test system is shown in [Figure 49](#).

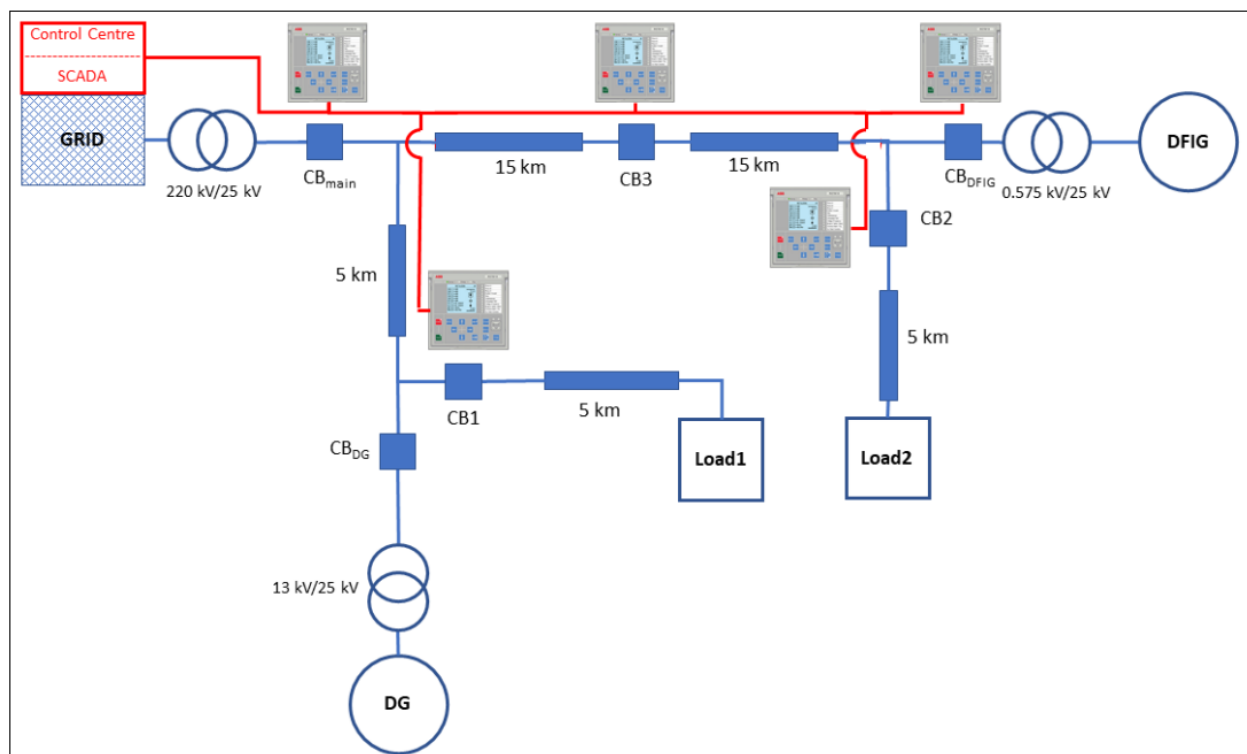


**Figure 49: The proposed test system (Reda, Ray, Peidaee, Anwar, Mahmood, Kalam, Islam, 2021)**



From the HIL-based simulations conducted, they were able to establish that the IEC61850 GOOSE protocol was susceptible to data attacks even with the IEC 62351 security scheme enabled.

The authors (Nomandela et al., 2023) conducted a based study into transformer differential protection. They set out to verify the efficacy of the settings configured in the protection IED against the theoretical assumptions made in the calculations. The tests conducted are not confined to just the transformer but extended to include the broader power system network. Shown in Figure 50 is the HIL test setup.

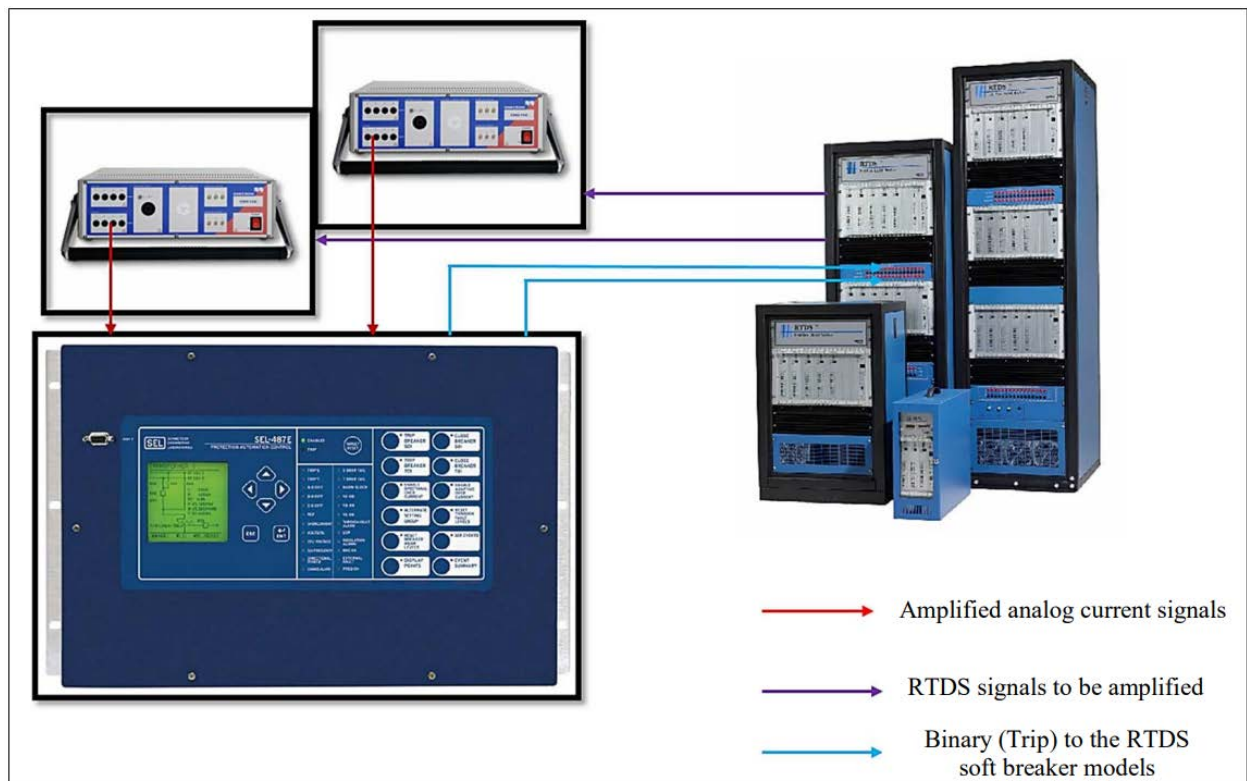


**Figure 50: The HIL test setup structure (Nomandela et al., 2023)**

The IEEE 9 bus power system network was modelled in the RSCAD software, and real-time signals were generated from the RTDS equipment supplied to two Omicron amplifiers. The amplified signals are sent to the SEL-487E transformer protection relay. The transformer relay monitors the signal and operates according to the engineering configuration setting programmed to the relay. The RTDS equipment monitors the relays relay outputs. The efficacy of the protection settings is then analyzed using the data from the RTDS equipment. The results obtained from the HIL simulations point to the effective integration of protection IEDs with the RTDS equipment. It serves as a platform for power system engineers to include HIL

simulations for transformer differential testing to prevent nuisance tripping during normal operating conditions.

A study was undertaken by (Yadav et al., 2023) into relay testing using HIL simulations. With the increase in consumer energy demand, the power system network needs to be expanded to keep up this increased demand. The network consisting of various equipment needs to be safeguarded against fault conditions, which could render the entire network out of service. Modern protective devices are employed to protect and isolate certain network sections during fault conditions to keep the rest of the power system network operational. In this study, two SEL-351 directional overcurrent relays were employed in the sample distribution network system to execute the protection functions. The settings for the protection relays were calculated and configured in such a way as to provide optimum coordination between the two directional overcurrent relays. HIL simulations were conducted in a closed-loop system using RTDS equipment to test the protection performance of the relays. [Figure 51](#) shows the network under study.

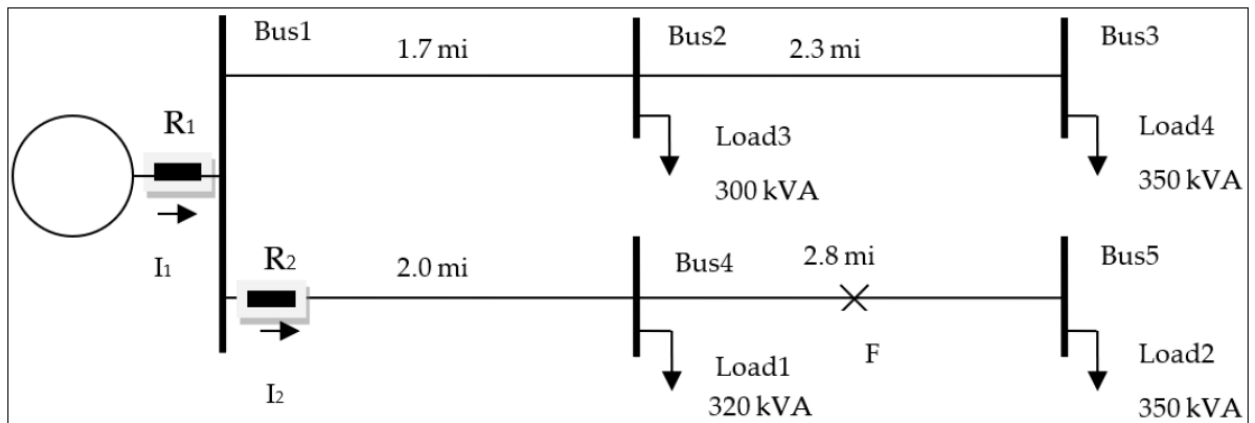


**Figure 51: Network under study (Yadav et al., 2023)**

The results from the HIL simulations conducted point to the proper protection coordination between the protection relays during fault conditions. The fault clearing times of the protection relays could be properly investigated from the data retrieved from the RTDS equipment. They concluded that HIL simulations would play a more crucial role in the future for power system design and protection.

A study by (Shangase et al., 2024) said the power transformer is a crucial element of the power system network to ensure the uninterrupted supply of reliable and stable energy. It is therefore of paramount importance to protect this element at all costs to

prevent unnecessary network outages. A HIL-based study was conducted into transformer differential protection, which included the IEC 61850 GOOSE protocol as a method of protection signal transmission. Real-time simulation testing was executed using the RTDS platform and the MiCOM-P645 IED as the protection IED in a modified version of the IEEE 9 bus network. Various external and internal faults were simulated, and the IEC 81650 GOOSE protection signals published by the MiCOM-P645 IED were analyzed by the RTDS equipment. After scrutinizing the test result they concluded that IEC 61850 GOOSE proved to be superior regarding interoperability between devices, signal transmission speed and reliability. Shown in Figure 52 is the modified version of the IEEE 9 bus network used for the HIL testing.

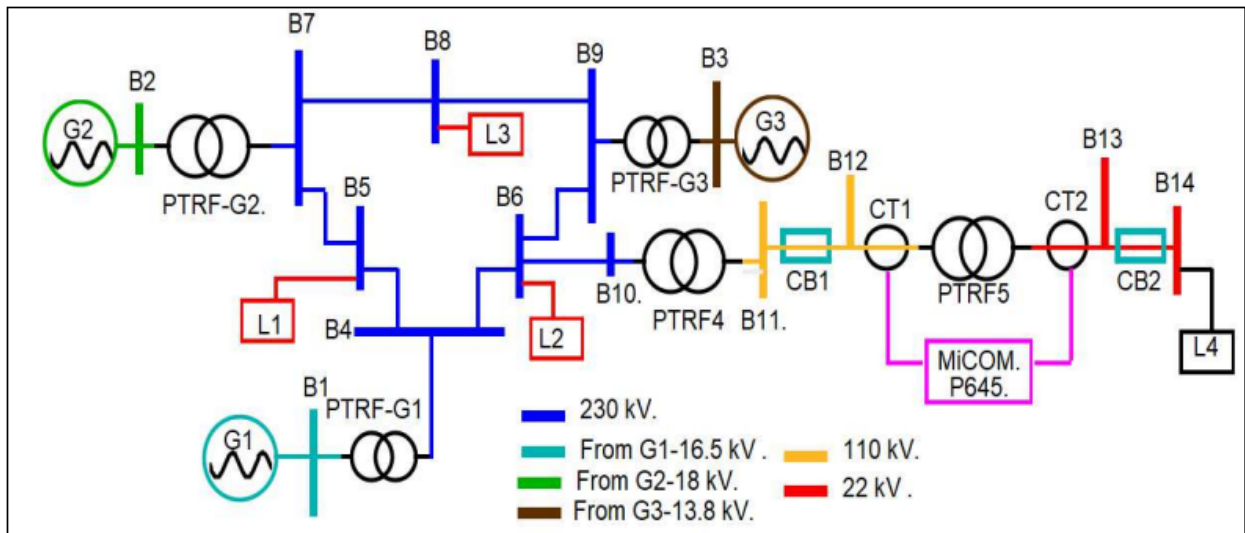


Figure 52: IEEE 9 bus network used for the HIL testing (Shangase et al., 2024)

### 2.4.3 Literature review summary on Hardware-in-the-loop simulations

**Table 10** provides a comprehensive summary of Hardware-in-the-loop simulations. Potential review papers are chosen from the literature to give the comparison study based on their research work goal, techniques, simulation and hardware tools, and project benefits, as stated in **Table 10** below.

**Table 10: Review the summary on Hardware-in-the-loop simulation**

<b>Paper</b>	<b>Aim</b>	<b>Method used</b>	<b>Simulation/ implementation Hardware/software</b>	<b>Benefits</b>
Qasmi, 2014	The research findings give a basic overview of the different protection mechanisms employed in the industry to protect power transformers.	The paper was formulated in a theoretical format to research and discuss the employment of IEDs as the main backup protection mechanism for power transformers.	The research provides different types of protection mechanisms used to protect the power transformers. The schemes used included current protection functions, earth fault protection, differential protection, a winding temperature indicator, and an oil temperature indicator.	The schemes designed for power transformer protection are proving effective in limiting damage to transformers and human life when faults occur.

			The relays used and programs used for simulations should be mentioned. Only diagrams are shown.	
Rudez, Osredkar, Mihalic, 2012	The testing of an overcurrent relay by incorporating special simulation hardware for a real-time digital simulation in a closed-loop configuration.	They tested an ABB REF 630 protective relay employing RTDS equipment in a closed-loop configuration.	The protective relay they used in the experiment was the ABB protection relay REF 630. The RSCAD software suite was used to simulate the testing conditions digitally, and RTDS equipment was used to create an analogue output signal.	They successfully demonstrated the use of RTDS equipment in a closed-loop configuration in the protection arena. Protection equipment can be tested in a controlled lab environment before live field testing.
Murugan, Simon, Sundareswaran, Panugothu, Padhy, 2019	Tested a differential relay to protect a power transformer using RTDS and DSP.	They tested the operation of this Empirical Fourier Transform-based transformer	They modelled the EFTDR in the DSP environment—TMS320F28335. Using the analogue and digital	After conducting HIL tests for various operating and fault conditions, they found that the EFTDR is superior in operating performance to the DFTDR.

		differential relay (EFTDR) under various power transformer operating conditions.	hardware circuit, the DSP circuit was interfaced with the RTDS system. They evaluated the EFTDR for the following conditions: internal fault, inrush current, and CT saturation.	They believe that HIL testing of protection systems has proven effective in validating and assessing them in real time.
Nguyen, Yang, Nielsen, Jenson, 2020	HIL is testing the automatic voltage regulator of the synchronous condenser.	Tests were conducted to determine AVR's steady-state and dynamic performance under various operating scenarios.	The grid and the SC were constructed in the RTDS software suite, and the AVR was implemented using an HIL structure. The system was evaluated for the following conditions: Over-excitation, under-excitation, and AVR set point loss.	They said that by including HIL in this study, they demonstrated that validating and modifying the control function is possible. This makes HIL a handy tool for enabling the protection engineer to test the performance of control and protection functions in a lab environment before the commencement of final construction and commissioning.

Dantas, Pellini, Junior, 2018	A study involving hardware-in-the-loop to validate and evaluate the energy and reactive power differential protection for the application in transformers.	The protection solutions for the study are based on two time-domain protection algorithms.	They used the 87E for energy differential protection and the 87Q for reactive power differential. A prototype relay was programmed with the relevant protection algorithms used for the study. The network was configured in the RSCAD software suite and applied to the prototype relay via the RTDS signal generators.	The tests conducted revealed that the prototype relay created presented excellent fault-clearing characteristics. With the help of HIL systems like RTDS, engineers can create and test custom prototype relays and test their performance and fault-clearing capabilities and characteristics.
Cha, Kwon, Wu, Nielsen, Ostergaard, 2012	The research was conducted to discuss hardware-in-the-loop testing of power electronic controllers.	C-programmed microcontrollers were tested using the real-time hardware-in-the-loop method.	The power system was modeled in the RTDS environment. The control algorithms were programmed using the C language on a TI	Employing hardware-in-the-loop simulations would reduce development costs and experimental risk during product development projects.

			<p>TMS320C28x DSP microcontroller for testing purposes. These C-programmed microcontrollers were tested using the real-time hardware-in-the-loop method. The TI TMS320C28x DSP microcontroller was programmed to perform the functions of a buck converter and a DC to AC inverter.</p>	
Alencar, Bezerra, Ferreira, 2014	<p>Research was conducted to find a system based on a differential current gradient that can differentiate between internal faults and</p>	<p>Their proposed system is based on computing the differential current gradient vector angles at the 3 phases.</p>	<p>Computerized simulations were conducted employing EMTP/ATP and MATLAB. They analyzed inrush current and internal faults.</p>	<p>The algorithm they created and tested gave satisfactory results when implemented in the differential protection scheme. In the case studies, inrush currents, internal and external faults were correctly identified and isolated.</p>



	inrush currents.			
Rahmati, Sanaye-Pasand, 2015	Research was conducted to create a power transformer protection system that makes decisions based on multiple input criteria.	The power transformer protection function the proposed used implemented an algorithm that makes decisions based on multiple inputs from different protective equipment. This contrasts traditional protection topologies, which have different protection functions operating in isolation.	Computerized simulations were conducted employing the differential protection relay programmed with a custom relay based on fuzzy logic. The algorithm makes decisions based on multiple inputs from different protective equipment instead of traditional protection topologies with varying functions of protection operating in isolation. An IPTP relay is modeled using part of the power system	The power transformer protection system they proposed proved to increase its overall reliability. The custom algorithm they created enabled the protection function to perform effectively even when false tripping and faulty signals were present from individual protective relays within the protection system.

			network. The relays used and programs used for simulations are not mentioned. Only results are shown.	
Reda, Ray, Peidaee, Anwar, Mahmood, Kalam, Islam, 2021	A HIL-based study is conducted to investigate and assess the security of the smart grid infrastructure due to the IEC 61850 GOOSE application.	They created simulated attacks on the smart grid to analyze and expose the IEC 61850 communication protocol vulnerabilities.	The IED from ABB, the REF615, was a dedicated feeder protection and control IED in the study. Communication between IEDs and HIL simulation equipment was a LAN-based network. HIL simulation is done by using the OP5600 chassis of the OPAL-RT platform which supports the IEC 61850	They were able to establish that the IEC61850 GOOSE protocol was susceptible to data attacks even with the IEC 62351 security scheme enabled. Further investigation is needed.

			protocol.	
Nomandela, Mnguni, Ratshitanga, Ntshiba, 2023	They set out to verify the efficacy of the settings configured in the protection IED against the theoretical assumptions made in the calculations.	The IEEE 9 bus power system network was modelled in the RSCAD software, and real-time signals were generated from the RTDS equipment supplied to two Omicron amplifiers. The amplified signals are sent to the SEL-487E transformer protection relay to monitor for fault conditions.	The IEEE 9 bus power system network was modelled in the RSCAD software. RTDS equipment supplied output signals to two Omicron amplifiers. SEL-487E is the transformer protection relay in the study.	The results obtained from the HIL simulations point to the effective integration of protection IEDs with the RTDS equipment. This platform allows power system engineers to include HIL simulations for transformer differential testing to prevent nuisance tripping during normal operating conditions.
Yadav, Liao, Burfield, 2023	Directional overcurrent relay testing using HIL simulations.	This study employed two SEL-351 directional overcurrent relays in	Two SEL-351 directional overcurrent relays were employed in the sample	The HIL simulations' results point to the proper protection coordination between the protection relays during fault

		the sample distribution network system to execute the protection functions. HIL simulations were conducted in a closed-loop system using RTDS equipment to test the protection performance of the relays.	distribution network system to execute the protection functions. HIL simulations were conducted in a closed-loop system using RTDS equipment.	conditions. They concluded that HIL simulations would play a more crucial and critical role for power system design and protection.
Shangase, Ratshitanga, Mnguni, 2024	A HIL-based study was conducted into transformer differential protection, which included the IEC 61850 GOOSE protocol as a method of protection signal transmission.	Real-time simulation testing was executed using the RTDS platform and the MiCOM-P645 IED as the protection IED in a modified version of the IEEE 9 bus network. Various	The RTDS platform was used for real-time simulation testing. The MiCOM-P645 IED served as the protection IED in a modified version of the IEEE 9 bus network. IEC 81650 GOOSE communication	After scrutinizing the test results, they concluded that IEC 61850 GOOSE proved superior in terms of interoperability between devices, signal transmission speed, and reliability. HIL simulations are critical to the design of network protection systems.

		external and internal faults were simulated, and the RTDS equipmentRTDS equipment analyzed the IEC 81650 GOOSE protection signals published by the MiCOM-P645 IED analyzed the IEC 81650 GOOSE protection signals published by the MiCOM-P645 IED.	was used to protect signal transmission.	
--	--	--	--	--

#### **2.4.4 Discussion of literature survey on Protection and Hardware-in-loop simulation**

Designers and manufacturers can test equipment in a real-time environment replicated by the RTDS environment and receive reliable input from protective equipment. This allowed designers and protection experts to preconfigure and test protective equipment before it was installed in the field. Because the RTDS environment is now IEC61850 standard compliant, communication conveying signals and IED reaction time could be verified in real-time. IED tripping response times could now be determined and compared to typical hardwiring response times. Protection schemes can be devised and implemented in software and tested in a lab environment using RTDS equipment to send faulty signals to real physical protection and control devices.

This testing simulates real-world situations, allowing protection and control functions to be changed and optimized before they are tested in the field. Doing hardware-in-the-loop testing before installation and commissioning also benefits personnel safety by allowing equipment to be evaluated in a safe lab setting under controlled conditions before exposure to live testing. Tripping and control reaction times of protection and control devices can be thoroughly examined using the RTDS equipment's feedback channels.

#### **2.5 Conclusion:**

This chapter gave an introductory framework of literature related to this study in preparation for the successful completion of this thesis. Reviewing related papers and journal articles established a deeper understanding of the subject matter, refined the approach taken, and enhanced the methodology for this project. The key insights from the literature review are that a modern approach is needed to solve the contemporary power system challenges. OLTCs with modern IEC61850 GOOSE protocol aim to modernize, simplify, and make the power grid protection and control functions more reliable.

The next chapter shares more insight into implementing the power system network under study in the DIgSilent environment. Load flow simulations are conducted for different network loading conditions.

## CHAPTER THREE

### OLTC THEORY AND MODELLING AND SIMULATION OF THE POWER SYSTEM NETWORK

#### 3.1 Introduction

The demand for high-quality energy has been rising constantly since mass industrialization's adoption. Electricity producers have been connecting distributed generation at various grid entry points in the distribution network to keep up with this energy demand. This, among many other factors, has led to unstable electrical supply issues for clients connected to the electrical grid. Overvoltage, conditions occur on the grid when electricity generation exceeds the demands during specific periods, caused by reverse power flow (Bimbira, 1995). Under voltage conditions, the generation capacity can't keep up with demand. To stabilize voltage conditions along the power system network, many methods are used, such as Shunt compensation, Series compensation, Transformer Tap Changers, Voltage Regulators, etc. Power transformers fitted with On Load Tap Changers have proven to be a very effective method of maintaining the voltage levels of a power system network at a desired level without the need to interrupt the power supply. About 96% of power transformers installed in power system networks with a rating of 10MVA or above use OLTC for voltage regulation (Banakar, Muralidhara, Maheswara Rao, 2016).

This chapter aims to provide some background information on essential transformers, OLTC implementation, and voltage regulation control methods on parallel transformers. The modified version of the IEEE 14 bus network is modelled in the DIgSilent software. Load flow studies are conducted on the network for different network loading conditions, and the results are analyzed and compared to the load flow results obtained in Chapter 5.

Section 3.1 covers the introduction, section 3.2 covers the transformer theory, and section 3.3 shows the Transformer Tap changers. Section 3.4 shows the Control methods for OLTCs of parallel transformers, and section 3.5 deals with the modeling

and simulation of the modified IEEE 14 bus network in DIgSilent. Section 3.6 covers the conclusion.

### 3.2 Transformers

A transformer is an electromagnetic device that, through a medium of the magnetic field, transfers energy from one alternating-current circuit to another without altering the frequency. The primary winding is located on the side that receives the alternating current from the supply. The secondary winding is located on the side that supplies the energy to a connected load said (Bimbira, 1995). This transfer of energy from one circuit to another takes place without the need for any moving parts. This makes a transformer a very efficient device that requires very low maintenance levels said (Kothari, Nagrath, 2010). Shown in Figure 53 is the equivalent circuit of a transformer.

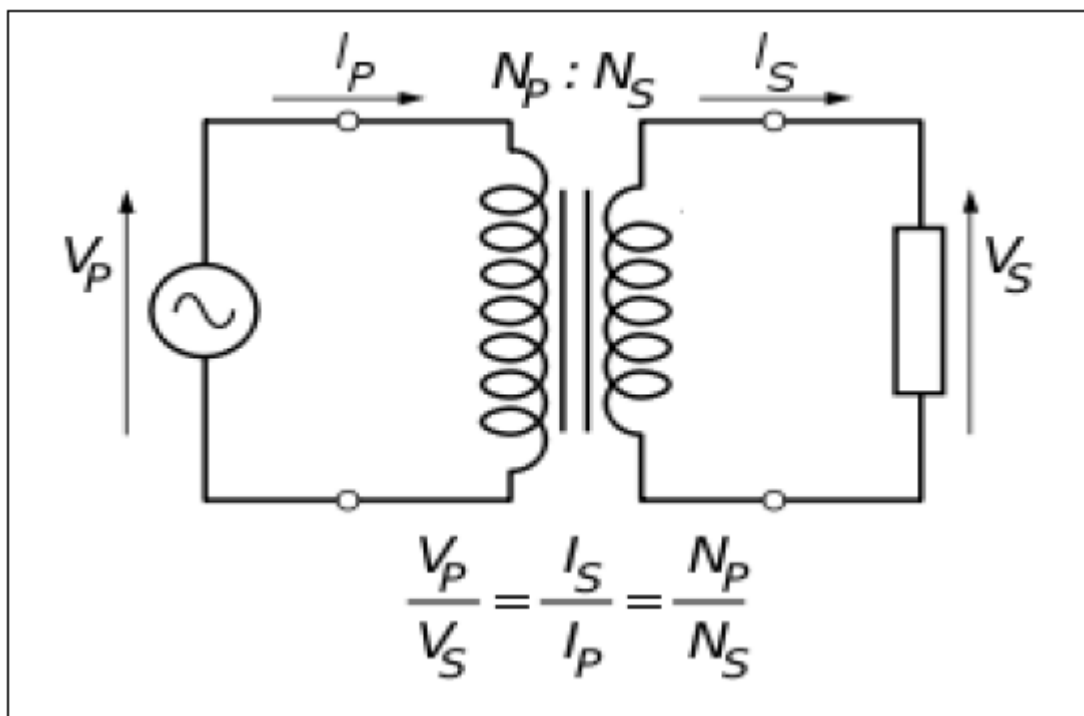


**Figure 53: Equivalent circuit of a transformer**

Where:

$V_P$  = voltage applied on primary winding

$V_S$  = voltage induced on secondary side winding

$I_S$  = current in secondary winding



$I_p$  = current in the primary winding

$N_p$  = turns ratio of the primary winding

$N_s$  = turns ratio of the secondary winding

Shown in the equation is the relationship between turns ratio, voltage, and current in a transformer:

$$\frac{N_p}{N_s} = \frac{V_p}{V_s} = \frac{I_s}{I_p} \quad (3.1)$$

From the equation, it can be established that by adjusting the transformer ratio, the voltage induced in the secondary side windings connected to the load can thus be regulated to a desired level.

From the equation (3.1) it can be derived that:

$$\text{Turns ratio} = \frac{N_p}{N_s} \quad (3.2)$$

And that:

$$\frac{V_p}{V_s} = \frac{N_p}{N_s} \quad (3.3)$$

Which derives that:

$$V_s = V_p \frac{N_p}{N_s} \quad (3.4)$$

Or:

$$V_s = \frac{V_p}{\left(\frac{N_p}{N_s}\right)} = \frac{V_p}{\text{Turns ratio}} \quad (3.5)$$

Transformer Tap changers are added to transformers to alter the transform's turns ratio, with the aim of maintaining a stable voltage on the secondary windings.

As the demand for electricity grows globally, in line with rapid population growth, utilities need to make certain changes to the electricity supply network to keep up with this increased demand. Some of those adaptations made are installing power transformers in parallel. Shown in [Figure 54](#) is the basic configuration of two parallel transformer pair supplied from the same power and connected to the same load.

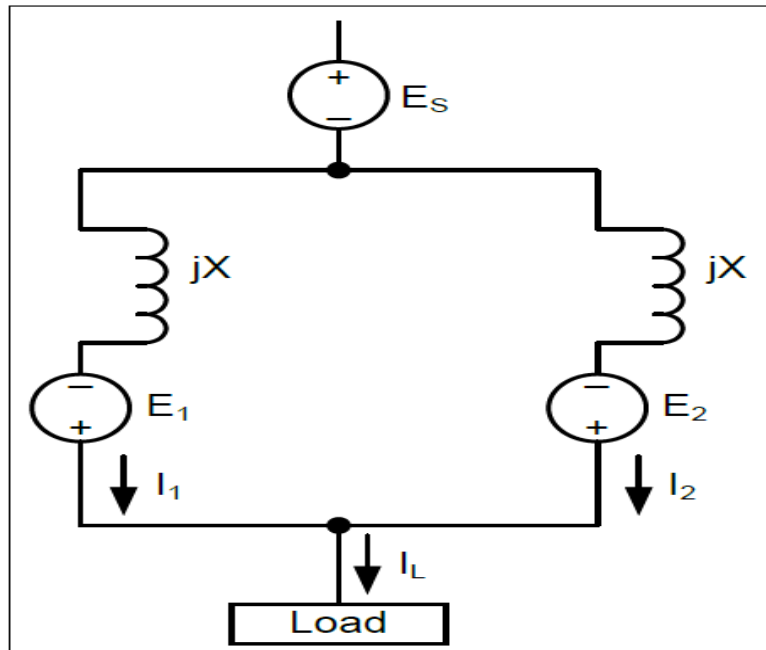


**Figure 54: Basic configuration of two parallel transformers**

Where:

$E_s$  = supply voltage

$E_1$  = voltage change in transformer 1

$E_2$  = voltage change in transformer 2

$I_1$  = current in transformer 1 windings

$I_2$  = current in transformer 2 windings

$jX$  = impedance

$I_L$  = load current

If the both transformers is identical,  $E_1 + E_2 = 0$  and  $I_1$  and  $I_2$  is equal, (3.6)

And:  $I_1 + I_2 = I_L$  (3.7)

A circulating current equal to zero will flow between identical transformers with equal voltages. The equation for circulating current flowing between transformers is shown in the equation:

$$I_{\text{circ}} = \frac{(E_1 - E_2)}{2jX} = \frac{-j(E_1 - E_2)}{2X} \quad (3.8)$$

The requirements for connecting power transformers in parallel are shown in [Table 3-12](#). Instead of replacing a single power transformer with a unit with a higher rated capacity, another transformer (or more) is placed parallel to the existing transformer mentioned (Trebolle, Valecillos, 2008). The advantages and disadvantages of putting power transformers in parallel can be seen in [Table 11](#).

**Table 11: Advantages and disadvantages of placing power transformers in parallel (Trebolle, Valecillos, 2008)**

<b>Advantages of parallel transformers</b>	<b>Disadvantages of parallel transformers</b>
Optimal efficiency is attained at a reduced cost.	Very high short-circuit currents are possible.
If one transformer needs maintenance, it can be taken out of commission while the other transformers continue to supply the load.	The system becomes more complex due to technical confusion.
Loads are spread over multiple transformers, lowering the risk of overloading a single transformer.	The complexity of the system means more auxiliary equipment is needed.
Greater flexibility as transformers can be switched on or off depending on demand.	Circulating currents might develop between transformers.
Better scalability as more transformers can be placed in parallel to increase the system's overall capacity.	The higher output current can cause big technical issues if not handled correctly.

**Table 12: Requirements for connecting power transformers in parallel (Trebolle, Valecillos, 2008)**

<b>Conditions for placing</b>	<b>Transformers in parallel</b>
Equal polarities	Equal frequencies
The HV-LV ratios should be the same	Equal phase sequence
Short-circuit impedances should not exceed 10%	Equal conversion ratios
Power ratios of 3/1 for transformers	Short circuit currents should match and

should not be exceeded	should not exceed 10%
------------------------	-----------------------

### 3.3 Transformer Tap Changers

The two main types of transformer tap changers found in power network systems are no-load tap changers (NLTC) and on-load tap changers (OLTC). As the name would suggest in the case of NLTC, the transformer is de-energized for the tap positions on the transformer to be changed. In most cases, this would involve an operator manually disengaging and engaging the taps to obtain the desired transformer ratio. As in the case of OLTC, as the name would suggest, it implies that the transformer's tap position is changed without needing to de-energize the transformer; it means that the transformer's tap position is altered without de-energizing it. The transformer would thus remain operational while the tap-changing process takes place. For this reason, power industries prefer transformers fitted with OLTCs. See [Figure 55](#) for the basic principle of how tap changers adjust the transformer ratio.

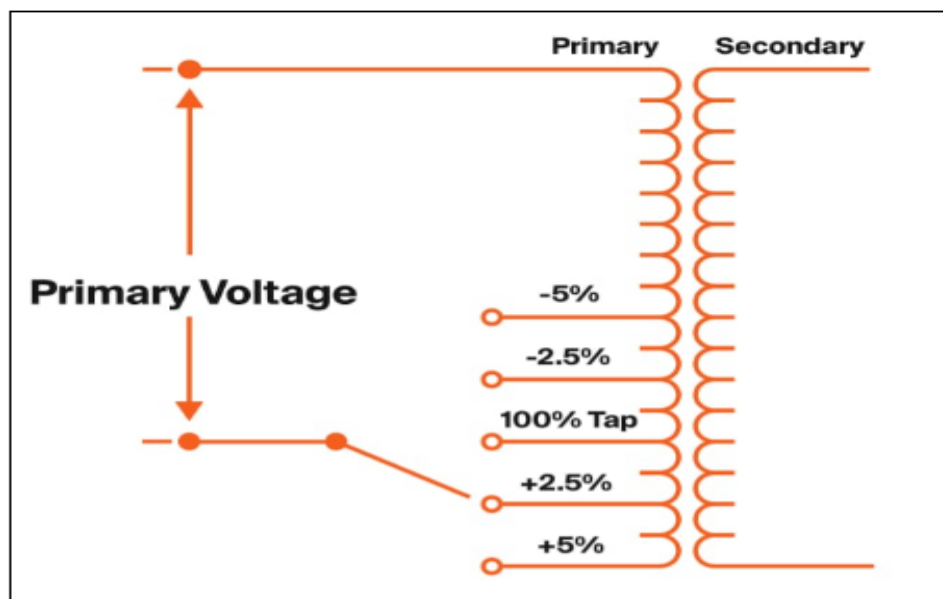


**Figure 55: Basic principle of how a tap changer adjusts the transformer ratio**

#### 3.3.1 On-Load-Tap-Changers

In most cases where OLTCs are utilized, it is installed on the power transformer's primary side (high voltage side) windings. The current flowing in the transformer's high-voltage side winding is much lower than the current that flows in the secondary side windings (Aung, Thike, 2019). Figure 56 shows the basic rotational adjustments for selecting different taps in the primary winding.

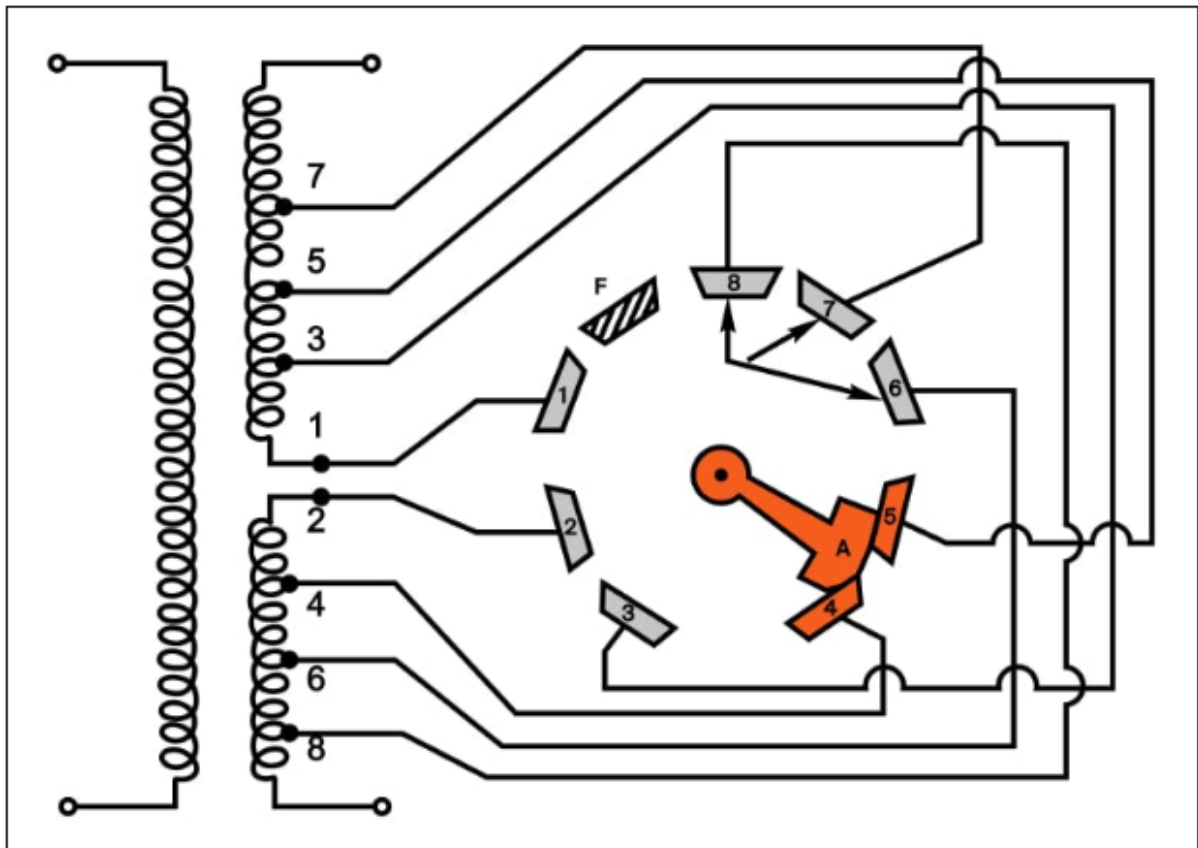


**Figure 56: Basic rotational adjustments for selecting taps (Aung, Thike, 2019)**

Studies conducted by a Cigré Working Group in 2015, TB 642 - Transformer Reliability Survey, determined that OLTCs are responsible for about 30% of transformer outages in substations. Taking this relatively high rate of OLTC failures due to aging conditions into consideration, (Erbrink, Gulski, Smit, Leich, 2009) mentioned some standard testing methods developed to monitor the condition of the OLTCs on power transformers as shown in **Table 13**. Conducting these tests enables technical staff to act preventatively before OLTC failures put the transformer out of commission.

**Table 13: Common procedures for testing OLTCs (Erbrink, Gulski, Smit, Leich, 2009)**

Measurement method	Purpose	Problems
<b>Static winding resistance</b>	Verify the integrity of the windings and the internal connections	Alignment and deterioration of electrical contact points
<b>Vibro-acoustic</b>	Use acoustic monitoring to	Mechanical components:

	detect mechanical movement and vibration	linkages, gears, timing, and sequencing. Electrical contacts: arcing, wear, and alignment. Thermal: overheating, coking and transition problems.
<b>Torque &amp; position</b>	Diagnose mechanical issues and assess the condition of drive mechanism components.	Mechanical components: linkages, gears, lubrication. Electrical components: Control/relays, motor, brake, contact alignment.
<b>Analysis of dissolved gas</b>	Diagnose an increased amount of gas concentration present within the tap changer compartment.	Thermal: overheating, coking, and transition problems.
<b>Dynamic resistance</b>	Analyze and document the rapid switching characteristics of the diverter switch.	Mechanical components: timing and sequencing. Electrical components: contacts wear & transition.

### 3.4 Control methods for OLTCs of parallel transformers

When employing OLTC for network voltage regulation, some method of control is needed to regulate and perform this control function. The control circuit needs to determine the maximum allowed voltage fluctuations from the optimal voltage level and the desired time allowed to correct the voltage levels. Shown in Figure 57 is the basic control operation flow diagram of OLTC to regulate the network voltage.

The OLTC control methods described are microprocessor-based, with the control device monitoring voltage and current signals. A communication protocol such as IEC 61850 GOOSE, MMS, DNP3, etc. is needed for peer-to-peer communication between the control devices and a SCADA system. The most frequently employed control methods for voltage regulation of parallel transformers using OLTCs .

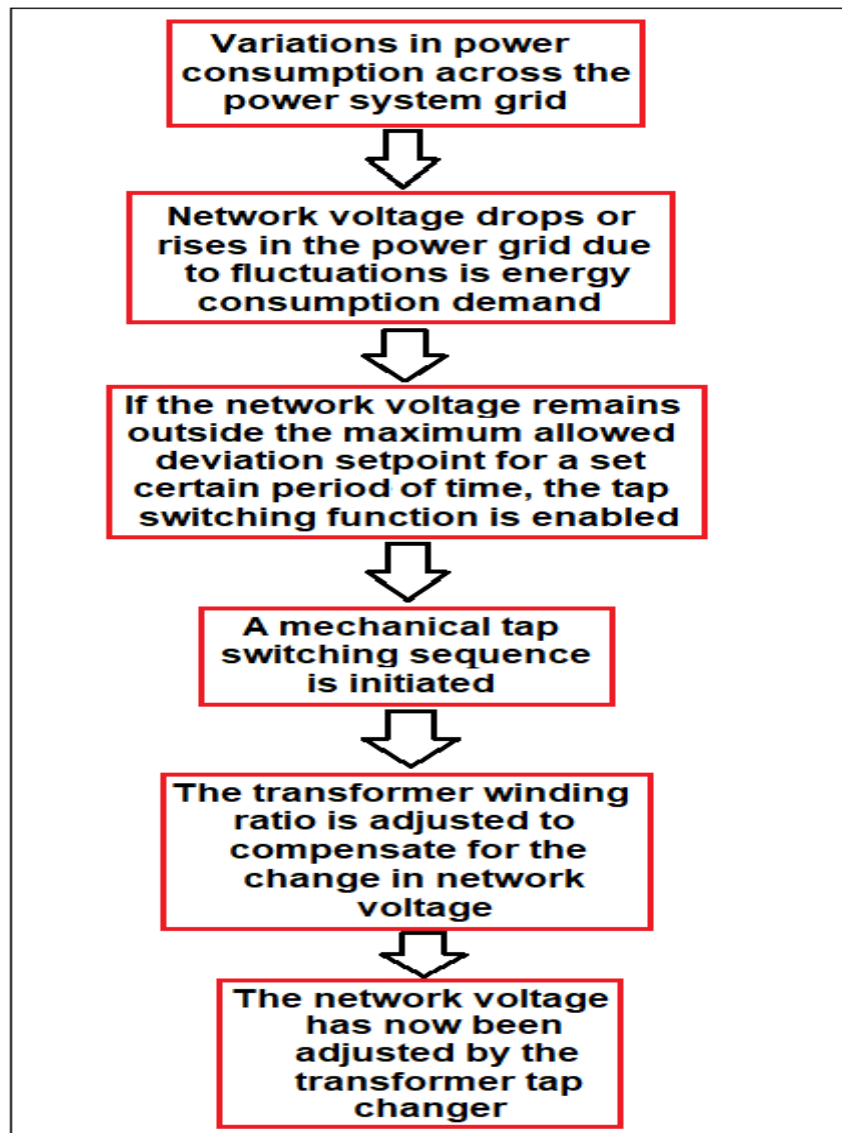


**Figure 57: Basic control operation of OLTC to regulate the network voltage (Banakar, Muralidhara, Maheswara Rao, 2016)**

The control methods for parallel transformers equipped with OLTCs is shown in 3.4.1 Master-Follower Control Method, 3.4.2 Circulating current method and 3.4.3 Negative reactance method.

### **3.4.1 Master-Follower Control Method**

The authors (Ferrero, Cimadevilla, Yarza, Solaun, 2014) indicated that the Master-Follower control method can be employed in scenarios where all the parallel power transformers have similar power ratings, the tap changers have an equal amount of steps, and they must be identical in voltage step ratio. To employ this control

method, (Constantin and Iliescu, 2012) said that only a voltage signal from the bus to be regulated is needed as input to the controller. Utilizing this control method essentially means that all the parallel transformers operate in unison, behaving as a single synchronized entity. An infinite number of transformers can be placed in parallel using this control method. The Master transformer monitors the system voltage and decides if corrections will be made when voltage levels fall below or rise above a certain threshold value for a predetermined time. When the system voltage deviates outside the dead band setting value, the master relay issues a lower or rise tap control signal. This signal is sent to the master OLTC. The current tap position of the master OLTC is sent to the Follower, which will also issue the appropriate signal to synchronize its tap position with that of the master. Out-of-step protection is recommended when the Master and Followers steps are not synchronised. This should stop the Master from issuing lowering or raising tap commands until tap synchronization is achieved. A drawback of this method is that a constant method of communication between the Master and Follower transformers is required.

### **3.4.2 Circulating current method**

The authors (Gajic, Aganovic, Benovic, Leci, Gazzari, 2010) proposed that the circulating current method can be utilized when the parallel transformers have an equal or different power rating. The OLTCs can also have different step voltage ratios when this control scheme and offer the optimal solution when connected to irregular reactive loads. This control method optimizes the load voltage while eliminating the circulating current flowing between the parallel transformers. (Yarza, Cimadevilla, 2014) indicated that a reactive circulating current is the result of parallel transformers not having matching voltages at when tap positions is synchronized. The impedance and the difference in voltage magnitude of the parallel transformers influence the extent of this circulating current. The transformer losses are proportional to the magnitude of the circulating current flowing between the parallel transformers. To use this OLTC control method, the controller requires voltage and current signals. A communication protocol such as IEC 61850 GOOSE, MMS or DNP3, etc., is needed for peer-to-peer communication between the control devices and a SCADA system. This communication protocol is also employed of the transmit magnitude and phase angle data required to calculate the circulating current flowing between transformers.



### 3.4.3 Negative reactance method

This method of OLTC control can be implemented as an alternative or substitute method for the circulating current control method. (Yarza, Cimadevilla, 2014) believes a proven benefit when using this method is that no communication protocol or structure of communication needs to be established between the controlling devices. The voltage regulation devices execute the controlling function entirely independently, and transformer ratings need not be equal. To use this method of OLTC control, the controllers require voltage and current signals. By comparing the phase angle measured by the controller to the load phase angle setting the circulating current can be determined. (Ferrero, Íñigo, Cimadevilla, Yarza, Solaun, 2014) said a crucial observation when employing this control method is that a stable load phase angle is required to maintain the expected voltage levels. Any fluctuations in the phase angle of the load will result in voltage deviations. This will adversely impact the voltage regulation function, resulting in an undesired and unstable voltage environment.

### 3.4.4 Discussion of the Control methods for OLTCs on parallel transformers

Some method of control is needed to regulate and perform this control function of the OLTC of power transformers. The type of control method significantly employed depends on the characteristics and parameters of the parallel transformers. As stated by (Ferrero, Cimadevilla, Yarza, Solaun, 2014) to employ a master-follower control method, the transformers in parallel need almost be identical in every aspect. The benefit of using this method, according to (Constantin and Iliescu, 2012), is that only a voltage signal is needed by the controller. The parallel transformers do not need to be identical when using a circulating current method. This control method optimizes the load voltage while eliminating the circulating current between the parallel transformers. For the master-follower and circulating current control method, communication structure is required between the controllers. The harmful reactance control method can be used as a substitute for the circulating current method. (Yarza, Cimadevilla, 2014) believes the main benefit of this method is that it requires no communication between the controllers of the parallel transformers. A crucial

requirement for the harmful reactance control method is that a stable load phase angle is necessary to maintain the expected voltage levels.

### **3.5 Modelling and simulation of the modified IEEE 14 bus network**

The IEEE 14 Bus Network was first introduced as far back as 1962. It is a power system network consisting of 14 buses, 11 loads, and 5 generators. The network was officially standardized in the 2000s by the IEEE PES to be used across different simulation platforms as a standard model. The network is widely used by researchers in power engineering, industry, and education to conduct power systems analysis. It is also frequently adapted and extended to cater to implementing modern technologies such as grid automation and integrated with renewable energy studies.

The aim of the DIgSilent implementation of the modified version of the IEEE 14 bus is to model the network in the DIgSilent PowerFactory 2023 software. An identical transformer is parallel to the existing transformer between 132kV Bus 5 and 33kV Bus 6 in the network. Load flow studies are conducted on the network for different network loading conditions, and the results are analyzed and compared to the load flow results obtained in Chapter 5.

Shown in [Figure 58](#) is the Modified IEEE 14 Bus Network with parallel transformers used in this study.

#### **3.5.1 Data of the Modified version of the IEEE 14 bus network**

The standard IEEE 14 Bus Network was obtained from the power system library within the DIgSilent software. The standard model parameters (data found in Appendix B) were the template from which the Modified IEEE 14 Bus Network was developed. Shown in [Table 14](#) Provides the details of the network's load demand.

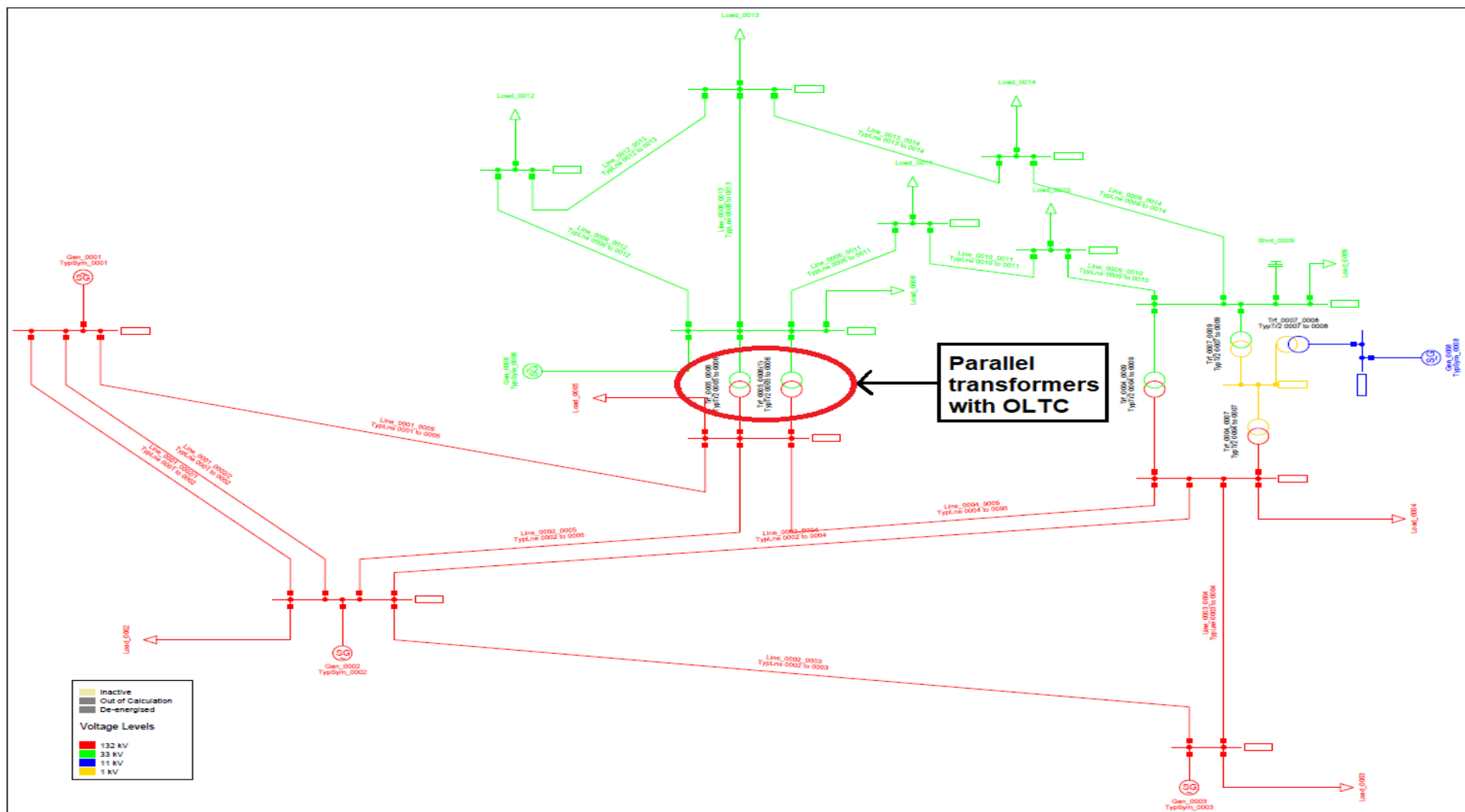


Figure 58: Modified IEEE 14 Bus Network with parallel transformers

**Table 14: Load demand of network**

Load	Bus	P in MW	Q in Mvar
Load 0002	Bus 0002	21.7	12.7
Load 0003	Bus 0003	94.2	19.0
Load 0004	Bus 0004	47.8	-3.9
Load 0005	Bus 0005	7.6	1.6
Load 0006	Bus 0006	11.2	7.5
Load 0009	Bus 0009	29.5	16.6
Load 0010	Bus 0010	9.0	5.8
Load 0011	Bus 0011	3.5	1.8
Load 0012	Bus 0012	6.1	1.6
Load 0013	Bus 0013	13.5	5.8
Load 0014	Bus 0014	14.9	5.0

Shown **Table 15** is the network's generator controller settings.

**Table 15: Generator controller settings**

Generator	Bus Type	Voltage in p.u.	Minimum capability in MVA	Maximum capability in MVA
Gen 0001	Slack	1.060	N.A.	N.A.
Gen 0002	PV	1.045	-40.0	50.0
Gen 0003	PV	1.010	0.0	40.0
Gen 0006	PV	1.070	-6.0	24.0
Gen 0008	PV	1.090	-6.0	24.0

Shown **Table 16** is the data of the lines of the network.

**Table 16: Data of lines in the model**

Line	From Bus	To Bus	Un in kV	R in $\Omega$	X in $\Omega$	B in $\mu S$
Line 0001 0002/1	1	2	132.0	6.753542	20.619560	151.5152
Line 0001 0002/2	1	2	132.0	6.753542	20.619560	151.5152

Line 0001 0005	1	5	132.0	9.414187	38.862490	282.3691
Line 0002 0003	2	3	132.0	8.187537	34.494280	251.3774
Line 0002 0004	2	4	132.0	10.125090	30.722000	214.6465
Line 0002 0005	2	5	132.0	9.922968	30.296850	195.1331
Line 0003 0004	3	4	132.0	11.675820	29.800270	198.5767
Line 0004 0005	4	5	132.0	2.326104	7.337246	73.4619
Line 0006 0011	6	11	33.0	1.034332	2.166021	0.0000
Line 0006 0012	6	12	33.0	1.338490	2.785771	0.0000
Line 0006 0013	6	13	33.0	0.720374	1.418640	0.0000
Line 0009 0010	9	10	33.0	0.346411	0.920205	0.0000
Line 0009 0014	9	14	33.0	1.384228	2.944439	0.0000
Line 0010 0011	10	11	33.0	0.893524	2.091643	0.0000
Line 0012 0013	12	13	33.0	2.405819	2.176693	0.0000
Line 0013 0014	13	14	33.0	1.861428	3.789938	0.0000

Shown **Table 17** is the data of the transformers of the network. The details of the added transformer are also included.

**Table 17: Data of transformers given on a base of 100MVA, included is rated voltages**

<b>Trans- former</b>	<b>From Bus</b>	<b>To Bus</b>	<b>Ur HV in kV</b>	<b>Ur LV in kV</b>	<b>r in p.u.</b>	<b>x in p.u.</b>	<b>Transformer final turns ratio</b>
Trf 0004 0007	4	7	132.0	1.0	0.0	0.20912	0.978
Trf 0004 0009	4	9	132.0	33.0	0.0	0.55618	0.969
Trf 0005 0006 [A]	5	6	132.0	33.0	0.0	0.25202	0.932
Trf 0005 0006 [B]	5	6	132.0	33.0	0.0	0.25202	0.932
Trf 0007 0008	7	8	11.0	1.0	0.0	0.17615	0.000

Trf 0007 0009	7	9	33.0	1.0	0.0	0.11001	0.000
------------------	---	---	------	-----	-----	---------	-------

### 3.5.2 Implementation of DigSilent Power Factory model

An identical transformer is placed parallel with the existing transformer between 132kV Bus 5 and 33kV Bus 6 in the network. Shown in Figure 59 is the parallel transformer pair between Bus 5 and Bus 6.

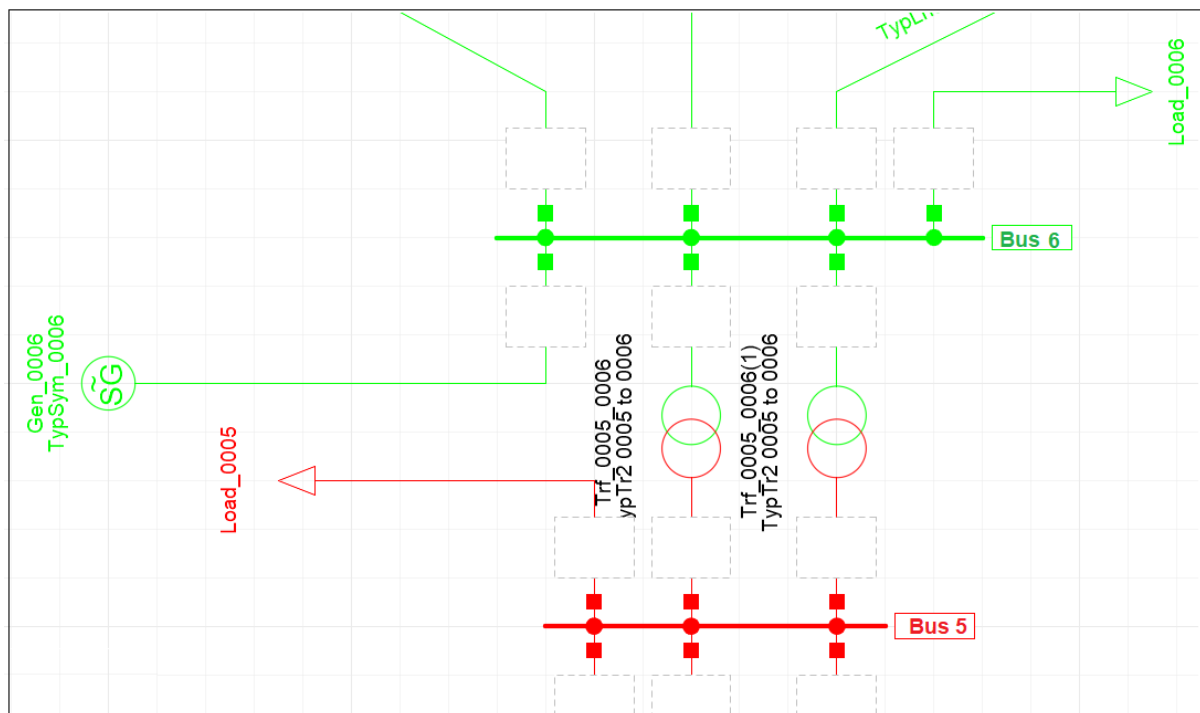


**Figure 59: Parallel transformers between Bus 5 & Bus 6**

Shown in Figure 60 is the Transformer between Bus 5 & Bus 6 . As can be seen from Figures 3-7, the transformer has a rating of 100MVA, an HV of 132 kV and LV side of 33 kV.

An identical 100MVA transformer is placed in parallel with this transformer between Bus 5 and Bus 6. Shown in Figure 61 is the procedure for adding the identical transformer.

2-Winding Transformer Type - Equipment Type Library\TypTr2 0005 to 0006.TypTr2

<b>Basic Data</b>	Name	TypTr2 0005 to 0006	
Description	Technology	Three Phase Transformer	
Version	Rated Power	100,	MVA
Load Flow	Nominal Frequency	60,	Hz
Short-Circuit VDE/IEC	Rated Voltage		
Short-Circuit Complete	HV-Side	132,	kV
Short-Circuit ANSI	LV-Side	33,	kV
Short-Circuit IEC 61363	Vector Group		
Short-Circuit DC	HV-Side	YN	
	LV-Side	YN	
	<input type="checkbox"/> Internal Delta Winding		
Simulation RMS	Phase Shift	0,	*30deg
Simulation EMT	Name	YNyn0	
Protection	Positive Sequence Impedance		
Power Quality/Harmonics	Reactance x1	0,25202	p.u.
Reliability	Resistance r1	0,	p.u.
Hosting Capacity Analysis	Zero Sequence Impedance		
Power Park Energy Analysis	Short-Circuit Voltage uk0	0,	%
Optimal Power Flow	SHC-Voltage (Re(uk0)) uk0r	0,	%

Figure 60: Transformer between Bus 5 & Bus 6

2-Winding Transformer - Grid\Trf\_0005\_0006.ElmTr2\*

<b>Basic Data</b>	<b>General</b>	<b>Grounding/Neutral Conductor</b>
Description	Name	Trf_0005_0006
Load Flow	Type	Equipment Type Library\TypTr2 0005 to 0006
Short-Circuit VDE/IEC	HV-Side	Grid\Bus_0005\Cub_4 Bus_0005
Short-Circuit Complete	LV-Side	Grid\Bus_0006\Cub_4 Bus_0006
Short-Circuit ANSI	Zone	HV-Side
Short-Circuit IEC 61363	Area	HV-Side
Short-Circuit DC	<input type="checkbox"/> Out of Service	
Simulation RMS	Number of parallel Transformers	2
Simulation EMT	Thermal Rating	
Protection	Meteo. Station	
Power Quality/Harmonics	Rating Factor	1, Nominal Power (act.) 200, MVA
Tie Open Point Opt.	<input type="checkbox"/> Auto Transformer	
Reliability	Supplied Elements	
Hosting Capacity Analysis	Mark Elements in Graphic	Edit Elements
Power Park Energy Analysis		
Optimal Power Flow		
Unit Commitment		
Optimal Equipment Placement		
State Estimation		

Indicates 2 parallel transformers

Figure 61: Indication of two parallel transformers between Bus 5 & Bus 6

OLTCs are added to both the parallel transformers. The OLTCs were added to the high-voltage windings of the transformers. See Figure 62 for configuring the OLTCs of the parallel transformers. Each tap would add or subtract 0.7% voltage. The

OLTCs will each have 20 taps, with Tap 10 being the neutral tap. Tap 20 is the maximum tap, and tap 0 is the minimum tap position.

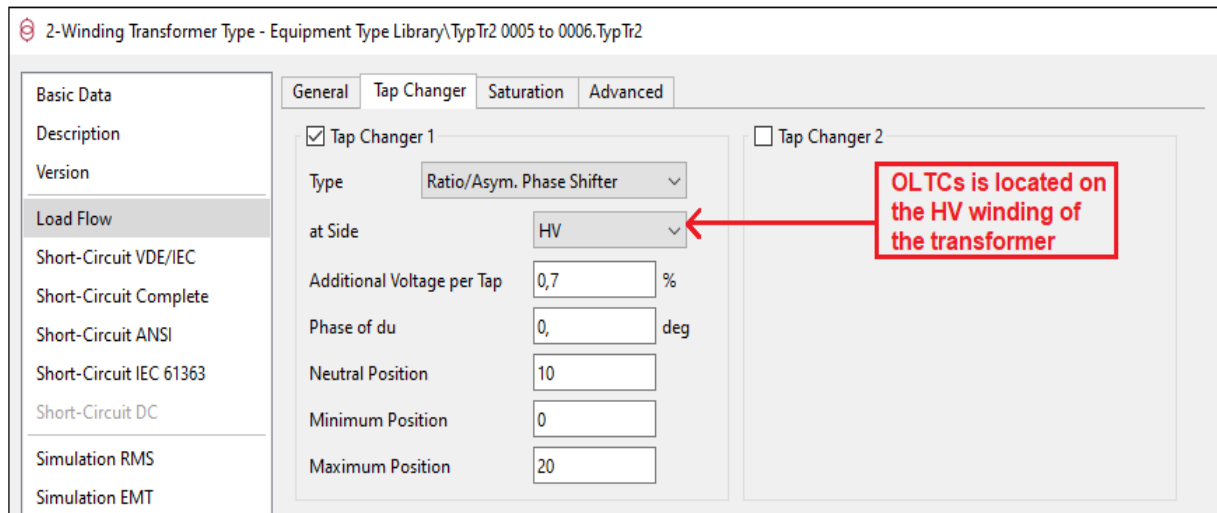


**Figure 62: Configuring the OLTCs of the parallel transformers**

Once the OLTCs have been configured, the base caseload flow can be calculated using the load flow calculating function of DlgSilent

### 3.5.3 Load Flow Analysis

Calculating load in a power system network is a computational procedure for analysing the power network under various operating conditions and scenarios. It gives the power system engineer a deeper understanding of how power is transferred in the network. Power flow calculations are based on Kirchhoff's circuit laws and aim to calculate the operating point where the circuit runs at its optimal steady-state condition. Shown in Figure 63 is the load flow analysis diagram with input and outputs is shown.

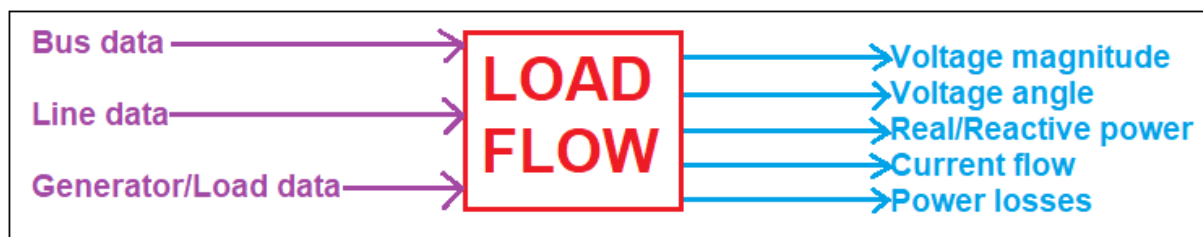


**Figure 63: Load Flow Analysis Diagram**



The results obtained from calculating the load flow of a network assist power systems engineers and planners analyze the loading capacity of transformers, transmission lines, generators, and various power system equipment. They can better plan to make sure that network voltage levels do not fluctuate from the statutory limits set for the network. The power system losses can be analyzed, and equipment operating near its overload capacity can be identified; plans can thus be put in place to address these network concerns. Future network expansion strategies can be developed to mitigate the problems the power system load flow analysis exposed. To calculate load flow analysis, different numerical techniques are used to determine the solution for resolving nonlinear power flow equations. The various methods and their characteristics used in DIgSilent for calculating load flow are shown in [Table 18](#).

**Table 18: Numerical techniques for calculating load flow in the power system in DIgSilent software (Dubey, 2016)**

<b>Gauss-Seidel Method</b>	<b>Newton-Raphson Method</b>	<b>Fast Decoupled Load Flow Method</b>
Step-by-step approximation method.	Power system engineers most often use this solution.	This solution is simpler and best suited for online applications.
Large and complex systems exhibit slow execution of solution convergence.	Better solution convergence achieved typically achieves results within 3-5 iterations	Decouples real & reactive power components, allowing for independent analysis.
Potential solution divergence caused by sensitivity to numerical perturbations.	Linear equation is solved by employing matrix inversion techniques.	Results are calculated faster but with reduced accuracy than the Newton-Raphson Method.
	Solution calculations are executed by employing the Jacobian matrix formulation.	

### 3.5.4 Load Flow Analysis

Load flow calculations were conducted on the Modified version of the IEEE 14 bus network. Load flow calculations were done under different network loading conditions with varying positions of tap of the OLTCs of parallel transformers. The results are scrutinized to verify the performance of the OLTC in correcting the voltage profile of the affected busses. See Figure 64 to perform load flow calculations in the DlgSilent software.

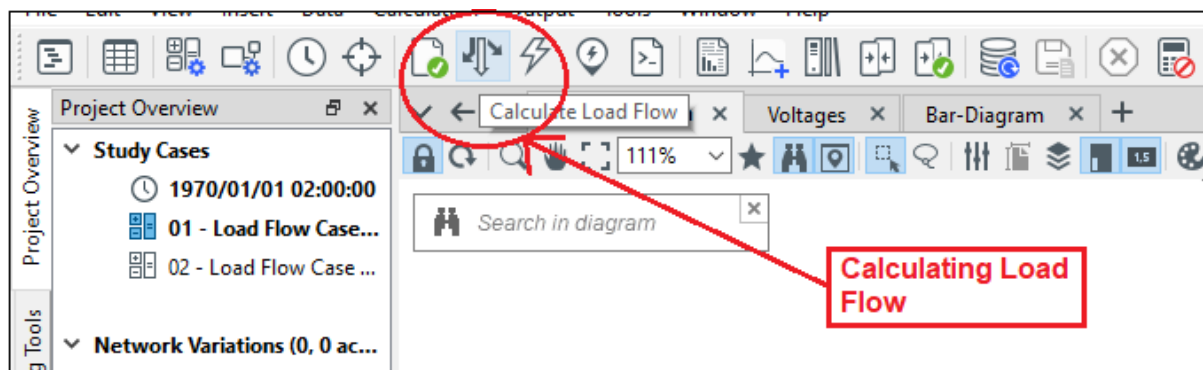


Figure 64: Calculating load flow in DlgSilent software

#### 3.5.4.1 Calculating Load Flow with base case values

Load flow calculation is conducted using the values from Table 14 to Table 17 with the two parallel transformers between Bus 5 and Bus 6. This was done to ensure that the results obtained with the parallel transformer added to the network under normal operating conditions yield similar results. Shown in Figure 65: Results for base case values of Bus 5 & Bus 6 from DlgSilent.

Shown in Figure 66 is the load flow results for base case values of Bus 5 & Bus 6 from RSCAD. Comparing the load flow results for the base values is tabled in Table 19. The load flow results yield similar values. This verifies that under normal operating conditions, the load flow results obtained with the parallel transformer added to the network yield similar results.

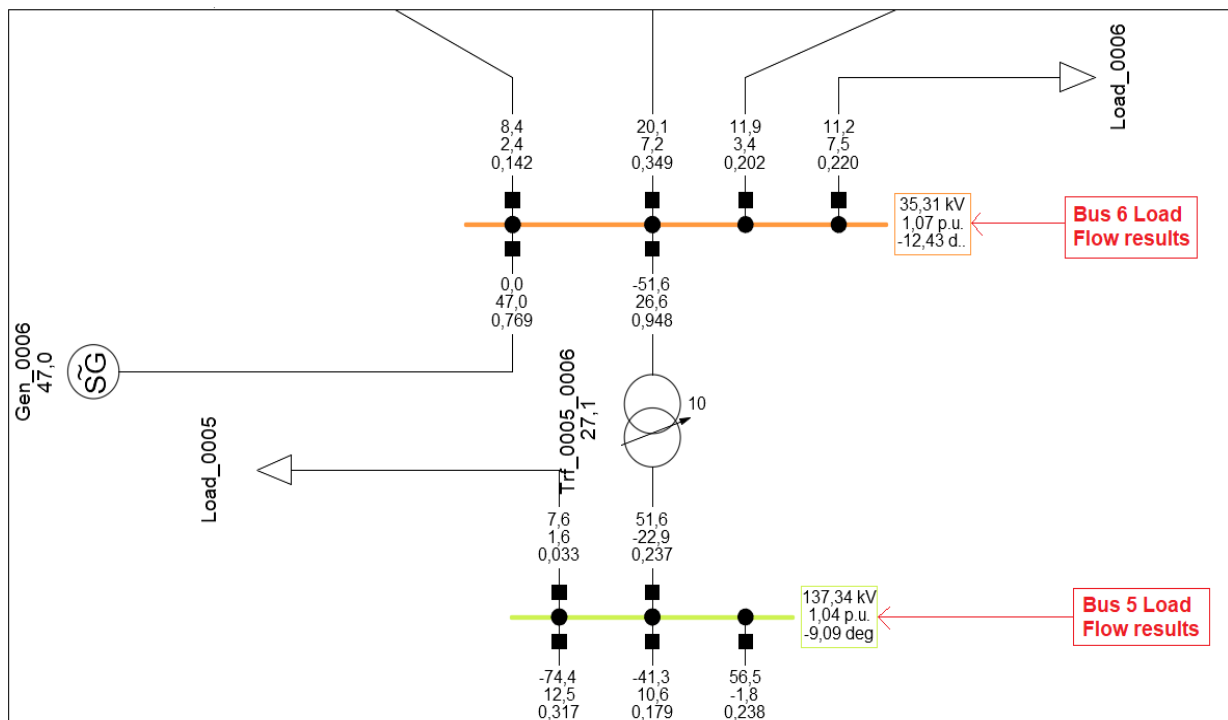


Figure 65: Results for base case values of Bus 5 & Bus 6 from DIgSILENT

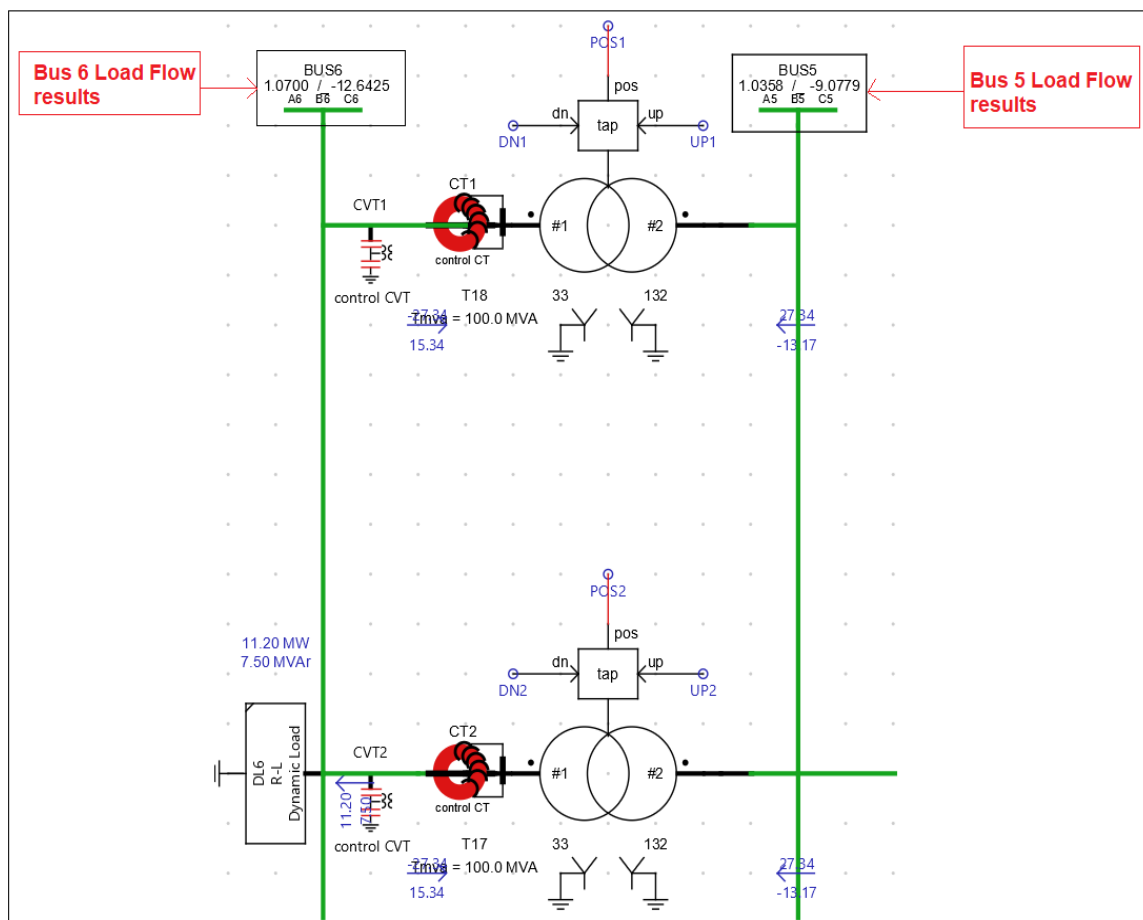


Figure 66: Results for base case values of Bus 5 & Bus 6 from RSCAD

**Table 19: Load flow results from Bus 5 & Bus 6 for the base case**

	DlgSilent			RSCAD		
	kV L-L	V  pu	Angle in degree	kV L-L	V  pu	Angle in degree
<b>Bus 5</b>	137.34	1.04	-9.09	136.72	1.0358	-9.0779
<b>Bus 6</b>	35.31	1.07	-12.43	35.31	1.07	-12.6425

### 3.5.4.2 Investigating the load flow for steady-state conditions

Investigating the power load flow, the dynamic load on Bus 6 is set to a value of **75 MW and 24 MVAR**. This loading condition of Bus 6 causes the voltage magnitude to rise to 32.16 kV L-L, which results in a per-unit voltage value of 0.97. The tap position for both OLTCs of the parallel transformer is at position 10. This loading condition is within the 5% acceptable voltage deviation value and thus requires no intervention from the automatic voltage control function. Shown in [Figure 67](#) is the load flow results for steady-state loading condition values of Bus 5 & 6 from DlgSilent.

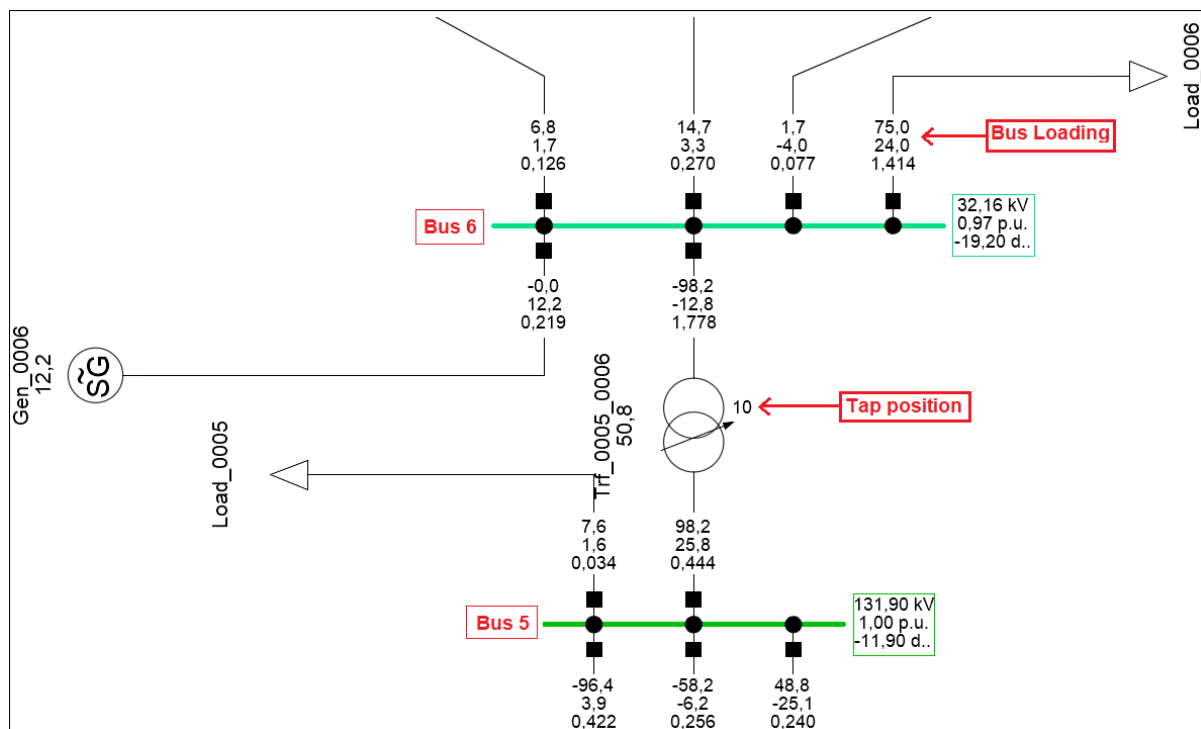


**Figure 67: Results for steady-state condition loading of Bus 5 & Bus 6 from DlgSilent**

Shown in Figure 68 is the result of the DlgSilent load flow calculations for bus voltage magnitudes at steady-state conditions.

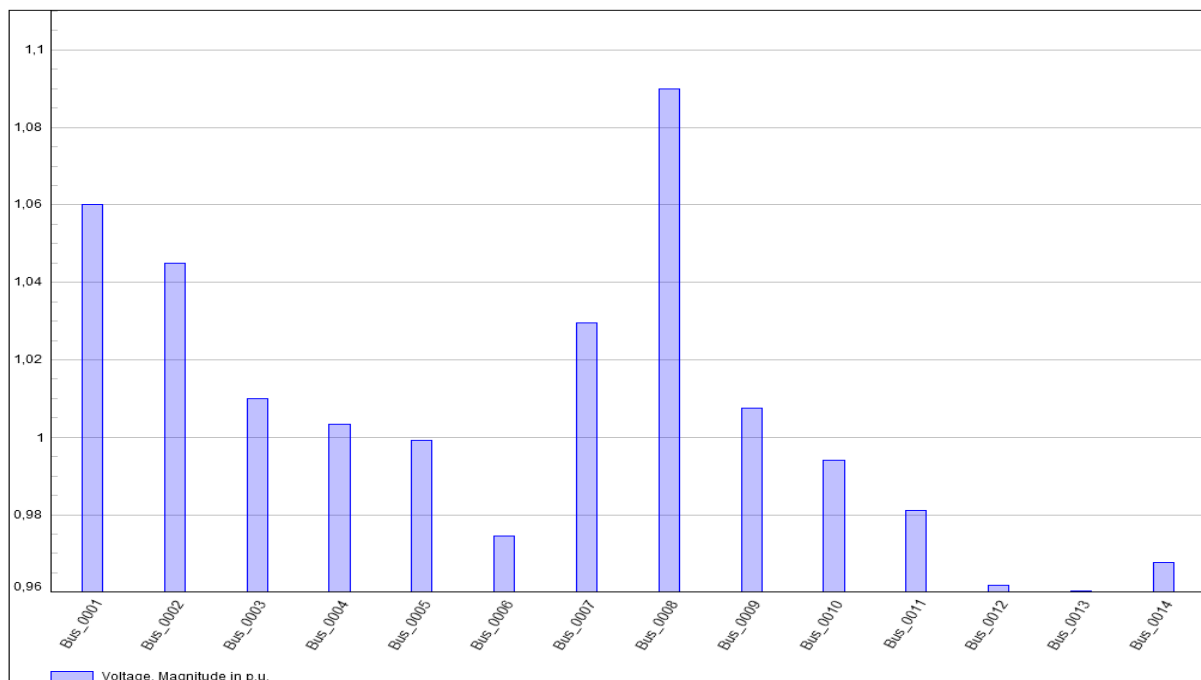


**Figure 68: Voltage magnitudes of Buses for steady-state conditions from DlgSilent**

Shown in Table 20 are the results from the DlgSilent load flow calculations for Bus 5 and Bus 6 voltage magnitudes at steady-state conditions.

**Table 20: Steady state load conditions for Bus 5 and Bus 6 voltage, with voltage magnitudes obtained from DlgSilent - no corrections needed**

Tap_Pos = 10	kV L-L	V  pu	Angle in degree
Bus 5	131.90	1.00	-11.90
Bus 6	32.16	0.97	-19.20

### 3.5.4.3 Investigating the Load Flow for over-voltage conditions

Investigating the power load flow, the dynamic load on Bus 6 is set to a value of **5.6 MW and 11 MVAR**. This loading condition of Bus 6 causes the voltage magnitude to rise to 33.69 kV L-L, which results in a per-unit voltage value of 1.02. Tap position for both OLTCs of the parallel transformer is at position 10. This loading condition is within the 5% acceptable voltage deviation value and thus requires intervention from

the OLTCs to better the voltage profile at Bus 6. Shown in Figure 69 are the initial load flow results for over-voltage loading condition values of Bus 5 & Bus 6 from DlgSilent before tap positions are adjusted.

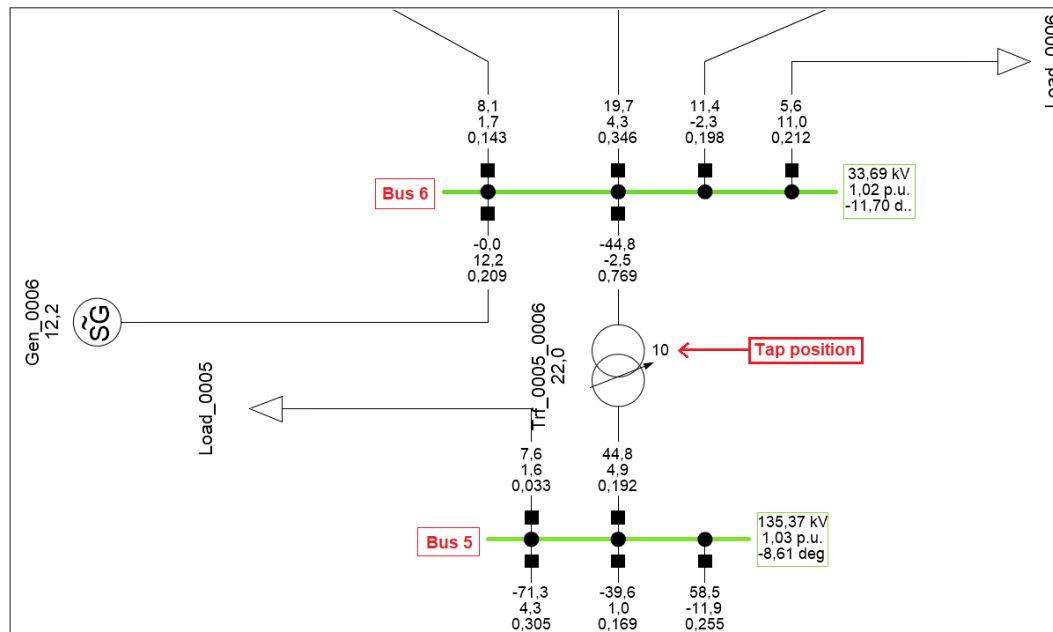


**Figure 69: Initial load flow results for over-voltage loading conditions of Bus 5 and Bus 6 from DlgSilent before tap positions are adjusted**

Shown in Figure 70 are the results from DlgSilent for voltage magnitudes of Buses for over-voltage conditions before tap positions are adjusted.

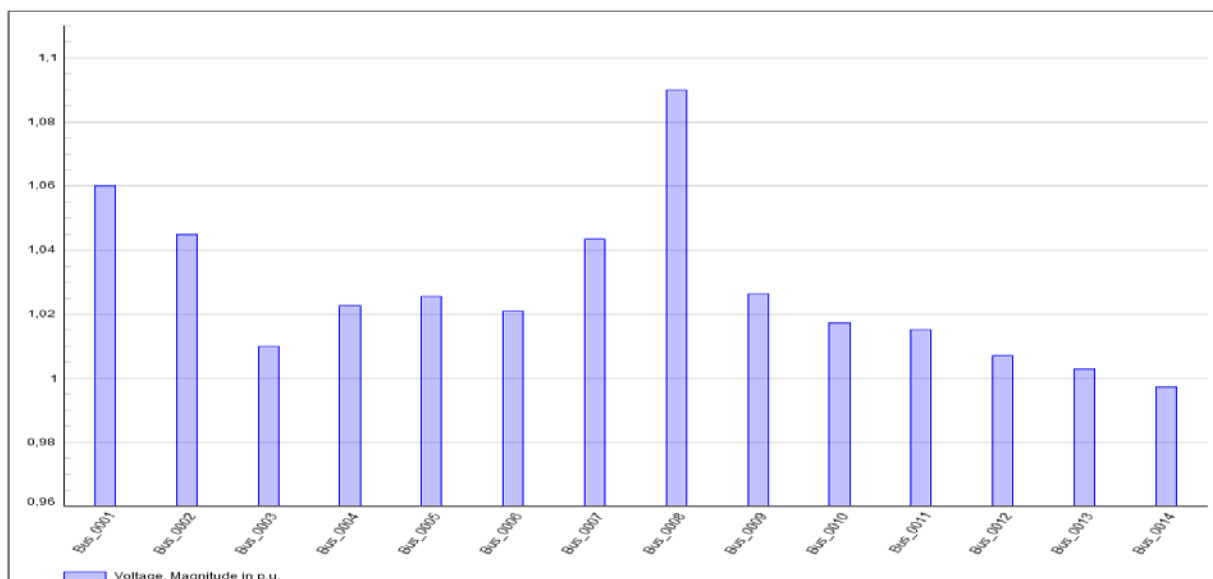


**Figure 70: Voltage magnitudes of Buses for initial over voltage conditions from DlgSilent - before tap position is adjusted**

Shown in **Table 21** are the results from the DIgSilent load flow calculations for Bus 5 and Bus 6 voltage magnitudes at overvoltage conditions before tap positions are adjusted.

**Table 21: Over voltage load conditions for Bus 5 and Bus 6 voltage, with voltage magnitudes obtained from DIgSilent – before tap position is adjusted**

Tap_Pos = 10	kV L-L	V  pu	Angle in degree
<b>Bus 5</b>	135.37	1.03	-8.61
<b>Bus 6</b>	33.69	1.02	-11.70

With the OLTCs positions raised 13; the parallel transformers achieved a better LV voltage magnitude at Bus 6. Shown in **Figure 71** are the corrected load flow results for the over-voltage loading condition values of Bus 5 and Bus 6 from DIgSilent after the tap positions are adjusted. With the OLTCs position at 13, a magnitude of 33.16 kV at Bus 6 is achieved.

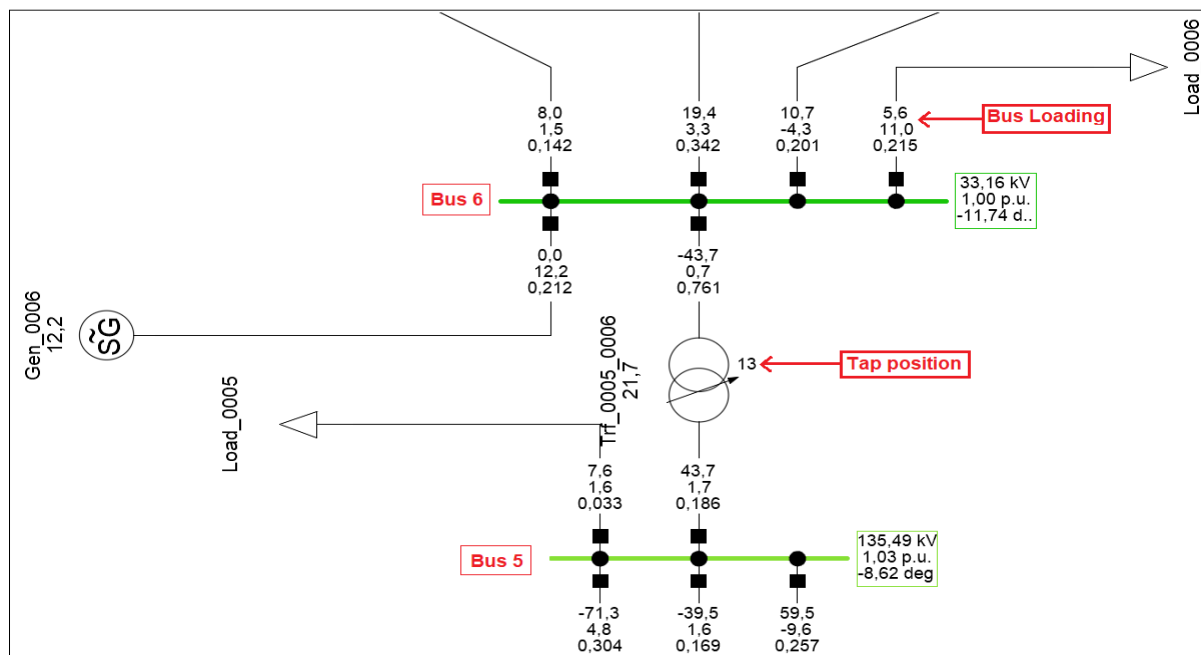


**Figure 71: Load flow results for the over-voltage loading condition values of Bus 5 and Bus 6 from DIgSilent after the tap positions are adjusted**

Shown in **Figure 72** are the results from DIgSilent for voltage magnitudes of Buses for over-voltage conditions before and after tap positions are adjusted.

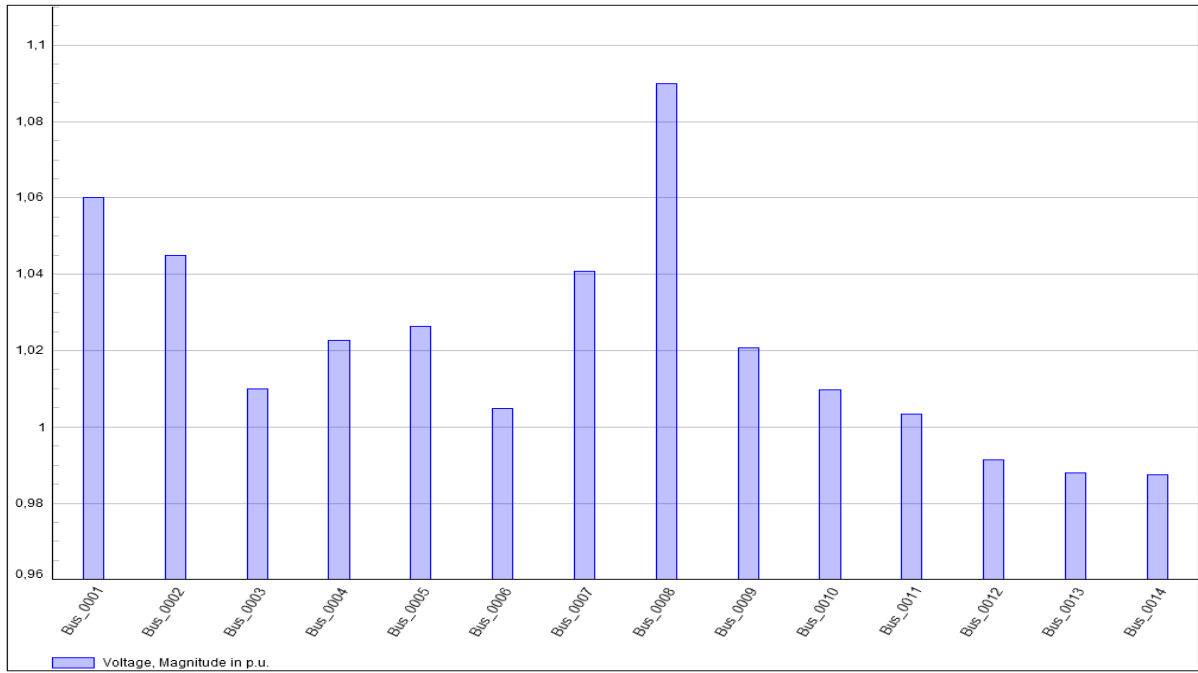


**Figure 72: Voltage magnitudes of Buses for over-voltage conditions from DIgSilent - after tap position is adjusted**

Shown in **Table 22** is the results from DIgSilent for voltage magnitudes of Buses for over-voltage conditions after tap positions are adjusted.

**Table 22: Over voltage load conditions for Bus 5 and Bus 6 voltage, with voltage magnitudes obtained from DIgSilent – after tap position is adjusted**

Tap_Pos = 13	kV L-L	V  pu	Angle in degree
Bus 5	135.49	1.03	-8.62
Bus 6	33.16	1.00	-11.74

#### 3.5.4.4 Investigating the Load Flow for under voltage conditions

Investigating the power load flow, the dynamic load on Bus 6 is set to a value of **150 MW and 24 MVAR**. This loading condition of Bus 6 causes the voltage magnitude to decrease to 30.56 kV L-L, which results in a per-unit voltage value of 0.93. The tap position for both OLTCs of the parallel transformer is at position 10. This loading condition is within the 5% acceptable voltage deviation value and thus requires no intervention from the OLTCs to better the voltage profile at Bus 6. Shown in **Figure**



73 are the initial load flow results for over-voltage loading condition values of Bus 5 & Bus 6 from DlgSilent before tap positions are adjusted.

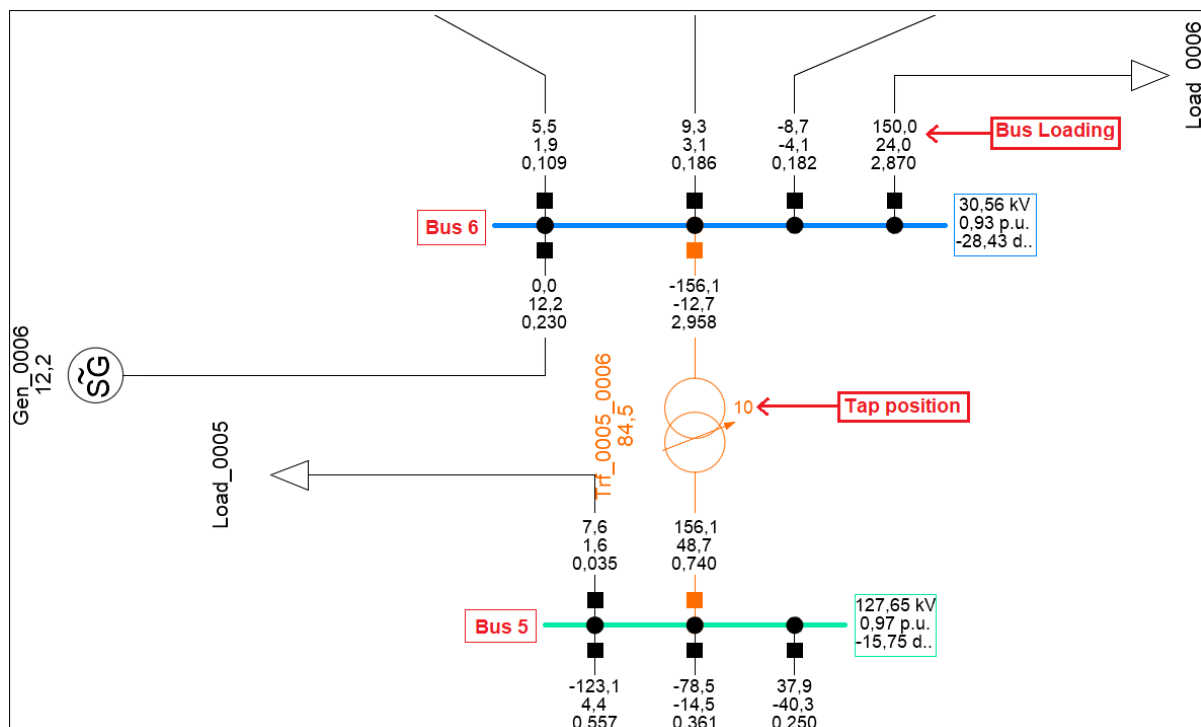


**Figure 73: Initial load flow results for under voltage loading conditions of Bus 5 & Bus 6 from DlgSilent - before tap positions is adjusted.**

Shown in Figure 74 are the results from DlgSilent for voltage magnitudes of Buses under voltage conditions before tap positions are adjusted.

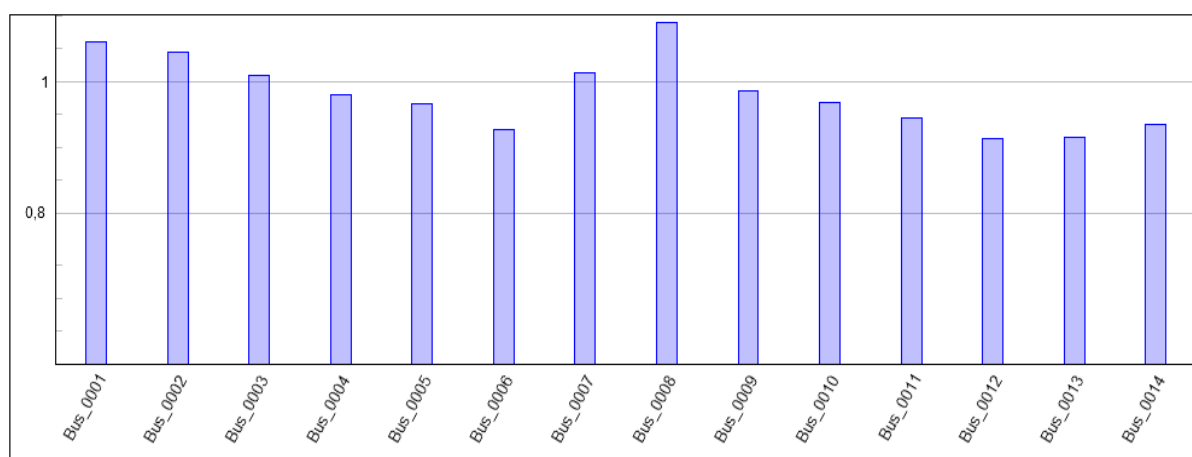


**Figure 74: Voltage magnitudes of Buses for initial under voltage conditions from DlgSilent - before tap position is adjusted**

Shown in **Table 23** are the results from the DlgSilent load flow calculations for Bus 5 and Bus 6 voltage magnitudes under voltage conditions before tap positions are adjusted.

**Table 23: Under voltage load conditions for Bus 5 and Bus 6 voltage, with voltage magnitudes obtained from DlgSilent – before tap position is adjusted**

Tap_Pos = 10	kV L-L	V  pu	Angle in degree
Bus 5	127.65	0.97	-15.75
Bus 6	30.56	0.93	-28.43

With the OLTCs positions lowered to 5; the parallel transformers achieved a better LV voltage magnitude at Bus 6. Shown in **Figure 75** are the corrected load flow results for the over-voltage loading condition values of Bus 5 and Bus 6 from DlgSilent after the tap positions are adjusted. With the OLTCs position at 5, a magnitude of 31.55 kV at Bus 6 is achieved.

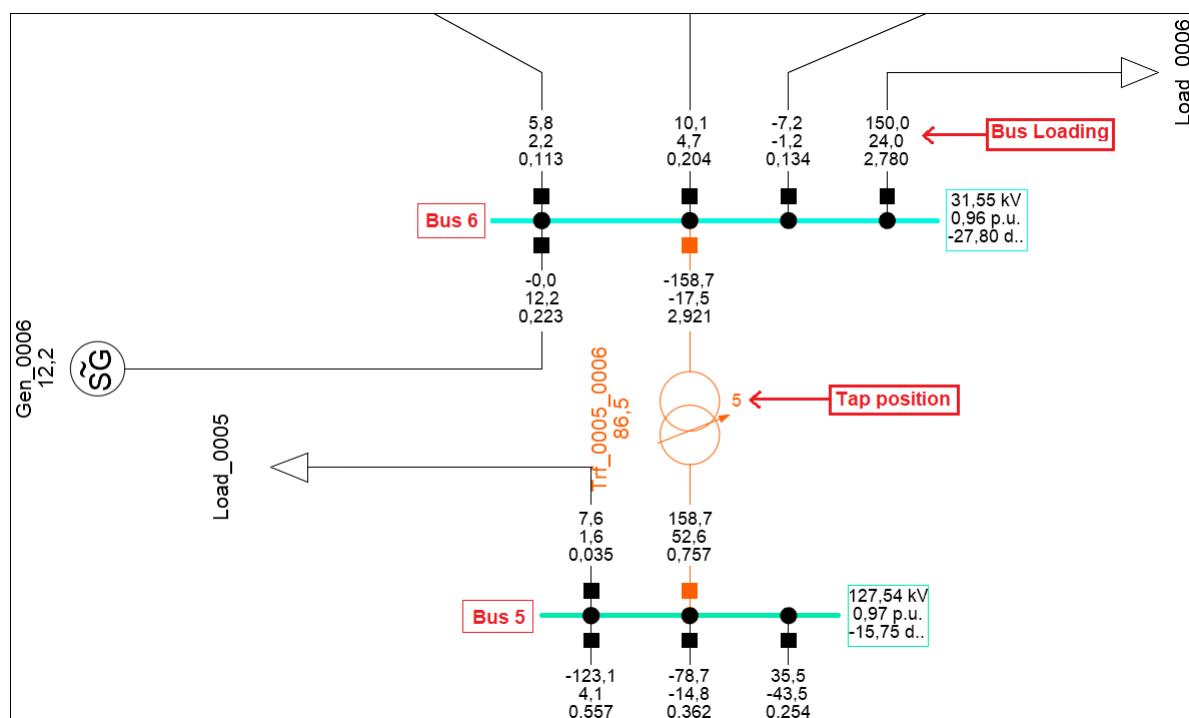


**Figure 75: Load flow results for over voltage loading condition values of Bus 5 & Bus 6 from DlgSilent - after tap positions is adjusted**

Shown in Figure 76 are the results from DlgSilent for voltage magnitudes of Buses under voltage conditions after tap positions are adjusted.

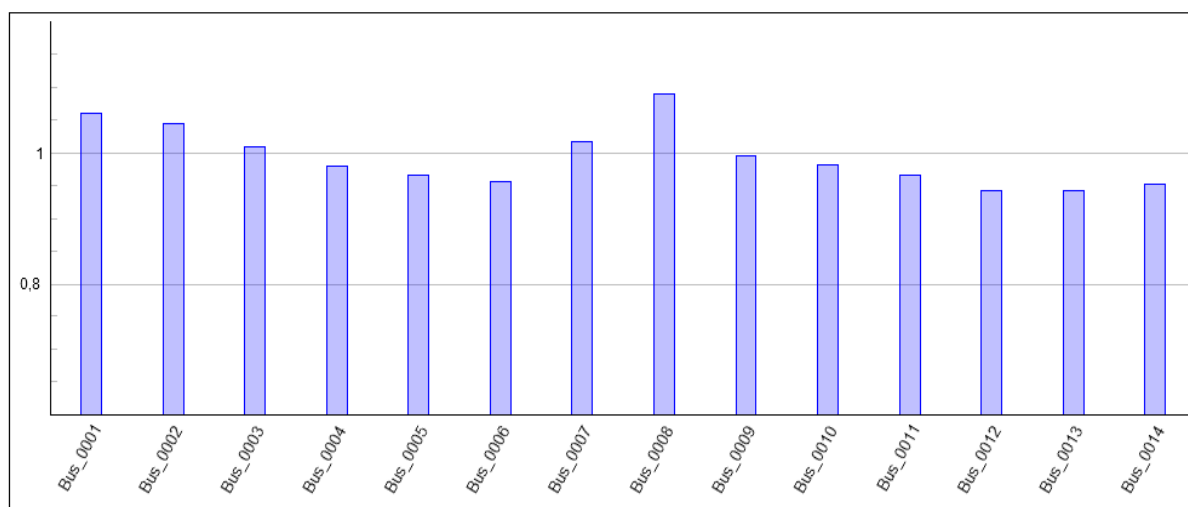


**Figure 76: Voltage magnitudes of Buses for under voltage conditions from DlgSilent - after tap position is adjusted**

Shown in Table 24 are the results from DlgSilent for voltage magnitudes of Buses under voltage conditions after tap positions are adjusted.

**Table 24: Under voltage load conditions for Bus 5 and Bus 6 voltage, with voltage magnitudes obtained from DlgSilent – after tap position is adjusted**

Tap_Pos = 5	kV L-L	V  pu	Angle in degree
Bus 5	127.54	0.97	-15.75
Bus 6	31.55	0.96	-27.80

### 3.5.4.5 Comparative study of the Load flow analysis for steady state, over voltage conditions, and under voltage conditions

This comparison of the results focuses on Bus 6, where the secondary side of the parallel transformers equipped with the OLTCs is located.

#### 3.5.4.5.1 Steady state load flow

This loading condition of **75 MW and 24 MVAR** on Bus 6 causes the voltage magnitude to rise to 32.16 kV L-L, which results in a per-unit voltage value of 0.97. The tap position for both OLTCs of the parallel transformer is at position 10. This

loading condition is within the 5% acceptable voltage deviation value and thus requires no intervention from the automatic voltage control function. Results of steady-state loading are shown in [Table 25](#).

**Table 25: Load flow results of steady-state loading conditions**

<b>Tap_Pos = 10</b>	<b>kV L-L</b>	<b> V  pu</b>	<b>Angle in degree</b>
<b>Bus 5</b>	131.90	1.00	-11.90
<b>Bus 6</b>	32.16	0.97	-19.20

### 3.5.4.5.2 Overvoltage load flow

A loading condition of **5.6 MW and 11 MVAR** on Bus 6 causes the voltage magnitude to rise to 33.69 kV L-L, which results in a per-unit voltage value of 1.02. The tap position for both OLTCs of the parallel transformer is at position 10. This loading condition is within the 5% acceptable voltage deviation value and thus requires intervention from the OLTCs to better the voltage profile at Bus 6. Although this loading condition is within the 5% voltage deviation range, the tap positions was adjusted to show the results of the improved voltage profile on Bus 6 of 33.16 kV L-L. The results of overvoltage loading on Bus 6 are shown in [Table 26](#). With the OLTC positions at Tap 13, the voltage profile is almost equal to the nominal voltage.

**Table 26: Load flow results of overvoltage loading conditions**

<b>Tap_Pos = 13</b>	<b>kV L-L</b>	<b> V  pu</b>	<b>Angle in degree</b>
<b>Bus 5</b>	135.49	1.03	-8.62
<b>Bus 6</b>	33.16	1.00	-11.74

### 3.5.4.5.3 Undervoltage load flow

A loading condition of 150 MW and 24 MVAR on Bus 6 causes the voltage magnitude to decrease to 30.56 kV L-L, which results in a per-unit voltage value of 0.93. The tap position for both OLTCs of the parallel transformer is at position 10. This loading condition is outside the 5% acceptable voltage deviation value and thus requires no intervention from the OLTCs to better the voltage profile at Bus 6. The OLTC tap positions are adjusted to show the improved voltage profile on Bus 6 of 31.55kV L-L. With the OLTC positions at Tap 5, the voltage profile is improved to

0.96 per unit, with a magnitude of 31.55 kV. This voltage level after tap adjustments is within the 5% dead band range and does not require further tap adjustments. **Table 27** shows the results of under-voltage loading on Bus 6.

**Table 27: Load flow results of under voltage loading conditions**

<b>Tap_Pos = 5</b>	<b>kV L-L</b>	<b> V  pu</b>	<b>Angle in degree</b>
<b>Bus 5</b>	127.54	0.97	-15.75
<b>Bus 6</b>	31.55	0.96	-27.80

### 3.6 Conclusion

From the comparison of load flow results of the different loading conditions, it can be concluded that the power transformers equipped with OLTCs are sufficient to maintain the voltage profile of Bus 6. OLTCs regulate and maintain the system voltage magnitude at the desired level on the load side at levels that clients connected to the grid would expect. Modern electrical supply networks' control of network voltages became more crucial due to the changing network topology. The power generating function is increasingly becoming more decentralized, with independent power producers connecting to the grid at various distributed entry points. These distributed entry points and changing load conditions on the power distribution side create the perfect conditions for voltage magnitudes to deviate and fluctuate from their desired set point. To stabilize the network voltage magnitude at a desired level, transformers fitted with OLTC is widely used for voltage regulation in power systems. The three most frequently implemented control methods for regulating system voltages employing OLTCs on parallel transformers is discussed.

DlgSilent Implementation demonstrates the implementation of the modified version of the IEEE 14 bus network modelled in the power system simulation tool DlgSilent PowerFactory 2023 software. Load flow studies are conducted on the network for different network loading conditions, and the results are analysed and compared to the load flow results obtained from the real-time results obtained from the RTDS software suite of the RSCAD environment in the next chapter and the comparison of results are discussed in chapter 4

## CHAPTER FOUR

### LAB SCALE SIMULATION AND TESTING OF THE POWER TRANSFORMER ON THE LOAD TAP CHANGER

#### 4.1 Introduction

Two **SEL-2414** Transformer Monitor relays were employed to perform the control function of the parallel power transformers in the network. These IEDs are programmed with custom-created algorithms to execute the automatic voltage control function using a **Master-Follower** control function. **IEC61850 GOOSE** communication will facilitate the interchange of communication between the two IEDs and the transmission of control signals to the RTDS equipment. The two SEL-2414 IEDs were configured and programmed utilizing the Quickset AcSELerator environment. One SEL-2414 relay will execute the function as the control relay for the OLTC of the Master transformer, and the other SEL-2414 relay will execute the function as the control relay for the OLTC of the Slave transformer. The Omicron Test Universe software was utilized to configure the Omicron CMC 356 signal generator device. The IEC 61850 GOOSE configuration was done using the Architect software.

This chapter aims to demonstrate the development and testing of the custom-created voltage control algorithms to control the OLTCs of the parallel transformer pair, the configuration settings of the Master and Slave-Follower relay, and the implementation of the IEC61850 GOOSE communication. The testing is executed by using the two Omicron CMC 356 test injection devices. The event files from the relays are scrutinized to analyze the voltage control function. The Wireshark Network Analyzer software was utilized to monitor the IEC 61850 GOOSE traffic on the network during the relay testing.

#### 4.2 Transformer Relay Control Configuration Settings

The two SEL-2414 IEDs were configured and programmed utilizing the Quickset AcSELerator software. One SEL-2414 relay will execute the control function of the relay for the OLTC of the Master transformer, and the other SEL-2414 relay will

execute the control function for the relay for the OLTC of the Slave-Follower transformer.

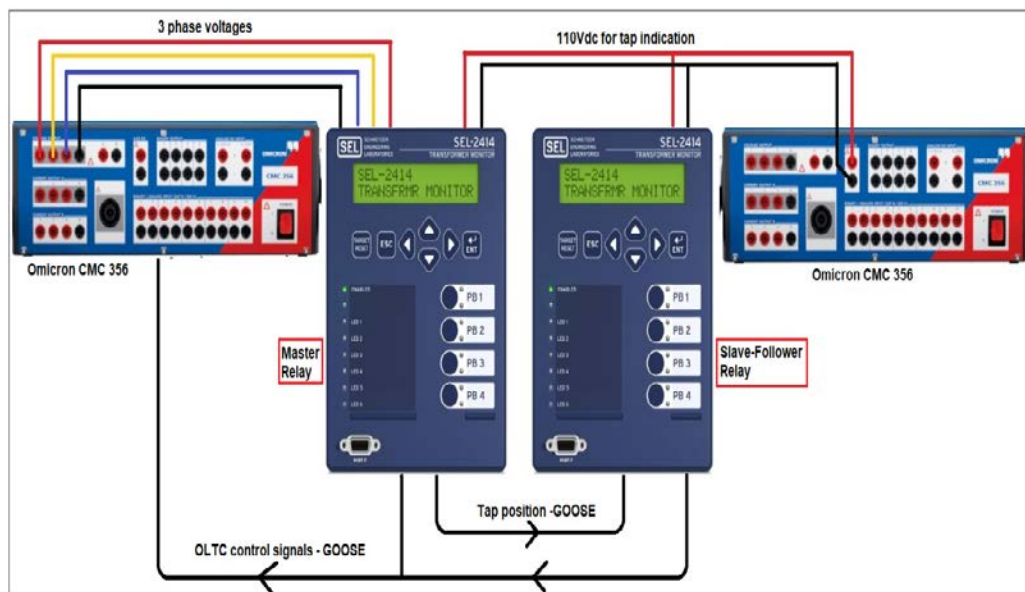


**Figure 77: Structure of the Lab-scale test bench setup for testing the Master- and Slave-Follower relays control algorithms and GOOSE configurations**

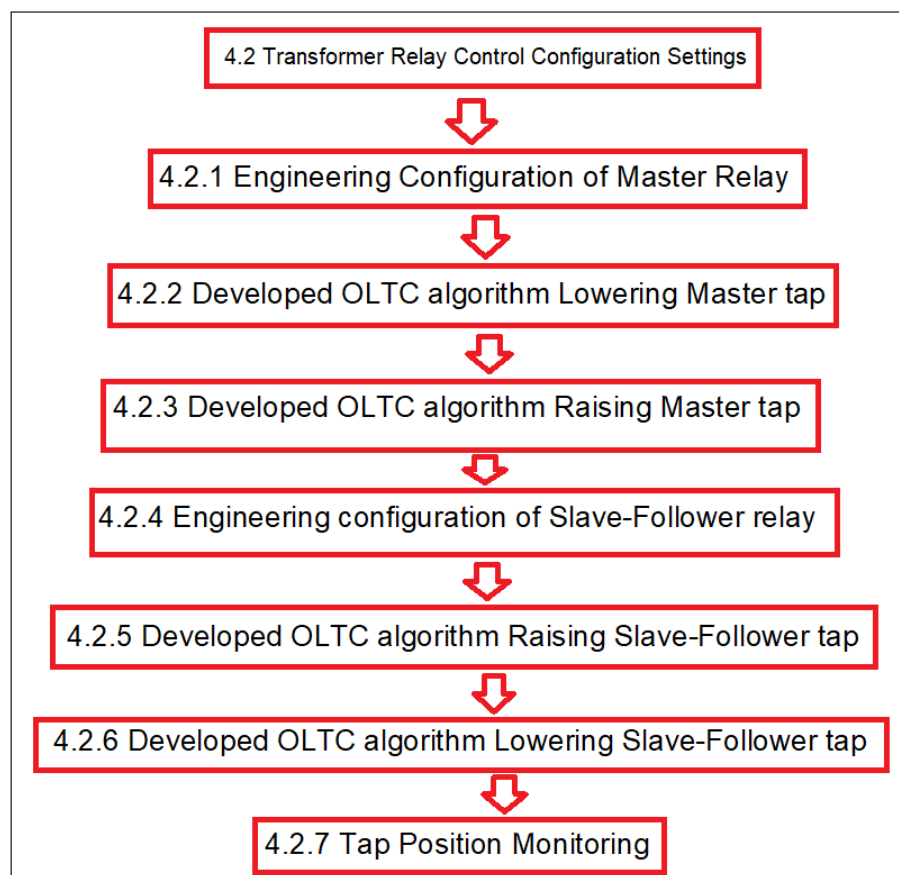


**Figure 78: Relay engineering configuration sequence followed**

The Omicron test universe software was utilized to configure the Omicron CMC 356 test signal generator device. The IEC 61850 GOOSE configuration was done using the Architect software. Shown in [Figure 77](#) is the structure of the Lab-scale test bench setup for testing the Master—and Slave-Follower relay control algorithms and GOOSE configurations. To configure the IEDs to execute the voltage control functions, the SEL-2414 relays were configured under the following sections following the sequence as depicted in [Figure 78](#).

#### 4.2.1 Engineering Configuration of Master Relay

Before the relay can be configured, a connection between it and the computer loaded with the Quickset software used to configure it needs to be established. The following methods can be used to connect to the relay.

- Ethernet connection RJ45 port
- Ethernet connection Fibre port
- Serial communication via serial port

See [Figure 79](#) for communication connection options to the relay and power connections for powering up the relay.

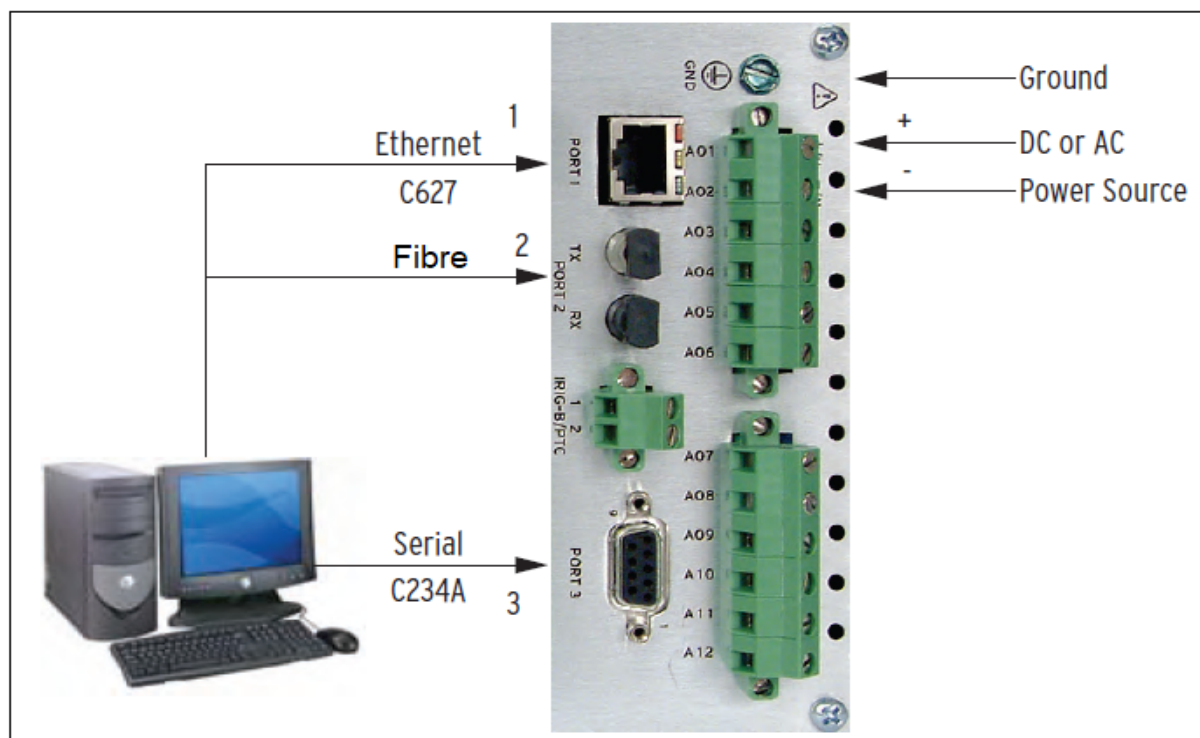


**Figure 79: Connecting to the relay, powering the relay**



This project used a fiber Ethernet connection to connect the SEL-2414 relays. The communication parameters must be entered to communicate between the computer and the relay. The connection type was chosen as a network connection. The relay IP address of 192.168.1.1 is entered in the Host IP address section. The file transfer type option selected was FTP. See [Figure 80](#) for communication parameters entered to establish communication with the Master relay.

Communication Parameters

Active Connection Type  
Network

Serial Network Modem Blueframe

Connection Name  
▼

Host IP Address  
192.168.1.1

Port Number(Telnet)  
23

Port Number(FTP)  
21

File Transfer Option  
☒ FTP ☐ Raw TCP  
☐ Telnet ☐ SSH

User ID  
FTPUSER

Password  
••••

Level One Password  
•••••

Level Two Password  
••••

Save to Address Book Default

OK Cancel Apply Help

**Figure 80: Establishing communication with Master relay**

The relay's part number can be found under the EDIT tab when communication is successfully established. The part number tells you how the relay's hardware has been configured, the classification of the cards installed, and the communication protocol available for the relay. See [Figure 81](#) for the part number of the Master relay.

**Part Number: 2414 \* \* \* C \* 9 X 7 4 8 5 1 8 4 \***

**Position C**  
C\* = 4 Digital Input, 3 Digital Output (Form C + 1 Form B) ▾

**Position D**  
9X = 10 RTD Input ▾

**Position E**  
74 = SElect 3ACI/3AVI (3-Phase 5A Current Input, 3-Phase 3) ▾

**Position Z**  
85 = 4 AC Current Input (5 A Phase, 5 A Neutral) ▾

**Communication Ports**  
18 = Dual 100BASE-FX Ethernet Port and Fiber Optic Port - M ▾

**Communications Protocol**  
4 = Standard Plus DNP and IEC-61850 ▾

**Figure 81: Part Number of Master relay**

**General settings:**

DELTA\_Y Transformer connection was set to WYE

**Transformer settings:**

The PTR Potential Transformer Ratio was set to 276,00

**Transformer monitoring:**

ETPM\_MDE Tap Position Monitoring Mode was set to BIN. This enables the relay to receive a digital binary code input to determine the OLTC's tap position.

**Load Tap Position and Control Monitoring Settings:**

The TP\_MAX Highest Tap Position on the Load Tap Changer was set to 20. The TP\_MIN Lowest Tap Position on the Load Tap Changer was set to 0. MULT\_NEU 3 Neutral positions on the Load Tap Changer were set to N. TPFB\_TIM Feedback time interval for load tap control monitoring alarms, in second was set 5,0. The load tap position and control monitoring settings is summarised in [Table 28](#).

**Table 28: Load Tap Position and Control Monitoring Settings of Master relay**

Load Tap Position and Control Monitoring Settings	Range
---	-------

TP_MAX Highest Tap Position	20
TP_MIN Lowest Tap Position	0
MULT_NEU 3 Neutral position	N
TPFB_TIM Feedback time interval	5.0

### Load Tap Position and Control Monitoring Inputs:

The TPM\_DI Digital inputs of the BCD/Binary Tap Position code, listed in least significant bit to most significant bit was set to IN101, IN102, IN301, IN302, IN303, IN304. The LTC\_RSE SELogic input that indicates the raised operation control status was set to LT02 AND TAP\_POS < 20 AND VB\_MAG < 22806. The LTC\_LWR SELogic input that indicates the lower operation control status was set to LT01 AND TAP\_POS > 0 AND VB\_MAG > 14289. The load tap position and control monitoring inputs is summarised in [Table 29](#).

**Table 29: Load Tap Position and Control Monitoring Inputs of Mater relay**

Load Tap Position and Control Monitoring Inputs	Range
TPM_DI Digital inputs	IN101,IN102,IN301,IN302,IN303, IN304
LTC_RSE SELogic input	LT02 AND TAP_POS < 20 AND VB_MAG < 23815
LTC_LWR SELogic input	LT01 AND TAP_POS > 0 AND VB_MAG > 14289

### SELogic Enables:

ELAT SELogic Latches was set to 2. ESV SELogic Variables/Timers was set to 5. EMV SELogic Math Variable Equations was set to 1.

### SELogic Variable/Timer Settings:

SV01 SeLogic Variable Input was set to VA\_MAG < 18055. SV01PU SELogic Variable Timer Pickup was set to 30. SV01DO SELogic Variable Timer Dropout was set to 0. SV02 SeLogic Variable Input was set to VA\_MAG > 20000. SV02PU SELogic Variable Timer Pickup was set to 30. SV02DO SELogic Variable Timer Dropout was set to 0. SV03 SeLogic Variable Input was set LT01. SV03PU SELogic Variable Timer Pickup was set to 13. SV03DO SELogic Variable Timer

Dropout was set to 15. SV04 SeLogic Variable Input was set LT02. SV04PU SELogic Variable Timer Pickup was set to 15. SV04DO SELogic Variable Timer Dropout was set to 13. The SELogic Variable/Timer Settings is summarised in [Table 30](#).

**Table 30: SELogic Variable/Timer Settings of Master relay**

<b>SELogic Variable/Timer Settings</b>	<b>Range</b>
SV01 SeLogic Variable Input	VA_MAG < 18099
SV01PU SELogic Variable Timer Pickup	30
SV01DO SELogic Variable Timer Dropout	0
SV02 SeLogic Variable Input	VA_MAG > 20005
SV02PU SELogic Variable Timer Pickup	30
SV02DO SELogic Variable Timer Dropout	0
SV03PU SELogic Variable Timer Pickup	3
SV03DO SELogic Variable Timer Dropout	15
SV04 SeLogic Variable Input	LT02
SV04PU SELogic Variable Timer Pickup	3
SV04DO SELogic Variable Timer Dropout	15

### **Output SELogic Equations:**

The OUT101 was set to LTC\_RSE. The OUT102 was set to LTC\_LWR.

### **Port 1 Settings:**

The FTPUSER File transfer User Name was set to FTPUSER. The IPDDR Device Address was set 192.168.1.1. The SUBNETM Subnet Mask was set to 255.255.255.0. The E61850 Enable IEC 61850 Protocol was set to Y. EGSE Enable IEC 61850 GSE was set to Y.

### **Graphical Logic:**

The master relay's graphical logic was configured with a custom algorithm to control the OLTC on the Master transformer T18. See Figure 2 for the custom algorithm configured within the master controller relay to control the lowering of the tap function.

See **Table 31** for summary of the configured elements of the SEL-2414\_A Master relay.

**Table 31: The SEL-2414\_A Master relay was configured according to the following settings**

<b>Master Relay Configuration Settings</b>	<b>Range</b>
DELTA_Y	WYE
PTR Potential Transformer Ratio	276,00
ETPM_MDE Tap Position Monitoring Mode	BIN
TP_MAX Highest Tap Position	20
TP_MIN Lowest Tap Position	0
MULT_NEU 3 Neutral position	N
TPFB_TIM Feedback time interval	5.0
TPM_DI Digital inputs	IN101,IN102,IN301,IN302,IN303, IN304
LTC_RSE SELogic input	LT02 AND TAP_POS < 20 AND VB_MAG < 23815
LTC_LWR SELogic input	LT01 AND TAP_POS > 0 AND VB_MAG > 14289
ELAT SELogic Latches	2
ESV SELogic Variables/Timers	5
EMV SELogic Math Variable Equations	1
SV01 SeLogic Variable Input	VA_MAG < 18099
SV01PU SELogic Variable Timer Pickup	30
SV01DO SELogic Variable Timer Dropout	0
SV02 SeLogic Variable Input	VA_MAG > 20005
SV02PU SELogic Variable Timer Pickup	30
SV02DO SELogic Variable Timer Dropout	0
SV03PU SELogic Variable Timer Pickup	3
SV03DO SELogic Variable Timer Dropout	15
SV04 SeLogic Variable Input	LT02
SV04PU SELogic Variable Timer Pickup	3
SV04DO SELogic Variable Timer Dropout	15

OUT101	LTC_RSE
OUT102	LTC_LWR.
FTPUSER File transfer User Name	FTPUSER
IPDDR Device Address	192.168.1.1.
SUBNETM Subnet Mask	255.255.255.0.
E61850 Enable IEC 61850 Protocol	Y
EGSE Enable IEC 61850	Y

OLTC voltage control algorithms for the SEL-2414 relays were developed as follows:  
4.2.2 the tap lowering algorithm of the Master relay and 4.2.3 the tap Raise algorithm of the Master relay

#### 4.2.2 Developed OLTC algorithm Lowering Master tap

The master relay's graphical logic was configured with a custom algorithm to control the tap-lowering function of the OLTC on the Master transformer T18 located in the RTDS equipment. See [Figure 82](#) for the custom algorithm configured within the master controller relay to control the lowering of the tap function. The 3-phase L-L nominal Bus voltage is 33 kV. The Line to neutral voltage of the bus is calculated using the following equation:

$$V(L-N) = \frac{V(L-L)}{\sqrt{3}} = \frac{33\,000}{\sqrt{3}} = 19,052 \text{ kV} \quad (4.1)$$

The set point for the bus voltage is to be controlled between 0.95 to 1.05 per-unit. Any voltage measured below this point would be considered outside the allowed deviation level, and the OLTC should issue tap operation signals to correct the voltage level. The lower set point is calculated using the following equation:

$$\text{Lower set point} = 95\% \text{ of } V(L-N) = 0.95 \times 19,052 = 18,099 \text{ kV} \quad (4.2)$$

The lowest level the bus voltage is allowed to deviate to is set to 75% below the nominal voltage. Any voltage measured below this point would be considered a fault condition and the OLTC should not issue tap operation signals. The minimum allowed voltage magnitude is calculated using the following equation:

$$\text{Minimum set point} = 75\% \text{ of } V(L-N) = 0.75 \times 19,052 = 14,289 \text{ kV} \quad (4.3)$$

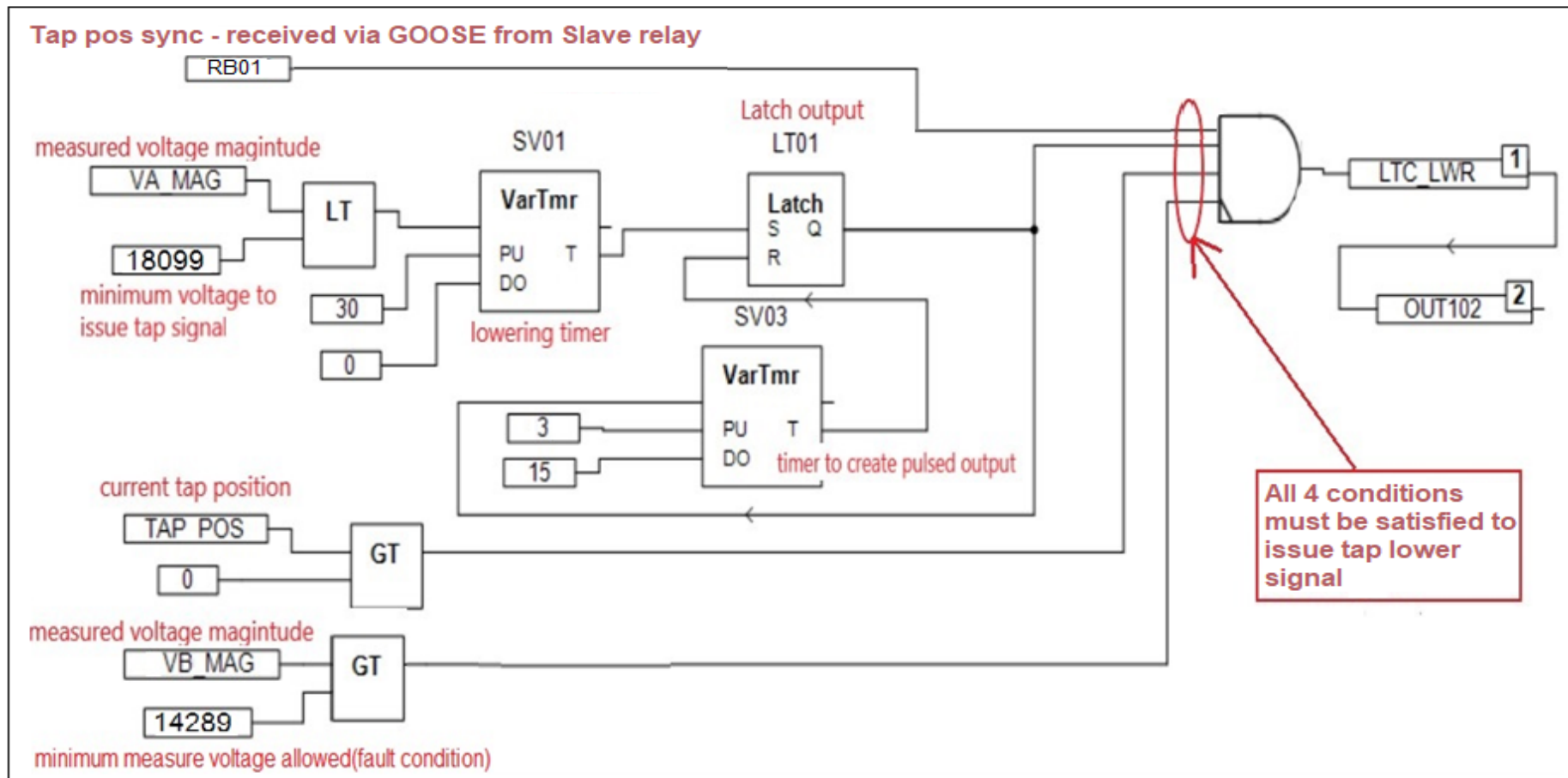


Figure 82: Algorithm to control the tap-lowering function of the Master transformer

If the VA (Line-to-Neutral) magnitude measured by the Master relay is lower than the limit set at 18,099 kV, the relay will sense that the measured value is below the minimum set, and the timer SV01 pick-up timer will start to time. If the low voltage condition remains for the entire 30-second set time, SV01 will issue a signal to the latch LT01. The output from the latch is logically high. The output from the latch goes to the input of timer SV03 with a pickup time of 3 seconds and dropout time of 15 seconds. If its logical input remains high, this will cause the latch LT01 to issue an output signal with a 3-second second length. This pulsed out from timer LT01 goes to a three-input AND gate. The tap position of the relay needs to be greater than 0, and the system voltage needs to be greater than the minimum voltage set point of 14,289 kV to satisfy the conditions for this AND gate to issue high signal to LTC\_LWR. LTC\_LWR is mapped to OUT102 on the Master relay.

A tap synchronisation bit RB01 is received via IEC61850 GOOSE message from the Slave-follower relay to verify that the Master Tap position and the Slave-Follower Tap position are synchronised. The Tap positions of the OLTCs need to be synchronised before Master relay can issue tap lowering signals.

### 4.2.3 Developed OLTC algorithm Raising Master tap

The master relay's graphical logic was configured with a custom algorithm to control the tap-lowering function of the OLTC on the Master transformer T18 located in the RTDS equipment. See [Figure 83](#) for the custom algorithm configured within the master controller relay to control the raising of the tap function. The 3-phase L-L nominal Bus voltage is 33 kV. The Line to neutral voltage of the bus is calculated using the following equation:

$$V(L-N) = \frac{V(L-L)}{\sqrt{3}} = \frac{33\,000}{\sqrt{3}} = 19,052 \text{ kV} \quad (4.4)$$

The set point for the bus voltage is to be controlled between 0.95 p.u to 1.05 per-unit. Any voltage measured above this set point would be considered outside the allowed deviation level, and the OLTC should issue tap operation signals to correct



the voltage level. The high voltage set point is calculated using the following equation:

$$\text{High voltage set point} = 105\% \text{ of } V(L-N) = 1.05 \times 19,052 = 20,005 \text{ kV} \quad (4.5)$$

The highest level the bus voltage is allowed to deviate to is set to 25% above nominal voltage. Any voltage measured below this point would be considered a fault condition and the OLTC should not issue tap operation signals. The maximum allowed voltage magnitude is calculated using the following equation:

$$\text{Maximum set point} = 125\% \text{ of } V(L-N) = 1.25 \times 19,052 = 23,815 \text{ kV} \quad (4.6)$$

If the VA (Line-to-Neutral) magnitude measured by the Master relay is above the limit set at 20,005 kV, the relay will sense that the measured value is above the set point, and the timer SV02 pick-up timer will start to time. If the low voltage condition remains for the entire 30-second set time, SV02 will issue a signal to the latch LT02. The output from the latch becomes logically high. The output from the latch goes to the input of timer SV04 with a pickup time of 3 seconds and dropout time of 15 seconds. This will cause the latch LT02 to issue an output signal with a 3-second length if its logical input remains high. This pulsed out from timer LT02 goes to a three input AND gate. The tap position of the relay needs to be less than 20, and the system voltage needs to be below the maximum set value of 23,815 kV to satisfy the conditions for this AND gate to issue a high signal to LTC\_RSE. LTC\_RSE is mapped to OUT101 on the Master relay.

A tap synchronisation bit RB01 is received via IEC61850 GOOSE message from the Slave-follower relay to verify that the Master Tap position and the Slave-Follower Tap position are synchronised. The Tap positions of the OLTCs need to be synchronised before Master relay can issue tap raising signals.

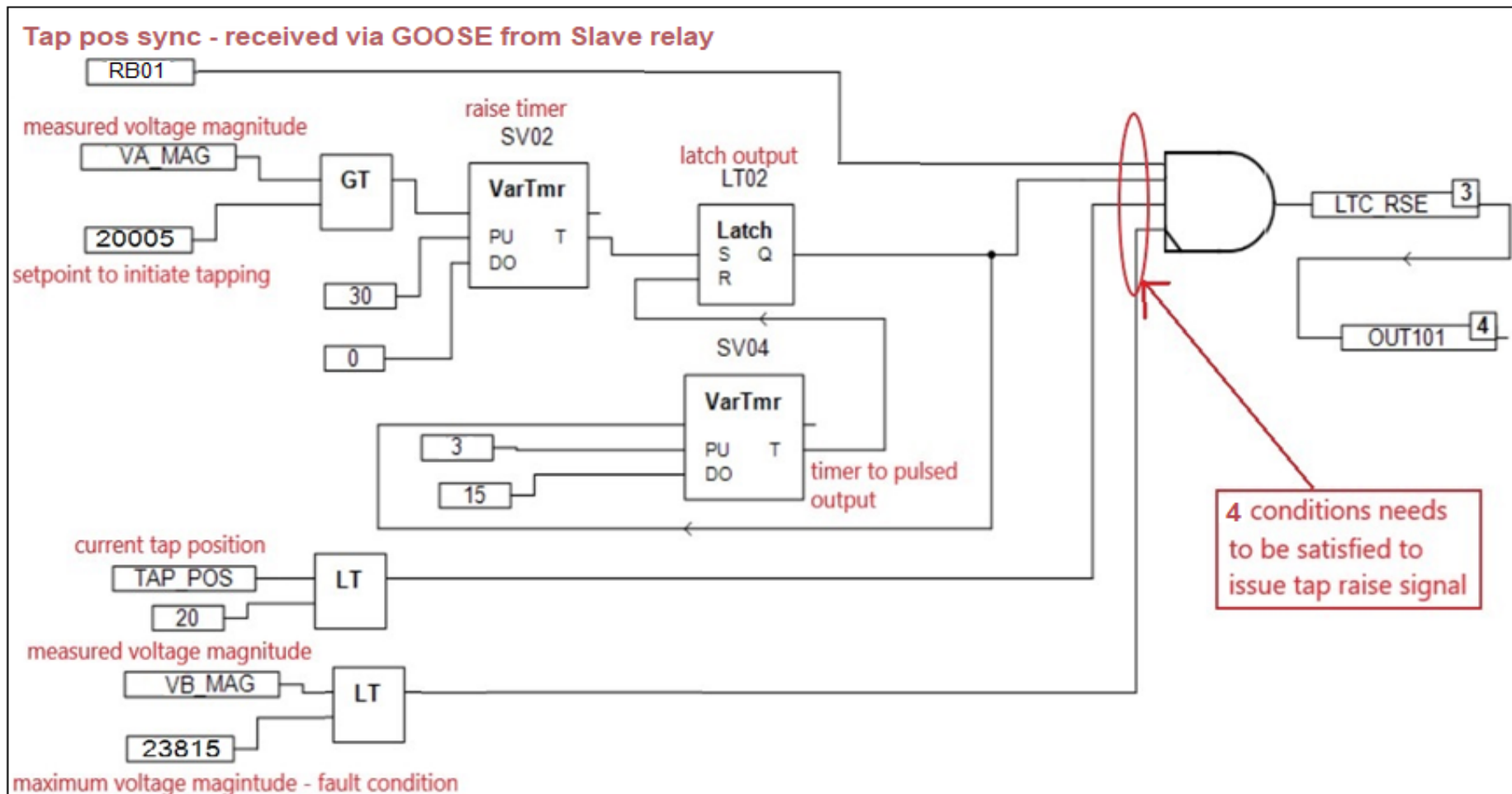


Figure 83: Algorithm to control the tap-raising function of the Master transformer

#### 4.2.4 Engineering configuration of Slave-Follower relay

The communication parameters must be entered to communicate between the computer and the relay. The connection type was chosen as a network connection. The relay IP address 192.168.1.2 is entered in the Host IP address section. The file transfer type option selected was FTP. See [Figure 84](#) for communication parameters entered to establish communication with the Slave-Follower relay.

Communication Parameters

Active Connection Type  
Network

Serial Network Modem Blueframe

Connection Name  
▼

Host IP Address  
192.168.1.2

Port Number(Telnet)  
23

Port Number(FTP)  
21

File Transfer Option  
☒ FTP ☐ Raw TCP  
☐ Telnet ☐ SSH

User ID  
FTPUSER

Password  
••••

Level One Password  
•••••

Level Two Password  
••••

Save to Address Book Default

OK Cancel Apply Help

**Figure 84: Establishing communication with Slave-Follower relay**

When communication is successfully established with, the part number of the relay can be found under the EDIT tab. The part number of the relay tells you how the hardware of the relay has been configured, the classification of the cards installed and the communication protocol that is available for the relay. See [Figure 85](#) for the part number of the Slave-Follower relay.

**Part Number: 2414 \* \* \* C \* 3 \* 3 \* 5 X 1 4 4 \***

**Position C**  
C\* = 4 Digital Input, 3 Digital Output (Form C + 1 Form B) ▾

**Position D**  
3\* = 8 Digital Input ▾

**Position E**  
3\* = 8 Digital Input ▾

**Position Z**  
5X = 8 Analog Input (8 Std Range Voltage or Current) ▾

**Communication Ports**  
14 = Single 100BASE-FX Ethernet Port and Fiber Optic Port - II ▾

**Communications Protocol**  
4 = Standard Plus DNP and IEC-61850 ▾

**Figure 85: Part Number of Slave-Follower relay**

### Transformer Tap monitoring

ETPM\_MDE Tap Position Monitoring Mode was set to BIN. This mode allows the relay to receive a digital binary code input to determine the OLTC's tap position.

### Load Tap Position and Control Monitoring Settings

The TP\_MAX Highest Tap Position on the Load Tap Changer was set to 20. The TP\_MIN Lowest Tap Position on the Load Tap Changer was set to 0. MULT\_NEU 3 Neutral positions on the Load Tap Changer were set to N. TPFb\_TIM Feedback time interval for load tap control monitoring alarms, in second was set 5,0. The load tap position and control monitoring settings are summarised in [Table 32](#).

**Table 32: Load Tap Position and Control Monitoring Settings of Slave-Follower relay**

Load Tap Position and Control Monitoring Settings	Range
TP_MAX Highest Tap Position	20
TP_MIN Lowest Tap Position	0
MULT_NEU 3 Neutral position	N
TPFB_TIM Feedback time interval	5.0

## Load Tap Position and Control Monitoring Inputs

The TPM\_DI Digital inputs of the BCD/Binary Tap Position code, listed in the least significant bit to a most important bit, set to IN101, IN102, IN301, IN302, IN303, IN304. The LTC\_RSE SELogic input that indicates the raised operation control status was set to LT01. The LTC\_LWR SELogic input that indicates the lower operation control status was set to LT02. The load tap position and control monitoring inputs of the Slave-Follower relay is summarised in [Table 33](#).

**Table 33: Load Tap Position and Control Monitoring Input of Slave-follower relay**

Load Tap Position and Control Monitoring Inputs	Range
TPM_DI Digital inputs	IN101,IN102,IN301,IN302,IN303, IN304
LTC_RSE SELogic input	LT01
LTC_LWR SELogic input	LT02

## SELogic Variable/Timer Settings

SV01 SeLogic Variable Input was set to MV01<RA004. SV01PU SELogic Variable Timer Pickup was set to 4. SV01DO SELogic Variable Timer Dropout was set to 0. SV02 SeLogic Variable Input was set to LT01. SV02PU SELogic Variable Timer Pickup was set to 10. SV02DO SELogic Variable Timer Dropout was set to 13. SV03 SeLogic Variable Input was set LT02. SV03PU SELogic Variable Timer Pickup was set to 10. SV03DO SELogic Variable Timer Dropout was set to 13. SV06 SeLogic Variable Input was set MV01 > RA004. SV06PU SELogic Variable Timer Pickup was set to 4. SV04DO SELogic Variable Timer Dropout was set to 0. SV07 SeLogic Variable Input was set MV01 = RA004. SV07PU SELogic Variable Timer Pickup was set to 5. SV07DO SELogic Variable Timer Dropout was set to 0. The SELogic Variable/Timer Settings is summarised in [Table 34](#).

**Table 34: SELogic Variable/Timer Settings is summarised of Slave-Follower relay**

<b>SELogic Variable/Timer Settings</b>	<b>Range</b>
SV01 SeLogic Variable Input	MV01<RA004.
SV01PU SELogic Variable Timer Pickup	4
SV01DO SELogic Variable Timer Dropout	0
SV02 SeLogic Variable Input	LT01
SV02PU SELogic Variable Timer Pickup	3
SV02DO SELogic Variable Timer Dropout	13
SV03 SeLogic Variable Input	LT02
SV03PU SELogic Variable Timer Pickup	3
SV03DO SELogic Variable Timer Dropout	13
SV06 SeLogic Variable Input	MV01 > RA004
SV06PU SELogic Variable Timer Pickup	4
SV06DO SELogic Variable Timer Dropout	0
SV07 SeLogic Variable Input	MV01 = RA004
SV07PU SELogic Variable Timer Pickup	5
SV07DO SELogic Variable Timer Drop out	0

See **Table 35** for summary of the configured elements of the SEL-2414\_B Slave-Follower relay.

**Table 35: The SEL-2414\_B Slave-Follower relay was configured according to the following settings**

<b>Slave-Follower relay ConfigurationSettings</b>	<b>Range</b>
ETPM_MDE Tap Position Monitoring Mode	BIN
TP_MAX Highest Tap Position	20
TP_MIN Lowest Tap Position	0
MULT_NEU 3 Neutral position	N
TPFB_TIM Feedback time interval	5.0
TPM_DI Digital inputs	IN101,IN102,IN301,IN302,IN303,IN304
LTC_RSE SELogic input	LT01

LTC_LWR SELogic input	LT02
SV01 SeLogic Variable Input	MV01<RA004.
SV01PU SELogic Variable Timer Pickup	4
SV01DO SELogic Variable Timer Dropout	0
SV02 SeLogic Variable Input	LT01
SV02PU SELogic Variable Timer Pickup	3
SV02DO SELogic Variable Timer Dropout	13
SV03 SeLogic Variable Input	LT02
SV03PU SELogic Variable Timer Pickup	3
SV03DO SELogic Variable Timer Dropout	13
SV06 SeLogic Variable Input	MV01 > RA004
SV06PU SELogic Variable Timer Pickup	4
SV06DO SELogic Variable Timer Dropout	0
SV07 SeLogic Variable Input	MV01 = RA004
SV07PU SELogic Variable Timer Pickup	5
SV07DO SELogic Variable Timer Drop out	0
OUT101	LTC_RSE
OUT102	LTC_LWR.
FTPUSER File transfer User Name	FTPUSER
IPDDR Device Address	192.168.1.2.
SUBNETM Subnet Mask	255.255.255.0.
E61850 Enable IEC 61850 Protocol	Y
EGSE Enable IEC 61850	Y

The OLTC voltage control algorithms for the SEL-2414 relays were developed as follows: 4.2.5, the tap Raise algorithm of the Slave-Follower relay, and 4.2.6, the tap Lower algorithm of the Slave-Follower relay and 4.2.7 the developed algorithm for Tap synchronisation in Slave-Follower relay.

#### 4.2.5 Developed OLTC algorithm Raising Slave-Follower tap

The slave relay's graphical logic was configured with a custom algorithm to control the OLTC on Slave transformer T17. See [Figure 86](#) for the custom algorithm configured within the Slave controller relay to prevent the raising of the tap function.

MV01 reads the current tap position of the Slave transformer. The Master transformer tap position is sent via GOOSE message to the Slave relay. If the Slaves transformer tap position is less than the Master transformer tap position, it will activate the timer SV01, sending a high signal to the Latch LT01. This will cause the Latch01s Q output to be activated. A timer SV02 is connected to the Latch LT01 output with a pickup time of 3 seconds and a dropout time of 15 seconds. This SV02 will cause Latch LT01 to create a pulsed-out with a pulse length of 3 seconds. This will initiate the LTC\_RSE to become active. LTC\_RSE is mapped to OUT101 on the Slave relay.



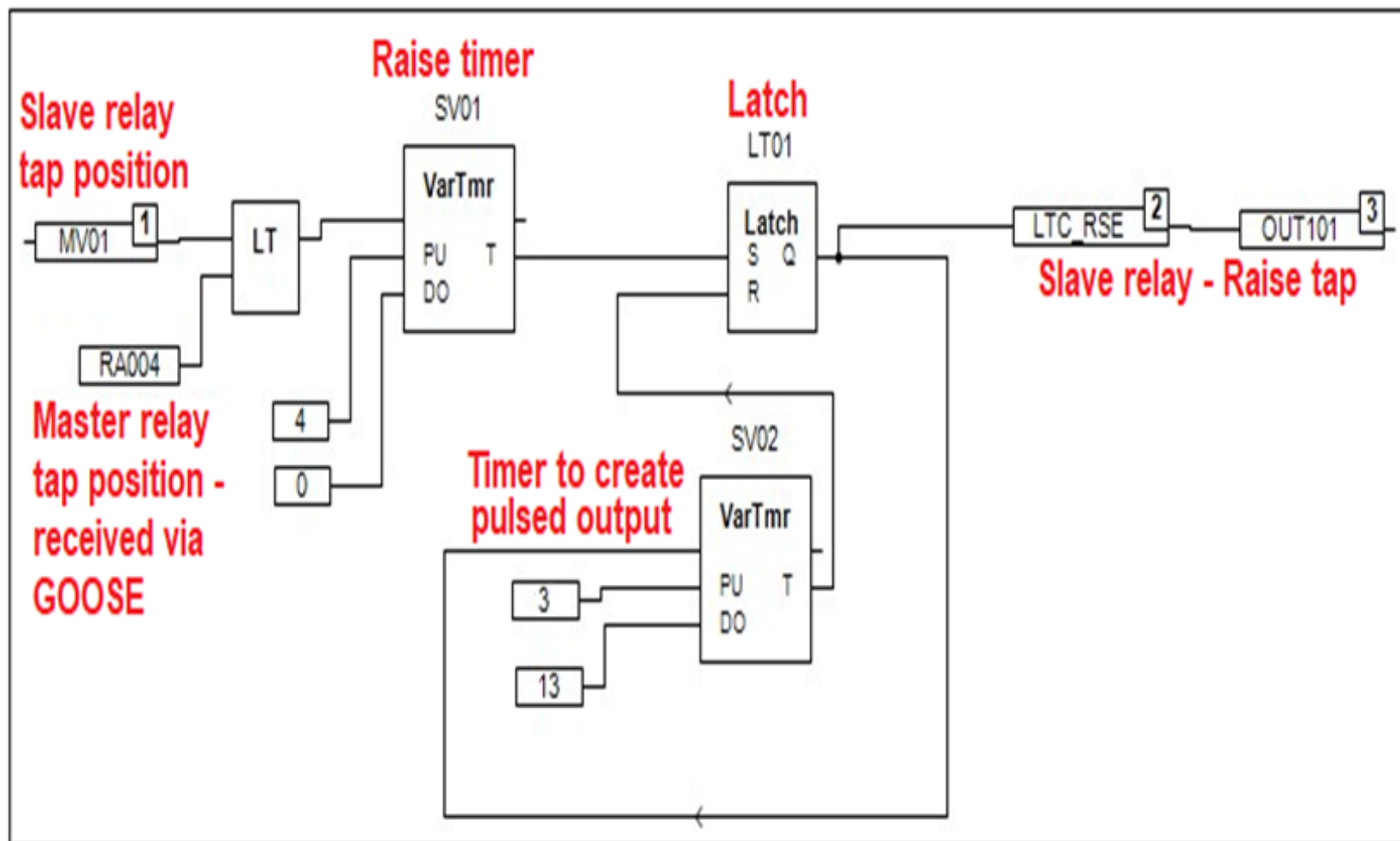


Figure 86: Algorithm to control the tap-raising function of the Slave-Follower transformer

#### 4.2.6 Developed OLTC algorithm Lowering Slave-Follower tap

The Slave-Follower relay's graphical logic was configured with a custom algorithm to control the OLTC on Slave transformer T17. See [Figure 87](#) for the custom algorithm configured within the Slave controller relay to control the lowering of the tap function. MV01 reads the current tap position of the Slave transformer. The Master transformer tap position is sent via GOOSE message to the Slave relay. If the Slaves transformer tap position is greater than the Master transformer tap position, it will activate the timer SV06, sending a high signal to the Latch LT02. This will cause the Latch LT02s Q output to be activated. A timer SV03 is connected to the Latch LT02 output with a pickup time of 3 seconds and a dropout time of 15 seconds. This SV03 will cause Latch LT01 to create a pulsed-out with a pulse length of 3 seconds. This will initiate the LTC\_LWR to become active. LTC\_LWR is mapped to OUT102 on the Slave-Follower relay.

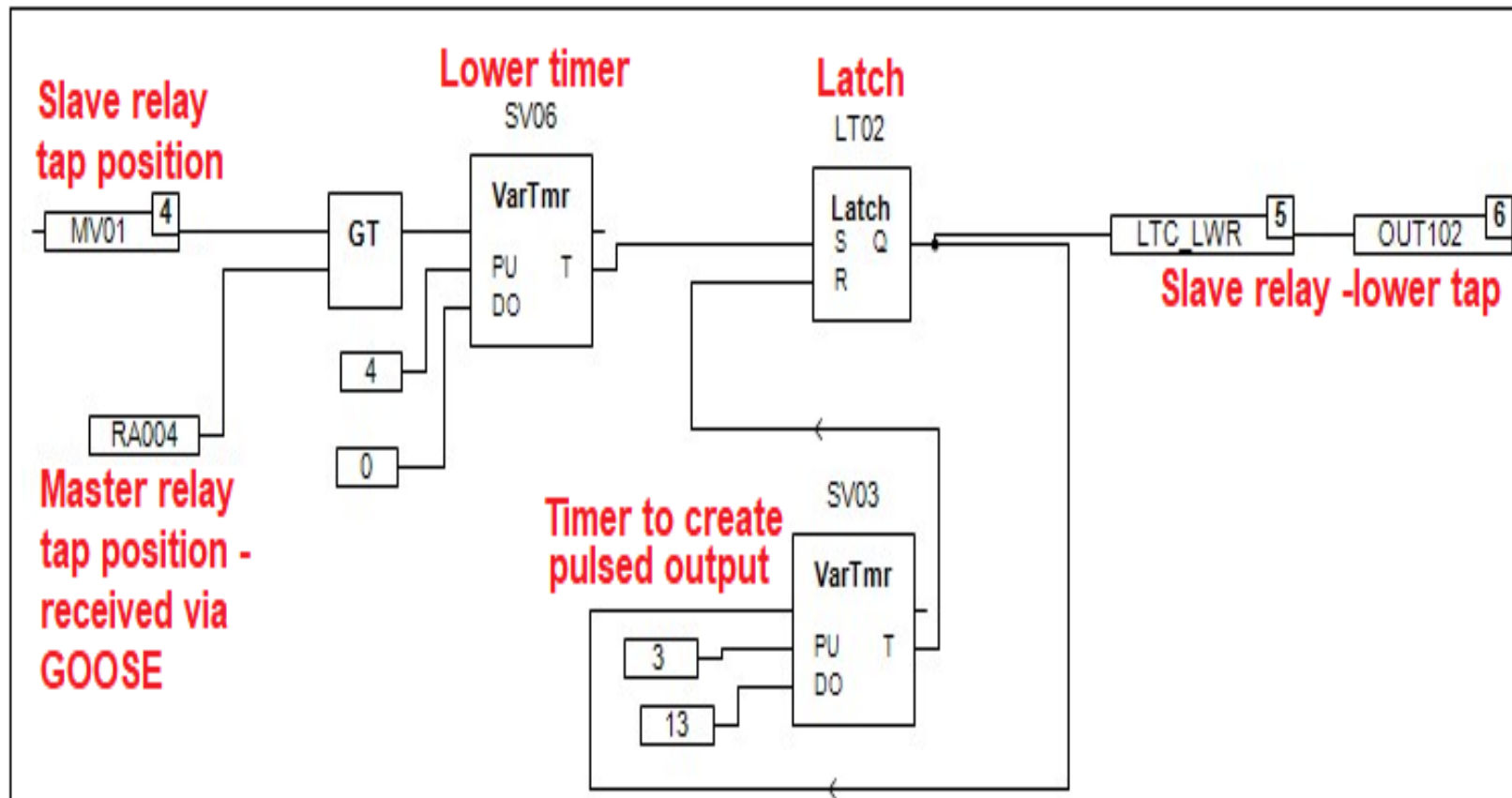
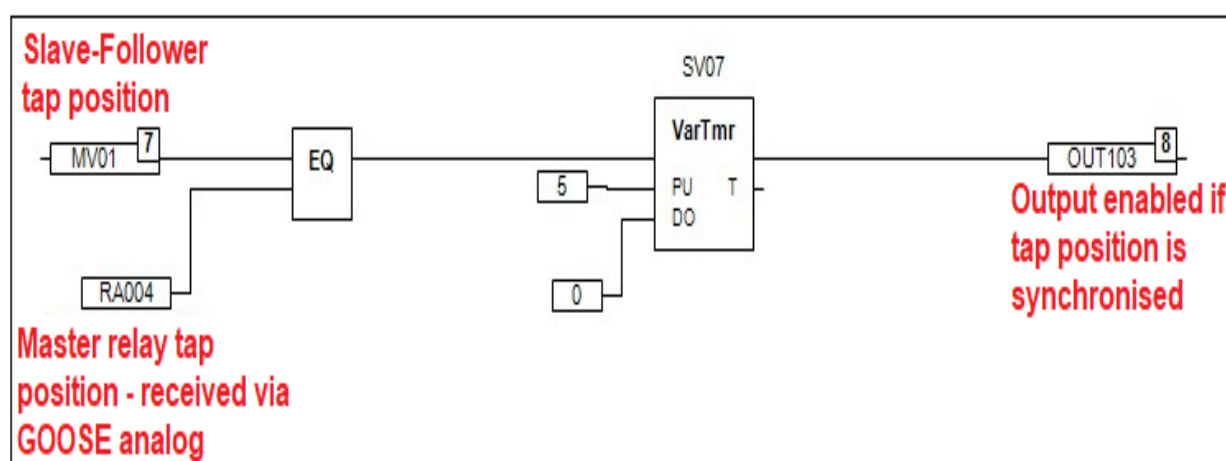


Figure 87: Algorithm to control the tap-lowering function of the Slave-Follower transformer

### 4.2.7 Developed OLTC algorithm for Tap synchronisation in Slave-Follower relay

The Slave-Follower relay's graphical logic was configured with a custom algorithm to verify that the Tap positions of the Master transformer and the Slave-Follower Transformer is synchronised. The Master transformers Tap position is sent transmitted via GOOSE message to the Slave-Follower relay and mapped to remote analog input RA004. If taps of Master transformer and Slave-Follower is synchronised, the Slave-Follower enables OUT103 bit. This OUT103 status is transmitted to Master relay to confirm Tap synchronisation. Unsynchronised taps results in a circulating current flowing between the parallel transformers. See [Figure 88](#) for the custom algorithm configured within the Slave-Follower controller relay to verify that Tap positions of the Master transformer and the Slave-Follower transformer is synchronised.



**Figure 88: Algorithm to verify Tap positions of the Master transformer and the Slave-Follower Transformer is synchronised**

### 4.2.8 Tap Position Monitoring

The SEL-2414 transformer monitor relay can monitor up to 32 tap positions. The relay uses digital input in binary-coded decimal or binary code input to determine its tap position. See [Figure 89](#) for Load Tap Position Control monitoring (TCPC).

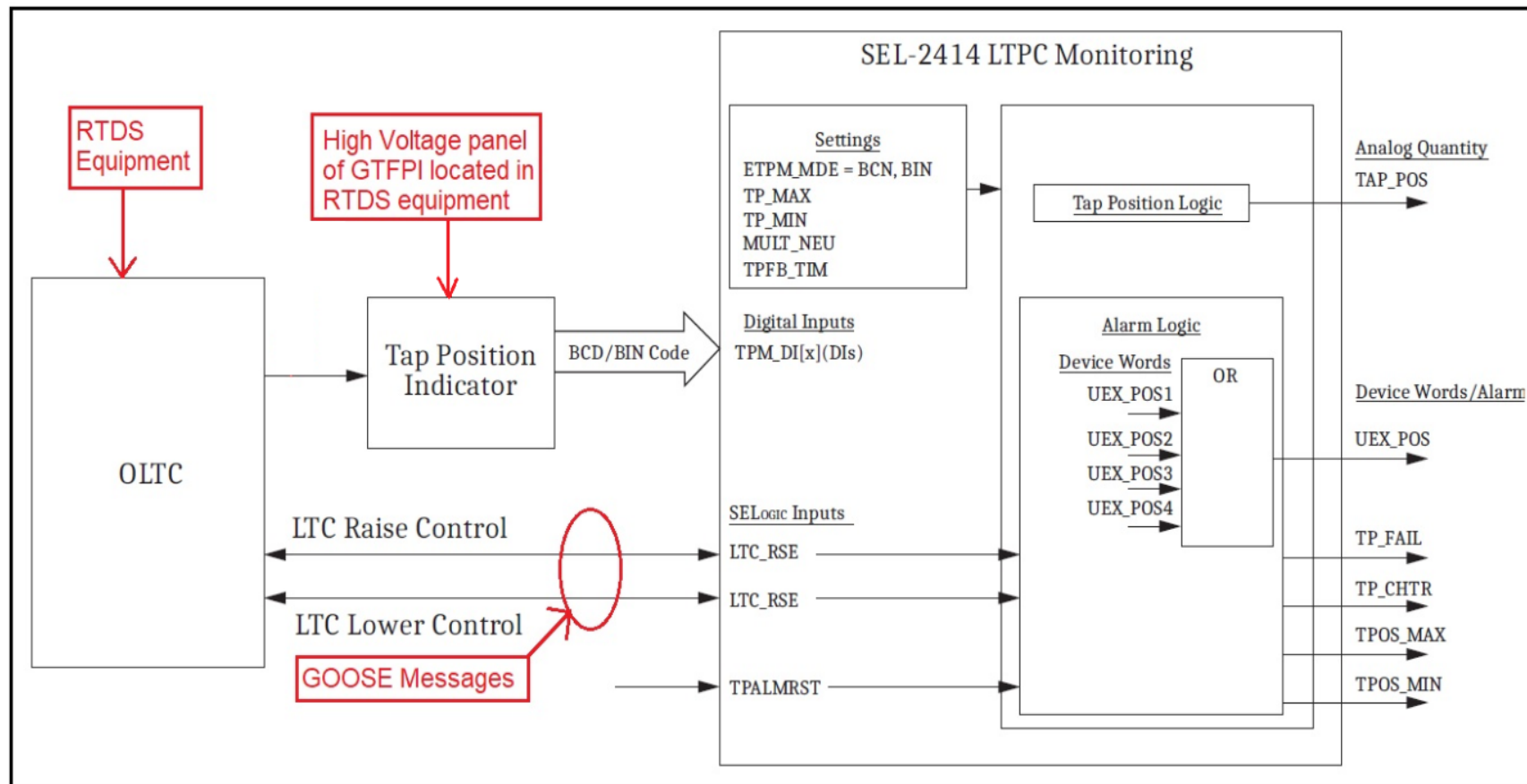


Figure 89: LTTPC Monitoring Block Diagram (SEL, 2017. SEL-2414 Relay Instruction Manual)

When the SEL-2414 relay is set to **ETPM\_MDE = BIN** (Binary code), it calculates the tap position (TAP\_POS) using the following equation:

$$\text{TAP\_POS} = \text{TPM\_DI1} + \text{TPM\_DI2} \cdot 2 + \text{TPM\_DI3} \cdot 4 + \text{TPM\_DI4} \cdot 8 + \text{TPM\_DI5} \cdot 16 + \text{TPM\_DI6} \cdot 32 + \text{TP\_MIN} \quad (4.6)$$

See **Table 36** for the calculation of TAP\_POS when ETPM\_MDE = BIN. The relay uses this binary code obtained via its digital input card to calculate its tap position.

**Table 36: TAP\_POS Calculation when ETPM\_MDE = BIN**

TPM_DI 6	TPM_DI 5	TPM_DI 4	TPM_DI 2	TPM_DI 2	TPM_DI 1	Position Number	TAP_POS
0	1	0	1	0	0	20	4
0	1	0	0	1	1	19	3
0	1	1	0	1	0	18	2
0	1	0	0	0	1	17	1
0	1	0	0	0	0	16	0
0	0	1	1	1	1	15	-1
0	1	1	1	1	0	14	-2
0	0	1	1	0	1	13	-3
0	0	1	1	0	0	12	-4
0	0	1	0	1	1	11	-5
0	0	1	0	1	0	10	-6
0	0	1	0	0	1	9	-7
0	0	1	0	0	0	8	-8
0	0	0	1	1	1	7	-9
0	0	0	1	1	0	6	-10
0	0	0	1	0	1	5	-11
0	0	0	1	0	0	4	-12
0	0	0	0	1	1	3	-13
0	0	0	0	1	0	2	-14
0	0	0	0	0	1	1	-15
0	0	0	0	0	0	0	-16

The digital input card of the SEL-2414 relay needs a signal with a voltage level of up to 125 VDC or VAC. An external voltage source is required to supply this voltage signal to the relay. The Omicron CMC 356 is used in this project to provide this external voltage. When running the hardware-in-the-loop simulations, the Omicron CMC 356 device supplies 110 VDC signal to the High Voltage Digital Interface Panel of the RTDS equipment. The High Voltage Digital Interface Panel then converts this signal to a binary code connected to the digital inputs IN101, IN102, IN301, IN302, IN303, and IN304 of the SEL-2414 relay. The relays use this binary code connected to digital inputs to calculate its OLTC tap position. See Figure 90 for supplying the binary input code to the relay's digital input card.

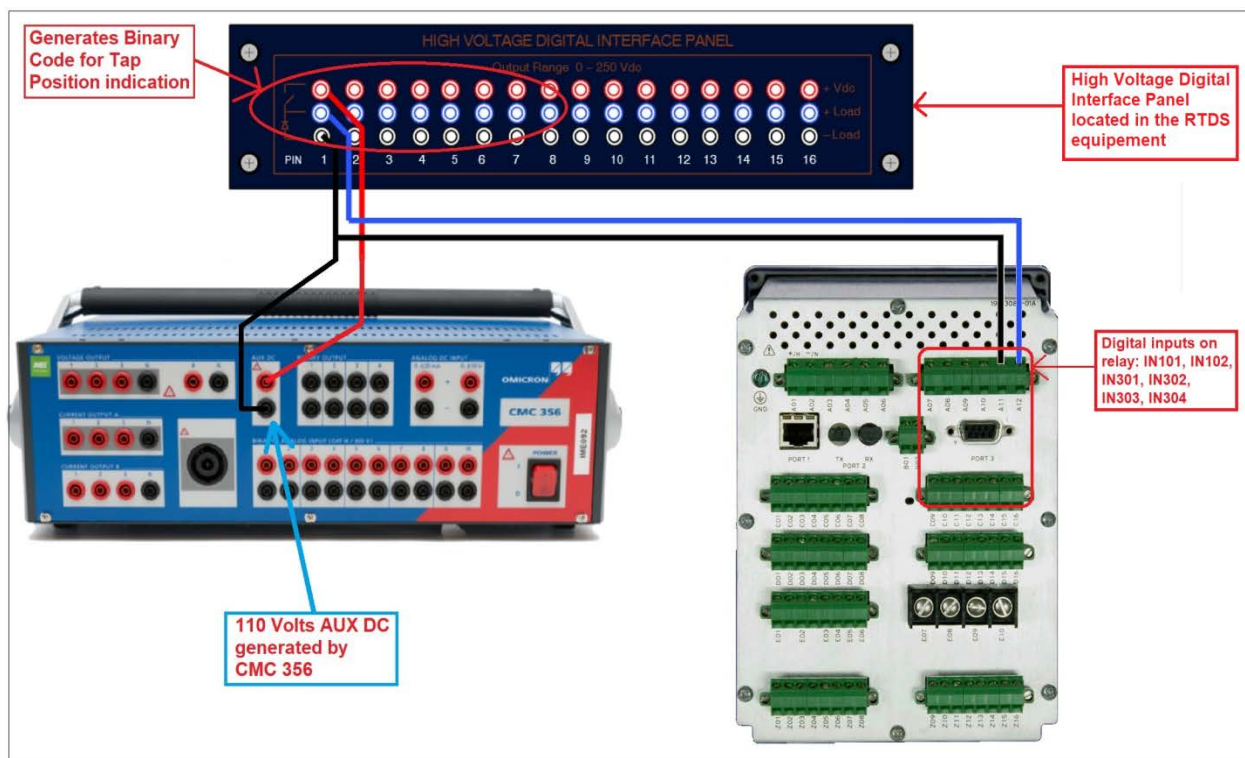


**Figure 90: High Voltage Digital Interface Panel generating binary code for relay to calculate OLTC tap position**

### 4.3 Transformer Relay IEC61850 GOOSE Configuration Settings

GOOSE communication will serve as the protocol for transmitting and receiving data between IEDs in the network and for transmitting control signals. The IEC 61850 standard allows for fast and effective communication between IEDs in a substation where a peer-to-peer structure is employed (Kriger, Behardien, Retonda-Modiya, 2013). The author (Mackiewicz, 2004) mentioned that the IEC 61850 standard for

communication aims to standardize the communication structure and should meet the following key requirements shown in [Table 37](#).

**Table 37: Key requirements for IEC61850 Standard (Mackiewicz, 2004)**

<b>Key requirements for IEC61850 Standard</b>	
Rapid data exchange between IEDs and IEDs	Compliant with industry standards
Seamless integration through the entire utility	Seamless interoperability between Multiple vendors
Continues uptime and reliability	Support time synchronised V&I samples
Reliable and predictable transmission times	Robust security features for data protection

Implementing the IEC61850 standard for communication function allows the engineer to reconfigure changes to the control system without altering any physical wiring, reducing commissioning costs and construction costs (Hakala-Ranta, Rintamäki, Starck, 2009). After considering the advantages of various communication protocols, the IEC 61850 GOOSE protocol was chosen for its superior benefits and suitability for this study. Figure 91: GOOSE configuration sequence.

#### **4.3.1 GOOSE Configuration of Master relay**

The GOOSE configurations of the Master- and Slave-Follower relays was configured using the sequence in [Figure 91](#).



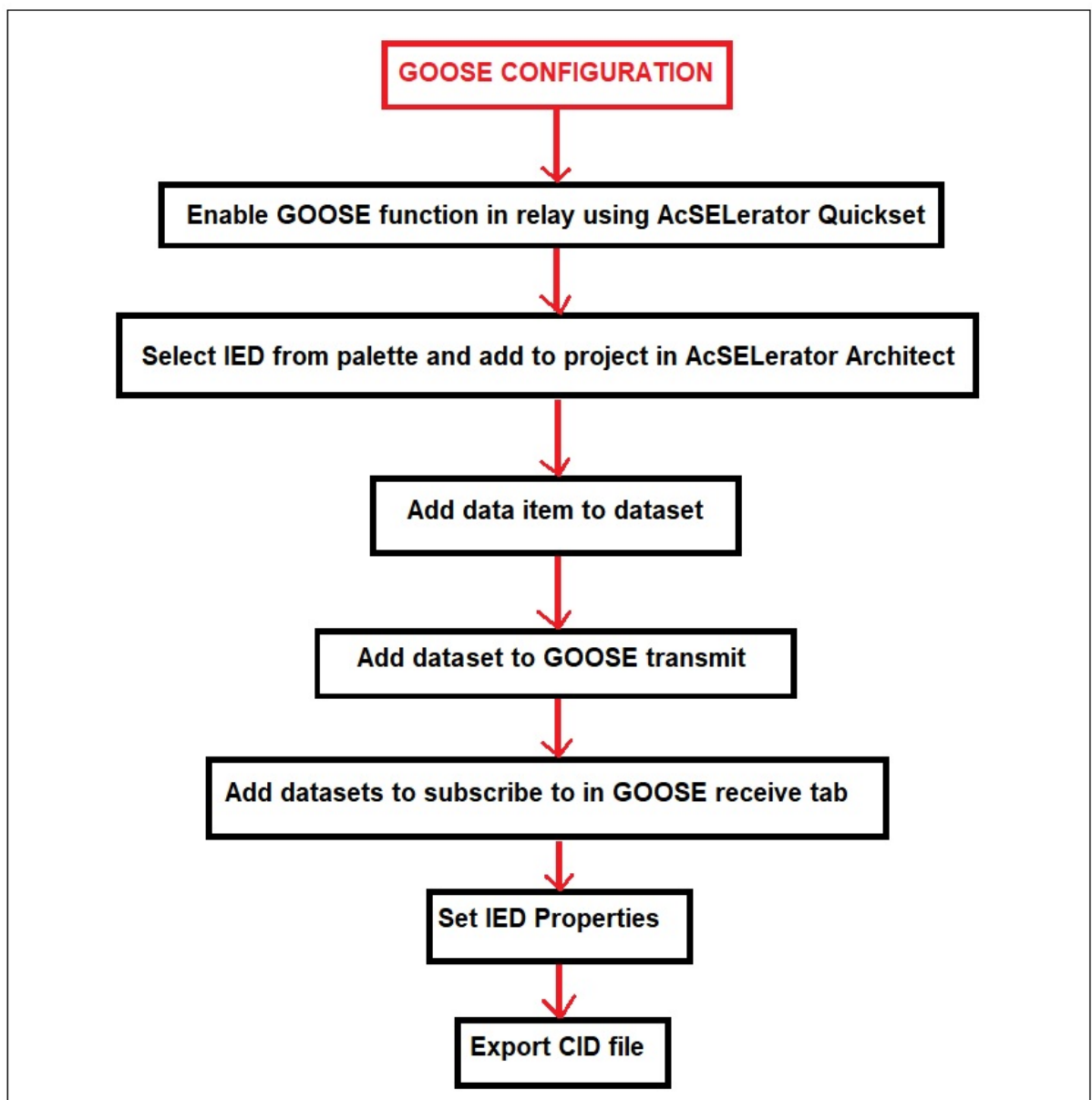


**Figure 91: GOOSE configuration sequence**

#### **4.3.1.1 Enable GOOSE protocol on relay**

The SEL-2414 transformer monitor relay is compliant with the IEC61850 GOOSE communication protocol. For the IEC61850 GOOSE to be configured on the relay, the IEC61850 standard protocol must be activated using the AcSELerator Quickset software. The E61850 Enable IEC 61850 Protocol setting must be set to Y, and the EGSE Enable IEC 61850 GSE must be set to Y. This enables the relays to transmit and subscribe to IEC61850 GOOSE messages. See [Figure 92](#) for enabling the IEC 61850 GOOSE functionality on the relay.

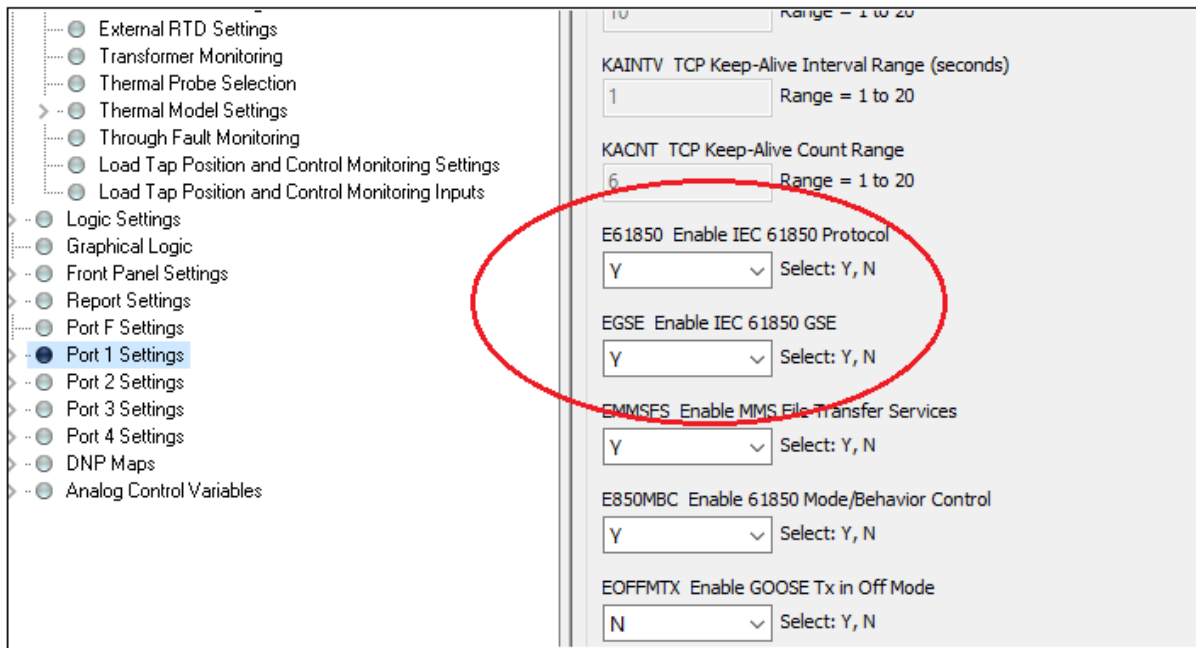


**Figure 92: Enabling IEC 61850 GOOSE functionality on the relay**

#### 4.3.1.2 Adding IED to project

The IEC 61850 GOOSE configuration of the two SEL-2414 relays is executed using the AcSEerator Architect software. An IED palette is available once the AcSEerator Architect software is opened. The relevant IED is selected from the list provided. The Class File Version corresponding with the chosen IED must then be selected. The correct Class File Version can be read from the Status section when connected to the relay using the HMI function. The IED is then added to the project. The process for adding IEDs to an AcSEerator Architect project is depicted in Figure 93.

#### 4.3.1.3 Adding data items to dataset

Figure 94 depicts the LTC\_RSE mapped to OUT101 and LTC\_LWR mapped to OUT102 of the Master relay during its Engineering configuration. OUT101 and OUT102 are included in the Master relay's dataset. Figure 95 depicts the TAP\_POS mapped to the math variable MV01 of the Master relay during the Engineering configuration of the relay. Mv01 is included in the Master relay's dataset.

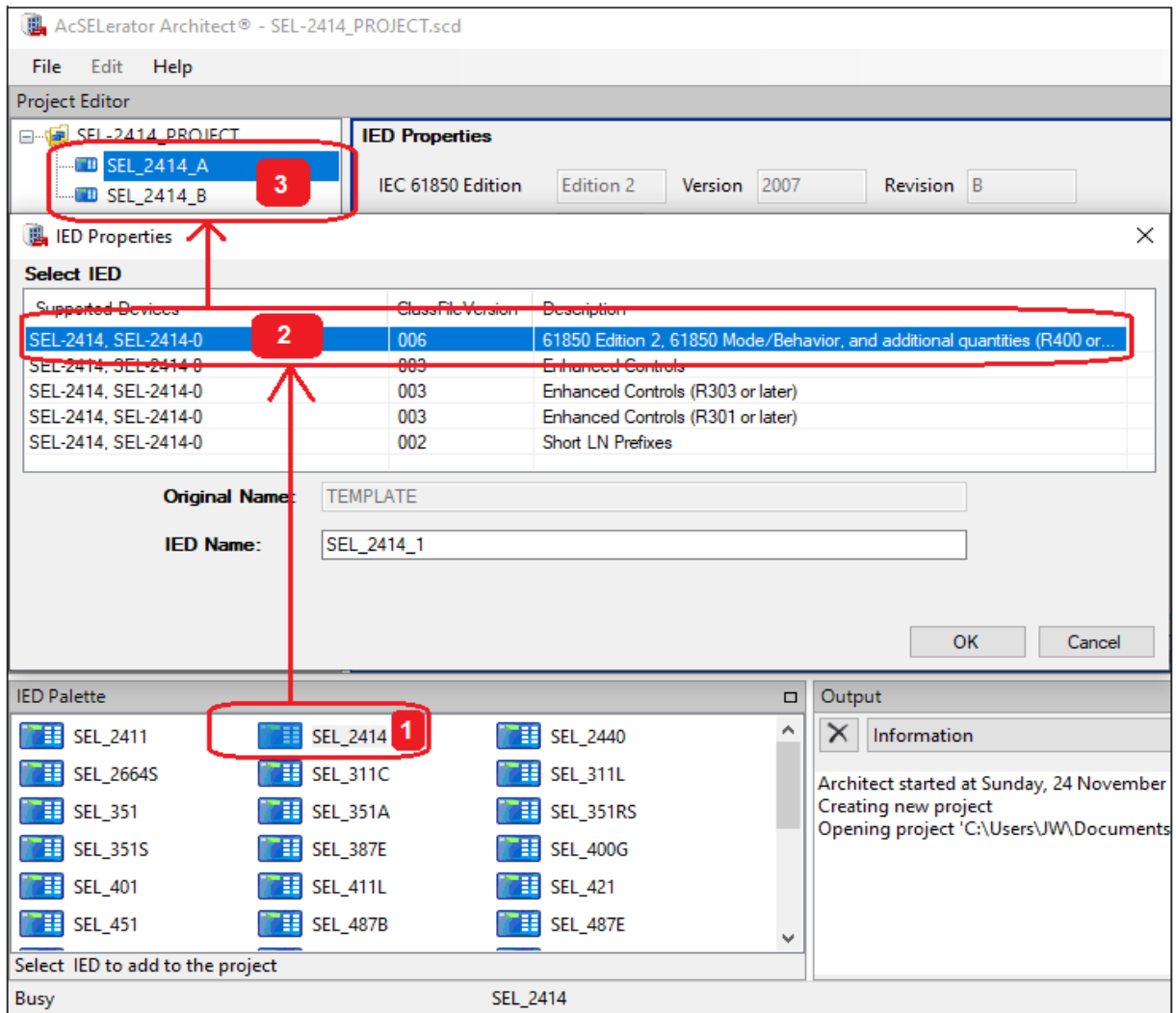


Figure 93: Added IEDs to an AcSElerator Architect project

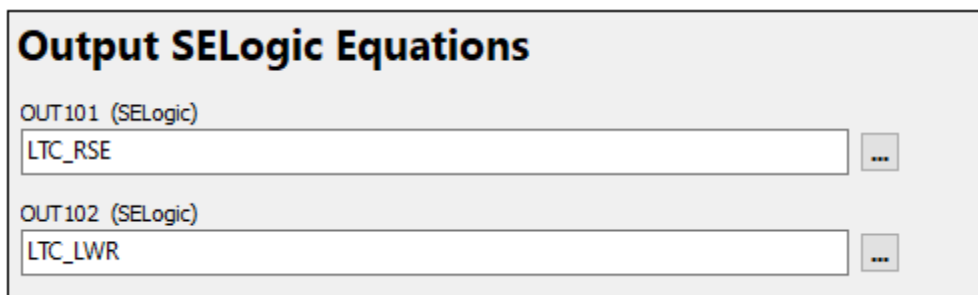


Figure 94: LTC\_RSE mapped to OUT101 and LTC\_LWR mapped to OUT102 of Master relay

### Math Variable SELogic Equations

MV01INV Nonvolatile Math Variable

Y

Select: Y, N

MV01 (SELogic)

TAP\_POS

...

Tap position of Master relay

**Figure 95: Tap the position of the Master relay mapped to Math Variable MV01**

The **Table 38** shows a list of the Logical Nodes included in the Master relay GOOSE communication structure. The master relay will publish and receive these datasets from external subscribing devices.

**Table 38: The datasets that is included in the Master relay GOOSE configuration**

Logical Device: ANN (Annunciation)		
Logical Nodes	Status or Measurand	Device Word Bits or Analog Quantities
Analog Quantities		
MVGGIO12	AnIn01.mag to AnIn32.mag	Math Variables (MV01 to MV32)
Device Word Bits		
OUTAGGIO2	Ind01.stVal	Digital Output (OUT101)—Slot A
OUTAGGIO2	Ind02.stVal	Digital Output (OUT102)—Slot A
Logical Nodes	Measurand	Comment
METMMXU1	PhV.phsA.instCVal.mag	Instantaneous, Voltage Magnitude, Phase A
METMMXU1	PhV.phsB.instCVal.mag	Instantaneous, Voltage Magnitude, Phase B
METMMXU1	PhV.phsC.instCVal.mag	Instantaneous, Voltage Magnitude, Phase C

**Figure 96** depicts adding the data item to the dataset of the Master relay Lower signal. The Master relay will publish this dataset, and external subscribing devices will receive it.

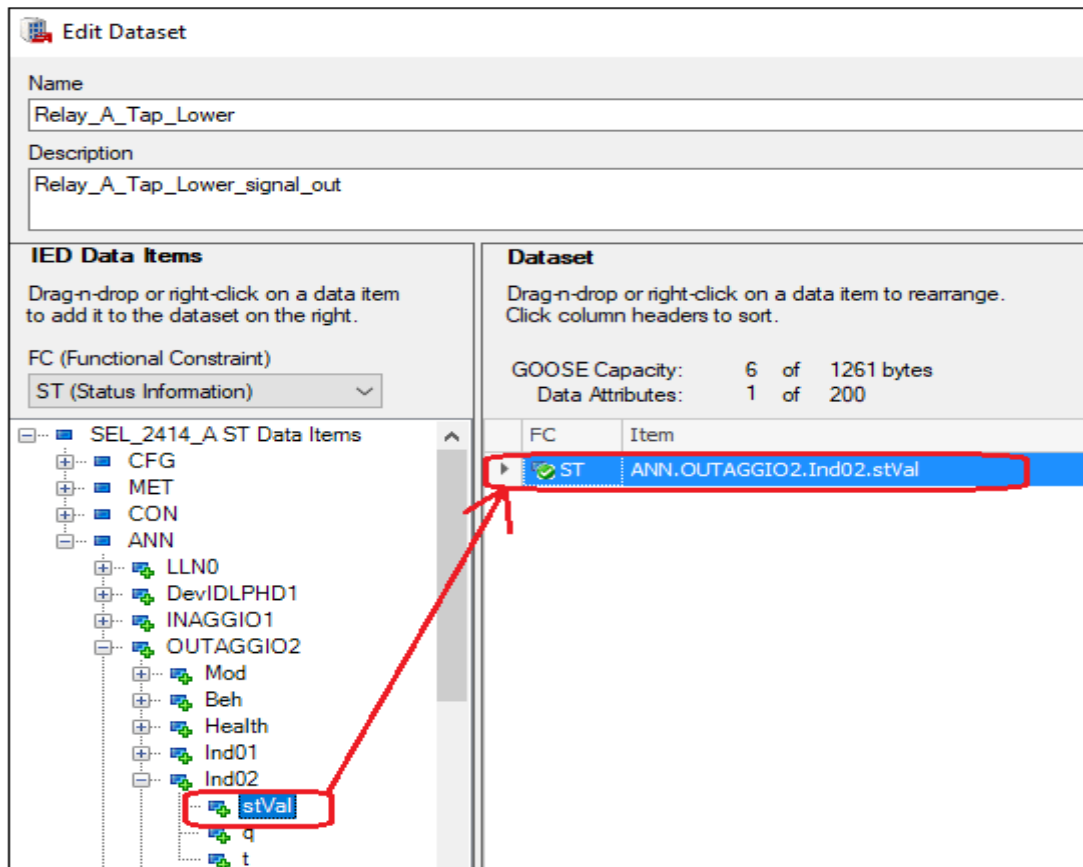


**Figure 96: Adding the data item to the dataset of the Master relay Lower signal**

Figure 98 shows the procedure for adding the data item to the dataset of the Master relay tap position. The master relay will publish this dataset, which is then received by the external subscribing Slave-Follower relay.

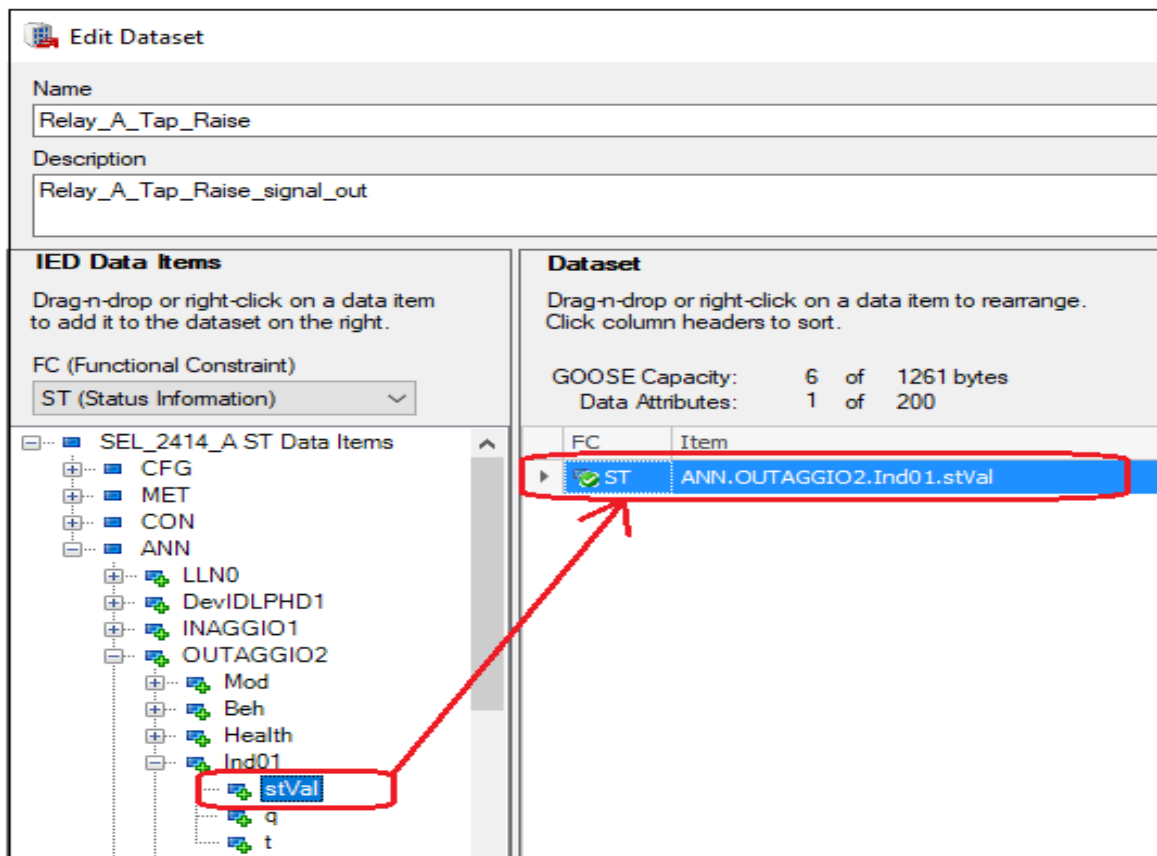


Figure 97: Adding the data item to the dataset of the Master relay Raise signal

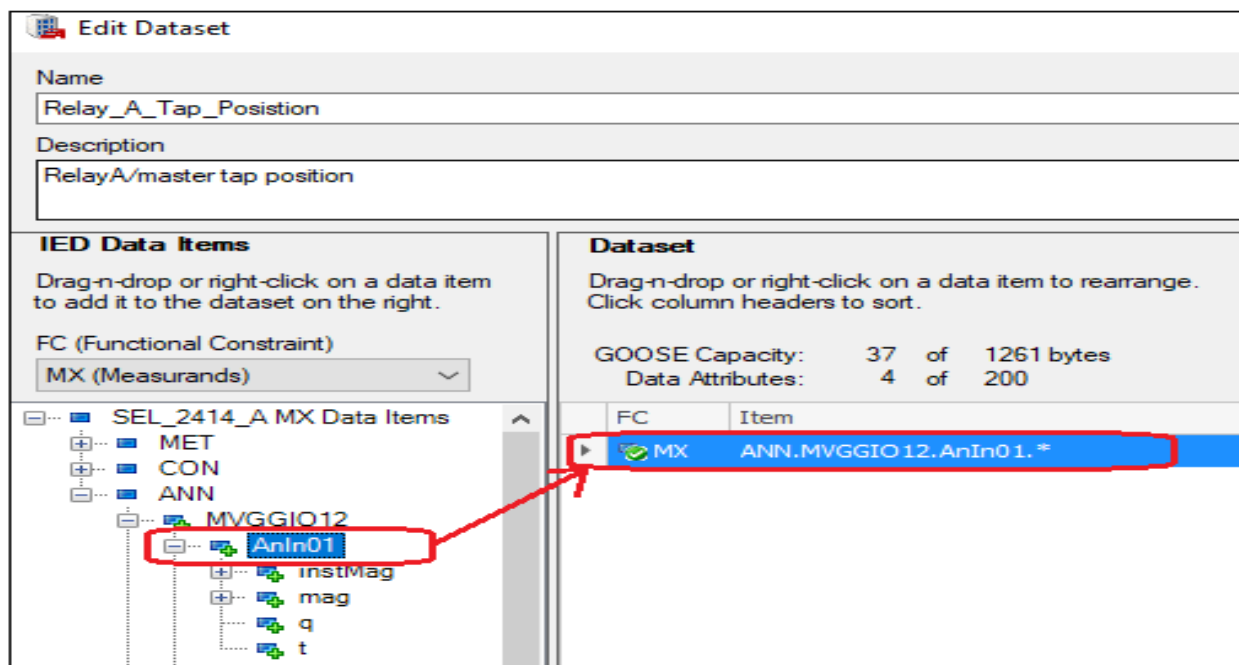


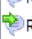
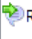



Figure 98: Adding the data item to the dataset of the Master Tap Position

#### 4.3.1.4 Adding datasets to GOOSE transmit

The datasets of the Master relay are published on external devices. These datasets are published within the communication network and can be subscribed to by multiple external devices. See Figure 99 for the GOOSE transmit tab of the Master relay.

GOOSE Transmit								
Name	Dataset	Description	LD	Interface	SubNetwork	Multicast MAC Address	APP ID	VLAN ID
 voltage	voltage		SEL_2414_ACFG	S1	W01	01-0C-CD-01-00-03	0003	003
 VOLTAGE_MAG	VOLTAGE_MAGNITUDE	VOLTAGE_MAGNITUDE	SEL_2414_ACFG	S1	W01	01-0C-CD-01-00-05	0005	003
 Relay_A_Tap_position	Relay_A_Tap_Posistion	RelayA/master tap position	SEL_2414_ACFG	S1	W01	01-0C-CD-01-00-06	0006	003
 RelayA_Raise_Tap	Relay_A_Tap_Raise	Relay_A_Raise_Tap_signal_out	SEL_2414_ACFG	S1	W01	01-0C-CD-01-00-07	0007	003
 RelayA_Lower_Tap	voltage	Relay_A_Lower_Tap_signal_out	SEL_2414_ACFG	S1	W01	01-0C-CD-01-00-08	0008	003

Messages: 5 of 8

[Properties](#) | [GOOSE Receive](#) | **[GOOSE Transmit](#)** | [Reports](#) | [Datasets](#) | [Dead Bands](#) | [Server Model](#)

Figure 99: The datasets of the Master relay that are published to the external devices

#### 4.3.1.5 Adding GOOSE subscriptions

Figure 100 shows the GOOSE receive tab of the Master relay. The dataset for the Tap synchronisation signal received from the Slave-Follower relay mapped to the Remote Bit 001 (RB001) address of the Master relay.

GOOSE Receive

IED

Control block

LD	LN	DO	DA
SEL_2414_B			
SEL_2414_BCFG/indication			
SEL_2414_BCFG/Relay_B_Lower			
SEL_2414_BCFG/Relay_B_Raise			
SEL_2414_BCFG/Relay_B_Sync			
ANN	OUTAGGIO2	Ind03	stVal

Category

intAddr	Source data item
RA	
RB	
RB01	SEL_2414_B/CFG/LLN0/Relay_B_Sync.ANN.OUTAGGIO2.Ind03.stVal
RB02	
RB03	
RB04	
RB05	
RB06	

Figure 100: The GOOSE datasets the Master relay receives from Slave-Follower relay

#### 4.3.1.5 Setting IED properties

**Figure 101** depicts the master relay's IED Properties. Details include the IP address, Subnet mask, and Gateway.

**IED Properties**

IEC 61850 Edition:  Version:  Revision:

UTC Offset:  *UTC Offset is configured in device settings.*

[MMS Settings](#)

MMS Authentication: OFF

MMS Inactivity Timeout: 900

**Communication Parameters\***

	Interface	IP address	Subnet mask	Gateway
▶	S1	192.168.1.1	255.255.255.0	0.0.0.0

**Figure 101: The IED Properties of the Master relay**

#### 4.3.1.6 Exporting CID file

Once the GOOSE configuration settings of the IED are complete, a CID file of the GOOSE configuration of the relay is exported. External devices import the CID file containing the details of the GOOSE configuration. This enables external devices to subscribe to GOOSE messages from this relay. See [Figure 102](#) for sending the CID file.

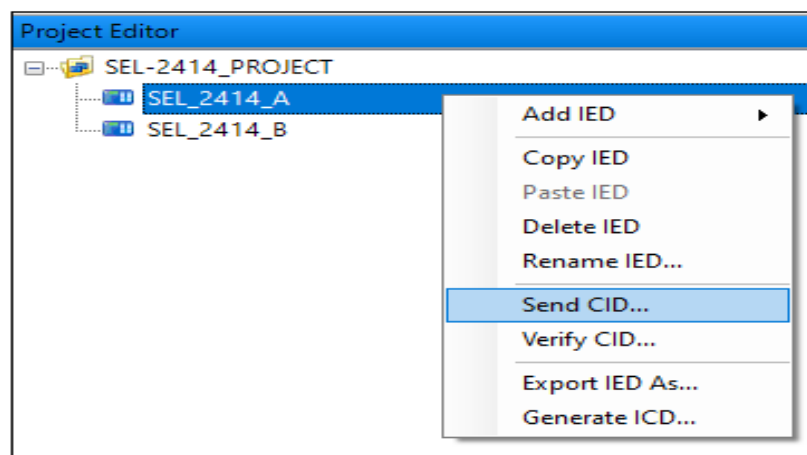


**Figure 102: Sending the CID file of the Master relay**

Once the option to send the relay's CID file has been selected, the program will prompt you to verify the FTP address, username, and password. Once these details have been filled out, external devices will export and import the relay's CID file. See



**Figure 103** This is to confirm the network settings of the Master relay before sending the CID file.

AcSElerator Architect

**SEL\_2414\_1**

Confirm Network Settings

SEL

FTP Address: 192.168.1.1  
Optional port number, append ':' and integer from 1 - 65535

User Name: FTPUSER

Password: •••••

Include Device Settings ☐

Cancel < Back Next > Finish

**Figure 103: Confirming the network settings of the Master relay before sending the CID file**

### 4.3.2 GOOSE Configuration of Slave-Follower Relay

The same procedure is followed to enable GOOSE protocol as mentioned in 4.3.1.1. and adding IED to project is the same as in 4.3.1.2.

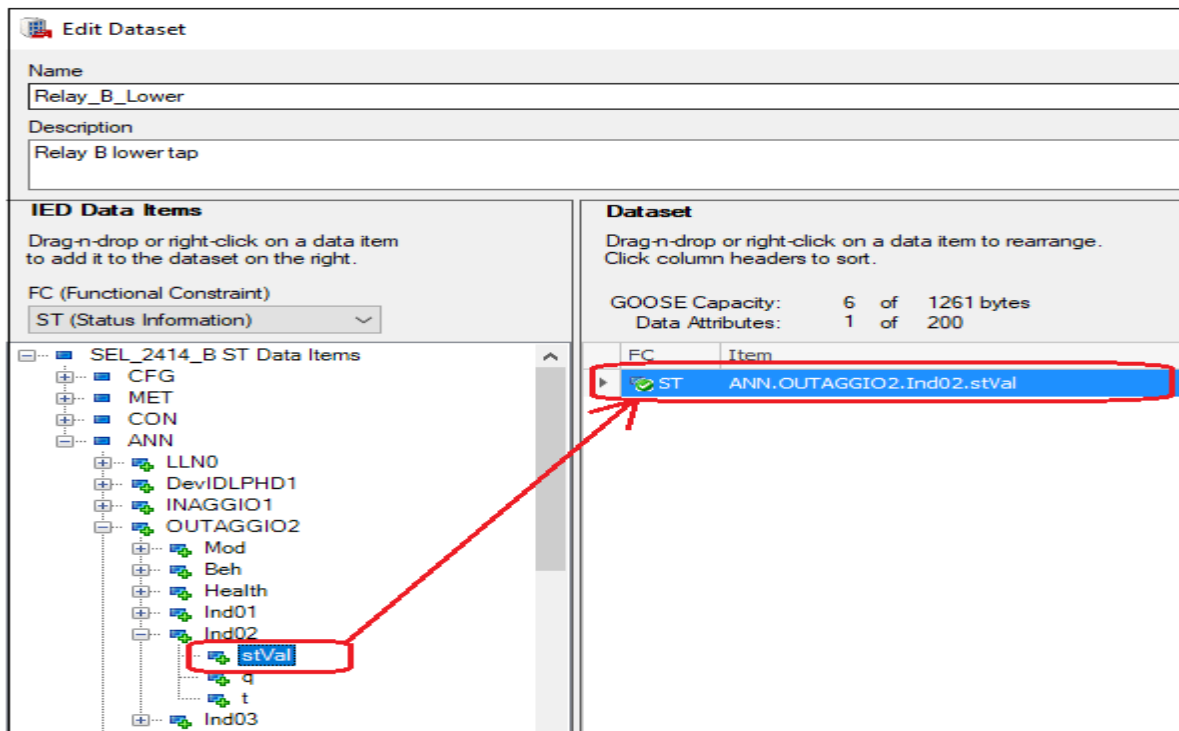
#### 4.3.2.1 Adding data items to dataset

The **Table 39** shows a list of the Logical Nodes included in the Slave-Follower relay's GOOSE communication structure. The relay will publish these datasets and receive them from external subscribing devices.

**Table 39: The datasets that is included in the Slave-Follower relay GOOSE configuration**

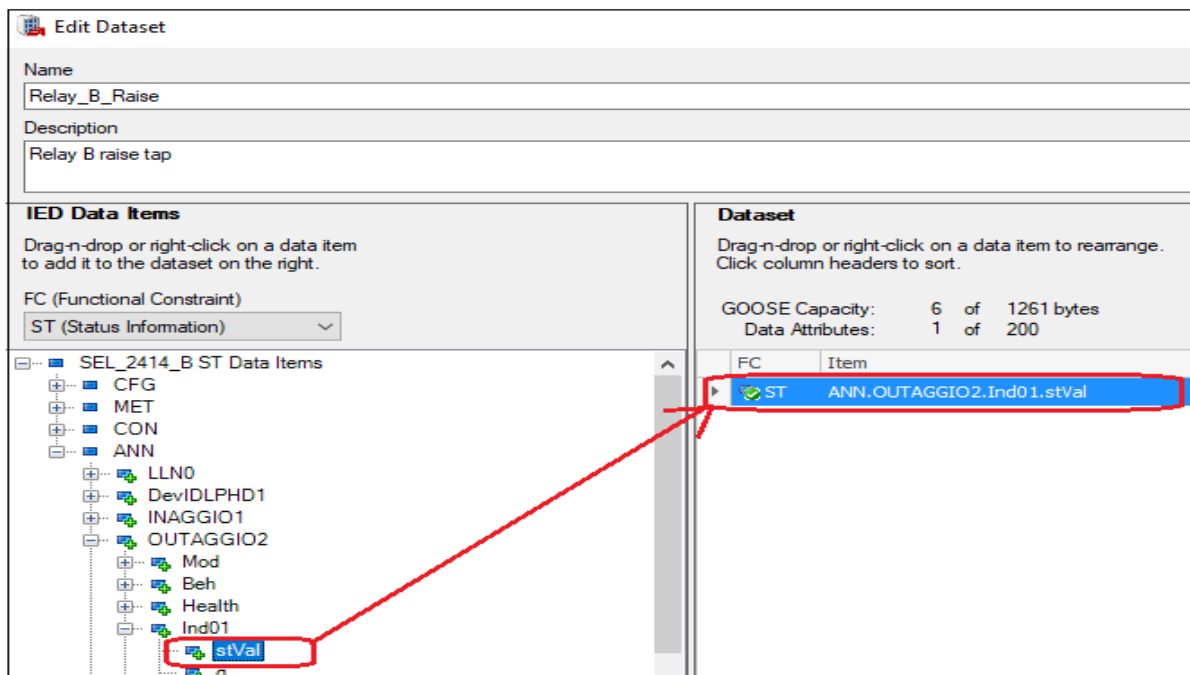
Logical Device: ANN (Annunciation)		
Logical Nodes	Status or Measurand	Device Word Bits or Analog Quantities
Device Word Bits		
OUTAGGIO2	Ind01.stVal	Digital Output (OUT101)—Slot A
OUTAGGIO2	Ind02.stVal	Digital Output (OUT102)—Slot A
OUTAGGIO2	Ind03.stVal	Digital Output (OUT103)—Slot A

**Figure 104** shows the procedure for adding the data item to the dataset of the Slave-Follower relay Lower signal. The Slave-Follower relay publishes this dataset, which external subscribing devices receive.



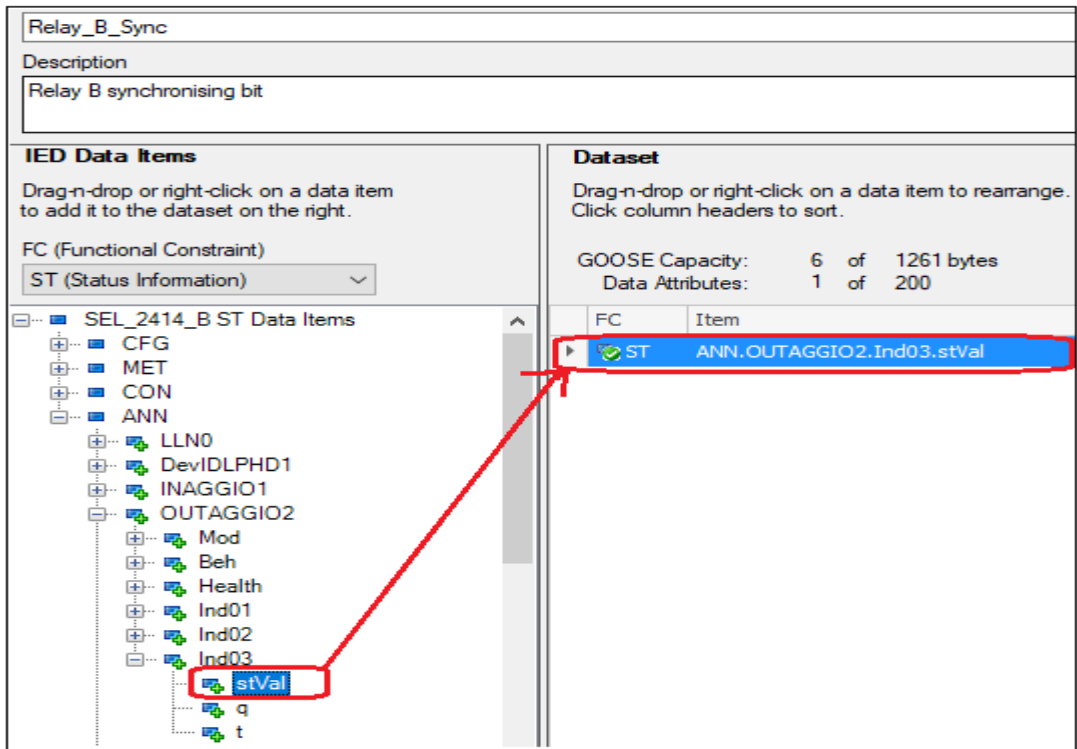
**Figure 104: Adding the data item to the dataset of the Slave-Follower relay lower signal**

Figure 105 shows procedure to add the data item to the Slave-Follower relay Raise signal dataset. The slave-follower publishes this dataset and receives it from external subscribing devices.



**Figure 105: Adding the data item to the dataset of the Slave-Follower relay raise signal**

Figure 106 depicts the procedure for adding the data item to the dataset of the Slave-Follower relay Tap synchronisation signal. This dataset is published by the Slave-Follower and received by external subscribing Master relay.



**Figure 106: Adding the data item to the dataset of the Slave-Follower relay for Tap synchronisation signal**

#### 4.3.2.2 Adding datasets to GOOSE transmit

The datasets of the Slave-Follower relay are published on external devices. These datasets are published within the communication network and can be subscribed to by multiple external devices. See Figure 107 for the GOOSE transmit tab of the Slave-Follower relay.

GOOSE Transmit								
Name	Dataset	Description	LD	Interface	SubNetwork	Multicast MAC Address	APP ID	VLAN ID
Indication	Indication		SEL_2414_BCFG	S1	W01	01-0C-CD-01-00-04	0004	003
Relay_B_Raise	Relay_B_Raise	Relay B Raise tap signal	SEL_2414_BCFG	S1	W01	01-0C-CD-01-00-09	0009	003
Relay_B_Lower	Relay_B_Lower	Relay B Lower tap signal	SEL_2414_BCFG	S1	W01	01-0C-CD-01-00-0A	000A	003
Relay_B_Sync	Relay_B_Sync	Tap sync between relays	SEL_2414_BCFG	S1	W01	01-0C-CD-01-00-0B	000B	003
<div> <div>New...</div> <div>Edit...</div> <div>Delete</div> </div> <div>Messages: 4 of 8</div>								
<div> <div>Properties</div> <div>GOOSE Receive</div> <div>GOOSE Transmit</div> <div>Reports</div> <div>Datasets</div> <div>Dead Bands</div> <div>Server Model</div> </div>								

**Figure 107: The datasets of the Slave-Follower relay that are published to the external devices**

### 4.3.2.3 Adding GOOSE subscriptions

Figure 108 shows the GOOSE receive tab of the Slave-Follower relay. The dataset for the tap position of the Master relay mapped to the Remote Analog 001(RA001) address of the Slave-Follower relay. Mapping datasets to address is achieved by dragging and dropping. The Voltages measured by the Master relay are mapped to the addresses RA002, RA003, and RA004 of the Slave-Follower relay.

GOOSE Receive				Category	
IED <span>▲</span>				Control block <span>▲</span>	
LD	LN	DO	DA	intAddr	Source data item
SEL_2414_A				RA	
SEL_2414_ACFG/Relay_A_Tap_position				RA001	SEL_2414_A/CFG/LLN0/VOLTAGE_MAG.MET.METMMXU1.PhV.phsA.instCVal.mag.f
● ANN	MVGGIO12	AnIn01	instMag.f	RA002	SEL_2414_A/CFG/LLN0/VOLTAGE_MAG.MET.METMMXU1.PhV.phsB.instCVal.mag.f
● ANN	MVGGIO12	AnIn01	mag.f	RA003	SEL_2414_A/CFG/LLN0/VOLTAGE_MAG.MET.METMMXU1.PhV.phsC.instCVal.mag.f
● ANN	MVGGIO12	AnIn01	q	RA004	SEL_2414_A/CFG/LLN0/Relay_A_Tap_position.ANN.MVGGIO12.AnIn01.instMag.f
● ANN	MVGGIO12	AnIn01	t	RA005	
SEL_2414_ACFG/RelayA_Lower_Tap				RA006	
SEL_2414_ACFG/RelayA_Raise_Tap				RA007	
SEL_2414_ACFG/voltage				RA008	
SEL_2414_ACFG/VOLTAGE_MAG				RA009	
● MET	METMMXU1	PhV	phsA.instCVal.mag.f	RA010	
● MET	METMMXU1	PhV	phsA.instCVal.ang.f	RA011	
● MET	METMMXU1	PhV	phsB.instCVal.mag.f	RA012	
● MET	METMMXU1	PhV	phsB.instCVal.ang.f	RA013	
● MET	METMMXU1	PhV	phsC.instCVal.mag.f	RA014	
● MET	METMMXU1	PhV	phsC.instCVal.ang.f	RA015	
● MET	METMMXU1	PhV	phsC.instCVal.mag.f	RA016	
● MET	METMMXU1	PhV	phsC.instCVal.ang.f	RA017	
● MET	METMMXU1	PhV	phsC.instCVal.mag.f	RA018	
● MET	METMMXU1	PhV	phsC.instCVal.ang.f	RA019	

**Figure 108: The GOOSE datasets Slave-Follower relay receives for Master relay**

### 4.3.2.4 Setting IED properties

The Figure 109 depicts the IED Properties of the Master relay. The details include the IP address, Subnet mask, and the Gateway of the Slave-Follower relay.

**IED Properties**

IEC 61850 Edition:  Version:  Revision:

UTC Offset:  *UTC Offset is configured in device settings.*

[MMS Settings](#)

MMS Authentication: OFF

MMS Inactivity Timeout: 900

Communication Parameters\*

	Interface	IP address	Subnet mask	Gateway
►	S1	192.168.1.2	255.255.255.0	0.0.0.0

**Figure 109: The IED Properties of the Slave-Follower relay**

The process of sending the CID file of the Slave-Follower relay is the same as that of the Master relay.

#### **4.4 Configuring the Omicron CMC 356 test injection device to receive GOOSE messages**

The Omicron CMC 356's GOOSE configuration was done using the Omicron Test Universe 4.31 software. The IEC 61850 GOOSE Configuration is selected from the program's main screen under the Test Modules & Tools tab. On the program's home screen, the Import SCL option is selected. This option allows you to import a project's CID file. The SEL-2414 CID file previously created and exported in the AcSELERator Architect software environment is selected. See [Figure 110: Importing the SCL file into the Omicron CMC 356 device](#).

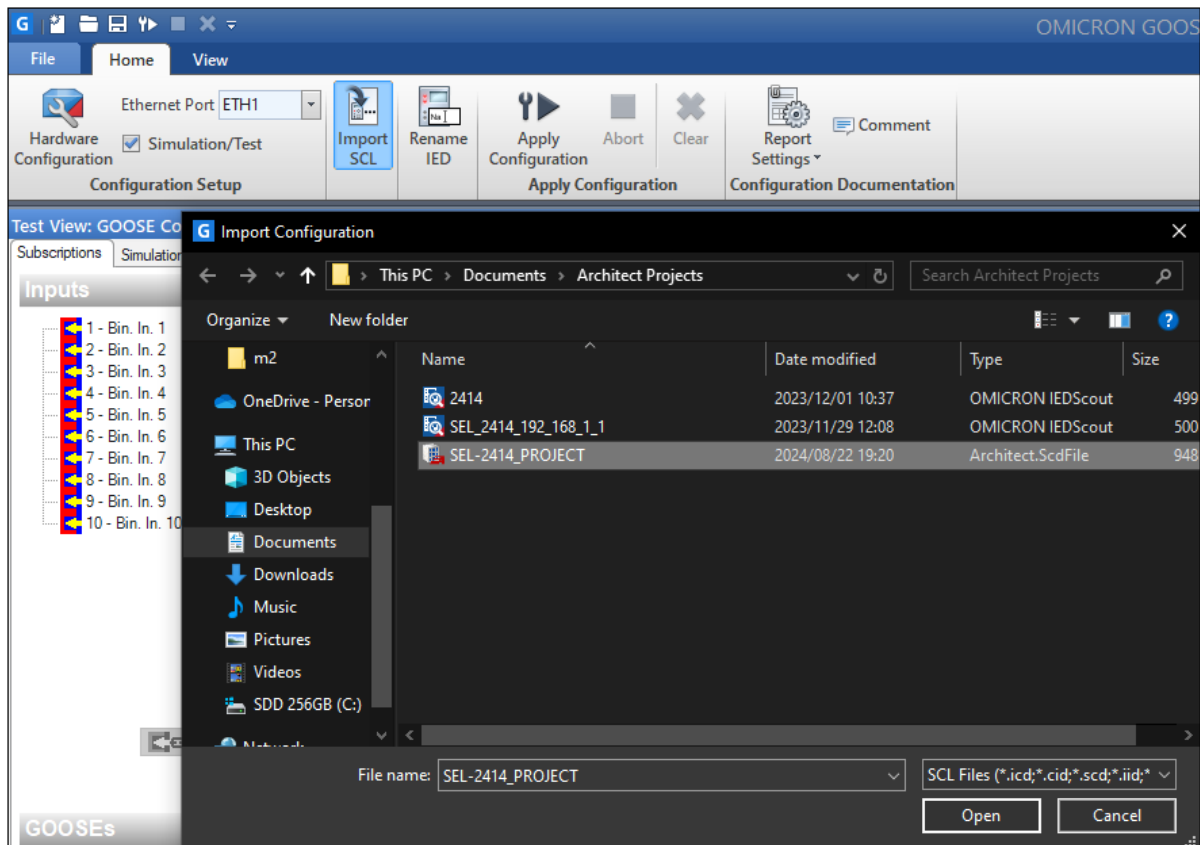


**Figure 110: Importing the SCL file into the Omicron CMC 356 device**

When selecting the SEL-2414 CID is selected, the import configuration tab opens up. This allows you to select the GOOSE dataset to be included. See [Figure 111](#) for choosing the GOOSE Datasets for which you wish to create subscriptions.

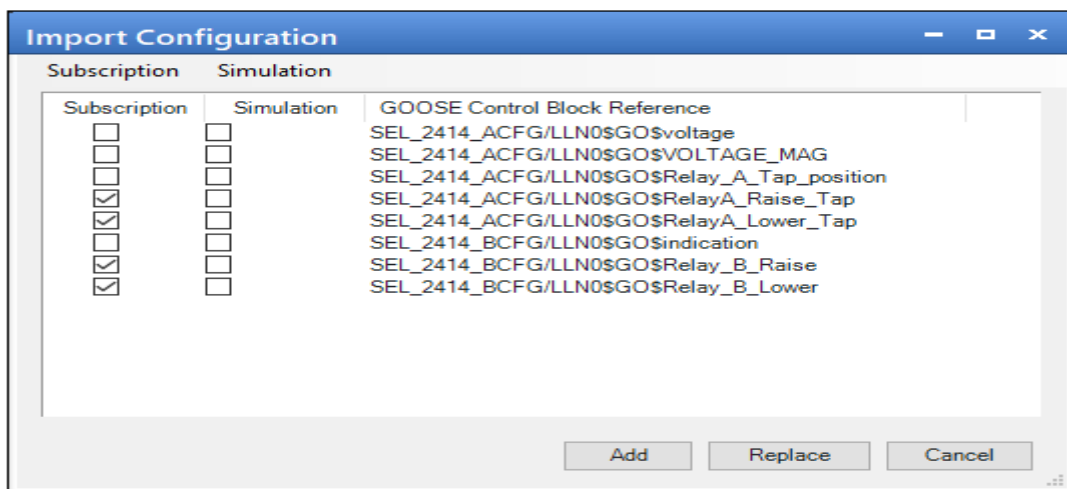


**Figure 111: Choosing the GOOSE Datasets for which you wish to create subscriptions**

Once the selection of items wished to be included has been made, they will appear at the bottom section of the program. The GOOSE dataset can now be dragged and dropped to the binary input section at the program's top. Once all the GOOSE datasets wished to include have been dragged to the relevant binary input, the Apply Configuration button must be clicked. The binary inputs of the Omicron CMC 356 have now been subscribed to the GOOSE messages published by the SEL-2414 relays. See Figure 112 for subscribing the GOOSE datasets to binary inputs on the Omicron CMC 356.

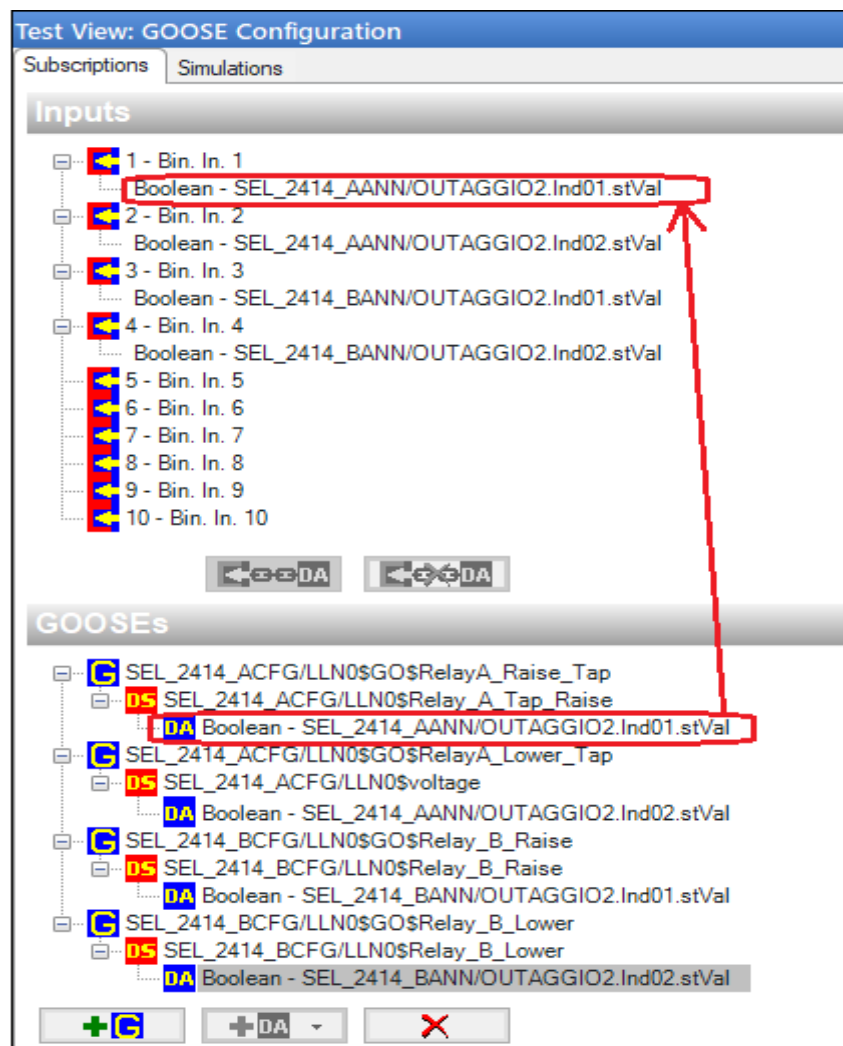


**Figure 112: Subscribing the GOOSE datasets to binary inputs on the Omicron CMC 356**

## 4.5 Configuring the Omicron CMC 356

Two Omicron CMC356 test injection devices create the lab-scale test bench setup for testing the master and slave-follower relay control algorithms and GOOSE

configurations. The first CMC 356 test injection device is configured to generate the three-phase voltage injected into the relay. The relay will measure this voltage and determine whether to initiate its internal programmed voltage control function. The second Omicron CMC 356 test injection device produces the 110VDC needed for the tap indication on the relays.

In 4.5.1, the first CMC test injection device is configured to generate the 3-phase voltages needed for the case studies. In 4.5.2, the second CMC test injection device is configured to generate an 110Vdc signal, which the relays use for tap indication.

#### 4.5.1 Configuring the Omicron CMC 356 to generate the 3-phase voltage

The Omicron QuickCMC application is used to generate the 3-phase voltage that is injected into the Master relay. From the main screen in the program, the QuickCMC is selected under the Test Modules & Tools tab. The current output section can be deactivated since only a voltage source is needed to perform the Lab-scale test bench setup. Under the Hardware Configuration tab, the Configure Device option is selected. The appropriate type of 3-phase voltage plus a neutral is chosen for this study. See [Figure 113](#) for configuring the hardware setup of the Omicron CMC 356

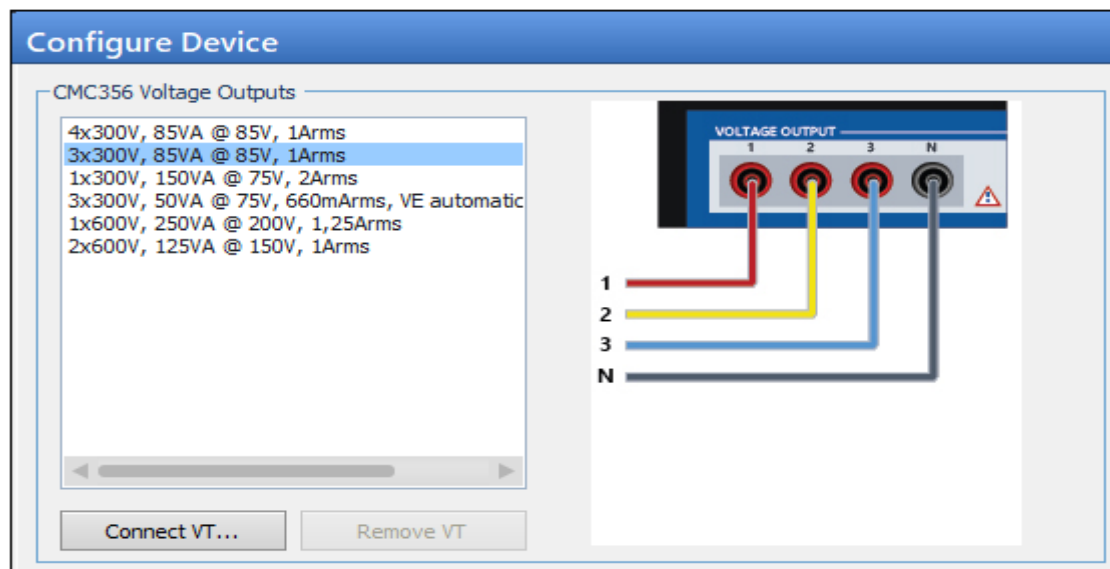


**Figure 113: Configuring the hardware setup of the Omicron CMC 356**

The number of binary inputs needed for this study must also be configured on the CMC 356 device. Four binary inputs are enabled to receive the previously



configured GOOSE messages. See Figure 114 for the selection of the inputs on the Omicron CMC 356 to monitor.

Hardware Configuration												
General			Analog Outputs		Binary / Analog Inputs		Binary Outputs		DC Analog Inputs			
			Function		Binary		Binary		Binary		Binary	
			Potential Free		<input checked="" type="checkbox"/>		<input checked="" type="checkbox"/>		<input checked="" type="checkbox"/>		<input checked="" type="checkbox"/>	
			Nominal Range									
			Clamp Ratio									
			Threshold									
Test Module Input Signal	Display Name	Connection Terminal	1+	1-	2+	2-	3+	3-	4+	4-	5+	5-
<b>Bin. in 1</b>	<b>Bin. in 1</b>		X									
Bin. in 2	Bin. in 2				X							
Bin. in 3	Bin. in 3						X					
Bin. in 4	Bin. in 4								X			
Not used	Bin. in 5										X	
Not used	Bin. in 6											

**Figure 114: Selecting the inputs on the Omicron CMC 356 to monitor**

The blank QuickCMC voltage generator test template is shown in Figure 115 with the section circled in red configures the voltage magnitude to be generated. The section circled in blue is the GOOSE inputs received from the external publishing relays as previously configured.

Test View: QuickCMC

analog outputs

Set Mode: Direct

V L1-E	0,00 V	0,00 *	50,000 Hz
V L2-E	0,00 V	-120,00 *	50,000 Hz
V L3-E	0,00 V	120,00 *	50,000 Hz

173,2 VA

1,0 kΩ

57,7 V

3,0 A

Analog Inputs

Vdc: 0,000 V Idc: 0,0000 mA

Binary Outputs

1 Bin. out 1	✓
2 Bin. out 2	✓
3 Bin. out 3	✓
4 Bin. out 4	✓

On Trigger

☒ Switch off Delay: 0,00 s

Step / Ramp

Signal(s): V L1-E Size: 0,00 V ☐ Auto step

Quantity: Magnitude Time: 1,000 s

☐ Pulse ramp Reset: 500,0 ms

Binary Inputs / Trigger

Bin. in 1	<input checked="" type="checkbox"/>	n/a
Bin. in 2	<input checked="" type="checkbox"/>	n/a
Bin. in 3	<input checked="" type="checkbox"/>	n/a
Bin. in 4	<input checked="" type="checkbox"/>	n/a

**Figure 115: Test template created in Quick CMC to inject 3-phase voltage into the Master relay**

### 4.5.2 Configuring the Omicron CMC 356 to generate the 110VDC used for the tap indication on the relays

The second Omicron CMC 356 test injection device supplies 110VDC needed for the tap indication on the relays. From the program's main screen, the AuxDC Configuration is selected under the Test Modules & Tools tab. The slider selects the desired voltage level. Select Apply Configuration to enable the voltage output. See Figure 116 for selecting the Aux DC voltage.

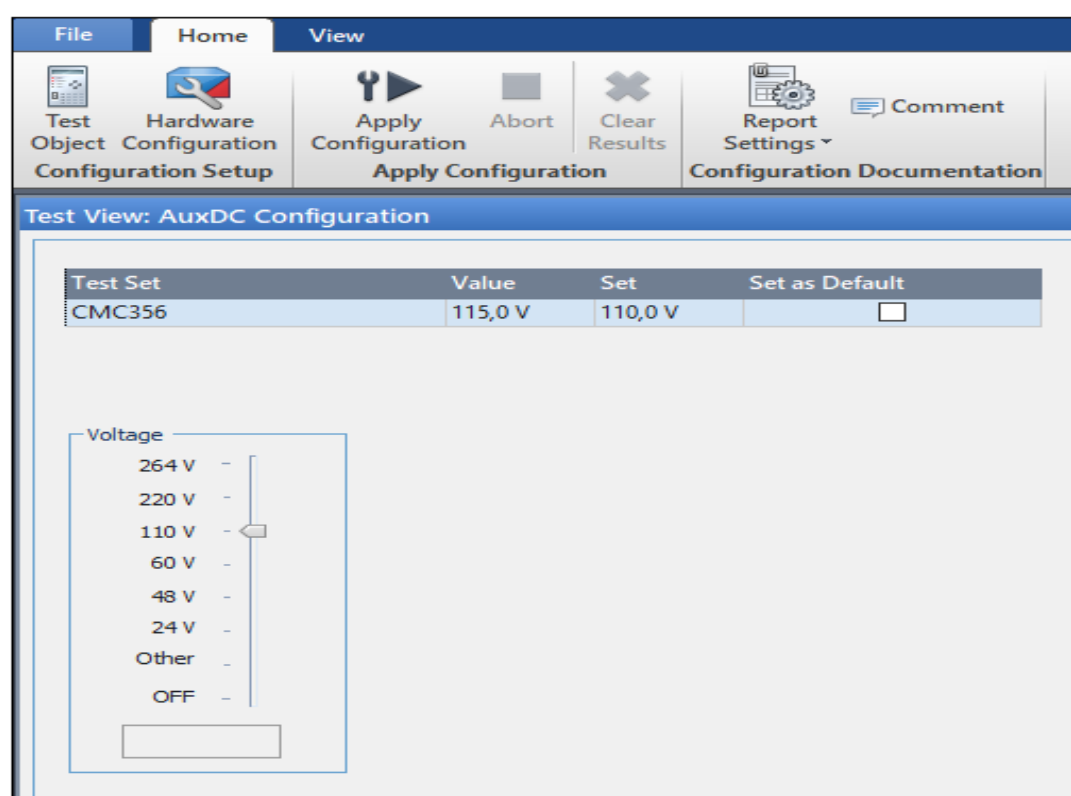


**Figure 116: Selecting the Aux DC voltage**

## 4.6 Lab-scale test bench setup for testing the Master- and Slave-Follower relays control algorithms and GOOSE configurations

Figure 117 depicts the basic structure of the Lab-scale test bench setup for testing the Master- and Slave-Follower relays control algorithms and GOOSE configurations. This test bench setup is created to verify the performance of the voltage control algorithms developed and to verify the successful implementation of

the GOOSE communication protocol for transmitting data between the relays and to transmit control signals to the CMC356 device. Following the successful lab scale test bench setup, the SEL-2414 relays are implemented into the hardware-in-the-loop test setup for real-world simulated testing.

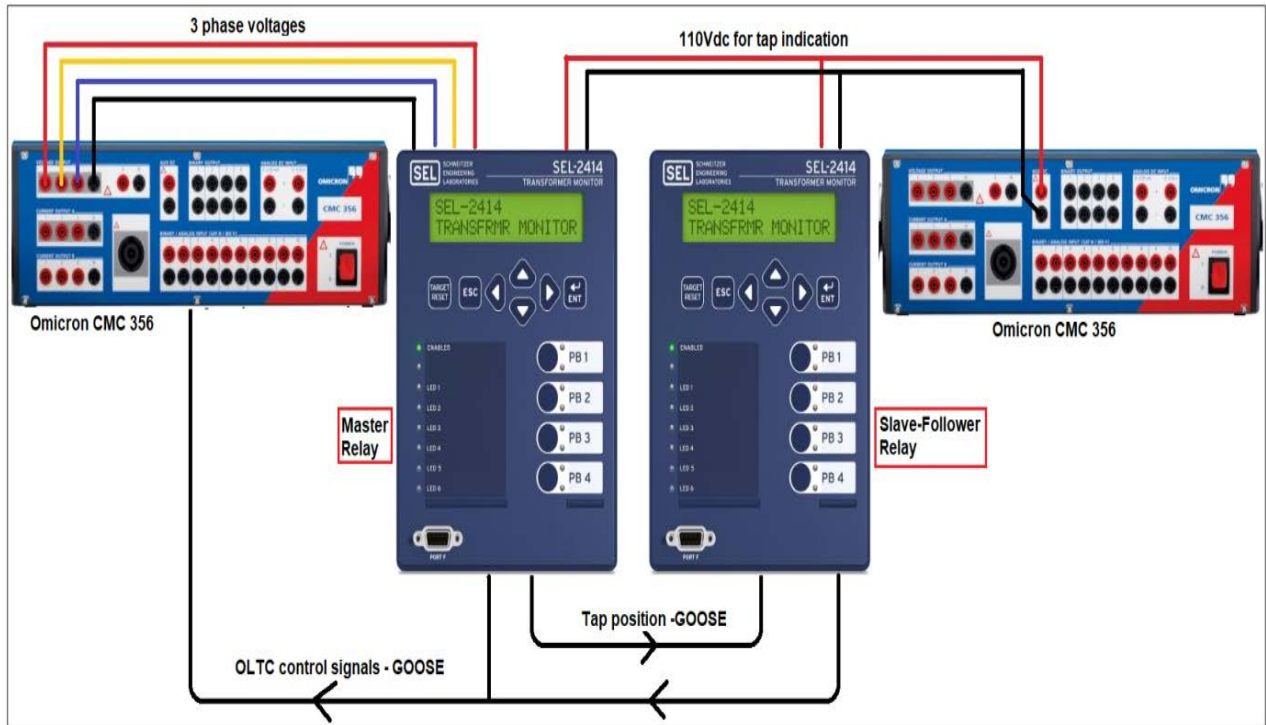


**Figure 117: Structure of the Lab-scale test bench setup for testing the Master- and Slave-Follower relays control algorithms and GOOSE configurations**

**Three case studies were conducted for the lab-scale testing:**

- 1) Signals simulating steady-state conditions were generated with the CMC 356 test injection device to simulate conditions where no tap change operations is needed
- 2) The CMC 356 test injection generated signals simulating overvoltage conditions. Tap change operations are needed.
- 3) The CMC 356 test injection generated signals simulating overvoltage conditions. Tap change operations are needed.

#### 4.6.1 Case Study 1: Steady-state condition

Utilizing the Omicron CMC 356 test injection device, a 3-phase 69 V AC signal is generated. The master relay monitors this voltage and determines whether a voltage control function should be activated.

**Voltage magnitude = test injecting voltage x PT ratio of relay = 69 x 276 = 19,05 kV L-N or 32,994 kV L-L. (4.7)**

This voltage magnitude is within the 5% acceptable voltage deviation from the nominal voltage value and thus requires no intervention from the IEDs to initiate the automatic voltage control functions. Figure 118 depicts the Quick CMC test template indicating the 3-phase 69 VAC generated. No GOOSE control signals are received on the binary inputs.

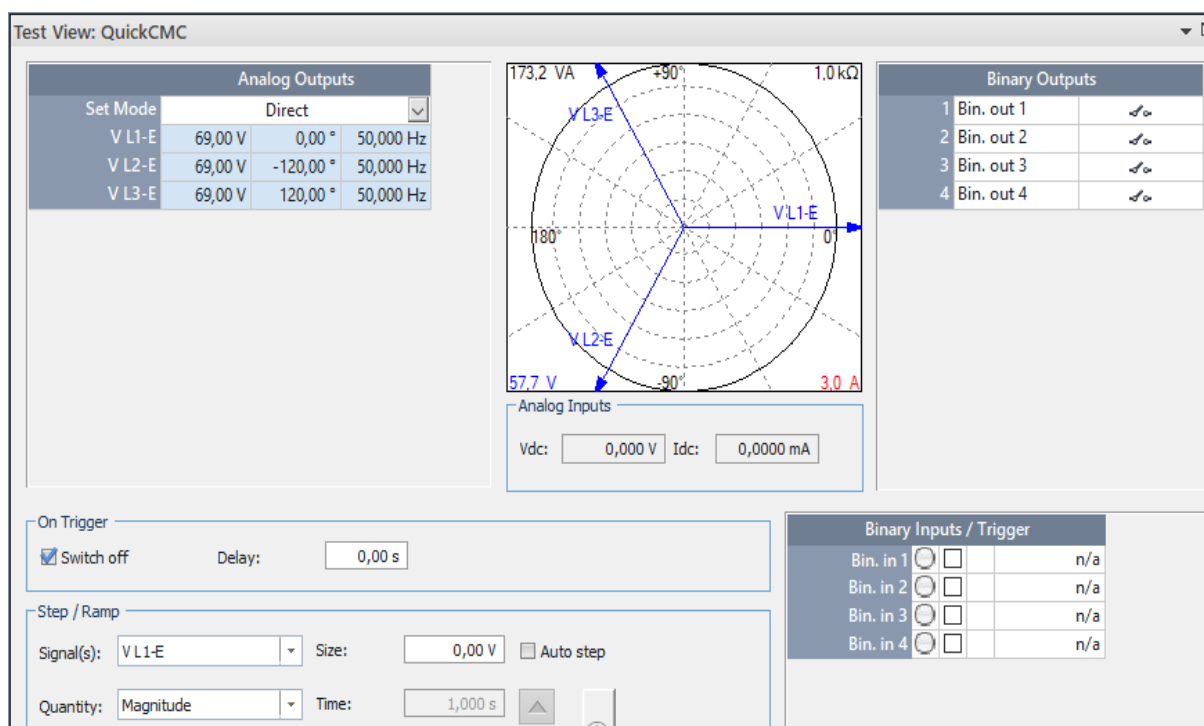


**Figure 118: Quick CMC test template indicating the 3 phase 69 VAC generated with no binary inputs**

Figure 119 depicts the Master relay's HMI, showing the measured values. The measured voltages are within the 5% dead band set point and thus require no voltage regulation. OUT101 and OUT102 are inactive.

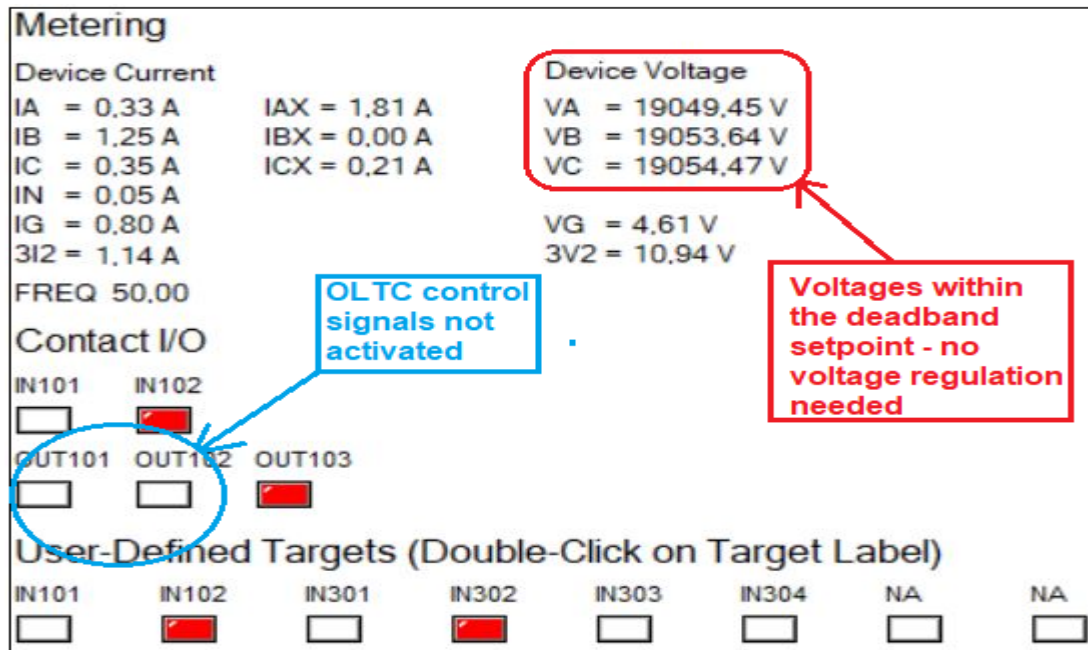


Figure 119: HMI of the Master relay showing the measured values

#### 4.6.2 Case Study 2: Overvoltage conditions

Utilizing the Omicron CMC 356 test injection device, a 3phase 69 V AC signal is generated. The Master relay monitors this voltage and determines if a voltage control function should be activated. The second CMC356 test device generates 110 VDC and is manually connected to the inputs of the Master relay to indicate a tap position of 10. The tap position of the Master relay is sent via analog GOOSE communication to the Slave-Follower relay. The slave-Follower tap position is 0.

$$\text{Voltage magnitude} = \text{test injecting voltage} \times \text{PT ratio of relay} = 73 \times 276 = 20,424 \text{ kV L-N or } 35,375 \text{ kV L-L.} \quad (4.8)$$

This voltage monitored by the Mater relay exceeds the 5% acceptable voltage deviation value, set at 20,005 kV for over-voltage pickup. The Master relay thus prompted the automatic voltage control function to be initiated. After 30.57 seconds, an OLTC GOOSE control signal is received by the CMC 356 device from the Master relay. The Slave-Follower also activates its tap raise function in response to matching the tap position of the master relay. The CMC 356 device receives the tap Raise signal of the Slave-Follower relay at binary input 3.

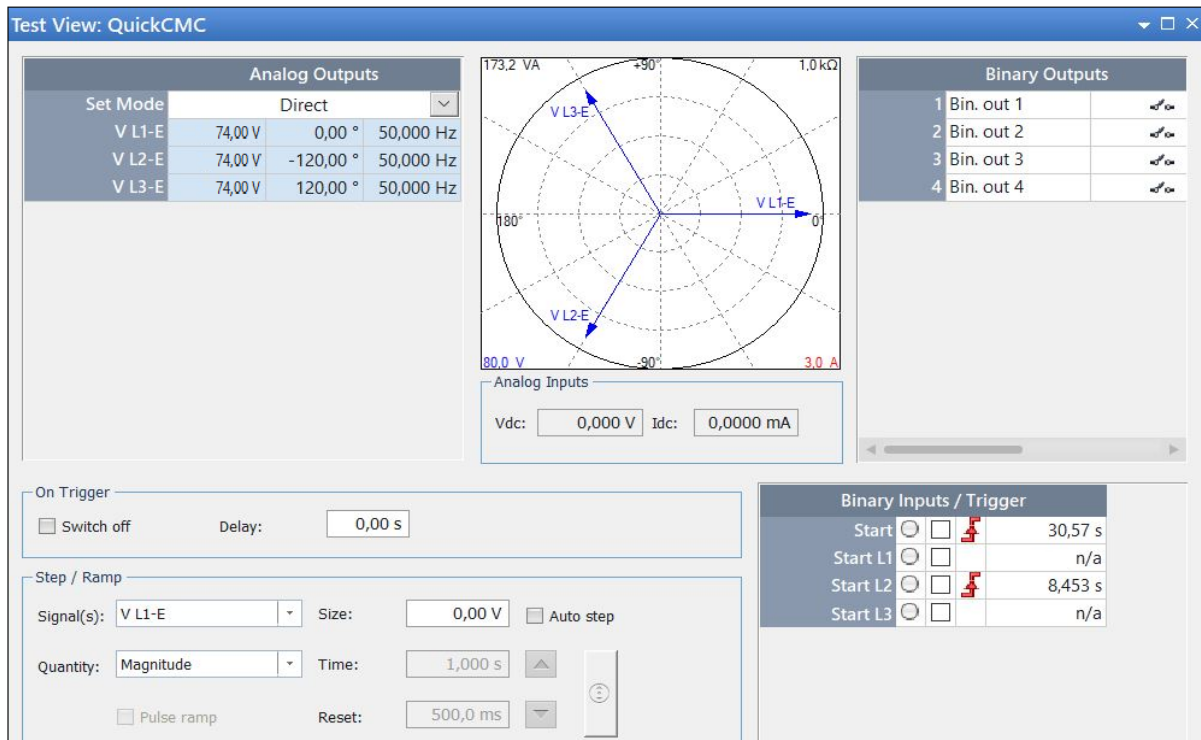


**Figure 120: Quick CMC test template indicating the 3 phase 74 VAC generated with binary inputs from Master- and Slave-Follower relays**

Figure 121 shows the relay event report of the Master relay indicates the voltage measured, which, after 30.57 seconds, activated the OLTC voltage regulation function. At the bottom of the graphs, elements from the tap Raise algorithm are shown, which activates the Tap Raise control function.

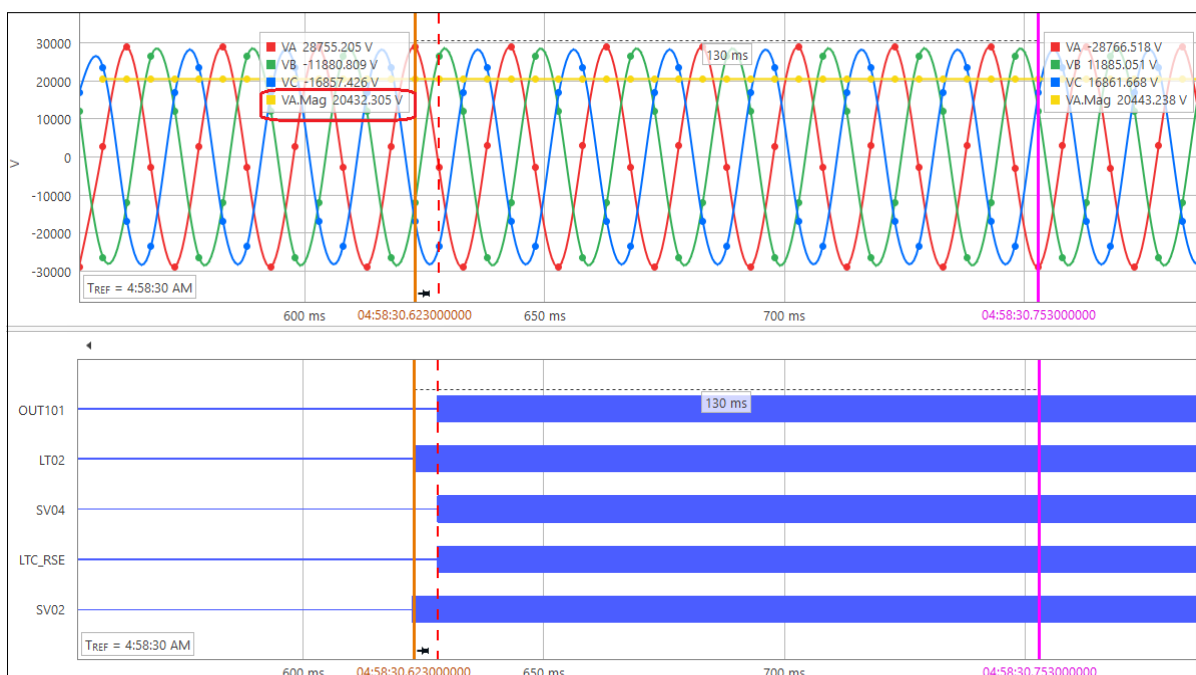


**Figure 121: Master relay event report for over voltage conditions**



Figure 122 shows the relay event report of the Slave-Follower relay, indicating elements from the tap Raise algorithm that activated the Tap Raise control function.

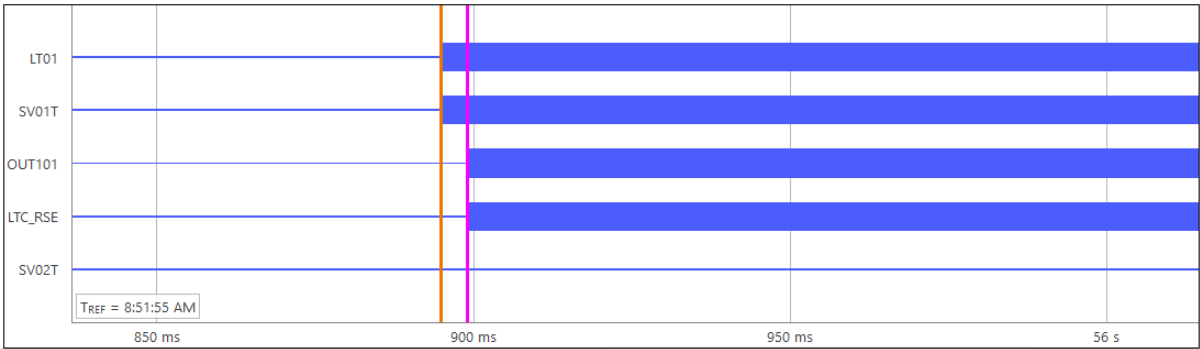


Figure 122: Slave-Follower relay event report for over-voltage conditions

The Wireshark Network Analyzer software was utilized to monitor the IEC 61850 GOOSE traffic on the network during the relay testing. This was done to verify that the GOOSE signals were successfully published across the network by the Master and Slave-Follower relays. Figure 123 shows the voltage magnitude measured by the Master relay published to the Slave-Follower relay.

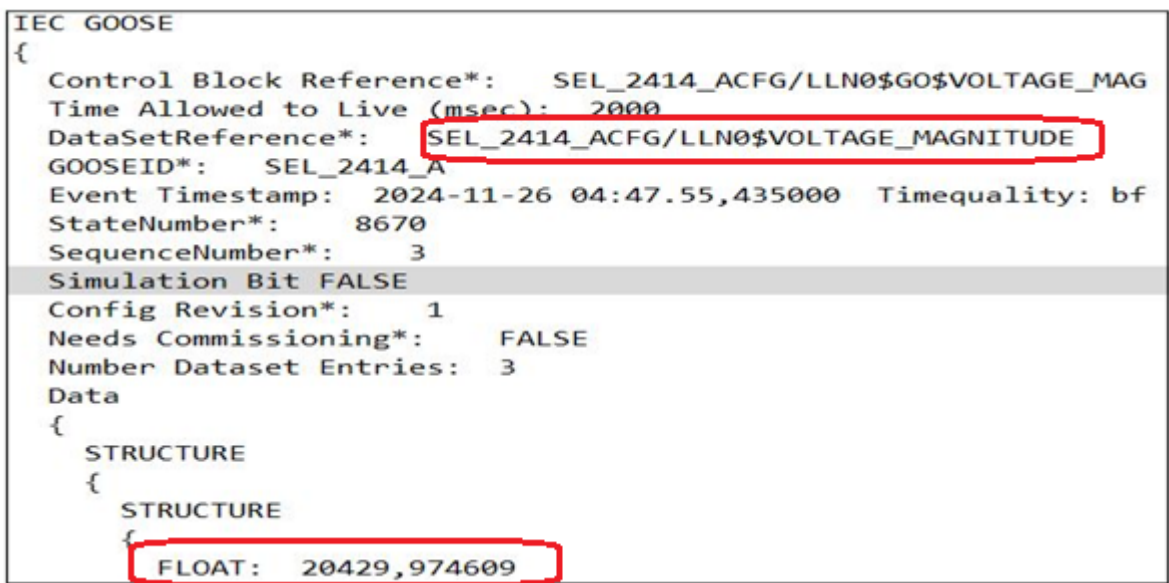


Figure 123: Voltage measured by the Master relay during over voltage conditions being published to the Slave-Follower relay via analog GOOSE

Shown in Figure 124 is the Master relay publishing a tap Raise control signal to the network. The CMC 356 subscribes to this GOOSE message and is received at binary 1 input on the CMC 356.

```
IEC GOOSE
{
  Control Block Reference*: SEL_2414_ACFG/LLN0$GO$RelayA_Raise_Tap
  Time Allowed to Live (msec): 2000
  DataSetReference*: SEL_2414_ACFG/LLN0$Relay_A_Tap_Raise
  GOOSEID*: SEL_2414_A
  Event Timestamp: 2024-11-26 04:21.46,131000 Timequality: bf
  StateNumber*: 92
  SequenceNumber*: 4
  Simulation Bit FALSE
  Config Revision*: 1
  Needs Commissioning*: FALSE
  Number Dataset Entries: 1
  Data
  {
    BOOLEAN: TRUE
  }
}
```

**Figure 124: The Master relay publishes a tap Raise control signal to the network**

Shown in Figure 125 is the Slave-Follower relay publishing a tap Raise control signal to the network. The CMC 356 subscribes to this GOOSE message and is received at binary 3 input on the CMC 356.

```
IEC GOOSE
{
  Control Block Reference*: SEL_2414_BCFG/LLN0$GO$Relay_B_Raise
  Time Allowed to Live (msec): 12
  DataSetReference*: SEL_2414_BCFG/LLN0$Relay_B_Raise
  GOOSEID*: SEL_2414_B
  Event Timestamp: 2024-11-26 04:18.57,327000 Timequality: bf
  StateNumber*: 278
  SequenceNumber*: 0
  Simulation Bit FALSE
  Config Revision*: 1
  Needs Commissioning*: FALSE
  Number Dataset Entries: 1
  Data
  {
    BOOLEAN: TRUE
  }
}
```

**Figure 125: The Slave-Follower relay publishes a tap Raise control signal to the network**

Shown in Figure 126 is the Tap position of the Master relay being published to the Slave-Follower relay via analog GOOSE. The Slave-Follower relay subscribes to this analog GOOSE message.



```

Time Allowed to Live (msec): 2000
DataSetReference*: SEL_2414_ACFG/LLN0$Relay_A_Tap_Posistion
GOOSEID*: SEL_2414_A
Event Timestamp: 2024-11-26 04:13.21,034000 Timequality: bf
StateNumber*: 6
SequenceNumber*: 1193
Simulation Bit FALSE
Config Revision*: 3
Needs Commissioning*: FALSE
Number Dataset Entries: 1
Data
{
  STRUCTURE
  {
    STRUCTURE
    {
      FLOAT: 10,000000
    }
  }
}

```

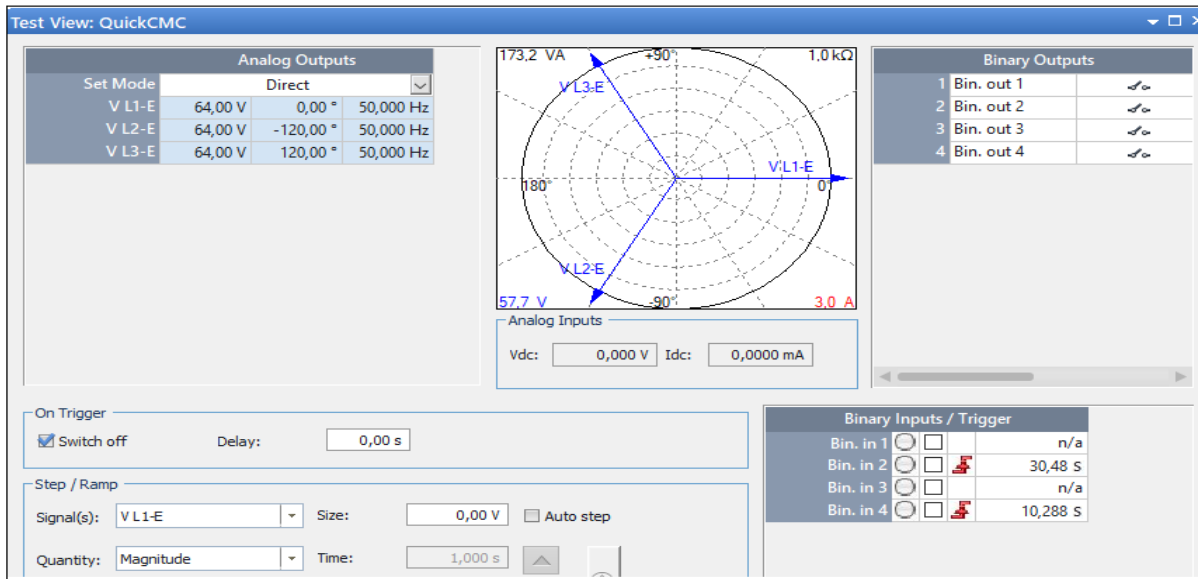
**Figure 126:** Shown in Figure # is the Tap position of the Master relay being published to the Slave-Follower relay via analog GOOSE

### 4.6.3 Case Study 3: Under voltage conditions

Utilizing the Omicron CMC 356 test injection device, a 3phase 64 V AC signal is generated. The Master relay monitors this voltage and determines if a voltage control function should be activated. The second CMC356 test device generates 110 VDC and is manually connected to the inputs of the Slave-Follower relay to indicate a tap position of 10. The tap position of the Master relay is sent via analog GOOSE communication to the Slave-Follower relay. The Master relay tap position is 0.

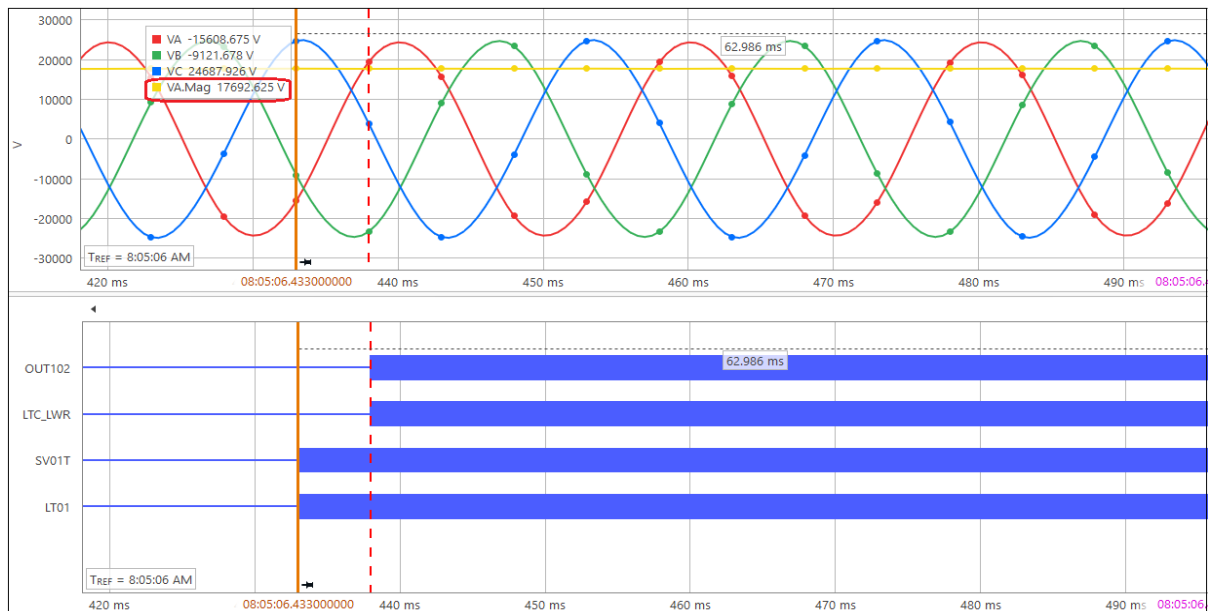
**Voltage magnitude = test injecting voltage x PT ratio of relay = 64 x 276 = 17,664 kV L-N or 30,594 kV L-L. (4.8)**

This voltage monitored by the Mater relay exceeds the 5% acceptable voltage deviation value, set at 18,099 kV for under-voltage pickup. The Master relay thus prompted the automatic voltage control function to be initiated. After 30.48 seconds, an OLTC GOOSE control signal is received by the CMC 356 device from the Master relay at binary 2 input. The Slave-Follower also activates its tap raise function in response to matching the tap position of the master relay. Tap Lower signal of the Slave-Follower relay is received by the CMC 356 device at binary input 4. Shown in [Figure 127](#) is the Quick CMC test template indicating the 3-phase 64 VAC generated with binary inputs received from Master- and Slave-Follower relays.



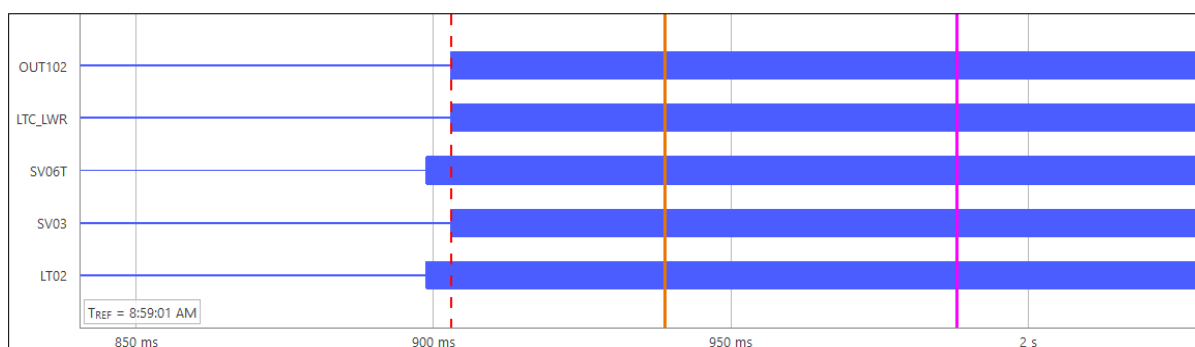
**Figure 127: Quick CMC test template indicating the 3-phase 64 VAC generated with binary inputs received from Master- and Slave-Follower relays**

Figure 128 Shows the relay event report of the Master relay indicating the voltage measured, which, after 30,48 seconds, activated the OLTC voltage regulation function. At the bottom section of the graphs, elements from the Tap Lower algorithm are shown, which activated the Tap Lower control function.



**Figure 128: Master relay event report for under voltage conditions**

Figure 129 shows the relay event report of the Slave-Follower relay, indicating elements from the tap Lower algorithm that activated the Tap Lower control function.



**Figure 129: Slave-Follower relay event report for under-voltage conditions**

The Wireshark Network Analyzer software was utilized to monitor the IEC 61850 GOOSE traffic on the network during the relay testing. This was done to verify that the GOOSE signals were successfully published across the network by the Master and Slave-Follower relays. Figure 130 shows the voltage magnitude measured by the Master relay published to the Slave-Follower relay.

```
IEC GOOSE
{
  Control Block Reference*:  SEL_2414_ACFG/LLN0$GO$VOLTAGE_MAG
  Time Allowed to Live (msec): 12
  DataSetReference*:  SEL_2414_ACFG/LLN0$VOLTAGE_MAGNITUDE
  GOOSEID*:  SEL_2414_A
  Event Timestamp:  2024-11-26 04:33.12,374000  Timequality: bf
  StateNumber*:  7495
  SequenceNumber*:  0
  Simulation Bit FALSE
  Config Revision*:  1
  Needs Commissioning*:  FALSE
  Number Dataset Entries:  3
  Data
  {
    STRUCTURE
    {
      STRUCTURE
      {
        FLOAT:  17123,238281
      }
    }
  }
}
```

**Figure 130: Voltage measured by the Master relay during under voltage conditions being published to the Slave-Follower relay via analog GOOSE**

Shown in Figure 131 is the Master relay publishing a tap Lower control signal to the network. The CMC 356 subscribes to this GOOSE message and is received at binary three input on the CMC 356.

```

AppID*: 8
PDU Length*: 131
Reserved1*: 0x0000
Reserved2*: 0x0000
PDU
  IEC GOOSE
  {
    Control Block Reference*: SEL_2414_ACFG/LLN0$GO$RelayA_Lower_Tap
    Time Allowed to Live (msec): 2000
    DataSetReference*: SEL_2414_ACFG/LLN0$Voltage
    GOOSEID*: SEL_2414_A
    Event Timestamp: 2024-11-26 04:33.10,238000 Timequality: bf
    StateNumber*: 192
    SequenceNumber*: 4
    Simulation Bit FALSE
    Config Revision*: 1
    Needs Commissioning*: FALSE
    Number Dataset Entries: 1
    Data
    {
      BOOLEAN: TRUE
    }
  }

```

**Figure 131: The Master relay publishes a tap Lower control signal to the network**

Shown in Figure 132 is the Slave-Follower relay publishing a tap Lower control signal to the network. The CMC 356 subscribes to this GOOSE message and is received at binary 4 input on the CMC 356.

```

> Frame 1321: 144 bytes on wire (1152 bits), 144 bytes captured (1152 bits) on interface 0
> Ethernet II, Src: Schweitz_0c:3c:5d (00:30:a7:0c:3c:5d), Dst: Iec-Tc57_01:00:0a (01:0c:cd:01:00:0a)
v goose
  AppID*: 10
  PDU Length*: 130
  Reserved1*: 0x0000
  Reserved2*: 0x0000
  v PDU
    IEC GOOSE
    {
      Control Block Reference*: SEL_2414_BCFG/LLN0$GO$Relay_B_Lower
      Time Allowed to Live (msec): 2000
      DataSetReference*: SEL_2414_BCFG/LLN0$Relay_B_Lower
      GOOSEID*: SEL_2414_B
      Event Timestamp: 2024-11-26 05:11.3,031000 Timequality: bf
      StateNumber*: 14
      SequenceNumber*: 5
      Simulation Bit FALSE
      Config Revision*: 1
      Needs Commissioning*: FALSE
      Number Dataset Entries: 1
      Data
      {
        BOOLEAN: TRUE
      }
    }
  }

```

**Figure 132: The Slave-Follower relay publishing a tap Lower control signal to the network**

## 4.7 Conclusion

This chapter demonstrated the development process and testing of the custom-created voltage control algorithms to control the OLTCs of the transformer pair and the configuration settings of the Master and Slave-Follower relay's implementation of the IEC61850 GOOSE communication. The lab-scale test bench setup was constructed, and two Omicron CMC 356 test injection devices were utilized to generate the relevant test signals. To verify that the GOOSE signals are successfully published across the network, the Wireshark Network Analyzer software was utilized to monitor the IEC 61850 GOOSE traffic during the relay testing. From the lab-scale testing conducted, it can be concluded that the Master and Slave-Follower relays, programmed with the created algorithms and engineering configurations, were able to successfully issue the appropriate voltage correction signals for various testing conditions. Wireshark Network Analyzer software verified that the GOOSE control signal was successfully published to the network and that Omicron could subscribe to them. However, this testing method has drawbacks because the Omicron CMC 356 device is not a live system that offers real-time feedback. The SEL-2414 relays are incorporated into an RTDS simulation environment with real-time feedback for live system testing.

The next chapter will focus on incorporating the two SEL-2414 relays into a modified version of the IEEE 14 Bus network built in the RSCAD FX environment. A hardware-in-the-loop setup is created for real-time digital simulation to properly scrutinize the voltage control functions of the Master and slave-follower relays. The relay settings will remain the same as those configured in Chapter 5. With GOOSE communication and control signal transmission to the RTDS equipment, peer-to-peer communication between the relays is established.

## CHAPTER FIVE

### HARDWARE-IN-THE-LOOP SIMULATION AND TESTING OF THE POWER TRANSFORMER TAP-CHANGE CONTROLLER

#### 5.1 Introduction

A modified version of the IEEE 14 Bus network was constructed in the RSCAD FX environment. An identical 100 MVA power transformer T18 was added to the network in parallel with the 100 MVA T17 transformer. Both T17 & T18 transformers have a primary side voltage of 132 kV connected to Bus5 and a secondary side voltage of 33 kV connected to Bus5. A hardware-in-the-loop network is constructed, incorporating the two SEL-2414 relays to monitor and control the voltage regulation function of the parallel transformers in the RTDS equipment. OLTCs with 20 steps were added to both Transformer T17 and T18. Step 10 of these OLTCs will serve as the neutral tap. The OLTCs of these transformers are situated on the HV side of the transformers. IEC61850 GOOSE communication will facilitate the interchange of communication between the two IEDs and convey control signals to the RTDS equipment. An Omicron CMS 156 amplifier device is used to amplify the analogue voltage signals generated within the RTDS equipment to functional magnitudes to be supplied to the SEL-2414 IED. A CMC 356 signal generator device will generate the high-voltage signals provided to the GTFPI of the RTDS equipment to be needed to develop the relevant signals to be required by the SEL-2414 IEDs. The dynamic load DL6 connected to the 33 kV Bus 6 is varied in this study to cause fluctuation in the voltage magnitude on the 33 kV Bus 6. The change in voltage magnitude is observed by the SEL-2414 relays monitoring the T17 and T18 transformers, and it will activate the voltage control function configured within the IEDs to perform corrections and maintain the voltage magnitude within the  $\pm 5\%$  tolerance range.

This chapter aims to demonstrate the development and testing of the modified version of the IEEE 14 Bus network constructed in the RSCAD FX environment. The RTDS equipment was configured, and hardware-in-the-loop simulation testing was conducted incorporating the two SEL-2414 relays responsible for controlling the OLTCs of the parallel transformers and the IEC61850 GOOSE protocol.

Section 5.1 of this chapter covers the introduction, modelling the Modified IEEE 14 Bus network is shown in section 5.2, modelling of Loads in RSCAD is shown in section 5.3, modelling the power sources in section 5.4, modelling the transmission lines in section 5.5, Configuring the RTDS Hardware components in section 5.6 , IEC61850 GOOSE configuration of the RTDS equipment in section 5.7, Case Studies conducted in section 5.8, section 5.9 shows the comparison between the DlgSilent simulation results and the HIL simulation results. The conclusion is in section 5.10.

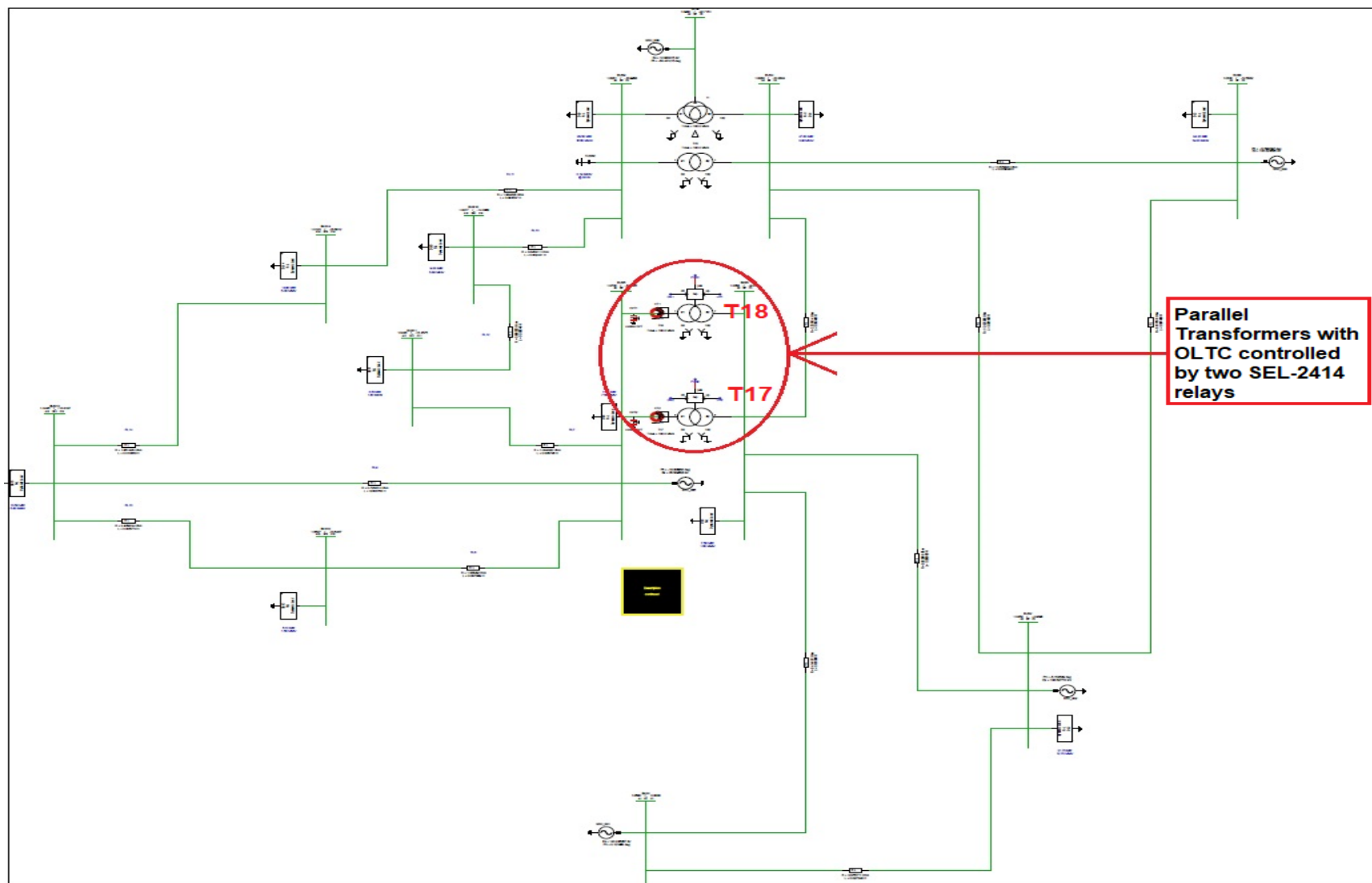


Figure 133: Modified IEEE 14 Bus network with an added transformer in RSCAD FX 2.1.1 environment



## 5.2 Modelling the Modified IEEE 14 Bus Network

For this study, the standard IEEE 14 Bus network (Appendix A) was modified to demonstrate the implementation of the parallel transformer control function. The modified network was modeled in the RSCAD FX 2.1.1 software environment.

Figure 134 shows the standard IEEE 14 Bus network without the added transformer.

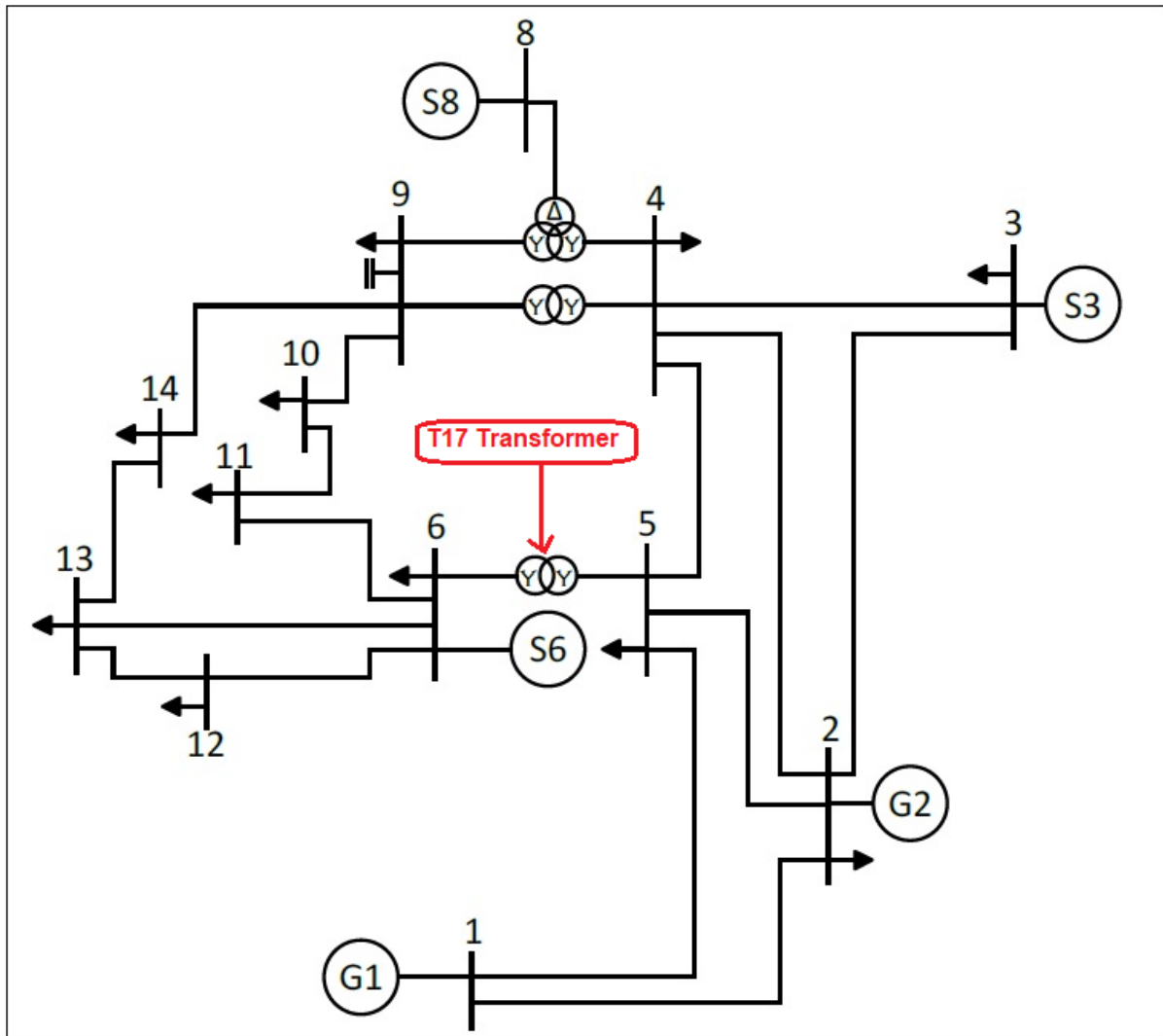


Figure 134: Standard IEEE 14 Bus network

The original voltage levels of the IEEE 14 Bus from the RSCAD library must be changed to match those of the equivalent IEEE 14 Bus network found in the DlgSilent software library. See Figure 135 for the original transformer voltage levels for primary side HV winding (1) and secondary side LV winding (2) from the RSCAD FX environment.

If_rtds_sharc_sld_TRF3P2W						
CONFIGURATION	Name	Description	Value	Unit	Min	Max
CORE ASSIGNMENT	VL1	Base primary voltage (L-L RMS )	18.00	kV	0.0001	
WINDING #1	Im1	Magnetizing Current	1E-4	%	1E-4	1e3
WINDING #2						
If_rtds_sharc_sld_TRF3P2W						
CONFIGURATION	Name	Description	Value	Unit	Min	Max
CORE ASSIGNMENT	VL2	Base secondary voltage (L-L RMS )	17.44	kV	0.0001	
WINDING #1	Im2	Magnetizing Current	1E-4	%	1E-4	1e3
WINDING #2						

**Figure 135: Voltage levels before transformer tap change of IEEE 14 Bus network**

The winding 1 Base primary voltage (L-L RMS) is 18.00kV, and the winding 2 Base primary voltage (L-L RMS) is 17.44kV. These voltage levels were changed to the corresponding voltage levels from the IEEE 14 Bus network in the DIgSilent environment. See Figure 136 for the voltage levels.

2-Winding Transformer Type - Equipment Type Library\TypTr2 0005 to 0006.TypTr2

<b>Basic Data</b>	Name	TypTr2 0005 to 0006
Load Flow	Technology	Three Phase Transformer
VDE/IEC Short-Circuit	Rated Power	100. MVA
Complete Short-Circuit	Nominal Frequency	60. Hz
ANSI Short-Circuit	Rated Voltage	
IEC 61363	HV-Side	132. kV
DC Short-Circuit	LV-Side	33. kV
RMS-Simulation	Vector Group	
EMT-Simulation	HV-Side	YN
Harmonics/Power Quality	LV-Side	YN
	<input type="checkbox"/> Internal Delta Winding	
	Phase Shift	0. °30deg
	Name	YNyn0
	Positive Sequence Impedance	
	Reactance x1	0.25202 p.u.
	Resistance r1	0. p.u.

**Figure 136: Transformer voltage levels from the power system simulation tool**

The HV-Side voltage magnitude is at 132kV and LV-Side voltage magnitude is at 33kV.

### 5.2.1 Modelling of transformers in RSCAD FX

Power transformers form an integral part of any power system network. It transforms voltage magnitude from one level to another through the difference in turn ratios on

the primary and secondary sides of the transformer. Located at various points within a power system network, a power transformer is able to supply the desired voltage level at multiple points. The power transformer fitted with tap changers is essential in maintaining a stable voltage magnitude along the entire electrical supply system. Various pre-modelled types of transformers are included in the RSCAD library.

The most frequently used transformers from the RSCAD library are as shown in [Table 40](#).

**Table 40: Most Frequently used transformers from the RSCAD library (RTDS Technologies, 2018)**

<b>Most frequently used transformers from the RSCAD library</b>	
2 Winding, 3 Phase Transformer	UMEC 2 Winding, 3 Phase Transformer
3 Winding, 3 Phase Transformer	UMEC 3 Winding, 3 Phase Transformer

When including transformer models from the RSCAD library for simulation cases the following parameters need to be considered, as shown in [Table 41](#).

**Table 41: Parameters considered when including transformer models from the RSCAD library (RTDS Technologies, 2018)**

<b>Parameters considered when including transformer models from the RSCAD library</b>		
Ratings (e.g. winding voltage and MVA)	Number of limbs on the core (e.g. core or shell type)	Losses (eddy current, magnetizing, winding)
Number of coupled windings	Leakage impedances	Saturation and hysteresis
Winding configuration (wye,delta, auto-transformer)	Magnetizing currents	Tap changers

When electing to enable tap changers on the transformer models; the choice is between a step/limit type tap changer or the more frequently used position table type tap changer. Up to 50 taps are available when incorporating the position table type

tap changer in a project. Tap change operation can be triggered by an arising edge or a falling edge signal.

## 5.2.2 Modelling the Transformer T16

The Transformer T16 was part of the original IEEE 14 bus network in the RSCAD case under study. It was, however, modified to comply with the new voltage magnitude level used for this study. Transformer T16 is a 3-winding, 3-phase transformer. No tap changer is enabled; it has a transformer rating of 100 MVA and an operating frequency of 60 Hz. See [Figure 137](#) for the configuration tab of transformer T16.

CONFIGURATION	Name	Description	Value	Unit	Min	Max
	Name	Transformer Name	T16			
PROCESSOR ASSIGNMENT	type	Include Saturation and Hysteresis	No			
WINDING #1	n3w	Enable 3rd Winding External Connections	Yes			
WINDING #2	tapCh	Tap Changer	No			
WINDING #3	edge	Tap Trigger on	Rising Edge			
	inps	Tap Changer Input Source	RunTime			
INTERNAL PLOT SELECTIONS	Tmva	3 Phase Transformer MVA	100.0	MVA	0	
AUTO-NAMING SETTINGS	f	Base Operating Frequency	60.0	Hz	0.0001	300
	Xl12	Pos. seq. leakage reactance(#1-#2)	0.319130	p.u.	0.001	1.0
	Xl13	Pos. seq. leakage reactance(#1-#3)	0.286160	p.u.	0.0001	1.0
	Xl23	Pos. seq. leakage reactance(#2-#3)	0.385270	p.u.	0.0001	1.0
	r12	Copper loss for winding(#1-#2)	0.0	p.u.	0.0	0.5
	r13	Copper loss for winding(#1-#3)	0.0	p.u.	0.0	0.5
	r23	Copper loss for winding(#2-#3)	0.0	p.u.	0.0	0.5
	nll	No Load Losses	0	p.u.	0.0	1
	phview	Single Line Diagram or three phase view	SLD view			

**Figure 137: Configuration tab of transformer T16**

Winding 1 of Transformer T16 has a rated line-to-line voltage of 33 KV and a Y-type connection. See [Figure 138](#) for the magnitude of winding 1 of transformer T16 and the connection type.

CONFIGURATION	Name	Description	Value	Unit
PROCESSOR ASSIGNMENT	YD1_W	Winding #1 Connection	Y-g	
	YD1_3W	Winding #1 Connection	Y	
WINDING #1	rot1	Winding Rotation	Lags	
WINDING #2	V1	Rated Line to Line Voltage (RMS)	33	kV
WINDING #3	Im1	Magnetizing Current	0	%
	trfbrkP	Enable Winding #1 Breaker ?	No	

**Figure 138: Winding 1 voltage magnitude of transformer T16**

Winding 2 of Transformer T16 has a rated line-to-line voltage of 132 KV and a Y-type connection. See [Figure 139](#) for the magnitude of winding 2 of transformer T16 and the connection type.

CONFIGURATION	Name	Description	Value	Unit
PROCESSOR ASSIGNMENT	YD2_W	Winding #2 Connection	Y-g	
	YD2_3W	Winding #2 Connection	Y	
WINDING #1	rot2	Winding Rotation	Lags	
WINDING #2	V2	Rated Line to Line Voltage (RMS)	132	kV
WINDING #3	Im2	Magnetizing Current	0	%
	trfbrkS	Enable Winding #2 Breaker ?	No	

**Figure 139: Winding 2 voltage magnitude of transformer T16**

Winding 3 of Transformer T16 has a rated line-to-line voltage of 11 KV and a Delta-type connection. See [Figure 140](#) for the magnitude of winding 3 of transformer T16 and the connection type.

CONFIGURATION	Name	Description	Value	Unit
PROCESSOR ASSIGNMENT	YD3_W	Winding #3 Connection	Delta	
	YD3_3W	Winding #3 Connection	Delta	
WINDING #1	rot3	Winding Rotation	Lags	
WINDING #2	V3	Rated Line to Line Voltage (RMS)	11	kV
WINDING #3	Im3	Magnetizing Current	0	%
	LDtype3W	Passive Load Type on Winding #3	R	

**Figure 140: Winding 3 voltage magnitude of transformer T16**

### 5.2.3 Modelling the Transformer T15

The Transformer T16 was part of the original IEEE 14 bus network in the RSCAD case under study. It was, however, modified to comply with the new voltage magnitude level used for this study. Transformer T15 is a two-winding, 3 phase transformer. No tap changer is enabled; it has a transformer rating of 100 MVA and an operating frequency of 60 Hz. See [Figure 141](#) for the configuration tab of transformer T15.

CONFIGURATION	Name	Description	Value	Unit
	Name	Transformer Name	T15	
PROCESSOR ASSIGNMENT	type	Include Saturation and Hysteresis?	No	
WINDING #1	tapCh	Include Tap Changer?	No	
WINDING #2	edge	Tap Trigger on (used if tapCh=Yes)	Rising Edge	
ENABLE MONITORING IN RUNTIME	inps	Tap Changer Input Source (used if tapCh=Yes)	RunTime	
AUTO-NAMING SETTINGS	Tmva	Transformer rating ( 3 Phase )	100.0	MVA
	f	Base Frequency	60.000000	Hz
	xl	Leakage Inductance	0.556180	p.u.
	NLL	No load losses	0.001000	p.u.
	CuL	Copper losses	0	p.u.
	NLLtp	No load loss branch type (used if NLL > 0)	Winding	
	phview	Single Line Diagram or three phase view	SLD view	

**Figure 141: Configuration tab of transformer T15**

Winding 1 of Transformer T15 has a rated line-to-line voltage of 33 KV and a Y-Gnd type connection. See [Figure 142](#) for the magnitude of transformer T16's winding 1 voltage and connection type.

CONFIGURATION	Name	Description	Value	Unit
	YD1	Winding #1 Connection	Y-Gnd	
PROCESSOR ASSIGNMENT	pol1	Primary Winding Polarity	+ve	
WINDING #1	rot1	Winding Rotation	ABC	
WINDING #2	VL1	Winding #1 Base Voltage (L-L, rms)	33	kV
ENABLE MONITORING IN RUNTIME	Im1	Magnetizing Current	0.0	%
	trfbrkP	Enable Winding #1 Breaker ?	No	

**Figure 142: Winding 1 voltage magnitude of transformer T15**

Winding 2 of Transformer T15 has a rated line-to-line voltage of 132 KV and a Y-Gnd type connection. See [Figure 143](#) for the magnitude of the winding two voltage of transformer T15 and the connection type.

CONFIGURATION	Name	Description	Value	Unit
	YD2	Winding #2 Connection	Y-Gnd	
PROCESSOR ASSIGNMENT	pol2	Secondary Winding Polarity	+ve	
WINDING #1	rot2	Winding Rotation	ABC	
WINDING #2	VL2	Winding #2 Base Voltage (L-L, rms)	132	kV
ENABLE MONITORING IN RUNTIME	Im2	Magnetizing Current	0.0	%
	trfbrkS	Enable Winding #2 Breaker ?	No	

**Figure 143: Winding two configuration of transformer T15**

## 5.2.4 Modelling the Transformer T18

The Transformer T18 was not part of the original IEEE 14 bus network in the RSCAD case under study. It was, however, added in parallel with Transformer T17 between the 132 kV Bus 5 and the 33 kV Bus 6. Transformer T18 is a 2-winding, 3-phase transformer. A position table-type tap changer is enabled, triggered by a falling edge signal. Transformer T18 rating of 100 MVA and an operating frequency of 60 Hz. See [Figure 144](#) for the configuration tab of transformer T18.

CONFIGURATION	Name	Description	Value	Unit
	Name	Transformer Name	T18	
PROCESSOR ASSIGNMENT	type	Include Saturation and Hysteresis?	No	
WINDING #1	tapCh	Include Tap Changer?	Pos Table	
WINDING #2	edge	Tap Trigger on (used if tapCh=Yes)	Falling Edge	
TAP CHANGER A	inps	Tap Changer Input Source (used if tapCh=Yes)	CC	
TAP SETTINGS (1-10)	Tmva	Transformer rating ( 3 Phase )	100.0	MVA
TAP SETTINGS (11-20)	f	Base Frequency	60.000000	Hz
ENABLE MONITORING IN RUNTIME	xl	Leakage Inductance	0.252020	p.u.
	NLL	No load losses	0.001000	p.u.
CURRENT NAMES	CuL	Copper losses	0	p.u.
	NLLtp	No load loss branch type (used if NLL > 0)	Winding	
AUTO-NAMING SETTINGS	phview	Single Line Diagram or three phase view	SLD view	

**Figure 144: Configuration tab of transformer T18**

Winding 1 of Transformer T18 has a rated line-to-line voltage of 33 KV and a Y-Gnd type connection. See [Figure 145](#) for the magnitude of winding 1 of transformer T18 and the connection type.

CONFIGURATION	Name	Description	Value	Unit
PROCESSOR ASSIGNMENT	YD1	Winding #1 Connection	Y-Gnd	
	pol1	Primary Winding Polarity	+ve	
WINDING #1	rot1	Winding Rotation	ABC	
WINDING #2	VL1	Winding #1 Base Voltage (L-L, rms)	33	kV
TAP CHANGER A	Im1	Magnetizing Current	0.0	%
	trfbrkP	Enable Winding #1 Breaker ?	No	

**Figure 145: Winding one configuration of transformer T18**

Winding 2 of Transformer T18 has a rated line-to-line voltage of 132 KV and a Y-Gnd type connection. See [Figure 146](#) for the magnitude of winding 2 of transformer T18 and the connection type.

CONFIGURATION	Name	Description	Value	Unit
PROCESSOR ASSIGNMENT	YD2	Winding #2 Connection	Y-Gnd	
	pol2	Secondary Winding Polarity	+ve	
WINDING #1	rot2	Winding Rotation	ABC	
WINDING #2	VL2	Winding #2 Base Voltage (L-L, rms)	132	kV
TAP CHANGER A	Im2	Magnetizing Current	0.0	%
	trfbrkS	Enable Winding #2 Breaker ?	No	

**Figure 146: Winding 2 configuration of transformer T18**

The TAP CHANGER A tab becomes available when the position table type tap changer is enabled in the configuration tab. The number of tap positions was set to 20 to correspond with the taps configured within the SEL-2414 relays. The starting tap position was set to 10, and it will serve as the neutral tap position. See [Figure 147](#) for the Tap changer configuration of transformer T18.



CONFIGURATION	Name	Description	Value
	NoTaps	Number of TAP positions (max=50)	20
PROCESSOR ASSIGNMENT	TR1	Starting Tap Position	10
WINDING #1			
WINDING #2			
TAP CHANGER A			

**Figure 147: Tap changer configuration of transformer T18**

In the TAP SETTINGS (1-10) tab, tap 10 will serve as the starting tap. Tap 10 will also be the neutral tap. Tap 10, being the neutral tap with 1.0 per-unit Value and will not add or subtract any additional voltage. The additional voltage added or subtracted per tap was set to 0.007 per-unit.

**33 kV x 0,007 = 0.231 kV per tap is added from Tap 9 to Tap 1 (5.1)**

See [Figure 148](#) for the additional voltage per unit added from tap 10 (P10) to tap 1 (P1).

CONFIGURATION	Name	Description	Value	Unit
	P1	Tap Setting for Position #1	1.063	p.u.
PROCESSOR ASSIGNMENT	P2	Tap Setting for Position #2	1.056	p.u.
WINDING #1	P3	Tap Setting for Position #3	1.049	p.u.
WINDING #2	P4	Tap Setting for Position #4	1.042	p.u.
TAP CHANGER A	P5	Tap Setting for Position #5	1.035	p.u.
	P6	Tap Setting for Position #6	1.028	p.u.
TAP SETTINGS (1-10)	P7	Tap Setting for Position #7	1.021	p.u.
TAP SETTINGS (11-20)	P8	Tap Setting for Position #8	1.014	p.u.
ENABLE MONITORING IN RUNTIME	P9	Tap Setting for Position #9	1.007	p.u.
CURRENT NAMES	P10	Tap Setting for Position #10	1.0	p.u.

**Figure 148: Tap settings (1-10) for transformer T18**

In the TAP SETTINGS (11-20) tab, tap 10 will serve as the starting tap. Tap 10 will also be the neutral tap. Tap 10, being the neutral tap, will have a 1.0 per-unit value and will not add or subtract any additional voltage. The additional voltage added or subtracted per tap was 0.007 per-unit.

**33 kV x 0,007 = 0.231 kV per tap is subtracted from Tap 11 to Tap 20 (5.2)**

See [Figure 149](#) for the additional voltage per unit subtracted from tap 11 (P11) to tap 20 (P20).

CONFIGURATION	Name	Description	Value	Unit
PROCESSOR ASSIGNMENT	P11	Tap Setting for Position #11	0.997	p.u.
	P12	Tap Setting for Position #12	0.986	p.u.
WINDING #1	P13	Tap Setting for Position #13	0.976	p.u.
WINDING #2	P14	Tap Setting for Position #14	0.972	p.u.
TAP CHANGER A	P15	Tap Setting for Position #15	0.965	p.u.
	P16	Tap Setting for Position #16	0.958	p.u.
TAP SETTINGS (1-10)	P17	Tap Setting for Position #17	0.951	p.u.
TAP SETTINGS (11-20)	P18	Tap Setting for Position #18	0.944	p.u.
ENABLE MONITORING IN RUNTIME	P19	Tap Setting for Position #19	0.937	p.u.
	P20	Tap Setting for Position #20	0.93	p.u.
CURRENT NAMES				

**Figure 149: Tap settings (11-20) for transformer T18**

### 5.2.5 Modelling the Transformer T17

The Transformer T17 was part of the original IEEE 14 bus network in the RSCAD case under study. However, an identical Transformer, T18, was added in parallel with Transformer T17, between the 132 kV Bus 5 and the 33 kV Bus 6. Transformer T17 is a 2-winding, 3-phase transformer. A position table-type tap changer is enabled, triggered by a falling edge signal. Transformer T17 rating of 100 MVA and an operating frequency of 60 Hz. See [Figure 150](#) for the Configuration tab of transformer T17.

CONFIGURATION	Name	Description	Value	Unit
	Name	Transformer Name	T17	
PROCESSOR ASSIGNMENT	type	Include Saturation and Hysteresis?	No	
WINDING #1	tapCh	Include Tap Changer?	Pos Table	
WINDING #2	edge	Tap Trigger on (used if tapCh=Yes)	Falling Edge	
TAP CHANGER A	inps	Tap Changer Input Source (used if tapCh=Yes)	CC	
	Tmva	Transformer rating ( 3 Phase )	100.0	MVA
TAP SETTINGS (1-10)	f	Base Frequency	60.000000	Hz
TAP SETTINGS (11-20)	xl	Leakage Inductance	0.252020	p.u.
ENABLE MONITORING IN RUNTIME	NLL	No load losses	0.001000	p.u.
	CuL	Copper losses	0	p.u.
CURRENT NAMES	NLLtp	No load loss branch type (used if NLL > 0)	Winding	
AUTO-NAMING SETTINGS	phview	Single Line Diagram or three phase view	SLD view	

**Figure 150: Configuration tab of transformer T17**

Winding 1 of Transformer T17 has a rated line-to-line voltage of 33 KV and a Y-Gnd type connection. See [Figure 151](#) for the magnitude of winding 1 of transformer T17 and the connection type.

CONFIGURATION	Name	Description	Value	Unit
	YD1	Winding #1 Connection	Y-Gnd	
PROCESSOR ASSIGNMENT	pol1	Primary Winding Polarity	+ve	
WINDING #1	rot1	Winding Rotation	ABC	
WINDING #2	VL1	Winding #1 Base Voltage (L-L, rms)	33	kV
	Im1	Magnetizing Current	0.0	%
TAP CHANGER A	trfbrkP	Enable Winding #1 Breaker ?	No	

**Figure 151: Winding one configuration of transformer T17**

Winding 2 of Transformer T17 has a rated line-to-line voltage of 132 KV and a Y-Gnd type connection. See [Figure 152](#) for the magnitude of winding 2 of transformer T17 and the connection type.

CONFIGURATION	Name	Description	Value	Unit
PROCESSOR ASSIGNMENT	YD2	Winding #2 Connection	Y-Gnd	
	pol2	Secondary Winding Polarity	+ve	
WINDING #1	rot2	Winding Rotation	ABC	
WINDING #2	VL2	Winding #2 Base Voltage (L-L, rms)	132	kV
TAP CHANGER A	Im2	Magnetizing Current	0.0	%
	trfbrkS	Enable Winding #2 Breaker ?	No	

**Figure 152: Winding 2 configuration of transformer T17**

The TAP CHANGER A tab becomes available when the position table type tap changer is enabled in the configuration tab. The number of tap positions was set to 20 to correspond with the taps configured within the SEL-2414 relays. The starting tap position was set to 10, and it will serve as the neutral tap position. See [Figure 153](#) for the Tap changer configuration of transformer T17.

CONFIGURATION	Name	Description	Value
PROCESSOR ASSIGNMENT	NoTaps	Number of TAP positions (max=50)	20
	TR1	Starting Tap Position	10
WINDING #1			
WINDING #2			
TAP CHANGER A			

**Figure 153: Tap changer configuration of transformer T17**

In the TAP SETTINGS (1-10) tab, tap 10 serves as the starting tap. Tap 10 is the neutral tap. Tap 10, being the neutral tap, will have a 1.0 per-unit and will not add or subtract any additional voltage. The additional voltage added or subtracted per tap was set to 0.007 per-unit

**33 kV x 0,007 = 0.231 kV per tap is added from Tap 9 to Tap 1 (5.3)**

See [Figure 154](#) for the additional voltage per-unit added from tap 10 (P10) to tap 1 (P1).

CONFIGURATION	Name	Description	Value	Unit
PROCESSOR ASSIGNMENT	P1	Tap Setting for Position #1	1.063	p.u.
	P2	Tap Setting for Position #2	1.056	p.u.
WINDING #1	P3	Tap Setting for Position #3	1.049	p.u.
WINDING #2	P4	Tap Setting for Position #4	1.042	p.u.
TAP CHANGER A	P5	Tap Setting for Position #5	1.035	p.u.
TAP SETTINGS (1-10)	P6	Tap Setting for Position #6	1.028	p.u.
	P7	Tap Setting for Position #7	1.021	p.u.
TAP SETTINGS (11-20)	P8	Tap Setting for Position #8	1.014	p.u.
ENABLE MONITORING IN RUNTIME	P9	Tap Setting for Position #9	1.007	p.u.
CURRENT NAMES	P10	Tap Setting for Position #10	1.0	p.u.

**Figure 154: Tap settings (1-10) for transformer T17**

In the TAP SETTINGS (11-20) tab, tap 10 will serve as the starting and neutral tap. Tap 10, the neutral tap, will have a 1.0 per unit value and will not add or subtract any additional voltage. The additional voltage added or subtracted per tap was set to 0.007 per voltage unit.

**33 kV x 0,007 = 0.231 kV per tap is subtracted from Tap 11 to Tap 20 (5.4)**

See Figure 155 for the additional voltage per unit subtracted from tap 11 (P11) to tap 20 (P20).

CONFIGURATION	Name	Description	Value	Unit
PROCESSOR ASSIGNMENT	P11	Tap Setting for Position #11	0.997	p.u.
	P12	Tap Setting for Position #12	0.986	p.u.
WINDING #1	P13	Tap Setting for Position #13	0.976	p.u.
WINDING #2	P14	Tap Setting for Position #14	0.972	p.u.
TAP CHANGER A	P15	Tap Setting for Position #15	0.965	p.u.
TAP SETTINGS (1-10)	P16	Tap Setting for Position #16	0.958	p.u.
	P17	Tap Setting for Position #17	0.951	p.u.
TAP SETTINGS (11-20)	P18	Tap Setting for Position #18	0.944	p.u.
	P19	Tap Setting for Position #19	0.937	p.u.
CURRENT NAMES	P20	Tap Setting for Position #20	0.93	p.u.

**Figure 155: Tap settings (11-20) for transformer T17**

## 5.3 Modelling of Loads in RSCAD FX

Pre-modelled types of dynamic loads are included in the RSCAD library. The loads can be customized to either or a combination of the following elements, as shown in [Table 5-42](#).

Loads can be configured to be in series or parallel connections and the P & Q of the loads can be controlled by the following means in the RSCAD FX, as shown in [Table 42](#).

**Table 42: Types of loads and controllers in RSCAD library**

Type of Loads	Load controller
Resistive	Slider
Inductive	Control Component (CC)
Capacitive	Const Z
	ZIP component

### 5.3.1 Modelling the Loads of the Modified IEEE 14 Bus network:

The Loads were part of the original IEEE 14 bus network in the RSCAD case under study. It was, however, modified to correspond with the new voltage magnitude level to where the load is connected. See [Table 43](#) for details of Loads included in this study.

**Table 43: Characteristics of Loads**

Dynamic Load	Line-Line Voltage kV	P MW	Q MVar
DL2	132	21.70	12.70
DL3	132	94.20	19.00
DL4	132	47.80	3.90
DL5	132	7.60	1.60
DL6	33	11.20	7.50
DL9	33	29.50	16.60
DL10	33	9.00	5.80
DL11	33	3.50	1.80
DL12	33	6.10	1.60
DL13	33	13.50	8.50
DL14	33	14.90	5.00

## 5.4 Modelling the power sources in RSCAD FX:

The original IEEE 14 Bus Network contained five generators. The generators from the original network needed to be adapted to the new voltage levels of the Modified IEEE 14 Bus Network. The original IEEE 14 Bus Network's generator parameters were insufficient to successfully adapt the generators to the new voltage levels. The network became unstable when the simulation was run in the RSCAD FX environment. The choice was made to substitute all the generators in the network with voltage sources to stabilize the network. See [Table 44](#) for details of Voltage Sources included in this study.

**Table 44: Details of Voltage Sources**

<b>Voltage Source Name</b>	<b>Connected to Bus</b>	<b>Voltage of connected Bus</b>	<b>Initial Source Mag (L-L, RMS) kV</b>	<b>Source Impedance Type</b>
SRC_001	1	132	143.246067	R-R//L
SRC_002	2	132	138.527713	R-R//L
SRC_003	3	132	133.324685	R-R//L
SRC_006	6	33	35.509628	R-R//L
SRC_008	8	11	12.883315	R-R//L

## 5.5 Modelling the transmission lines in RSCAD FX

The original IEEE 14 Bus Network contained 15 transmission lines. The transmission lines from the original network needed to be adapted to the new voltage levels of the Modified IEEE 14 Bus Network. The transmission line parameters from the original IEEE 14 Bus Network were insufficient to successfully adapt the transmission line parameters to the new voltage levels. The network became unstable when the simulation was run in the RSCAD FX environment. The series resistance parameter of the transmission line is not dependent and, thus, voltage-dependent and, thus, does not need to be adapted. The series inductance parameter of the transmission line is voltage-dependent and thus needs to be adapted to the new applicable voltage levels. The series inductance parameter for the transmission required in RSCAD FX should be in Henry (H). See [Figure 156](#) for the configuration tab for the transmission line between Bus 2 and Bus 5.

Name	Description	Value	Unit	Min	Max
R	Series Resistance per phase	9.922968	Ohm	0.0	
L	Series Inductance per phase	0.080365	H	0.0	1E6
CuF	Series Capacitance per phase	0.0	uF	0.0	1E6
Imon	Monitor Branch Current in RunTime?	No			
DA	Monitor Branch Current at Analogue Output Port?	No			
TXT	Display RLC values in icon?	Yes			
phview	Single Line Diagram or three phase view	SLD view			

**Figure 156: Configuration tab for a transmission line between Bus 2 and Bus 5**

To obtain the necessary applicable values for the transmission lines at the adapted voltage levels, the parameters were obtained from the equivalent IEEE 14 Bus Network in the DIgSilent environment, as shown in Figure 157.

Name: TypLne 0002 to 0005

Rated Voltage: 132, kV

Rated Current: 1, kA

Cable / OHL: Overhead Line

System Type: AC Phases: 3 Number of Neutrals: 0

Nominal Frequency: 50, Hz

Parameters per Length 1,2-Sequence

AC-Resistance R'(20°C): 9,922968 Ohm/km

Reactance X': 30,29685 Ohm/km

Parameters per Length Zero Sequence

AC-Resistance R0': 0, Ohm/km

Reactance X0': 0, Ohm/km

**Figure 157: Parameters for a transmission line between Bus 2 and Bus 5 in DigSilent environment**

The series inductance value from the DIgSilent environment is given in Ohm/km. This value must be converted to Henry (H) to be entered in the RSCAD FX software. The following equations are used for the conversion:

$$XL = 2 \pi f L \quad (5.5)$$



$$L = \frac{2\pi f}{XL} \quad (5.6)$$

Calculating series inductance (L) for Bus 2 – 5:

$$L = \frac{2\pi f}{XL} = \frac{2\pi 50}{30.29685} = 0.080364890 \text{ Henry} \quad (5.7)$$

All the other transmission lines series inductance (L) was calculated to this procedure. See **Table 45** for calculated parameters for the transmission lines.

**Table 45: Calculated Transmission Line data**

Bus	R in $\Omega$	X in $\Omega$	L in Henry
2-5	9.922968	30.29685	0.080364890
3-4	11.67582	29.80027	0.079047671
4-5	2.326104	7.337246	0.019462649
6-11	1.034332	2.166021	0.005745549
6-13	0.720374	1.418640	0.003763059
10-11	0.893540	2.091643	0.005548255
9-10	0.346411	0.920205	0.002440919
9-14	1.384228	2.944439	0.007810367
13-14	1.861428	3.789938	0.010053122
12-13	2.405819	2.176693	0.005773857
6-12	1.338490	2.785771	0.007389487
1-2	6.753542	20.61956	0.054695081
1-5	9.414187	38.86249	0.103085956
2-3	8.187537	34.49428	0.091498919
2-4	10.12509	30.722	0.081492636

## 5.6 Configuring the RTDS Hardware Components

The RTDS hardware components were configured using the following steps in the 5.6.1 Gigabit Transceiver Analogue Output Card (GTAO) and the 5.6.2 Front Panel Interface Card (GTFPI) configuration.

### 5.6.1 Gigabit Transceiver Analogue Output Card (GTAO)

The GTAO generates the analog voltage and current signals produced within the RSCAD FX software through the RTDS equipment to be interfaced with the external equipment. The GTAO card has a voltage analog output range of  $\pm 10$  volts. The

analog output signals produced by the GTAO card is used as input for testing external protective and control devices. See [Figure 158](#) for the configuration of GTAO card for this project. The scaling was set to 69.

CONFIGURATION	Name	Description	Value
ENABLE D/A OUTPUT CHANNELS	scl1	Chnl 1 Peak value for 5 Volts D/A out:	187.79
	scl2	Chnl 2 Peak value for 5 Volts D/A out:	187.79
D/A OUTPUT SCALING	scl3	Chnl 3 Peak value for 5 Volts D/A out:	187.79
PROJECTION ADVANCE FACTORS	scl4	Chnl 4 Peak value for 5 Volts D/A out:	69
OVERSAMPLING FACTORS	scl5	Chnl 5 Peak value for 5 Volts D/A out:	69
	scl6	Chnl 6 Peak value for 5 Volts D/A out:	69
SIGNAL ALIGNMENT DELAY OPTION	scl7	Chnl 7 Peak value for 5 Volts D/A out:	187.79
AUTO-NAMING SETTINGS	scl8	Chnl 8 Peak value for 5 Volts D/A out:	187.79

**Figure 158: Configuration of the GTAO card**

### 5.6.2 Front Panel Interface Card (GTFPI)

The GTFPI card executes the function as the digital link between the inputs and outputs modeled in the RSCAD FX software and the digital signal sent or received by external devices to the RTDS equipment. This GTFPI also has an option high voltage panel for switching external voltage supplied by external protective and control devices. See [Figure 159](#) for the configuration of the GTFPI card for this project.

Name	Description	Value
Port	GTIO Fiber Port Number	1
Card	GTFPI Card Number (refer to on-board 7 segment card# display)	1
CardVersion	GTFPI Card Version	V2
DIGEn	Enable Digital I/O Panel Signals?	None
Inv	Invert Digital I/O Panel Input Signals (16 bit word)	No
InitState	Initial State of Digital I/O Panel Input Channels	0000
IOIsb	Starting bit number for Digital Output Panel	1
IObits	Number of consecutive bits for Digital Output Panel	16
HVPanel	Include HV Panel Signals?	Yes
NUMHVinp	Number of HV Panel Inputs (HVPanel=Yes)	None
HVIsb	Starting bit number for HV Panel Output	1
HVbits	Number of consecutive bits for HV Panel Output	6
InvHVinp	Invert HV I/O Panel Input Signals	No
ctrlGrp	Assigned Control Group	1
Pri	Priority Level	5

Figure 159: Configure the GTFPI card for this project.

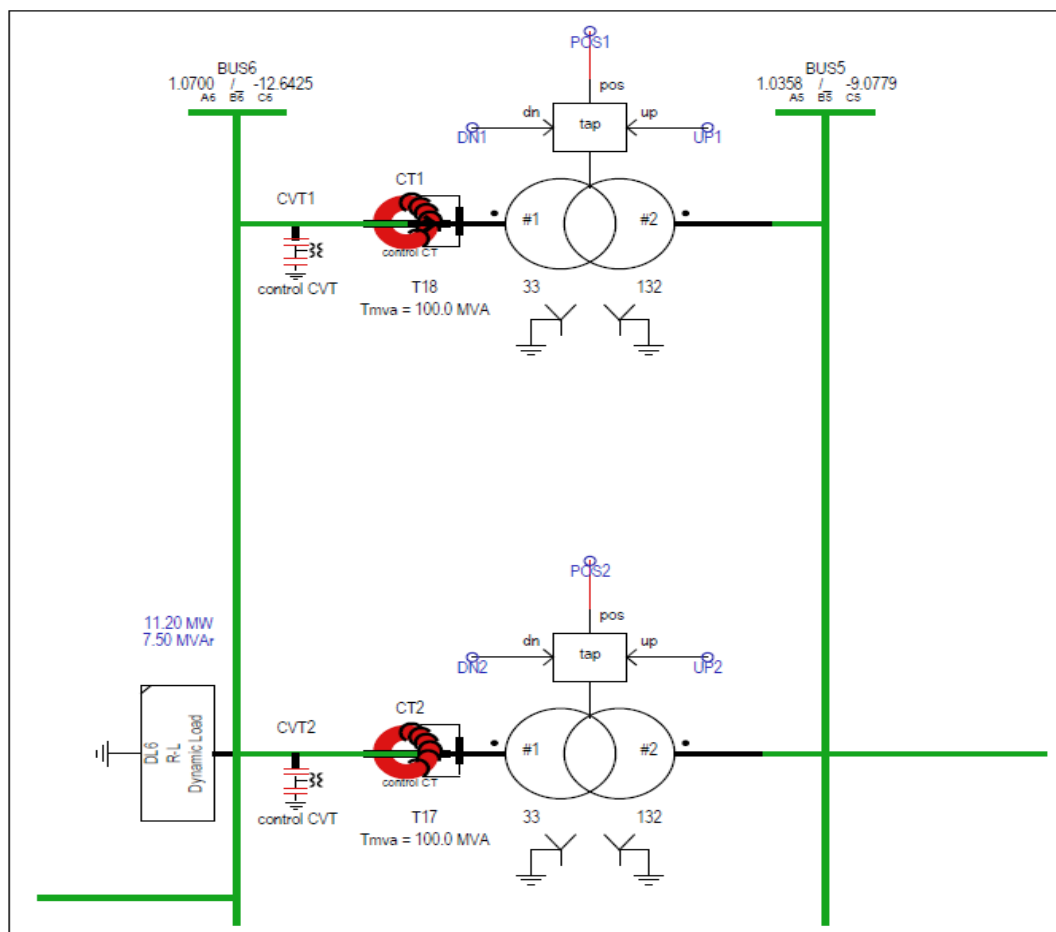


Figure 160: Parallel transformers T18 & T17 controlled by two SEL-2414 relays

Figure 160 shows the T17 and T18 parallel transformers within the modified version of the IEEE 14 Bus network. The tap positions of transformers T18 and T17 are represented by POS1 and POS2, respectively.

POS1 and POS2 are mapped to high-voltage GTFPI (GT Front Panel Interface) and GTFPIv2 (GT Front Panel Interface version 2) cards in the RTDS equipment. An external Omicron CMC 356 device supplies an 110VDC signal to the GTFPI and GTFPIv2 of the RTDS equipment. This 110VDC is converted to a high-voltage signal as a binary-coded decimal signal, which is hardwired to SEL -2414 relays. The relay decodes this binary code signal to determine the current tap position of its OLTC.

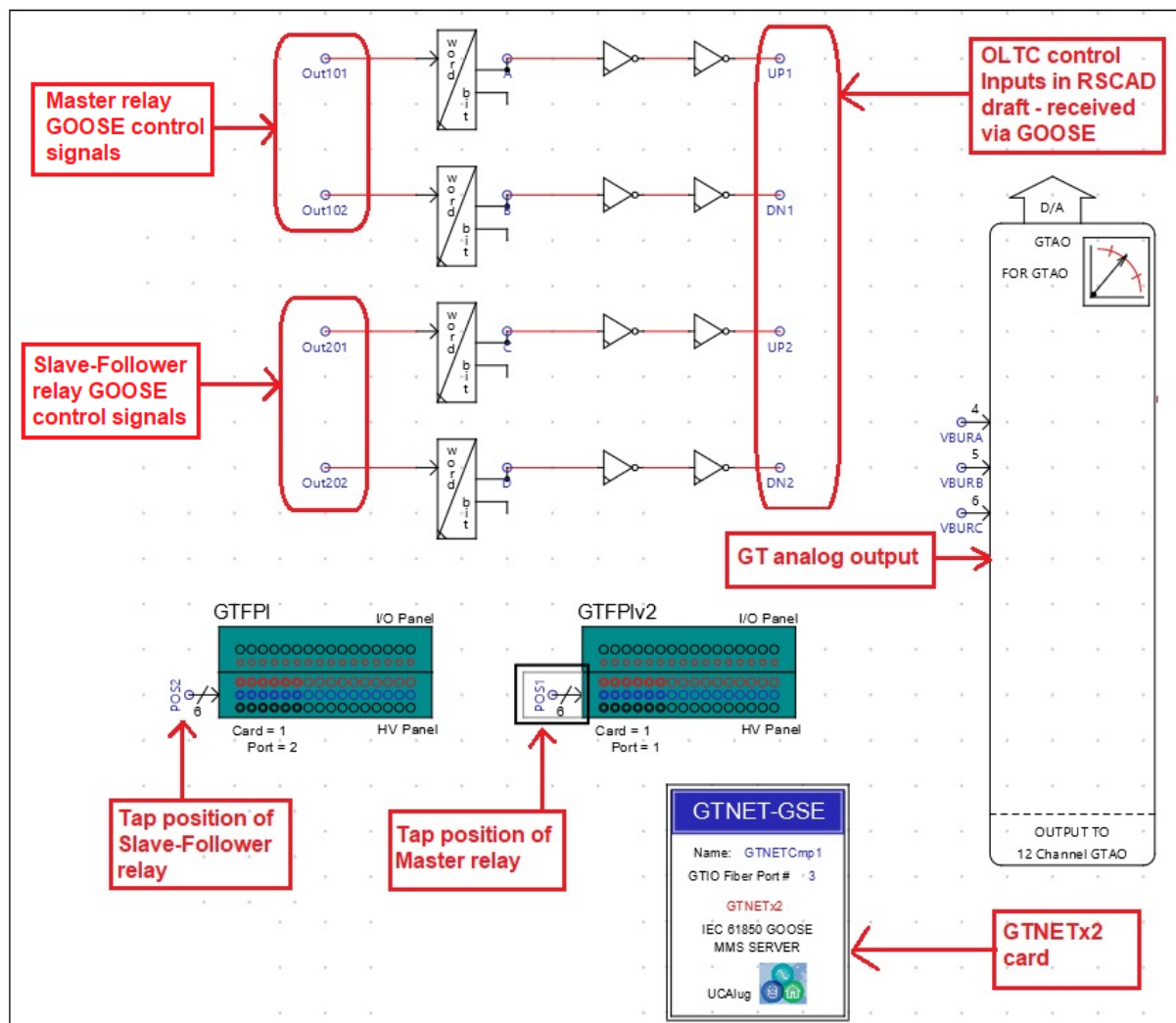


Figure 161: GTAO, GTFPI & GTFPIv2 and Out101, Out102, Out201 and Out202 and GTNETx2

Control CVT1 sent voltage signal measured VBURA, VBURB, and VBURC to the GTAO (GT analog output) card of the RTDS equipment. The output voltage signal from the GTAO card is amplified via the Omicron CMS 156 and supplied to the voltage input card of the Master IED. See [Figure 161](#) for the configuration of the GTAO, GTFPI, and GTFPIv2 as well as Out101, Out102, Out201, and Out202, which is received via IEC61850 GOOSE for the control of the OLTCs.

## 5.7 IEC61850 GOOSE configuration of the RTDS equipment

The IEC61850 GOOSE configuration for the SEL-2414 IEDs was executed in the AcSELeRator Architect environment. The Master transformer IED lower and raise control signals are mapped to Out101 and Out102, respectively. These GOOSE messages are sent to the GTNETx2 card located in the RTDS equipment. The Master transformer tap position is sent to the Slave transformers IED via GOOSE messages. To configure the GTNETx2 card located in the RTDS NovaCor chassis of the RTDS equipment was done under the following headings as seen in [Figure 127](#):

- Component name was chosen as GTNETCmp1.
- GTIO Fiber Port Number was selected as 3, as this is the physical port number in the chassis to which the card is connected to.
- The GTNET Type was selected as GTNETx2, as this identifies the physical type of card used.

CONFIGURATION	Name	Description	Value
GOOSE Configuration	sCompName	Component name	GTNETCmp1
	Port	GTIO Fiber Port Number	3
GSE Version	Card	GTNET_GSE Card Number	1
AUTO-NAMING SETTINGS	gtnettype	GTNET Type	GTNETx2 ▼
	ctrlGrp	Assigned Control Group	1
	Pri	Priority Level	6
	TSYNCEN	Use GTSYNC time of day for MMS and/or RefrTm	NO ▼
	GT_SOC	GTSYNC advance TIME signal name	ADVSECD
	GT_STAT	GTSYNC advance STAT signal name	ADVSTAT

**Figure 162: Configuration tab for GTNETx2**

The GTNET Goose version was selected as version 7, supported by the GTNETx2 card. GOOSE version 7 supports the IEC 61850-7-4 version of the standard. See [Figure 163](#) for the GOOSE version selection.

CONFIGURATION	Name	Description	Value
GOOSE Configuration	GSEv	GTNET-GSE version	7
GSE Version	TrMod	Trip Mode	3Pole
AUTO-NAMING SETTINGS			

**Figure 163: Selecting the GTNET GOOSE version**

Launching the ICT Configuration program from within the RSCAD FX environment, a data model is created in the RTDS equipment to receive IEC61850-7-4 GOOSE messages. See [Figure 164](#) for the process of making the IED model. The Process of creating the IED model is done in 3 steps:

**Step 1:** The ATCC (Automatic Tap Change Controller) logical nodes created within the RTDS equipment receive the GOOSE control signal from the external publishing SEL-2414 IEDs. The ATCC logical node is selected from the dropdown menu. The TapOpR for the Tap raise function and the TapOpL for the Tap lowering function are selected.

**Step 2:** The ATCC logical node is added to the template manager using the apply and create options. It is now available for addition to the IED model.

**Step 3:** Four instances of the ATCC logical nodes are added to the project: two instances for the control signal from the Master relay and two instances for the control signal from the Slave-Follower relay.

The ATCC (Automatic Tap Change Controller) logical nodes created within the RTDS equipment receive the GOOSE control signal from the external publishing SEL-2414 IEDs. A new IED has been added to the ICT Configuration program, which will be the receiving point for data from external devices. This new IED needs to be configured from the Data Model tab in the ICT Configuration program. Under the Data Model tab, the LN Class Database standard logical nodes included in the

IEC61850 standard can be chosen depending on the application. For this application of automatic voltage control by implementing OLTC, the appropriate ATCC logical node was selected.

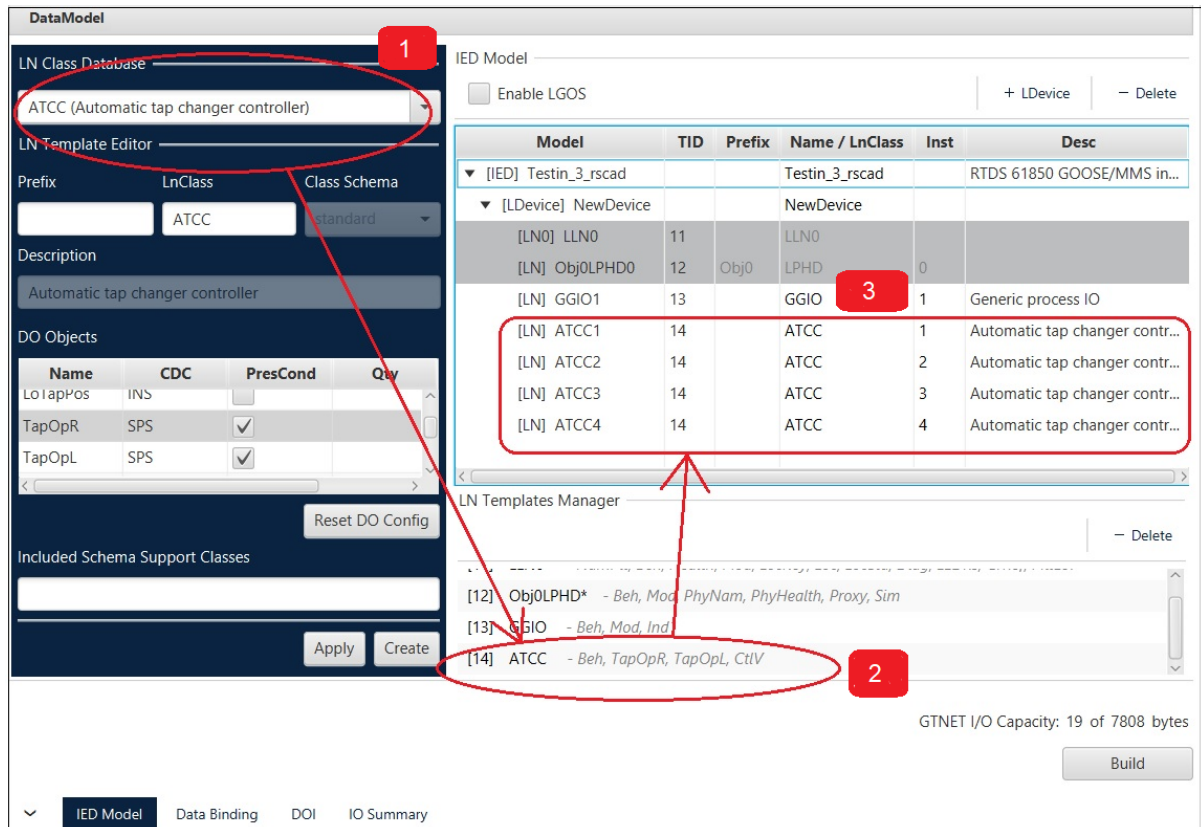


**Figure 164: Process of creating the IED model**

After creating the IED model in the ICT Configuration program, the external publishing IEDs need to be added to the project. Under the File tab in the program, the Import option is selected. This option allows you to import the IED Publishers into the project. The appropriate SCL file created in the AcSElerator Architect is selected and imported into the project. Once the SCL file is imported, the external publishing IEDs are visible under the External Publishing IEDs drop-down menu. See Figure 165 for external publishing IEDs imported into the project.

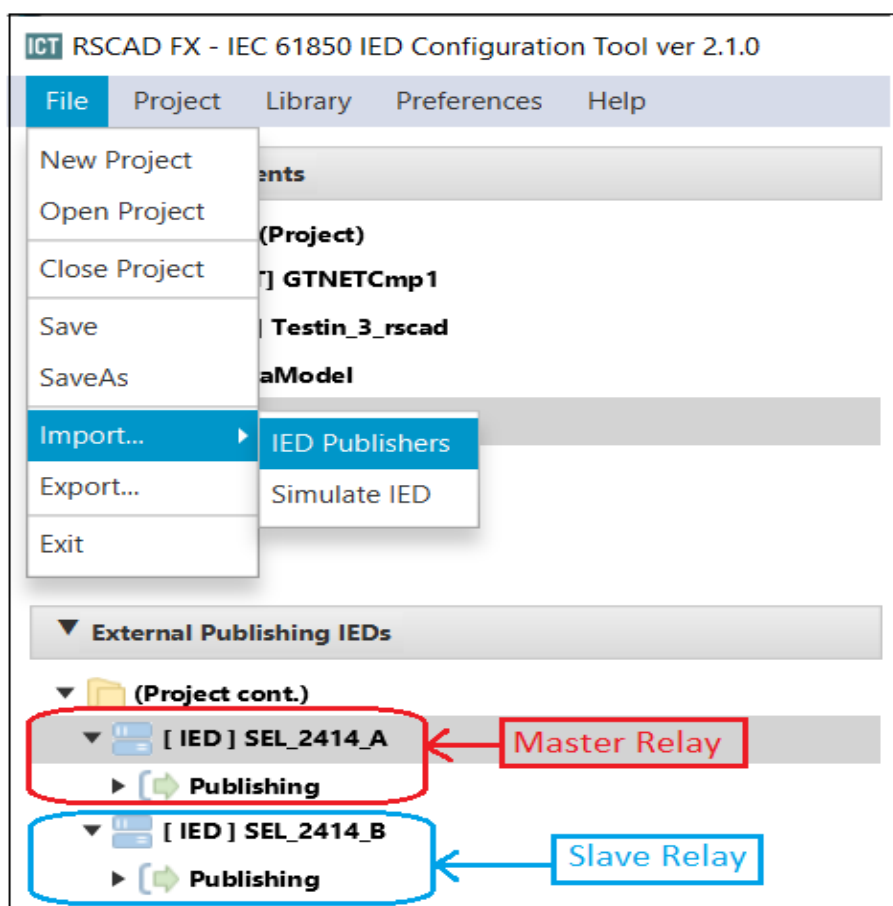


**Figure 165: Importing the external publishers into RSCAD**

After importing the external publishing IEDs into the project, subscriptions need to be created within the IED model to subscribe to the external publishing IEDs. By choosing the EDIT option under the subscription tab, you can now add the 4 ATCC logical nodes that were added to the IED model earlier. See [Figure 166](#) for the Logical Node subscriptions that were added.



Subscriptions			
Testin_3_rscad Inputs			
Edit Mode	Location		Del
	LD*	LN*	
EDIT	NewDevice	ATCC1	Del
EDIT	NewDevice	ATCC2	Del
EDIT	NewDevice	ATCC3	Del
EDIT	NewDevice	ATCC4	Del
ADD			

Master Relay Raise Tap

Master Relay Lower Tap

Slave Relay Raise Tap

Slave Relay Lower Tap

**Figure 166: Adding Logical Node subscriptions**

With the subscriptions added to the IED model, it is now possible to add the logical nodes from the external publishing relays to the relevant input logical nodes for RSCAD IED to subscribe to. The master relay raises the tap logical node OUTAGGIO2.Ind01.stVal was matched to the ATCC1 logical node in the RSCAD IED. See [Figure 167](#) for RSCAD IED subscriptions to external publishing IED.

**Draft Components**

- Testing\_3 (Project)
  - [CMPNT] GTNETCmp1
    - [IED] Testin\_3\_rscad
      - DataModel
      - Subscriptions
      - Publishing

**External Publishing IEDs**

- Publishing
  - [LD] CFG
    - [DS] voltage/voltage
    - [DS] VOLTAGE\_MAGNITUDE/VOLTAGE\_MAG
    - [DS] Relay\_A\_Tap\_Posistion/Relay\_A\_Tap\_position
    - [DS] Relay\_A\_Tap\_Raise/RelayA\_Raise\_Tap
    - [DS] voltage/RelayA\_Lower\_Tap
  - [LD] MET
  - [LD] CON

[DS] Relay\_A\_Tap\_Raise/RelayA\_Raise\_Tap

Desc	Type
OUTAGGIO2.Ind01.stVal [ST]	BOOLEAN

**Subscriptions**

Testin\_3\_rscad Inputs

Edit Mode	Location	Del
	LD* LN*	
EDIT	NewDevice ATCC1	Del
EDIT	NewDevice ATCC2	Del
EDIT	NewDevice ATCC3	Del
EDIT	NewDevice ATCC4	Del
ADD		

ExtRefs

IED	LD	LN	DO	DA
SEL_2414_A	ANN	OUTAGGIO2	Ind01	stVal

ExtRefs Count: 1  
Inputs Count: 4  
Sup. Subscription Count: 0  
GTNET I/O Capacity: 1

Update Monit

**Figure 167: Creating RSCAD IED subscriptions from external Master relay to raise tap**

With the subscriptions added to IED model, it is now possible to add the logical nodes from the external publishing relays to the relevant input logical nodes for RSCAD IED to subscribe to. The Master relay lower tap logical node OUTAGGIO2.Ind02.stVal was matched to the ATCC2 logical node in the RSCAD IED. See [Figure 168](#) for RSCAD IED subscriptions to external publishing IED.

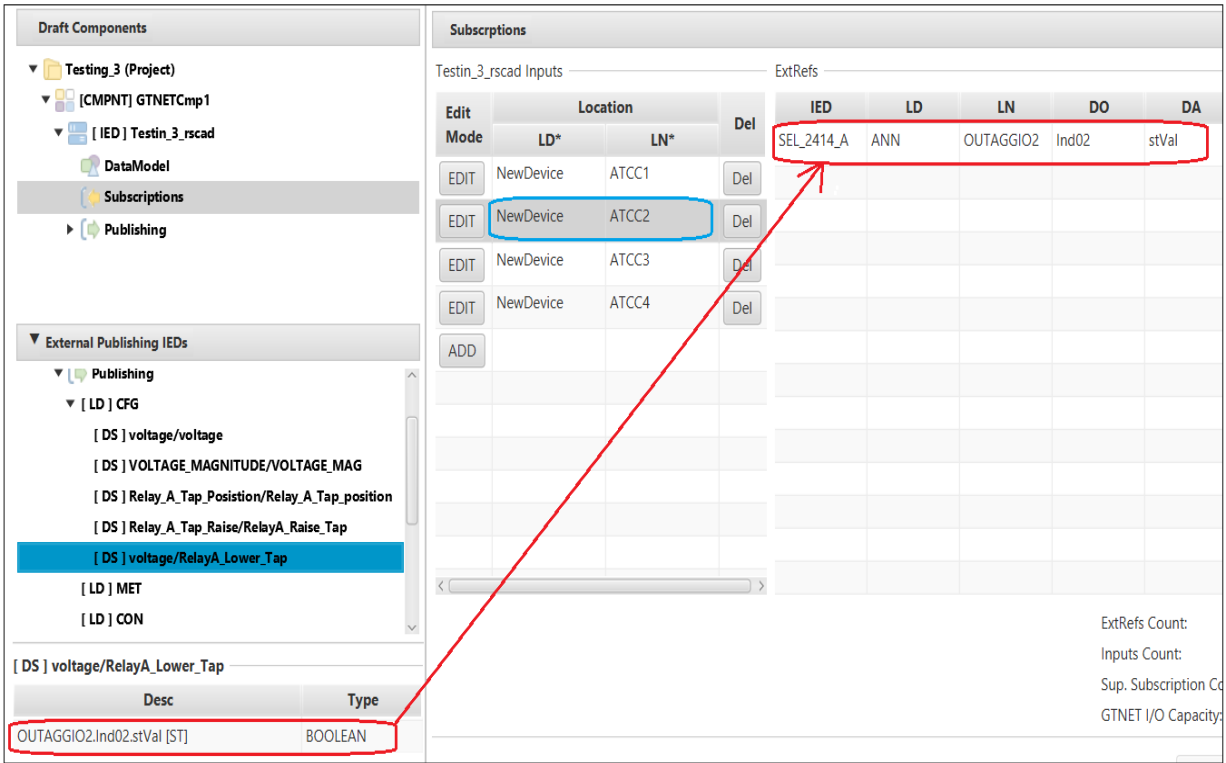


**Figure 168: Creating IED subscription from external Master relay to lower tap**

With the subscriptions added to IED model, it is now possible to add the logical nodes from the external publishing relays to the relevant input logical nodes for RSCAD IED to subscribe to. The Slave relay raise tap logical node OUTAGGIO2.Ind01.stVal was matched to the ATCC3 logical node in the RSCAD IED. See [Figure 169](#) for RSCAD IED subscriptions to external publishing IED.

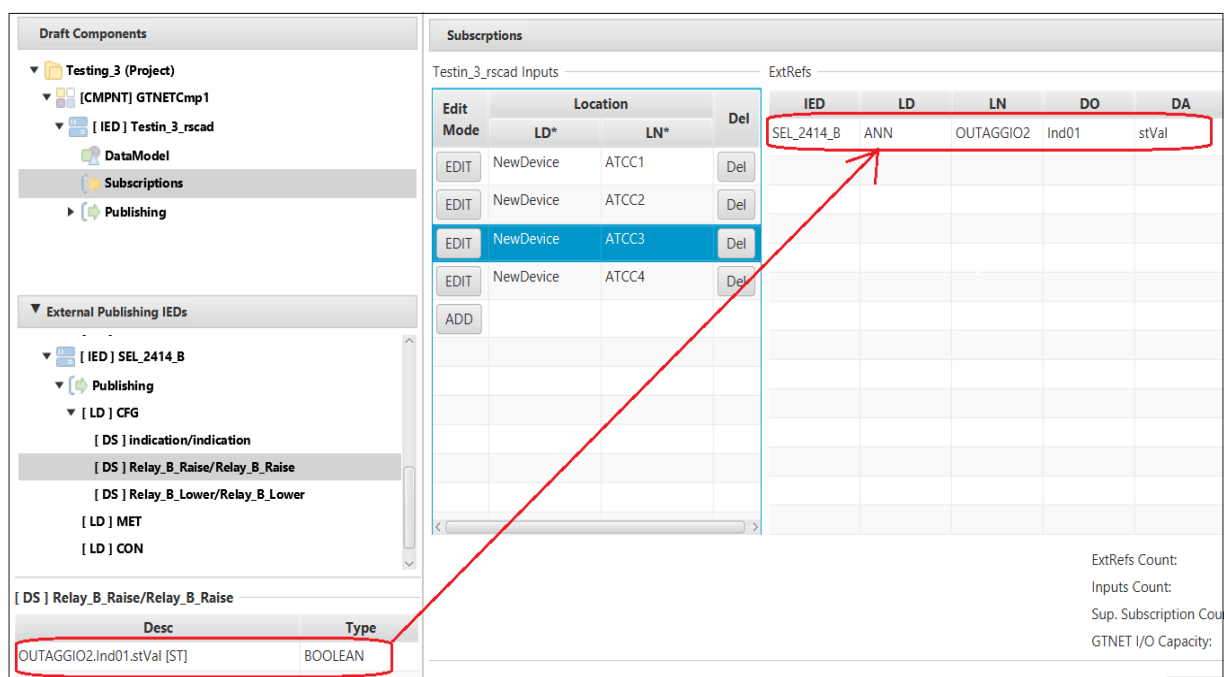


**Figure 169: Creating IED subscription from external Slave relay to raise tap**

With the subscriptions added to IED model, it is now possible to add the logical nodes from SEL from the external publishing relays to the relevant input logical nodes for RSCAD IED to subscribe to. The Slave relay lower tap logical node OUTAGGIO2.Ind02.stVal was matched to the ATCC4 logical node in the RSCAD IED. See Figure 170 for RSCAD IED subscriptions to external publishing IED.

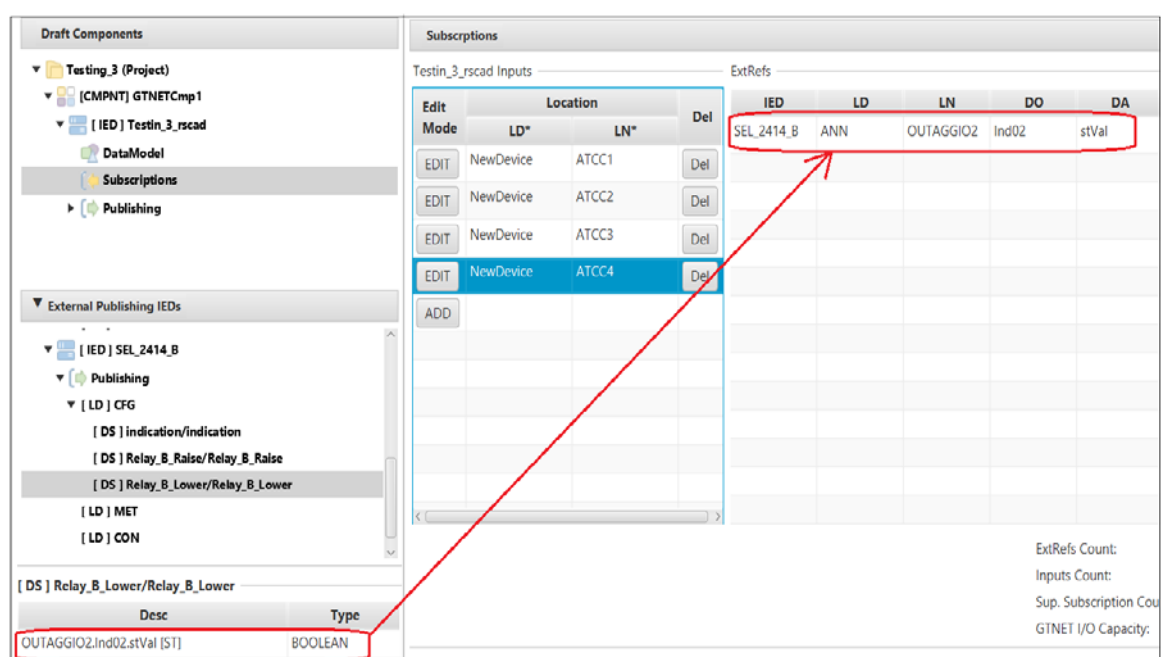


**Figure 170: Creating IED subscription from external Slave relay to lower tap**

For the subscribed logical nodes to be available within the RSCAD FX draft for simulation, these logical nodes need to be bound with the relevant signal names. This function is executed under the Data Binding tab. The IO name provided must match the name of the relevant signal in the RSCAD FX draft simulation. The direction must be chosen as Input, as this subscribed signal will go into the RSCAD IED. See Figure 171 for binding the GOOSE data model in the RSCAD FX draft model for receiving the IEC61850-7-4 GOOSE messages from the external publishing SEL-2414 IEDs.

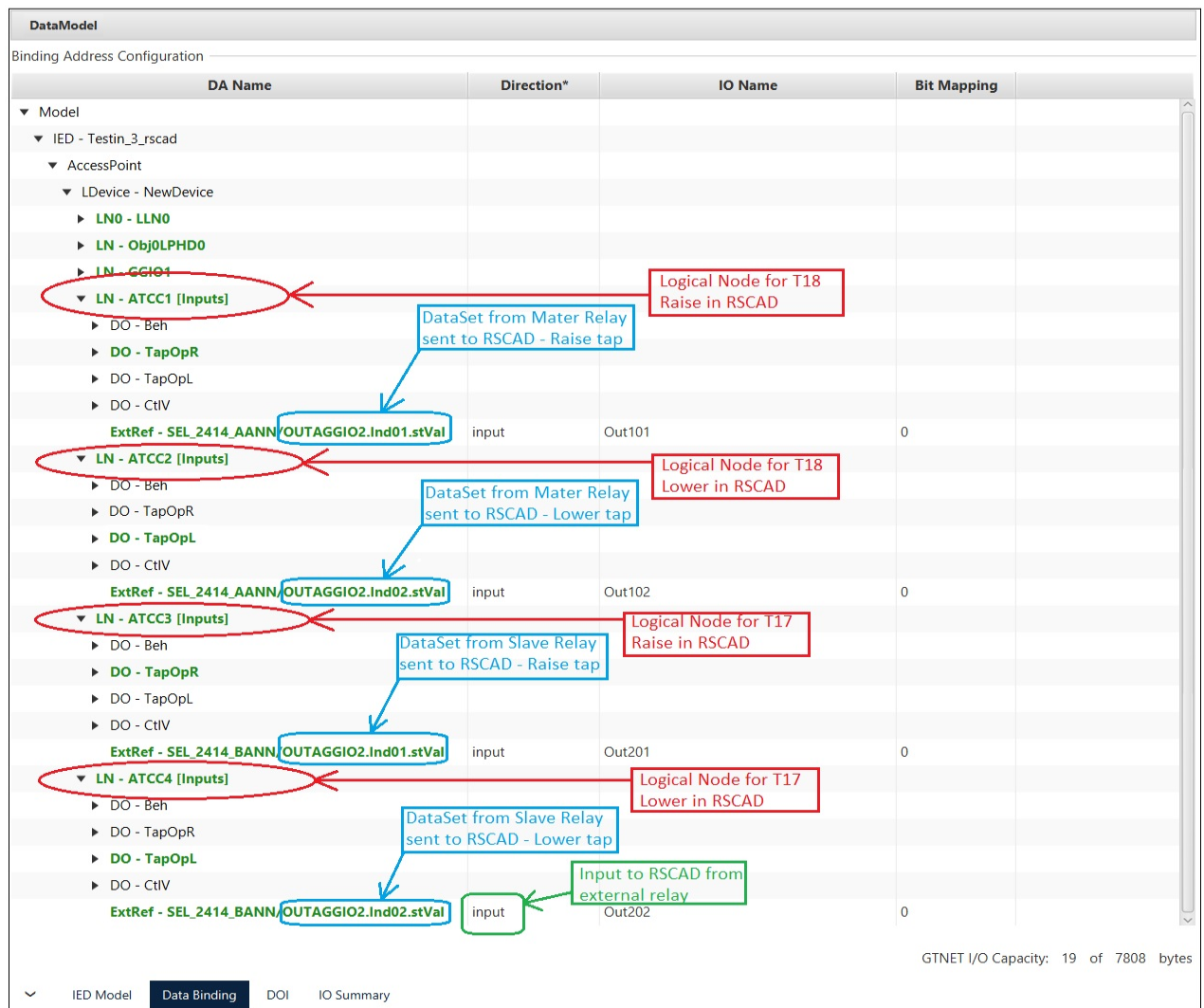


**Figure 171: Binding the GOOSE data model in the RSCAD FX draft model for receiving the IEC61850-7-4 GOOSE messages from the SEL-2414 IEDs**

Under the Access Points Configuration tab the IP address and Subnet mask of the GTNETx2 card was entered. See [Figure 172](#) for Access Points Configuration.

Project Properties							
AccessPoints Configuration							
Edit Mode	ConnectedAP		SubNetwork	IP Parameters			
	IED	AccessPoint	Name	IP	Subnet	Gateway	TCP Port
EDIT	Testin_3_rscad	P1	SubNetworkName	192.168.1.206	255.255.255.0		102

**Figure 172: Access Points Configuration of the GTNETx2**

## 5.8 Case Studies

The following case studies are considered 1) Simulating steady state conditions – no intervention from OLTC control function needed as Bus 6 voltage profile is within the 0.95 p.u to to1.05 per-unit dead band range in the control algorithm 2) Simulating over voltage conditions - intervention from OLTC control function needed as Bus 6 voltage profile is above the 0.95 p.u to1.05 per-unit dead band range in the control algorithm 3) Simulating at under voltage conditions - intervention from OLTC control function needed as Bus 6 voltage profile is below the 0.95 to 1.05 per-unit dead band range in the control algorithm.

### 5.8.1 Case Study 1: Steady-state condition

Running the simulation case of the RTDS equipment, the dynamic load DL6 is set to an initial value of 75 MW and 24 MVAR. This loading condition of Bus 6 causes the voltage magnitude to rise to 33.04 kV L-L, which results in a per-unit voltage value of 1.001. This loading condition is within the 5% acceptable voltage deviation value and thus requires no intervention from the IEDs to initiate the automatic voltage control function. See [Table 46](#) for initial loading values.

**Table 46: Steady state voltage conditions - no corrections needed**

Bus 6 kV L-L	Bus 6  V  pu	DL6 (P & Q)	Tap Pos T18 Master	Tap Pos T17 Follower
33.04	1.001	75 MW & 24 MVAR	10	10

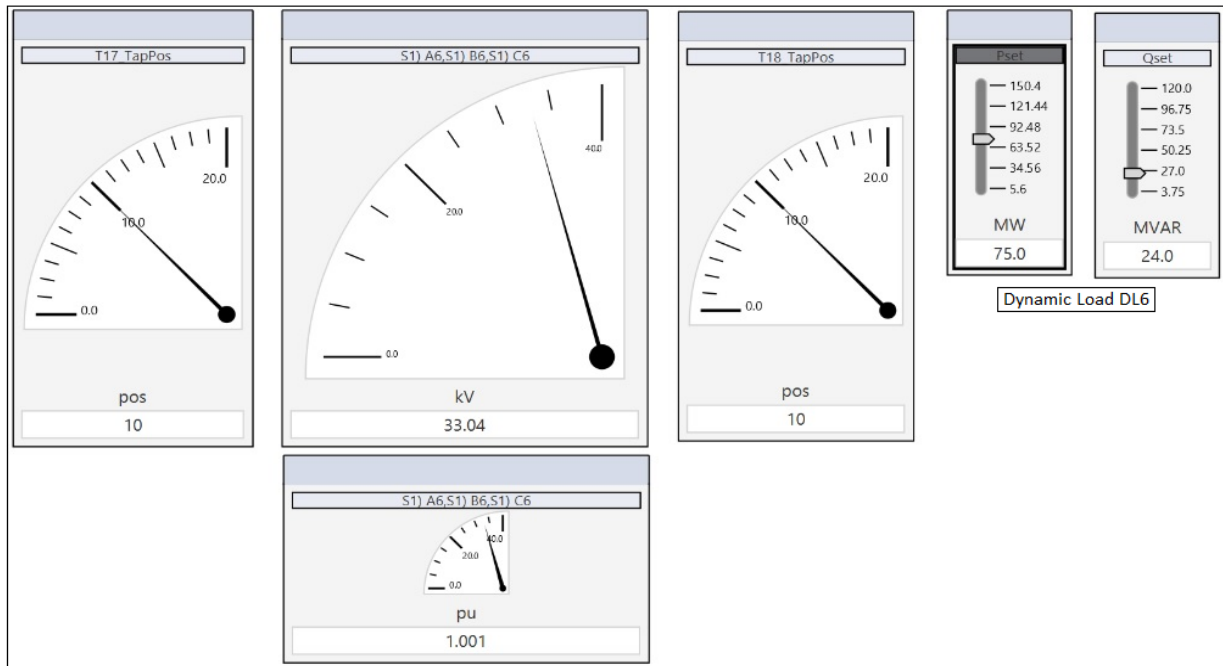


**Figure 173: Dashboard with steady state voltage conditions – no voltage regulation needed**

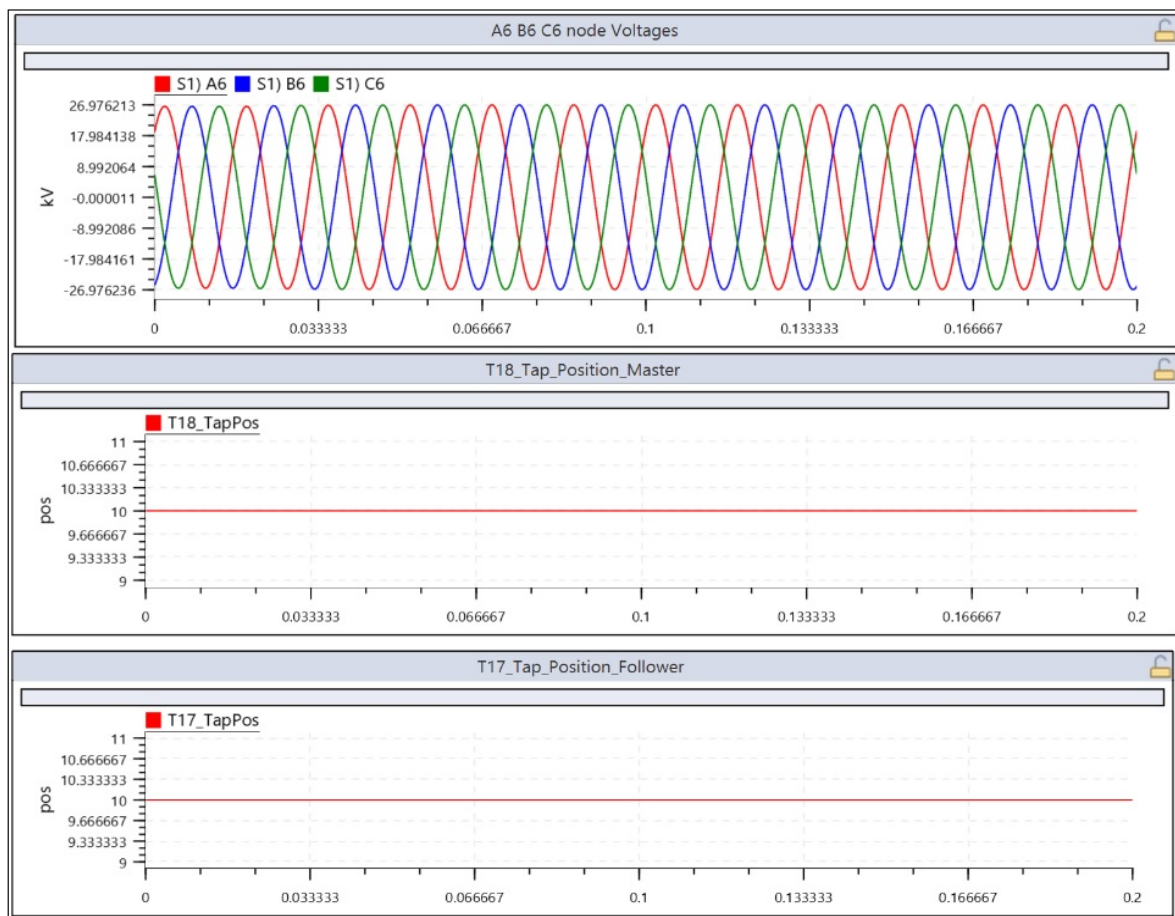


**Figure 174: Measured voltage at Bus 6 and the tap positions at steady state loading conditions - no voltage regulation needed**

With the Bus 6 voltage being measured outside the 5% acceptable voltage deviation set point, the IEDs constantly monitor the loading conditions. They will issue a corrective control signal if a deviation outside its maximum preset limit is detected. The Master or Slave SEL-2414 relays, in this case, do not need to issue any corrective control signals as the voltage magnitude is within the 5% acceptable voltage deviation value. See Figure 174 for measured voltage at Bus 6 and the tap positions at steady-state loading conditions.

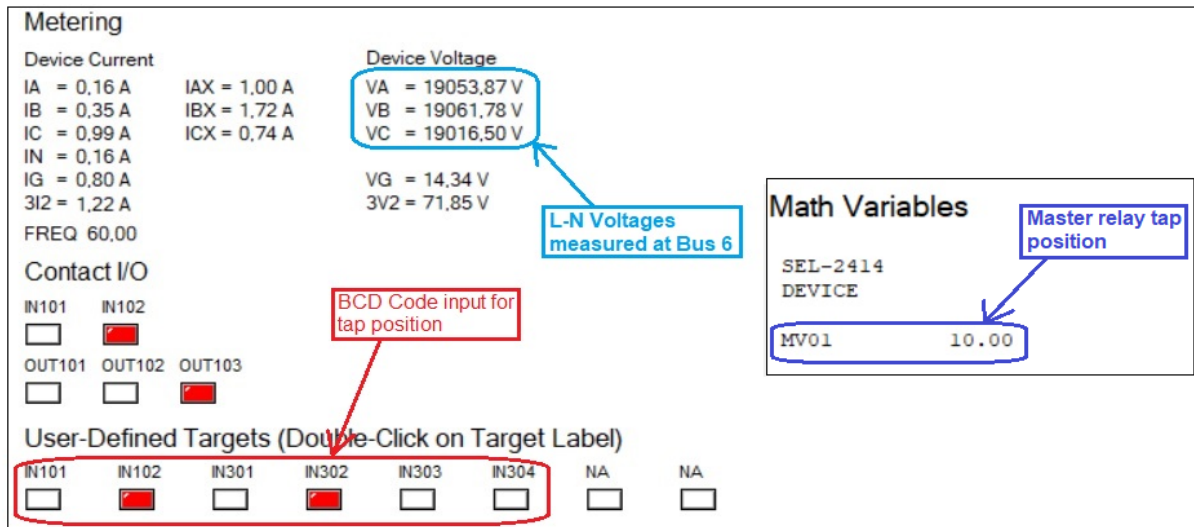


**Figure 175: HMI from Master relay with measured voltages and an indication of binary inputs for tap position**

### 5.8.2 Case Study 2: Overvoltage conditions

Running the simulation case of the RTDS equipment, the dynamic load DL6 is set to an initial value of 5.6 MW and 11 MVAR. This loading condition of Bus 6 causes the voltage magnitude to rise to 35.26 kV L-L, which results in a per-unit voltage value of 1.068. This loading condition is out of the 5% acceptable voltage deviation value and thus prompts the IEDs to initiate the automatic voltage control function. See Table 47 for initial loading values.

**Table 47: Initial loading condition values - overvoltage**

Bus 6 kV L-L	Bus 6  V  pu	DL6 (P & Q)	Tap Pos T18 Master	Tap Pos T17 Follower
35.26	1.068	5.6 MW & 11 MVAR	10	10



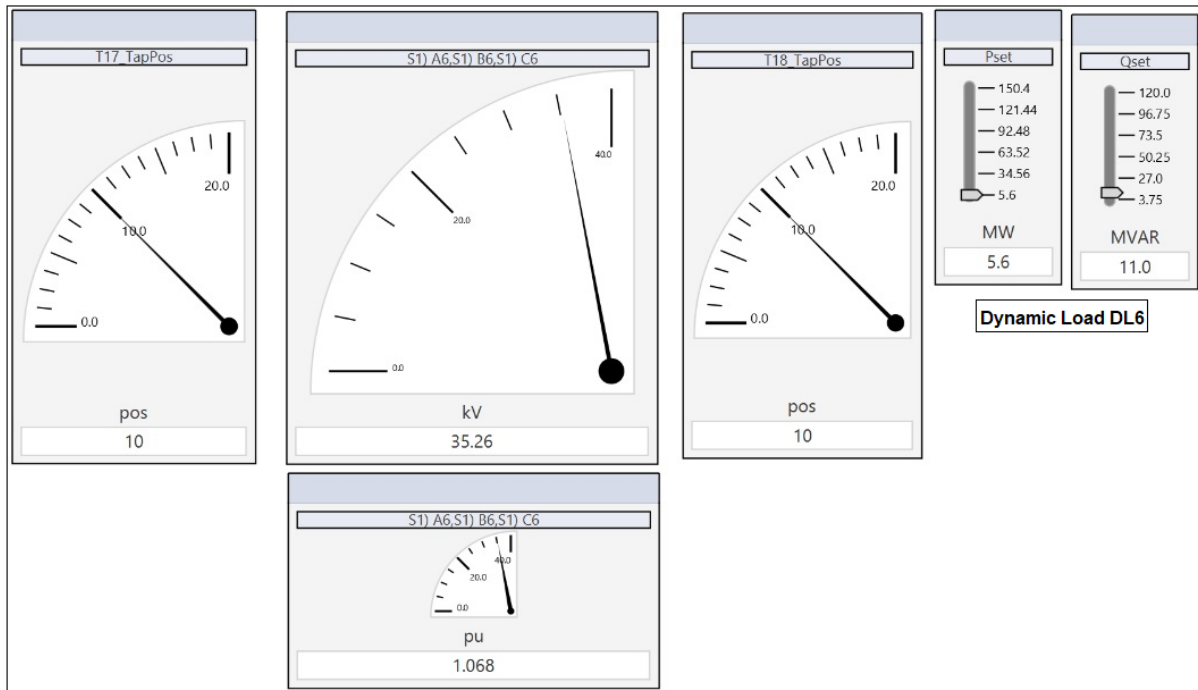


Figure 176: Dashboard with initial under voltage conditions before voltage correction

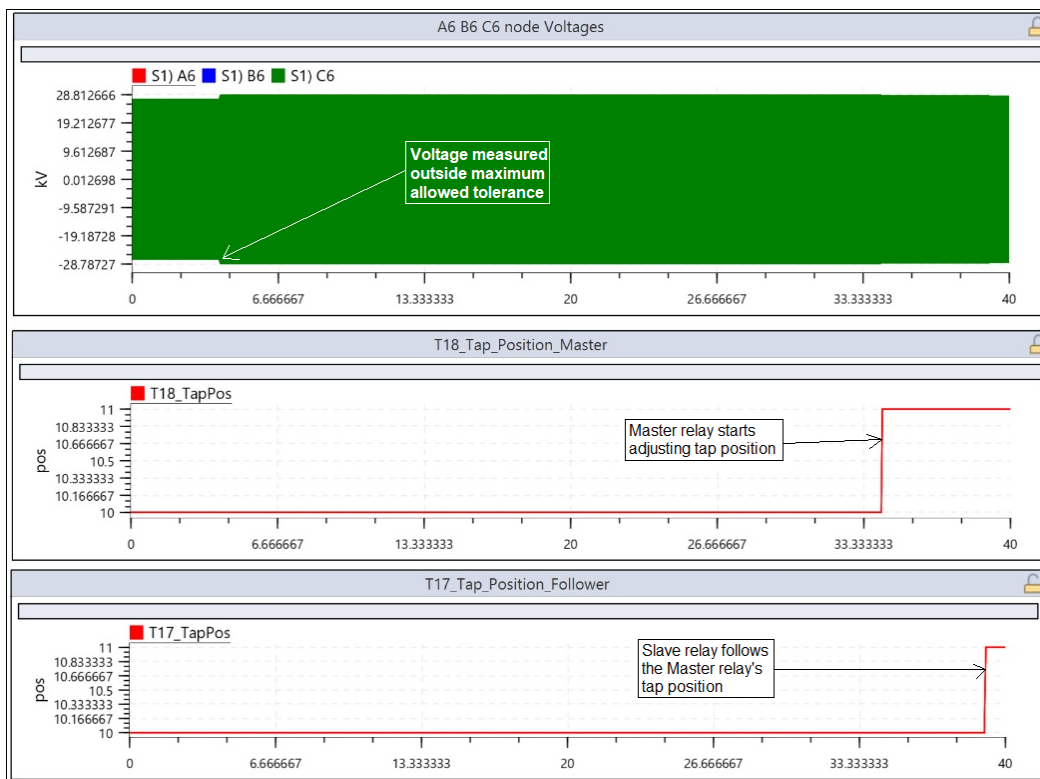
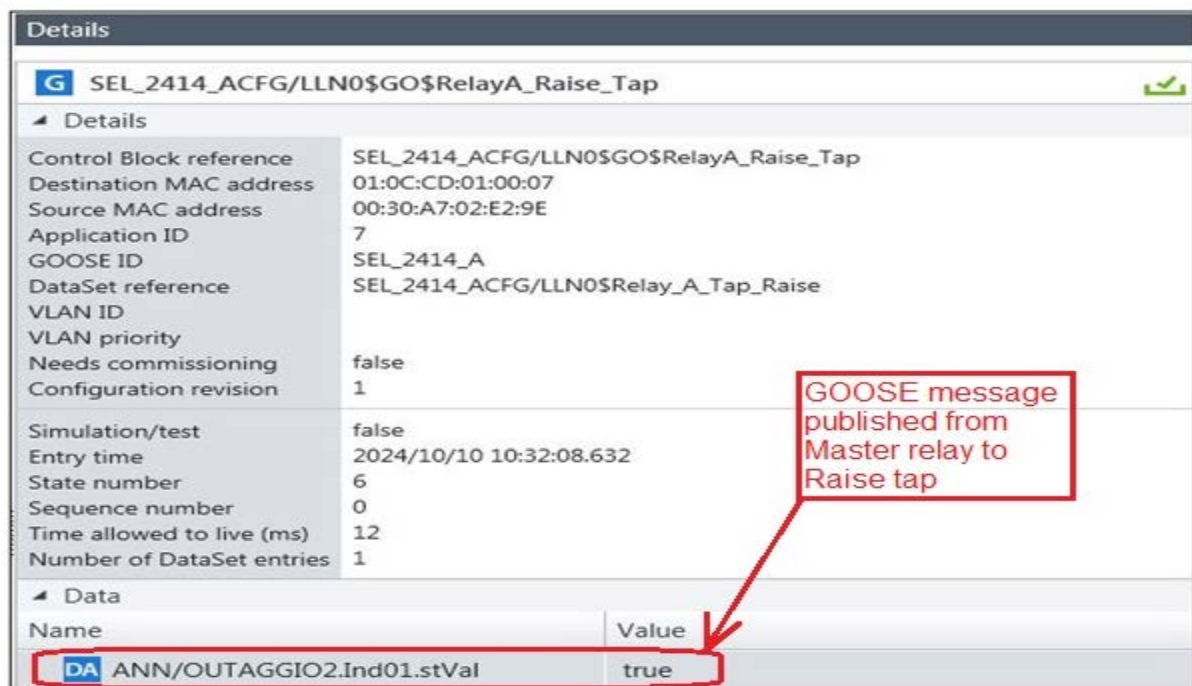


Figure 177: Measured voltage at Bus 6 and the tap raise operation in progress during over voltage conditions.



With the Bus 6 voltage being measured outside the 5% acceptable voltage deviation set point, the IEDs are prompted to initiate the automatic voltage control function. The Master SEL-2414 starts raising the taps of the master transformer as instructed by its incorporated voltage control algorithm. The master IED sent this control GOOSE message to the GTNETx2 card in the RTDS equipment. The master IED also sent its current tap position of the master transformer to the slave transformer's IED, which prompted the slave transformer to match its tap position to that of the master tap position. See [Figure 177](#) for the tap raise operation in progress.

With the OMICRON IEDScout software running, it is possible to view the live GOOSE message signals published by the Master and Slave relay. The GTNETx2 card in the RTDS equipment subscribes to these GOOSE messages and executes the OLTC control function. See [Figure#](#) for the GOOSE message for raising tap signals being issued by the Master relay and [Figure 178](#) for the GOOSE message for raising tap signals issued by the Slave relay.



Details	
<b>SEL_2414_ACFG/LLN0\$GO\$RelayA_Raise_Tap</b>	
Details	
Control Block reference	SEL_2414_ACFG/LLN0\$GO\$RelayA_Raise_Tap
Destination MAC address	01:0C:CD:01:00:07
Source MAC address	00:30:A7:02:E2:9E
Application ID	7
GOOSE ID	SEL_2414_A
DataSet reference	SEL_2414_ACFG/LLN0\$Relay_A_Tap_Raise
VLAN ID	
VLAN priority	
Needs commissioning	false
Configuration revision	1
Simulation/test	false
Entry time	2024/10/10 10:32:08.632
State number	6
Sequence number	0
Time allowed to live (ms)	12
Number of DataSet entries	1
Data	
Name	Value
DA ANN/OUTAGGIO2.Ind01.stVal	true

**Figure 178: GOOSE message for raising tap signals being issued by the Master relay**

SEL_2414_BCFG/LLN0\$GO\$Relay_B_Raise	
Details	
Control Block reference	SEL_2414_BCFG/LLN0\$GO\$Relay_B_Raise
Destination MAC address	01:0C:CD:01:00:0A
Source MAC address	00:30:A7:0C:3C:5D
Application ID	14
GOOSE ID	SEL_2414_B
DataSet reference	SEL_2414_BCFG/LLN0\$Relay_B_Raise
VLAN ID	
VLAN priority	
Needs commissioning	false
Configuration revision	1
Simulation/test	false
Entry time	2024/10/10 10:39:12.452
State number	63
Sequence number	0
Time allowed to live (ms)	12
Number of DataSet entries	1
Data	
Name	Value
DA ANN/OUTAGGIO2.Ind01.stVal	true

GOOSE message published from Slave relay to raise tap

**Figure 179: GOOSE message for raising tap signals being issued by the Slave relay**

AcSElerator® QuickSet - [Device ID: SEL-2414 (SEL-2414 011 HMI Driver)]	
File Edit View Communications Tools Windows Help Language	
Device Overview	Remote Analogs
Metering	SEL-2414
Temperature	DEVICE
Analog Inp	RA001 19413.03
Remote Ar	RA002 19448.30
Math Varia	RA003 19427.09
Fundamen	RA004 13.00
Demand	
Peak	
Energy	

Master relay tap position sent to Slave relay via GOOSE

AcSElerator® QuickSet - [Device ID: SEL-2414 (SEL-2414 011 HMI Driver)]	
File Edit View Communications Tools Windows Help Language	
Device Overview	Math Variables
Metering	SEL-2414
Temperature	DEVICE
Analog Inp	
Remote Ar	
Math Varia	MV01 13.00
Fundamen	
Demand	
Peak	

Slave relay tap position - matching tap position of Master relay

**Figure 180: HMI from Slave relay with indicating the Master relay tap position sent via GOOSE**

After the IED executes the control function to operate the OLTCs on the transformers, the voltage magnitude at Bus 6 is within the 5% acceptable voltage deviation value. See [Table 48](#) for voltage magnitude after corrections and Figure # for the dashboard in Runtime of RSCAD FX for visual indicators of live running conditions.

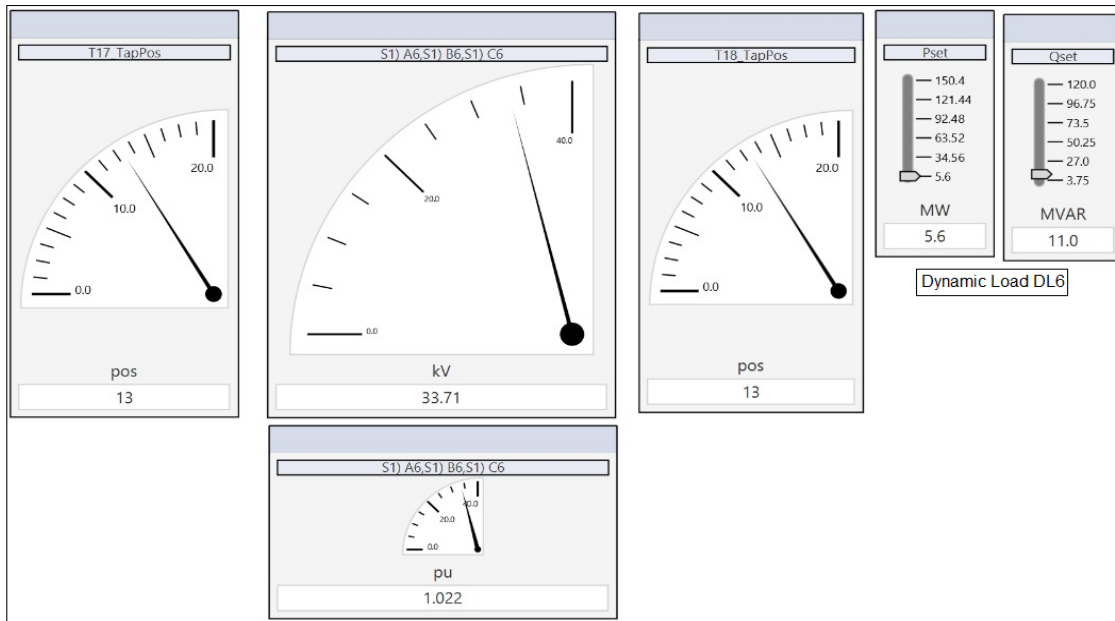


Figure 181: Dashboard with results after under voltage conditions is corrected

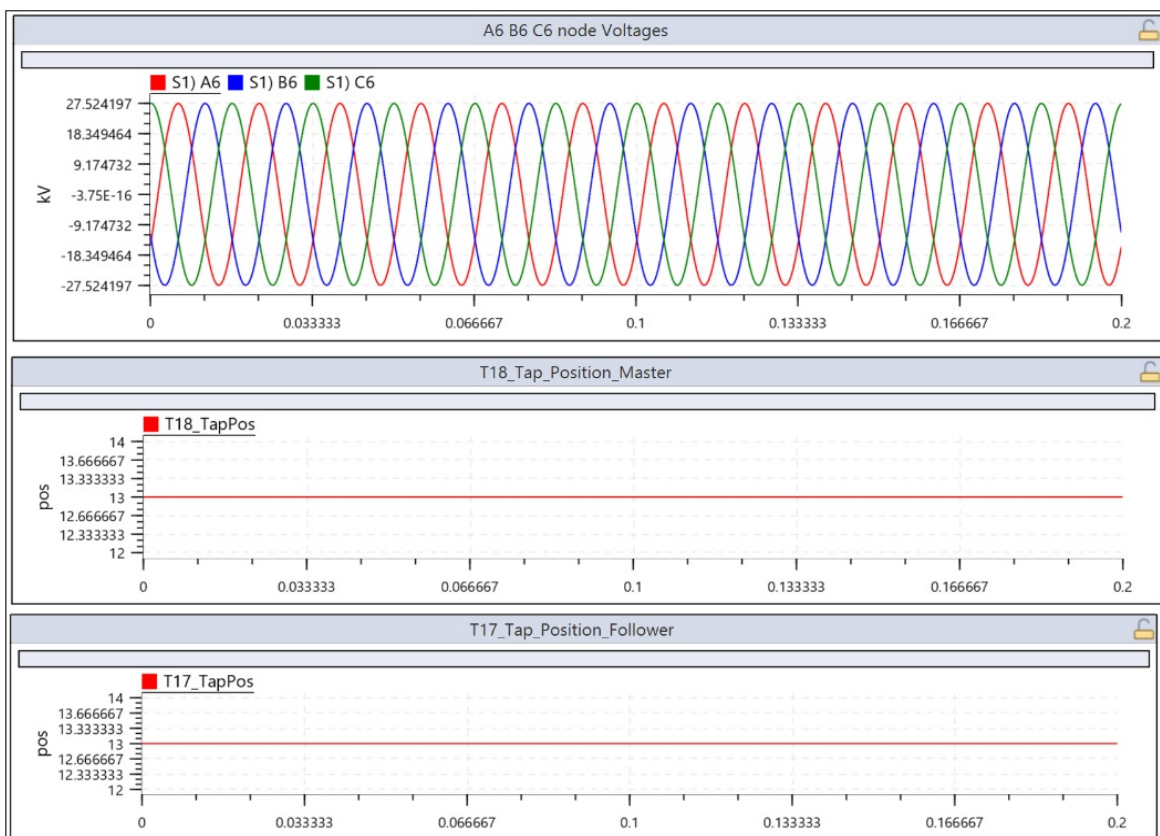


Figure 182: Measured voltage at Bus 6 and the tap positions after overvoltage conditions are corrected

**Table 48: Bus 6 voltage magnitude now within the acceptable range – after overvoltage condition is corrected**

Bus 6 kV L-L	Bus 6  V  pu	DL6 (P & Q)	Tap Pos T18 Master	Tap Pos T17 Follower
33.71	1.022	5.6 MW & 11 MVAR	13	13

### 5.8.3 Case Study 3: Under voltage conditions

Running the simulation case of the RTDS equipment, the dynamic load DL6 is set to an initial value of 150 MW and 24 MVAR. This loading condition of Bus 6 causes the voltage magnitude to rise to 30.39 kV L-L, which results in a per-unit voltage value of 0.9209. This loading condition is out of the 5% acceptable voltage deviation value and thus prompts the IEDs to initiate the automatic voltage control function. See [Table 49](#) for initial loading values.

**Table 5-49: Initial loading condition values – under voltage**

Bus 6 kV L-L	Bus 6  V  pu	DL6 (P & Q)	Tap Pos T18 Master	Tap Pos T17 Follower
30.39	0.9209	150 MW & 24 MVAR	10	10

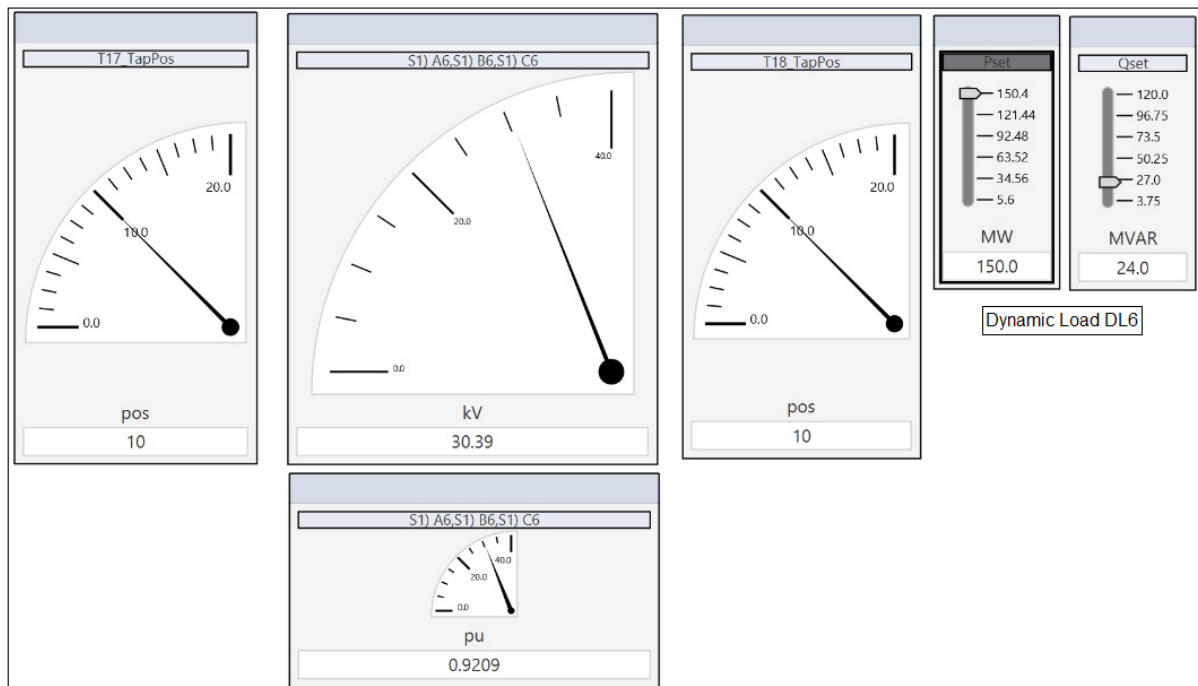


**Figure 183: Dashboard with initial under voltage conditions before voltage correction**

With the Bus 6 voltage being measured outside the 5% acceptable voltage deviation set point, the IEDs are prompted to initiate the automatic voltage control function. The Master SEL-2414 starts lowering the taps of the master transformer as instructed by its incorporated voltage control algorithm. The master IED sent this control GOOSE message to the GTNETx2 card in the RTDS equipment. The master IED also sent its current tap position of the master transformer to the slave transformer's IED, which prompts the slave transformer to match its tap position to that of the master tap position. See Figure 184 for the tap lowering operation in progress.

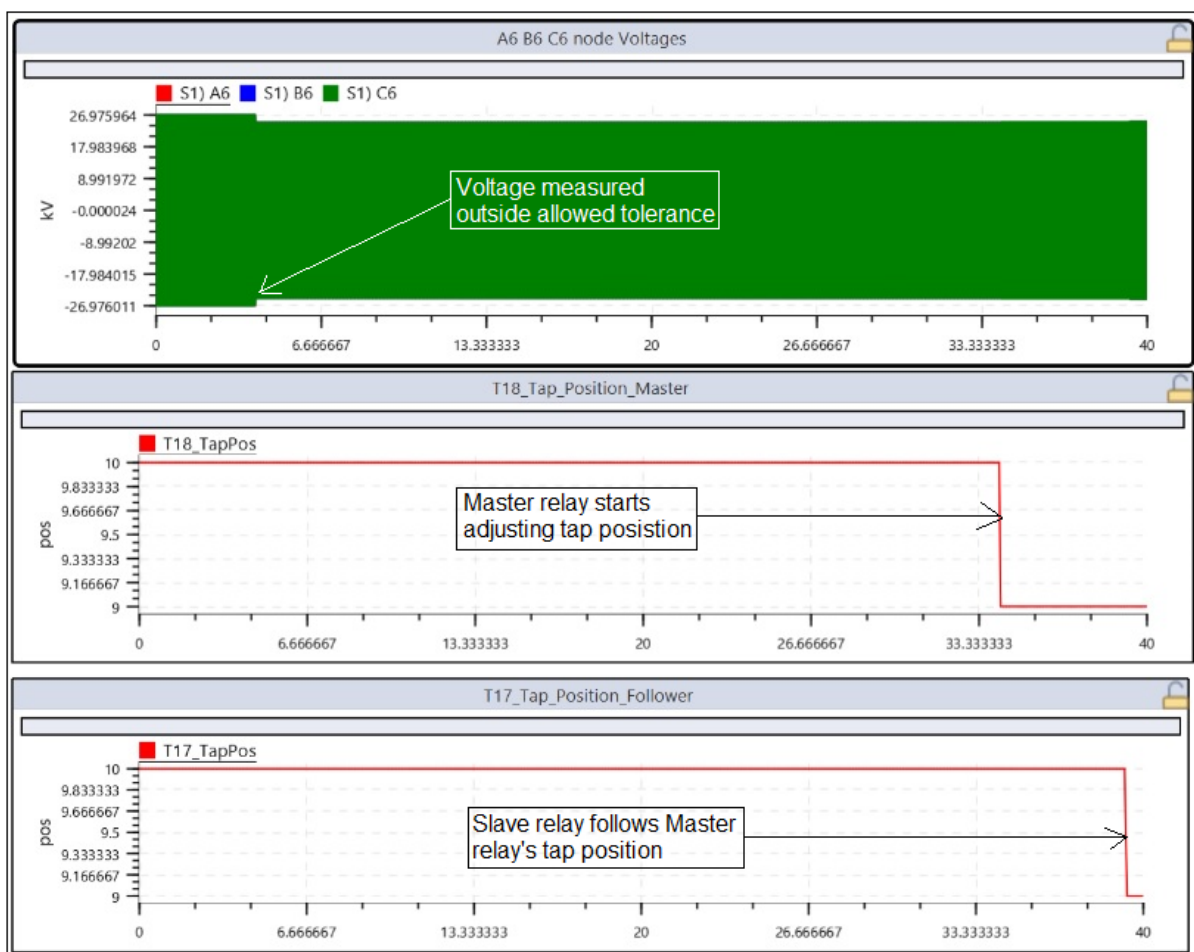


**Figure 184: Measured voltage at Bus 6 and the tap lowering operation in progress under voltage conditions.**

With the OMICRON IEDScout software running, it is possible to view the live GOOSE message signals published by the Master and Slave relay. The GTNETx2 card in the RTDS equipment subscribes to these GOOSE messages and executes the OLTC control function. See Figure 185 for the GOOSE message-lowering tap

signals being issued by the Master relay and [Figure 186](#) for the GOOSE message-lowering tap signals being issued by the Slave relay.

SEL_2414_ACFG/LLN0\$GO\$RelayA_Lower_Tap	
Details	
Control Block reference	SEL_2414_ACFG/LLN0\$GO\$RelayA_Lower_Tap
Destination MAC address	01:0C:CD:01:00:07
Source MAC address	00:30:A7:02:E2:9E
Application ID	8
GOOSE ID	SEL_2414_A
DataSet reference	SEL_2414_ACFG/LLN0\$RelayA_Lower_Tap
VLAN ID	
VLAN priority	
Needs commissioning	false
Configuration revision	1
Simulation/test	false
Entry time	2024/10/10 10:33:08.638
State number	12
Sequence number	0
Time allowed to live (ms)	12
Number of DataSet entries	1
Data	
Name	Value
DA ANN/OUTAGGIO2.Ind02.stVal	true

GOOSE message published from Master relay to lower tap

**Figure 185: GOOSE message for lowering tap signals being issued by the Master relay**

SEL_2414_BCFG/LLN0\$GO\$Relay_B_Lower	
Details	
Control Block reference	SEL_2414_BCFG/LLN0\$GO\$Relay_B_Lower
Destination MAC address	01:0C:CD:01:00:0A
Source MAC address	00:30:A7:0C:3C:5D
Application ID	10
GOOSE ID	SEL_2414_B
DataSet reference	SEL_2414_BCFG/LLN0\$Relay_B_Lower
VLAN ID	
VLAN priority	
Needs commissioning	false
Configuration revision	1
Simulation/test	false
Entry time	2024/10/10 10:39:06.458
State number	58
Sequence number	0
Time allowed to live (ms)	12
Number of DataSet entries	1
Data	
Name	Value
DA ANN/OUTAGGIO2.Ind02.stVal	true

GOOSE message published from Slave relay to lower tap

**Figure 186: GOOSE message for raising tap signals being issued by the Slave relay**



After the IED executes the control function to operate the OLTCs on the transformers, the voltage magnitude at Bus 6 is within the 5% acceptable voltage deviation value. See [Table 50](#) for voltage magnitude after corrections and Figure # for dashboard in Runtime of RSCAD FX for visual indicators of live running conditions.

**Table 50: Bus 6 voltage magnitude now within the acceptable range – after under voltage condition is corrected**

Bus 6 kV L-L	Bus 6  V  pu	DL6 (P & Q)	Tap Pos T18 Master	Tap Pos T17 Follower
31.44	0.9527	150 MW & 32 MVAR	5	5

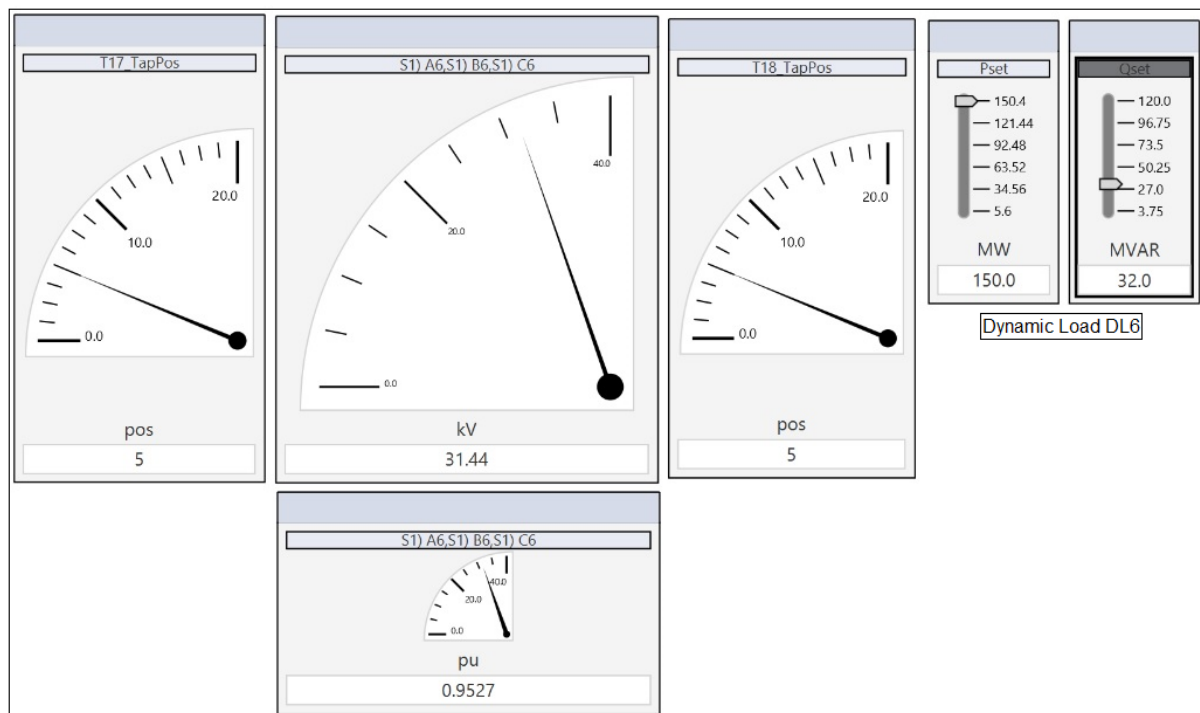


**Figure 187: Dashboard with results after under voltage conditions is corrected**

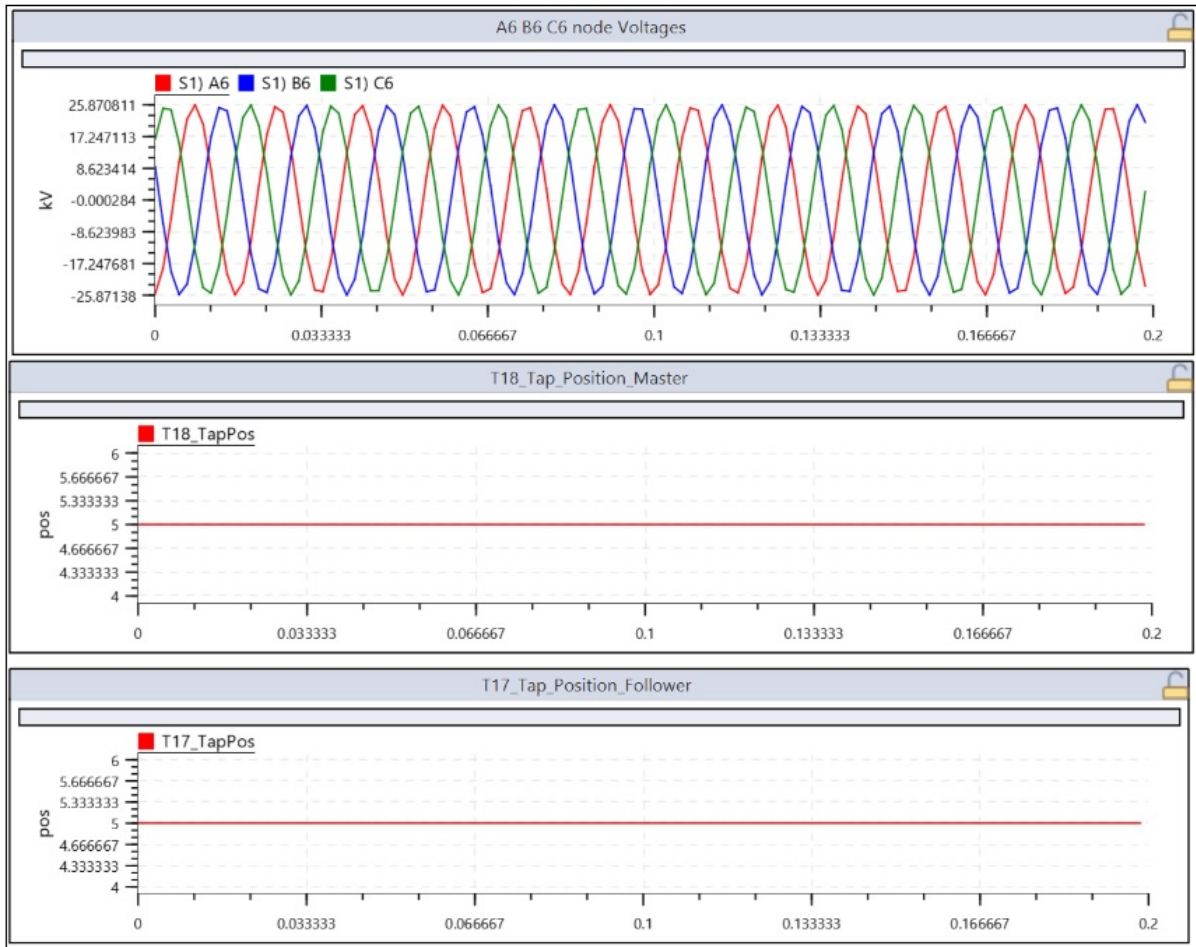


**Figure 188: Measured voltage at Bus 6 and the tap positions after under voltage conditions is corrected**

## 5.9 Comparison of DigSilent load flow results and RTDS real-time results

The results obtained from the load flow studies conducted in the DigSilent software for different loading conditions are compared to the real-time results from the RTDS environment. The comparison focuses on Bus 6, the secondary side of the parallel transformers. Steady-state results are compared in 5.9.1, overvoltage results are compared in 5.9.2, and undervoltage results are compared in 5.9.3.

### 5.9.1 Steady state results comparison



Applying a load of **75 MW and 24 MVAR** on Bus 6 in the DlgSilent and the RTDS environment yielded the following results. Results from DigSilent is shown in [Table 5-51](#) And real-time results from RTDS are shown in [Table 52](#).

**Table 51: Steady state load conditions for Bus 5 and Bus 6 voltage, with voltage magnitudes obtained from DlgSilent - no corrections needed**

Tap_Pos = 10	kV L-L	V  pu	Angle in degree
Bus 5	131.90	1.00	-11.90
Bus 6	32.16	0.97	-19.20

As can be seen from the DlgSilent load flow results, **75 MW and 24 MVAR** on Bus 6 causes the voltage magnitude to rise to 32.16 kV L-L, which results in a per-unit voltage value of 0.97. The tap position for both OLTCs of the parallel transformer is at position 10. This loading condition is within the 5% acceptable voltage deviation value and thus requires no intervention from the automatic voltage control function

**Table 52: Steady state load conditions for Bus 6 voltage, with voltage magnitudes obtained from RTDS - no corrections needed**

Bus 6 kV L-L	Bus 6  V  pu	DL6 (P & Q)	Tap Pos T18 Master	Tap Pos T17 Follower
33.04	1.001	75 MW & 24 MVAR	10	10

As can be seen from the RTDS real-time results **75 MW and 24 MVAR** on Bus 6 causes a voltage magnitude of 33.04 kV L-L, which results in a per-unit voltage value of 1.001. This loading condition is within the 5% acceptable voltage deviation value and thus requires no intervention from the IEDs to initiate the automatic voltage control function.

As seen from the results obtained from both environments, **75 MW and 24 MVAR** loading on Bus 6 results in a voltage profile within the acceptable range of 0.95 to 1.05 per unit. No intervention from the OLTCs is needed.

### 5.9.2 Overvoltage Results Comparison

A 5.6 MW and 11 MVAR load is applied on Bus 6 to create overvoltage conditions.

### 5.9.2.1 Overvoltage results comparison –before tap adjustments

Applying a load of **5.6 MW and 11 MVAR** on Bus 6 in the DIgSilent and the RTDS environment yielded the following results. The initial results from DIgSilent is shown in **Table 53** and real-time results from RTDS is shown in **Table 54**.

**Table 53: Over voltage load conditions for Bus 5 and Bus 6 voltage, with voltage magnitudes obtained from DIgSilent – before tap position is adjusted**

<b>Tap_Pos = 10</b>	<b>kV L-L</b>	<b> V  pu</b>	<b>Angle in degree</b>
<b>Bus 5</b>	135.37	1.03	-8.61
<b>Bus 6</b>	33.69	1.02	-11.70

As can be seen from the initial DIgSilent load flow results, 5.6 MW and 11 MVAR Bus 6 cause the voltage magnitude to rise to 33.69 kV L-L, which results in a per-unit voltage value of 1.02. The tap position for both OLTCs of the parallel transformer is at position 10. This loading condition is within the 5% acceptable voltage deviation value and thus requires no intervention from the OLTCs to improve the voltage profile at Bus 6.

**Table 54: Over voltage load conditions for Bus 6 voltage, with voltage magnitudes obtained from RTDS – before tap position is adjusted**

<b>Bus 6 kV L-L</b>	<b>Bus 6  V  pu</b>	<b>DL6 (P &amp; Q)</b>	<b>Tap Pos T18 Master</b>	<b>Tap Pos T17 Follower</b>
35.26	1.068	5.6 MW & 11 MVAR	10	10

As can be seen from the RTDS real-time results, 5.6 MW and 11 MVAR on Bus 6 cause the voltage magnitude to increase to 35.26 kV L-L, which results in a per-unit voltage value of 1.068. This loading condition is outside the 5% acceptable voltage deviation value and thus requires intervention from the IEDs to initiate the automatic voltage control function.

### 5.9.2.2 Overvoltage results in comparison – after tap adjustments

As seen from the initial DIgSilent loadflow results, although this loading condition is within the 5% voltage deviation range, the tap positions was adjusted to show the results of the improved voltage profile on Bus 6 of 33.16 kV L-L. Results of overvoltage loading on Bus 6 are shown in [Table 55](#). With the OLTC positions at Tap 13, the voltage profile is almost equal to the nominal voltage.

**Table 55: Over voltage load conditions for Bus 5 and Bus 6 voltage, with voltage magnitudes obtained from DIgSilent – after tap position is adjusted**

Tap_Pos = 13	kV L-L	V  pu	Angle in degree
Bus 5	135.49	1.03	-8.62
Bus 6	33.16	1.00	-11.74

After the IED executes the control function to operate the OLTCs on the transformers, the voltage magnitude at Bus 6 is within the 5% acceptable voltage deviation value. See [Table 56](#) for voltage magnitude after tap adjustments. Bus 6 now has a voltage magnitude of 1.022 per-unit. No further tap adjustments are required.

**Table 56: Over voltage load conditions for Bus 6 voltage, with voltage magnitudes obtained from RTDS – after tap position is adjusted**

Bus 6 kV L-L	Bus 6  V  pu	DL6 (P & Q)	Tap Pos T18 Master	Tap Pos T17 Follower
33.71	1.022	5.6 MW & 11 MVAR	13	13

### 5.9.3 Under voltage results comparison

A load of **150 MW and 24 MVAR** is applied on Bus 6 to create overvoltage conditions.

#### 5.9.3.1 Under voltage results comparison – before tap adjustments

Applying a load of **150 MW and 24 MVAR** on Bus 6 in both the DIgSilent and the RTDS environment yielded the following results. The initial results from DIgSilent are shown in [Table 57](#) and real-time results from RTDS are shown in [Table 58](#).

**Table 57: Under voltage load conditions for Bus 5 and Bus 6 voltage, with voltage magnitudes obtained from DIgSilent – before tap position is adjusted**

Tap_Pos = 10	kV L-L	V  pu	Angle in degree
Bus 5	127.65	0.97	-15.75
Bus 6	30.56	0.93	-28.43

As can be seen from the initial DIgSilent load flow results, 150 MW and 24 MVAR on Bus 6 cause the voltage magnitude to decrease to 30.56 kV L-L, which results in a per-unit voltage value of 0.93. The tap position for both OLTCs of the parallel transformer is at position 10. This loading condition is outside the 5% acceptable voltage deviation value and thus requires intervention from the OLTCs to improve the voltage profile at Bus 6.

**Table 58: Under voltage load conditions for Bus 6 voltage, with voltage magnitudes obtained from RTDS – before tap position is adjusted**

Bus 6 kV L-L	Bus 6  V  pu	DL6 (P & Q)	Tap Pos T18 Master	Tap Pos T17 Follower
30.39	0.9209	150 MW & 24 MVAR	10	10

As can be seen from the RTDS real-time results, 150 MW and 24 MVAR on Bus 6 cause the voltage magnitude to decrease to 30.39 kV L-L, which results in a per-unit voltage value of 0.9209. This loading condition is outside the 5% acceptable voltage deviation value and thus requires intervention from the IEDs to initiate the automatic voltage control function.

### 5.9.3.2 Under voltage results comparison – after tap adjustments

As seen from the initial DIgSilent loadflow results, although this loading condition is within the 5% voltage deviation range, the tap positions were adjusted to show the results of the improved voltage profile on Bus 6 of 31.55 kV L-L. Results of under-voltage loading on Bus 6 are shown in **Table 59**. With the OLTC positions at Tap 5, the voltage profile is almost equal to 0.96 per-unit.

**Table 59: Under voltage load conditions for Bus 5 and Bus 6 voltage, with voltage magnitudes obtained from DIgSilent – after tap position is adjusted**

Tap_Pos = 5	kV L-L	V  pu	Angle in degree
Bus 5	127.54	0.97	-15.75
Bus 6	31.55	0.96	-27.80

After the IED executes the control function to operate the OLTCs on the transformers, the voltage magnitude at Bus 6 is within the 5% acceptable voltage deviation value. See **Table 60** for voltage magnitude after tap adjustments. Bus 6 now has a voltage magnitude of 0.9527 per unit. No further tap adjustments are required.

**Table 60: Under voltage load conditions for Bus 6 voltage, with voltage magnitudes obtained from RTDS – after the tap position is adjusted**

Bus 6 kV L-L	Bus 6  V  pu	DL6 (P & Q)	Tap Pos T18 Master	Tap Pos T17 Follower
31.44	0.9527	150 MW & 32 MVAR	5	5

#### 5.9.4 Discussion of comparison between DIgSilent load flow results and RTDS real-time results

From the comparison of load flow results of the DIgSilent software and the real-time results from the RTDS environment for different loading conditions, it can be concluded that the power transformers equipped with OLTCs are sufficient in maintaining the voltage profile of Bus 6. OLTCs regulate and maintain the system voltage magnitude at the desired level on the load side. Results from both environments point to similar tap change operational results, except for a deviation from the over-voltage loading conditions, which shows that the voltage profile of Bus 6 from the DIgSilent environment did not increase to the same level as the equivalent RTDS simulation. This might be attributed to the RTDS incorporating additional real-time parameters into account that are beyond DIgSilent's scope.

## 5.10 Conclusion

The chapter shows how the original IEEE 14 Bus Network was adapted for the new voltage levels and how the Modified IEEE 14 Bus network was modeled in the RSCAD FX software. An in-depth illustration of how the GTNETx2 card of the RSCAD equipment was configured to subscribe to the IEC61850 GOOSE messages published from the external SEL-2414 relays is demonstrated. It also reflects the process of developing the hardware-in-the-loop testbed and the procedure to configure its various components. This chapter reveals how hardware-in-the-loop simulations were conducted and the results obtained from the simulations.

When conducting hardware-in-the-loop simulations, whenever voltage deviations more extraordinary than the allowable 5% were detected, the external SEL-2414 relays employed the internal voltage control algorithms to successfully correct the bus voltage magnitudes. The IEC 61850-7-4 GOOSE messages proved to be a capable and reliable method of communication for sharing information between the IEDs and transmitting control signals to the RTDS equipment.

The next chapter shows the deliverables of the thesis, the recommended work to be conducted in the future, and the conclusions made from conducting the studies in this thesis.

## CHAPTER SIX

### CONCLUSION

#### 6.1 Introduction

Maintaining a stable grid voltage level is critical for all industrial and residential customers connected to the power system network. Fluctuating grid voltage levels wreak havoc on all linked customers. Power transformer voltage regulation is a serious concern in the industry. According to a literature survey, power transformer protection and control relays have evolved into smart relays with highly complex technology capable of performing various protection and control functions in an "all in one" package. The SEL-2414 transformer monitor relay was chosen to execute the transformer voltage control in this project. The two SEL-2414 relays were configured and programmed with a custom-created control algorithm to implement the transformer OLTCs control functions in order to maintain a stable voltage profile. The settings and parameters of the relays are determined by the specifications of the parallel transformers and the modified version of the IEEE 14 Bus network specifications. A hardware-in-the-loop test bench was built to evaluate the operational performance of the control algorithm created to control the OLTC operations.

RTDS simulation equipment was employed to simulate a real-time testing environment. Low-level signals generated within the RTDS equipment were amplified to usable levels by the Omicron CMS 156 amplifier. The connected SEL-2414 monitored the amplified signals. The IEC61850 standard compatibility of the SEL-2414 IED allowed it to send and receive control signals over an Ethernet connection. The relays' algorithm that controls the OLTCs was tested using the IEC61850 GOOSE messaging application to control signal transfer and transmit data between the relays. The control signals from the SEL-2414 IEDs were sent via IEC61850 GOOSE communication to the RTDS equipment to control the OLTCs. Data obtained from the RTDS equipment was analyzed to scrutinize the operational performance of the control algorithm and verify the effectiveness of using IEC61850 GOOSE communication for control signal transmission.

This chapter will summarise this research's key findings and conclusions and discuss the study's deliverables. The study's research aim and objectives are shown in section 6.2, deliverables in section 6.3, industry application in section 6.4, future work recommendations in section 6.5, publications in section 6.6, and Conclusion in 6.7. The bibliography follows.

## 6.2 Research Aim & Objectives

Control and maintain power system voltages within predefined voltage levels using automatic voltage regulation by tap changer technology on power transformers and IEC 61850 GOOSE messages for control signal transmission.

The study's objectives included reviewing documents related to the subject matter and developing an OLTC control algorithm. Modeling the network in the DIgSilent software, lab-scale testing, and control IED configuration. HIL closed-loop testing to verify the operational performance of the control algorithm and IEC61850 GOOSE-based communication for control signal transmission as follows:

- ix) To conduct a literature review on transformer voltage control, IEC61850-7-4, automatic transformers, tap changers, tap changer controller algorithms, and hardware-in-the-loop simulations in a closed-loop simulation environment.
- x) To investigate and comprehend the transformer tap change controller and its automatic operation, parallel transformer operation, and IEC61850 GOOSE message applications for transformer tap changer application.
- xi) Modelling and simulating the proposed power system network with the DigSilent and RTDS software suites RSCAD.
- xii) Using the IEC61850 accessible, logical nodes, create a novel algorithm for voltage control of transformers. a) Tap changer (YLTC), b) Automatic tap change control (ATCC), and c) Voltage control (AVCO) OR design custom IEC61850-7-4 based logical nodes for a) to c).
- xiii) Perform the relay engineering configuration to set up for online transformer-tap change control (OLTC).



- xiv) Perform the engineering configuration to the IEC61850 GOOSE message for OLTC operation.
- xv) Perform the engineering configuration to use a transformer tap changer and its controller to modulate the system voltage on a lab scale.
- xvi) Implement hardware-in-the-loop simulation in a closed-loop simulation environment using RTDS and relay and validate simulation results

### 6.3 Deliverables

Different network loading conditions influence the voltage profile of the monitored bus. The sudden unloading of the power system network causes system voltage to fluctuate above the maximum acceptable voltage level. In contrast, increasing loading will cause the network voltage to decrease below the minimum acceptable levels. Power transformers equipped with OLTCs regulate the system voltage levels by adjusting the winding ratios of the transformers to maintain voltage levels within the acceptable dead band value. This study controls the OLTCs of the transformers with a custom algorithm and transmits control signals using IEC61850 GOOSE-based communication. The deliverables for this study are as follows:

- Literature review conducted on OLTC.
- Modelling and simulation of the network in DigSilent & RTDS and base caseload flow analysis
- Lab-scale setup to validate the OLTC operation for different use case scenarios.
- HIL lab-scale setup to validate the OLTC operation.
- Engineering configuration of the OLTC relay and OLTC control configurations
- Simulation, validation, and results analysis of the OLTC operation for different use case scenarios.
- IEC61850 GOOSE Engineering configuration of the OLTC relay
- Simulation, validation, and results analysis of the IEC61850 GOOSE application for the OLTC operation for different use case scenarios.

### **6.3.1 Literature review**

The literature review examined the diverse strategies employed for voltage regulation of the power transformer. The algorithms reviewed for the control function of the OLTCs in terms of operational performance, application type, and reliability were examined. The benefits associated with conducting closed-loop testing using real-time simulators were also reviewed. From the literature reviewed on IEC61850-based communication, it can be concluded that incorporating IEC61850-based communication protocols into protection and control schemes has numerous benefits compared to traditional hardwired schemes. From the literature, IED testing conducted using real-time simulators with IEC61850 protocol proved to be a reliable, fast, and effective signal transmission verification and analysis method.

### **6.3.2 Modelling and simulation of the network in DigSilent & RTDS and base caseload flow analysis**

The modified version of the IEEE 14 bus network is modelled in the DIgSilent PowerFactory 2023 software and the RSCAD FX 2.2.1 software. Load flow studies are conducted on the network for different loading conditions, and the results are analyzed. The tap positions of the OLTCs of the parallel transformers are adjusted for both over- and under-voltage conditions. The influence of different tap positions on the voltage profile of the monitored bus is observed and analyzed. It is clear from the results obtained from the DIgSilent load flow simulations and RSCAD that by adjusting the parallel transformers' tap positions, the monitored bus's voltage load profile can be significantly improved under different loading conditions. The results from the tests conducted in the DIgSilent software are compared to those obtained from the RTDS environment. Comparing the load flow results from DIgSilent and RSACD for the base values yields similar values. This verifies that the load flow results obtained from both simulation software, with the parallel transformer added to the network, yield similar results under normal operating conditions.

### **6.3.3 Lab-scale setup to validate the OLTC operation for different case scenarios**

The two SEL-2414 IEDs were programmed with custom-created algorithms to execute the automatic voltage control function using a Master-Follower control scheme. The development and testing of the custom-created voltage control algorithms to control the OLTCs of the parallel transformer pair, the configuration settings of the Master and Slave-Follower relay, and the implementation of the IEC61850 GOOSE communication were done in preparation for HIL testing. The lab-scale test bench setup was constructed. Two Omicron CMC 356 test injection devices were utilized to generate the relevant test signals. The Wireshark Network Analyzer software was used to monitor the IEC61850 GOOSE traffic during the relay testing to verify that the GOOSE signals were successfully published across the network. The scale testing proved successful; the control IEDs issued the appropriate voltage correction signals via GOOSE messaging for various testing conditions.

### **6.3.4 HIL lab-scale setup to validate the OLTC operation**

A modified version of the IEEE 14 Bus network was constructed in the RSCAD FX environment. A hardware-in-the-loop network is built, incorporating the two SEL-2414 relays to monitor and control the voltage regulation function of the parallel transformers in the RTDS equipment using a Master-Follower control structure. IEC61850 GOOSE messages were used to transmit the control signals published by the Master and Follower relays to the RTDS equipment. GOOSE traffic on the network was monitored using the OMICRON IEDScout software during HIL testing. By varying the dynamic load connected to Bus 6, the voltage profile deviated outside the 0.95 p.u to 1.05 p.u. Control range of the algorithm. The IEDs managed to control the OLTCs of the transformers by publishing GOOSE control signals to bring the voltage profile back into the dead band range setting. Thus, the voltage control algorithm proved to be successful in the voltage regulation of parallel power transformers. IEC61850 GOOSE communication successfully performed the control signal transmission function during HIL testing.

### **6.3.5 Engineering configuration of the OLTC relay and OLTC control configurations**

The two SEL-2414 IEDs were configured and programmed with the custom-created algorithm utilizing the Quickset AcSELeator software. One SEL-2414 relay executes the control function of the relay for the OLTC of the Master transformer, and the other SEL-2414 relay executes the control function for the OLTC of the Slave-Follower transformer. The Omicron test universe software was utilized to configure the Omicron CMC 356 test signal generator device.

### **6.3.6 Simulation, validation, and results analysis of the OLTC operation for different case scenarios**

A test bench setup was created to verify the performance of the developed voltage control algorithms and the successful implementation of the GOOSE communication protocol for transmitting data between the relays and to transmit control signals to the CMC356 device. Different voltage magnitudes were injected into the SEL-2414 Master relay to simulate steady state--, over-voltage, and under-voltage conditions. The Master and Slave-Follower relays utilized their internally programmed control algorithm to issue the appropriate control signals for the simulated conditions. To analyze the operational performance results of the OLTC, a hardware-in-the-loop network was constructed, incorporating the two SEL-2414 relays to monitor and control the voltage regulation function of the parallel transformers in the RTDS equipment. Under different loading conditions, steady state-, over-voltage, and under-voltage conditions were simulated. The change in voltage magnitude is observed by the SEL-2414 relays monitoring the system voltage, and it will activate the voltage control algorithm configured within the IEDs to perform corrections and maintain the voltage magnitude within the  $\pm 5\%$  tolerance range.

### **6.3.7 IEC61850 GOOSE Engineering configuration of the OLTC relay**

GOOSE communication serves as the protocol for transmitting and receiving data between IEDs in the network and for transmitting control signals. The SEL-2414 transformer monitor relays used in this study are compliant with the IEC61850 GOOSE communication protocol. For the IEC61850 GOOSE to be configured on the relay, the IEC61850 standard protocol must be activated using the AcSELeator Quickset software.

### **6.3.8 Simulation, validation, and results analysis of the IEC61850 GOOSE application for the OLTC operation for different use case scenarios**

A lab-scale test bench setup was created to verify the performance of the developed voltage control algorithms and successfully implement the GOOSE communication protocol for data transmission between the relays and to transmit control signals to the CMC356 device. After successful testing in the lab scale test bench setup, a hardware-in-the-loop network was built, incorporating the two SEL-2414 relays to monitor and control the voltage regulation function of the parallel transformers in the RTDS equipment using a Master-Follower control structure. IEC61850 GOOSE messages were used to transmit the control signals published by the Master and Slave-Follower relays to the RTDS equipment.

## **6.4 Application**

This research provides a guideline to academia for creating custom algorithms, not limited to tap changers. The detailed DIgSilent and RTDS implementation guidelines can benefit academia and industry in similar contexts. The IEC61850 GOOSE step-by-step configuration can be a benchmark for incorporating modern, reliable, fast communication structures in protection and control applications.

## **6.5 Future work**

For future work recommendations, it would be worthwhile to investigate OLTC control schemes employing the circulating current and harmful reactance control methods by incorporating the IEC61850 GOOSE message application function. Including the transformer protection functions within the same IED conducting the OLTC function would also be recommended. To investigate IEDs' interoperability, I recommend researching OLTC controllers by using IEDs from different vendors to control parallel transformer OLTCs.

## **6.6 Publications**

Two SAUPEC papers and one journal paper are produced out of this research work as follows:

J. Wellen and S. Krishnamurthy, "IEC61850 standard-based motor protection scheme," *2020 IEEE PES/IAS PowerAfrica*, Nairobi, Kenya, 2020, pp. 1-5, doi: 10.1109/PowerAfrica49420.2020.9219855.

J. Wellen and S. Krishnamurthy and M Ratshitanga. IEC61850 GOOSE message application for a power transformer voltage control. *IEEE SAUPEC 2025 at TUT*, pp. 1-6.

J. Wellen, S. Krishnamurthy, and M. Ratshitanga. Enhanced Voltage Regulation and Real Journal of Electrical Engineering & Technology will be submitted for review in due course.

## 6.7. Conclusion

Traditional transformer voltage regulation was achieved by mechanically changing the tap positions of the power transformers. Modern power system requires constant monitoring of system power quality and for timely voltage corrections to be made if voltage level deviates from the acceptable pre-set values. From the hardware-in-the-loop real-time simulations and DIgSilent implementation conducted, OLTC operation for different voltage magnitudes, using the IEC61850 GOOSE message application as a communication medium, resulted in efficient tap changer operations. The SEL-2414 relays, programmed with the custom voltage control algorithm, successfully enhanced the voltage profile by adjusting the tap positions of the OLTCs of parallel transformers. This study revealed that GOOSE messages proved reliable and highly adaptable for future changes in operating structures without the need to change any physical hard-wired configurations. Combining the IEC61850 GOOSE message application with OLTCs enables remote monitoring and control of the OLTCs. In agreement with the findings from the literature review conducted, IEC61850-based communication provides superior performance in terms of speed, reliability for control, and protection signal transmission. The standardized logical nodes in IEC61850 GOOSE-based structures allow for more standardized communication streams for greater interoperability between IEDs from different vendors.

## Bibliography

1. Alencar, R. J. N., Bezerra, U. H., & Ferreira, A. M. D. (2014). A method to identify inrush currents in power transformers protection based on the differential current gradient. *Electric Power Systems Research*. <https://doi.org/10.1016/j.epsr.2014.02.009>
2. Ali Qasmi, Talha. (2014). Power Transformer Protection. <https://www.researchgate.net/publication/275042159>
3. Alkahdely, Sinan & Alsammak, Ahmed. (2023). Normal operation and reverse action of on-load tap changing transformer with its effect on voltage stability. *Bulletin of Electrical Engineering and Informatics*. 12. 650-658. 10.11591/eei.v12i2.4556.
4. Apostolov, A., & Vandiver, B. (2011). IEC 61850 GOOSE applications to distribution protection schemes. In 2011 64th Annual Conference for Protective Relay Engineers. <https://doi.org/10.1109/CPRE.2011.6035618>
5. Apostolov, A., Auperrin, F., Passet, R., Guenego, M., & Gilles, F. (2006). IEC 61850 process bus based distributed waveform recording. 2006 IEEE Power Engineering Society General Meeting, PES. <https://doi.org/10.1109/pes.2006.1709631> April 3–5, 2007.
6. Banakar, S. V., Muralidhara, V., & Maheswara Rao, N. (2016). Technological development of on - load tap changing mechanism in power transformer - a review. *Power Research - A Journal of CPRI*, 12(3), 487–496. Retrieved from <https://cprijournal.in/index.php/pr/article/view/281>
7. Bhamare, Y. (2009). IEC 61850 based distribution automation system. *Water and Energy International*.
8. Bonetti, Andrea & Zhu, Hongliang & Ignatovski, Nikolay. (2021). IEEE GPECOM 2021 - Use of IEC 61850 to increase the security of the protection system. 220-226. 10.1109/GPECOM52585.2021.9587715.
9. Brand, Klaus-Peter & Brunner, Christoph. (2011). Design of IEC 61850 Based

- Substation Automation Systems According to Customer Requirements.
10. Bugade, V. S. (2018). Automatic Voltage Control of Load using on Load Tap Changer. International Journal for Research in Applied Science and Engineering Technology. <https://doi.org/10.22214/ijraset.2018.3681>
  11. Carlen, M., Jakobs, R., Slupinski, A., Cornelius, F., Schneider, M., Buschmann, I., Tepper, J., & Wiesler, H. (2015). Line Voltage Regulator for Voltage Adjustment in MV-Grids. CIRED 23rd International Conference on Electricity Distribution.
  12. Cigré Working Group A2.3, 2015, TB 642 - Transformer Reliability Survey
  13. Cimadevilla, R., Ferrero, Í., & Yarza, J. M. (2014). IEC61850-9-2 process bus implementation on IEDs. Proceedings of the IEEE Power Engineering Society Transmission and Distribution Conference. <https://doi.org/10.1109/tdc.2014.6863506>
  14. Coffele, F., Blair, S., Booth, C., Kirkwood, J., & Fordyce, B. (2013). Demonstration of adaptive overcurrent protection using IEC 61850 communications. In IET Conference Publications. <https://doi.org/10.1049/cp.2013.0646>
  15. Constantin, I. C., & Iliescu, S. S. (2012). Automatic voltage regulation of the transformer units implemented in digital multifunction protection systems. Proceedings of the International Conference on Optimisation of Electrical and Electronic Equipment, OPTIM. <https://doi.org/10.1109/OPTIM.2012.6231763>
  16. D.P. Kothari & I.J. Nagrath, "Basic Electrical Engineering", Tata McGraw hills publishers, Second Edition.
  17. Dantas, D. T., Pellini, E. L., & Manassero Junior, G. (2018). Energy and reactive power differential protection hardware-in-the-loop validation for transformer application. The Journal of Engineering. <https://doi.org/10.1049/joe.2018.0223>
  18. Dr. P. S. Bimbra, "Generalized Theory of Electrical Machines" Khanna publishers, Fifth Edition.
  19. Dubey, Ashirwad. (2016). Load flow analysis of power systems. International Journal of Scientific and Engineering Research. 7. 06.
  20. Ferrero, I., Cimadevilla, R., Yarza, J. M., & Solaun, I. (2014). Analysis of oltc control of parallel transformers. ZIV grid report.



21. Ferrero, Íñigo, Roberto Cimadevilla, José Miguel Yarza and Iñaki Solaun. "Analysis of OLTC control of parallel transformers." (2014).
22. Fusco, G., & Russo, M. (2007). The Voltage Control Problem in Power Systems. In: Adaptive Voltage Control in Power Systems. Advances in Industrial Control. Springer, London. [https://doi.org/10.1007/978-1-84628-565-3\\_1](https://doi.org/10.1007/978-1-84628-565-3_1)
23. Gajić, Z., Aganović, S., Benović, J., Leci, G., & Gazzari, S. (2010). Using IEC 61850 analogue GOOSE messages for OLTC control of parallel transformers. *IET Conference Publications*. <https://doi.org/10.1049/cp.2010.0227>
24. Gajic, Zoran & Aganovic, Senad & Benovic, J. & Leci, G. & Gazzari, S.. (2010). Using IEC 61850 analogue GOOSE messages for OLTC control of parallel transformers. 1 - 5. 10.1049/cp.2010.0227.
25. H. de Graaff Genis and S. Krishnamurthy, "Microgrid Protection Simulation and Testing using a Relay-Secondary Injection Device Testbed," 2024 32nd Southern African Universities Power Engineering Conference (SAUPEC), Stellenbosch, South Africa, 2024, pp. 1-6, doi: 10.1109/SAUPEC60914.2024.10445048. keywords: {Bidirectional power flow;Power system stability;Power system reliability;Reliability;Relays;IEC Standards;Testing;Distributed generation (DG);DOCR;GOOSE;IEC 61850;IED;microgrid (MG)},
26. Hakala-Ranta, A., Rintamäki, O. & Starck, J. (2009). Utilizing possibilities of IEC 61850 and GOOSE. (CIRED 2009), Paper 0741
27. Hampson, B. (2018). Power System Operation and Control Solutions Using IEC 61850. 22nd Conference of the Electric Power Supply Industry, September 2018
28. Han, L.; Yin, J.; Wu, L.; Sun, L.; Wei, T. Research on the Novel Flexible On-Load Voltage Regulator Transformer and Voltage Stability Analysis. *Energies* 2022, 15, 6189. <https://doi.org/10.3390/en15176189>
29. Hasan, E. O., Hatata, A. Y., Badran, E. A. E., & Yossef, F. H. (2019). Voltage Control of Distribution Systems Using Electronic OLTC. In 2018 20th International Middle East Power Systems Conference, MEPCON 2018 - Proceedings. <https://doi.org/10.1109/MEPCON.2018.8635151><https://iopscience.iop.org/artic>

- 30.. C. Constantin and S. S. Iliescu, "Master-follower method for controlling parallell transformers implemented in a numerical protection system," *Proceedings of 2012 IEEE International Conference on Automation, Quality and Testing, Robotics*, Cluj-Napoca, Romania, 2012, pp. 32-37, doi: 10.1109/AQTR.2012.6237671.
31. Ibrahim, M. (2012). Performance evaluation of measurement algorithms used in IEDs.  
<https://digital.library.adelaide.edu.au/dspace/bitstream/2440/77855/8/02whole.pdf>
32. Isaac Kofi Otchere, Desmond Ampofo, Joshua Dantuo, Emmanuel Asuming Frimpong, The Influence of Voltage Regulation Devices Based Distributed Generation in Distribution Networks, *Electrical and Electronic Engineering*, Vol. 13 No. 1, 2023, pp. 1-5. doi: 10.5923/j.eee.20231301.01.
33. Jur Erbrink, Edward Gulski, Johan Smit, Rory Leich, 20th International Conference on Electricity Distribution 2009, Experimental Model for diagnosing on-load tap changer contact aging with dynamic resistance measurements
34. Jur Erbrink, Edward Gulski, Johan Smit, Rory Leich, 20th International Conference on Electricity Distribution 2009, Experimental Model for diagnosing on-load tap changer contact aging with dynamic resistance measurements
35. Jurišić, Goran et al. "Laboratory Test Bed for Analyzing Fault-Detection Reaction Times of Protection Relays in Different Substation Topologies." *Energies* (Basel) 11.9 (2018): 2482–. Web.
36. Kabiri, R., Holmes, D. G., & McGrath, B. P. (2014). Voltage regulation of LV feeders with high penetration of PV distributed generation using electronic tap changing transformers. In 2014 Australasian Universities Power Engineering Conference, AUPEC 2014 - Proceedings. <https://doi.org/10.1109/AUPEC.2014.6966635>
37. Krishnamurthy, S., Elenga Baringobera, B. IEC61850 standard-based harmonic blocking scheme for power transformers. *Prot Control Mod Power Syst* 4, 10 (2019). <https://doi.org/10.1186/s41601-019-0123-7>

38. Leon, H., Montez, C., Stemmer, M., & Vasques, F. (2016). Simulation models for IEC 61850 communication in electrical substations using GOOSE and SMV time-critical messages. IEEE International Workshop on Factory Communication Systems - Proceedings, WFCS. <https://doi.org/10.1109/WFCS.2016.7496500>
39. Li, Y., Nair, N. K. C., & Nguang, S. K. (2010). Improved coordinated control of on-load tap changers. AUPEC 2010 - 20th Australasian Universities Power Engineering Conference: "Power Quality for the 21st Century."
40. Ma, L. L., Pan, Z. C., Gao, Z. J., Wei, C., & Gao, G. L. (2008). The information modeling and communication mapping implementation of merging unit based on electronic transformer. 2008 China International Conference on Electricity Distribution, CICED 2008. <https://doi.org/10.1109/CICED.2008.5211787>
41. Madzonga, L. S., Munda, J. L., & Jimoh, A. A. (2009). Analysis of bus voltage regulation and OLTC performance on mismatched parallel-connected transformers. In IEEE AFRICON Conference. <https://doi.org/10.1109/AFRCON.2009.5308082>
42. Mahoney, K., Coyne, K., & Waldron, B. (2019). Lessons Learned in Implementing IEC 61850 Communications Solutions. In Power and Energy Automation Conference Spokane, Washington. 2019.
43. Małkowski, R., Izdebski, M., & Miller, P. (2020). Adaptive algorithm of a tap-changer controller of the power transformer supplying the radial network reducing the risk of voltage collapse. Energies. <https://doi.org/10.3390/en13205403>
44. Mnguni, M & Tzoneva, R. (2015). Comparison of the Operational Speed of Hard-wired and IEC 61850 Standard-based Implementations of a Reverse Blocking Protection Scheme. Journal of Electrical Engineering and Technology. 10. 740-754. [10.5370/JEET.2015.10.3.740](https://doi.org/10.5370/JEET.2015.10.3.740).
45. Monroy, D., Gómez-Expósito, A., & Romero-Ramos, E. (2007). Improving the voltage regulation of secondary feeders by applying solid-state tap changers to MV/LV transformers. In 2007 9th International Conference on Electrical Power Quality and Utilisation, EPQU. <https://doi.org/10.1109/EPQU.2007.4424122>
46. Murugan, S. K., Simon, S. P., Sundareswaran, K., Panugothu, S. R. N., &

- Padhy, N. P. (2019). Hardware-in-the Loop Testing of Power Transformer Differential Relay Using RTDS and DSP. Electric Power Components and Systems. <https://doi.org/10.1080/15325008.2019.1659449>
47. N. N. Shangase, M. Ratshitanga and M. Mnguni, "Transformer Differential Protection System with IEC 61850 GOOSE Communication Protocol," 2024 32nd Southern African Universities Power Engineering Conference (SAUPEC), Stellenbosch, South Africa, 2024, pp. 1-6, doi: 10.1109/SAUPEC60914.2024.10445097.
48. Nguyen Thi Ngoc Dung. Voltage Tap Changer of Power Transformer: Structure, Control and Application. International Journal of Research and Review. 2023; 10(12): 343-351. DOI: <https://doi.org/10.52403/ijrr.20231237>
49. Nguyen, H. T., Yang, G. Y., Nielsen, A. H., & ... (2018). Hardware-in-the-loop test for automatic voltage regulator of synchronous condenser. In Conference on Power .
50. Ntokozo N. Shangase, Mukovhe Ratshitanga, and Mkhululi E. S. Mnguni, "Interoperability Challenges in Multivendor IEC 61850 Devices for Parallel Power Transformer Differential Protection," International Journal of Electrical and Electronic Engineering & Telecommunications, Vol. 13, No. 1, pp. 45-57, 2024. doi: 10.18178/ijeetc.13.1.45-57
51. Okanik, P., Kurth, B., & Harlow, J. H. (1999). Update on the paralleling of OLTC power transformers. Proceedings of the IEEE Power Engineering Society Transmission and Distribution Conference. <https://doi.org/10.1109/tdc.1999.756164>
52. Oliviera, L. Dutra, C. Silveira, L. Cruz, I. Richards, S. (2015). Importance of IED performance on process bus applications. Actual trends in development of Power System Relay Protection and Automation. Sochi (Russia), 1–5 June. 20152015<http://cigre.ru/activity/conference/relayprotect5/materials/S.6.pdf>
53. OMICRON, Standard electrical tests for power transformers, [www.omicron.at](http://www.omicron.at)
54. Rahmati, A., & Sanaye-Pasand, M. (2015). Protection of power transformer using multi criteria decision-making. International Journal of Electrical Power and Energy Systems. <https://doi.org/10.1016/j.ijepes.2014.12.073>
55. Rangelov, Y., Nikolaev, N., & Ivanova, M. (2016). The IEC 61850 standard -

Communication networks and automation systems from an electrical engineering point of view. 2016 19th International Symposium on Electrical Apparatus and Technologies, SIELA 2016.  
<https://doi.org/10.1109/SIELA.2016.7543038>

56. Reda, Haftu & Ray, Biplob & Peidaee, Pejman & Anwar, Adnan & Mahmood, Abdun & Kalam, Akhtar & Islam, Nahina. (2021). Vulnerability and Impact Analysis of the IEC 61850 GOOSE Protocol in the Smart Grid. *Sensors*. 21. 1554. 10.3390/s21041554.
57. Reyes-López, Christopher & Yepez-Nicola, Jose. (2024). Protection of single busbar substations through coordination between overcurrent IEDs and the transformer differential based on IEC 61850. 10.18687/LACCEI2024.1.1.120.
58. Roostaei, S. (2015). Automatic Voltage regulation using IEC 61850. *International Journal Series in Multidisciplinary Research (IJSMR)*, Volume 1, Issue 2, 2015.
59. RTDS Hardware Manual. (2018) RTDS Technologies, Winnipeg, Manitoba, Canada
60. S. Devi and P. P. Kumar, "Methodology to Prevent Voltage Collapse During On Load Tap Changing Transformer Operation Under Network Contingencies," 2023 IEEE 8th International Conference on Recent Advances and Innovations in Engineering (ICRAIE), Kuala Lumpur, Malaysia, 2023, pp. 1-9, doi: 10.1109/ICRAIE59459.2023.10468436.
61. S. Nomandela, M. Mnguni, M. Ratshitanga and S. Ntshiba, "Transformer Differential Protection System Testing for Scholarly Benefits Using RTDS Hardware-in-the-Loop Technique," 2023 31st Southern African Universities Power Engineering Conference (SAUPEC), Johannesburg, South Africa, 2023, pp. 1-6, doi: 10.1109/SAUPEC57889.2023.10057606.
62. S. T. Cha, Q. Wu, A. H. Nielsen, J. Østergaard and I. K. Park, "Real-Time Hardware-In-The-Loop (HIL) Testing for Power Electronics Controllers," 2012 Asia-Pacific Power and Energy Engineering Conference, 2012, pp. 1-6, doi: 10.1109/APPEEC.2012.6307219.
63. Sangeerthana. R and Priyadharsini. S, "Controlling of Power Transformer Tap Positions (OLTC) Using Facts Devices", *pices*, vol. 4, no. 7, pp. 170-181, Nov. 2020.

64. Sarika Tasnim, Charles R. Sarimuthu, Boon Leong Lan, Chee Pin Tan, A game theory approach for OLTC voltage control operation in an active distribution network, *Electric Power Systems Research*, Volume 214, Part A, 2023, 108861, ISSN 0378-7796, <https://doi.org/10.1016/j.epsr.2022.108861>. (<https://www.sciencedirect.com/science/article/pii/S0378779622009142>)
65. Schwarz, K. (2005). IEC 61850 also outside the substation for the whole electrical power system. In 15th Power Systems Computation Conference, PSCC 2005.
66. SEL-2414. (2017) Instruction Manual, Schweitzer Engineering Laboratories Inc, Pullman, WA.
67. Sen, K. (2015). Overview Of Voltage Regulation Schemes For Utility And Industrial Applications. How2Power. 2015.
68. Sichwart, N., Eltom, A., & Kobet, G. (2013). Transformer Load Tap Changer control using IEC 61850 GOOSE messaging. In IEEE Power and Energy Society General Meeting. <https://doi.org/10.1109/PESMG.2013.6672628>
69. Skendzic, V., Énder, I.A., & Zweigle, G. (2007). IEC 61850-9-2 Process Bus and Its Impact on Power System Protection and Control Reliability. 9th Annual Western Power Delivery Automation Conference. Spokane, Washington,
70. Starck, J., & Hakala-Ranta, A. (2012). Switchgear Optimization Using IEC 61850-9-2 and Non-Conventional Measurements.
71. Starck, J., Wimmer, W. & Majer, K. (2013). "Switchgear optimization using IEC 61850-9-2," 22nd International Conference and Exhibition on Electricity Distribution (CIRED 2013), 2013, pp. 1-4, doi: 10.1049/cp.2013.0616.
72. Tlali, Nkeli. (2017). APPLICATION OF IEC 61850 ON SUBSTATION DESIGN AND ITS IMPACTS ON THE DESIGN OF THE SUBSTATION ITSELF. 10.13140/RG.2.2.35775.41121.
73. Treballe, David & Valecillos, Baudilio. (2008). Optimal Operation of Paralleled Power Transformers. *Renewable Energy and Power Quality Journal*. 1. 10.24084/repqj06.392.
74. Tu, J. & Mi, Y. (2019). Research on Transformer Fast OLTC System. *J. Phys.: Conf. Ser.* 1187 022002.
75. Wang, Y., Gao, P., Dong, E., Liu, Z., Zou, J., & Chen, X. (2011). Intelligent control of on-load tap changer of transformer. In 2011 1st International Conference on Electric Power Equipment - Switching Technology,

- ICEPE2011 - Proceedings. <https://doi.org/10.1109/ICEPE-ST.2011.6122963>
76. Wannous, K., & Toman, P. (2018). Sharing sampled values between two protection relays according to standard IEC 61850-9-2LE. 2018 19th International Scientific Conference on Electric Power Engineering, EPE 2018 - Proceedings. <https://doi.org/10.1109/EPE.2018.8396000>
77. Wróblewski, W.; Kowalik, R.; Januszewski, M.; Kurek, K. A.; Fuzzy OLTC Controller: Applicability in the Transition Stage of the Energy System Transformation. *Energies* 2024, 17, 2716. <https://doi.org/10.3390/en17112716>
78. Xie, Q., Shentu, X., Wu, X., Ding, Y., Hua, Y., & Cui, J. (2019). Coordinated voltage regulation by on-load tap changer operation and demand response based on voltage ranking search algorithm. *Energies*. <https://doi.org/10.3390/en12101902>
79. Xu, H., Dominguez-Garcia, A. D., & Sauer, P. W. (2020). Optimal Tap Setting of Voltage Regulation Transformers Using Batch Reinforcement Learning. *IEEE Transactions on Power Systems*. <https://doi.org/10.1109/TPWRS.2019.2948132>
80. Xyngi, I., & Popov, M. (2010). Integrated busbar protection scheme based on IEC61850-9-2 process bus concept. IEEE PES General Meeting, PES 2010. <https://doi.org/10.1109/PES.2010.5590022>
81. Yadav, Gaurav & Liao, Yuan & Burfield, Austin. (2023). Hardware-in-the-Loop Testing for Protective Relays Using Real Time Digital Simulator (RTDS). *Energies*. 16. 1039. [10.3390/en16031039](https://doi.org/10.3390/en16031039).
82. Yarza, Jose & Cimadevilla, Roberto. (2014). Advanced tap changer control of parallel transformers based on IEC 61850 GOOSE service. 1-5. [10.1109/TDC.2014.6863476](https://doi.org/10.1109/TDC.2014.6863476).
83. Yuvaraja, T., & Vigneshwaran, S. (2015). Voltage Regulation by Solid State Tap Change Mechanism for Distributing Transformer. *International journal of engineering research and technology*, 4.
84. Zhou, H., Yan, X., & Liu, G. (2019). A review on voltage control using on-load voltage transformer for the power grid. In *IOP Conference Series: Earth and Environmental Science*. <https://doi.org/10.1088/1755-1315/252/3/032144>
85. Zin Wah Aung Aung Thike "Analysis of on Load Tap Changing Transformer for Substation" Published in *International Journal of Trend in Scientific*

Research and Development (ijtsrd), ISSN: 2456-6470, Volume-3 Issue-5,  
August 2019, pp.1144-1146, <https://doi.org/10.31142/ijtsrd26556>



## APPENDIX A

This paper describes the IEEE 14 Bus System in RSCAD FX 2.2.1.

### 1 SYSTEM DATA: Real-Time Simulation Model of IEEE 14 Bus Power System

#### 1.1 Steady-State Data

Table A-1: Bus Data (RTDS)

BUS	Type	V  (pu)	Gen (MW)	Shunt (MVar)	Load	
					P (MW)	Q (MVar)
1	SLACK	1.060	-	-	-	-
2	P-V	1.045	40	-	21.7	12.7
3	P-V	1.010	0	-	94.2	19.0
4	P-Q	-	-	-	47.8	-3.9
5	P-Q	-	-	-	7.6	1.6
6	P-V	1.070	0	-	11.2	7.5
7 <sup>1</sup>	P-Q	-	-	-	-	-
8	P-V	1.090	0	-	-	-
9	P-Q	-	-	190	29.5	16.6
10	P-Q	-	-	-	9.0	5.8
11	P-Q	-	-	-	3.5	1.8
12	P-Q	-	-	-	6.1	1.6
13	P-Q	-	-	-	13.5	5.8
14	P-Q	-	-	-	14.9	5.0

Table A-2: Regulated Bus Data (RTDS)

BUS	V  (pu)	Qmax (MVar)	Qmin (MVar)
2	1.045	-40	50
3	1.010	0	40
6	1.070	-6	24
8	1.090	-6	24

Table A-3: Branch Data (RTDS)

From BUS	To BUS	R (pu)	X (pu)	B (pu)
1	2	0.01938	0.05917	0.0264
1	5	0.05403	0.22304	0.0246
2	3	0.04699	0.19797	0.0219
2	4	0.05811	0.17632	0.0187
2	5	0.05695	0.17388	0.0170
3	4	0.06701	0.17103	0.0173
4	5	0.01335	0.04211	0.0064
6	11	0.09498	0.19890	-
6	12	0.12291	0.25581	-
6	13	0.06615	0.13027	-
9	10	0.03181	0.08450	-
9	14	0.12711	0.27038	-
10	11	0.08205	0.19207	-
12	13	0.22092	0.19988	-
13	14	0.17093	0.34802	-

Table A-4: Transformer Data (RTDS)

From BUS	To BUS	R (pu)	X (pu)	Tap Ratio <sup>2</sup>
4	7	0.0	0.20912	0.978
4	9	0.0	0.55618	0.969
5	6	0.0	0.25202	0.932
7	8	0.0	0.17615	1.000
7	9	0.0	0.11001	1.000

## 1.2 Dynamic Data

Table A-5: Generator Data-1 (RTDS)

GEN	Base (MVA)	Xa (pu)	Xd (pu)	Xd' (pu)	Xd'' (pu)	Xq (pu)	Xq' (pu)	Xq'' (pu)
1	615	0.1450	1.7241	0.2586	0.2029	1.6587	0.4524	0.2029
2	60	0.1450	1.7241	0.2586	0.2029	1.6587	0.4524	0.2029
3	60	0.1450	1.7241	0.2586	0.2029	1.6587	0.4524	0.2029
6	25	0.1450	1.7241	0.2586	0.2029	1.6587	0.4524	0.2029
8	25	0.1450	1.7241	0.2586	0.2029	1.6587	0.4524	0.2029

Table A-6: Generator Data-2 (RTDS)

GEN	Base (MVA)	Ra (pu) <sup>3</sup>	Tdo' (s)	Tdo'' (s)	Tqo' (s)	Tqo'' (s)	H (s)	D(pu/pu)
1	615	0.000125	3.8260	0.0225	0.5084	0.0225	3.41	0.0
2	60	0.000125	3.8260	0.0225	0.5084	0.0225	3.41	0.0
3	60	0.000125	3.8260	0.0225	0.5084	0.0225	3.41	0.0
6	25	0.000125	3.8260	0.0225	0.5084	0.0225	3.41	0.0
8	25	0.000125	3.8260	0.0225	0.5084	0.0225	3.41	0.0

Table A-7: Exciter data-1 (IEEET1) (RTDS)

GEN	Tr	Ka	Ta	Vmax	Vmin	Ke	Te	Kf	Tf
1	0.0	6.2	0.05	5.2	-4.16	1.0	0.83	0.057	0.5
2	0.0	6.2	0.05	5.2	-4.16	1.0	0.83	0.057	0.5
3	0.0	6.2	0.05	5.2	-4.16	1.0	0.83	0.057	0.5
6	0.0	6.2	0.05	5.2	-4.16	1.0	0.83	0.057	0.5
8	0.0	6.2	0.05	5.2	-4.16	1.0	0.83	0.057	0.5

Table A-8: Governor Data (TGOV1) (RTDS)

GEN	R	T1	Vmax	Vmin	T2	T3	Dt
1	0.05	0.49	15.00	0.00	2.1	7.0	0.0
2	0.05	0.49	15.00	0.00	2.1	7.0	0.0

### 1.3 COMPARISON OF LOADFLOW RESULTS

Table A-9: Load Flow Results of Generator Buses (RTDS)

BUS	V  (pu)		$\angle V$ (deg) <sup>4</sup>		P <sub>G</sub> (MW)		Q <sub>G</sub> (MVar)	
	RTDS	PSSE	RTDS	PSSE	RTDS	PSSE	RTDS	PSSE
1	1.0600	1.0600	0.000	0.000	232.735	232.534	-15.842	-15.854
2	1.0450	1.0450	-4.990	-4.985	40.000	40.000	45.766	45.791
3	1.0100	1.0100	-12.727	-12.735	0.000	0.000	25.352	25.471
6	1.0700	1.0700	-14.414	-14.419	0.000	0.000	21.054	21.115
8	1.0900	1.0894	-43.269	-13.263	0.000	0.000	24.228	24.000

Table A-10: Load Flow Results of Load Buses (RTDS)

BUS	V  (pu)		$\angle V$ (deg)	
	RTDS	PSSE	RTDS	PSSE
4	1.0152	1.0151	-10.2671	-10.2686
5	1.0181	1.0180	-8.7710	-8.7735
9	1.0343	1.0341	-14.8531	-14.8427
10	1.0330	1.0329	-15.0577	-15.0506
11	1.0477	1.0477	-14.8544	-14.8544
12	1.0552	1.0535	-15.1590	-15.2719
13	1.0465	1.0472	-15.3535	-15.3128
14	1.0213	1.0216	-16.0964	-16.0718

## APPENDIX B

This paper describes the 14 Bus System in PowerFactory 2023 SP5. The parameters of the individual elements like generators, loads, shunts, transformers and lines are explained.

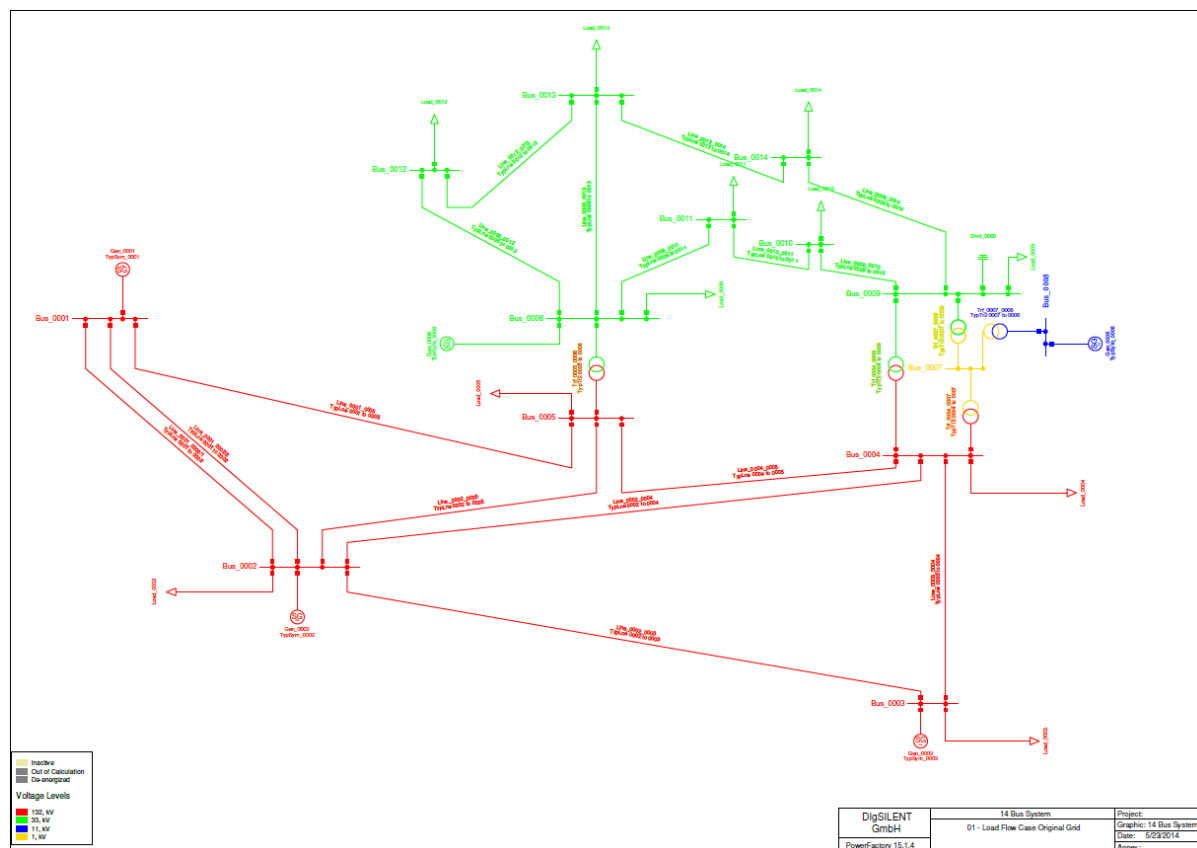


Figure B-1: Single line diagram of the 14 Bus System

Table B-1: Load demand

Load	Bus	P in MW	Q in Mvar
Load_0002	Bus_0002	21.7	12.7
Load_0003	Bus_0003	94.2	19.0
Load_0004	Bus_0004	47.8	-3.9
Load_0005	Bus_0005	7.6	1.6
Load_0006	Bus_0006	11.2	7.5
Load_0009	Bus_0009	29.5	16.6
Load_0010	Bus_0010	9.0	5.8
Load_0011	Bus_0011	3.5	1.8
Load_0012	Bus_0012	6.1	1.6
Load_0013	Bus_0013	13.5	5.8
Load_0014	Bus_0014	14.9	5.0

Table B-2: Generator dispatch

Generator	Bus	P in MW	Q in Mvar
Gen_0001	Bus_0001	N.A.	N.A.
Gen_0002	Bus_0002	40.0	N.A.
Gen_0003	Bus_0003	0.0	N.A.
Gen_0006	Bus_0006	0.0	N.A.
Gen_0008	Bus_0008	0.0	N.A.

Table B-3: Generator controller settings

Generator	Bus Type	Voltage in p.u.	Minimum capability in MVA	Maximum capability in MVA
Gen_0001	Slack	1.060	N.A.	N.A.
Gen_0002	PV	1.045	-40.0	50.0
Gen_0003	PV	1.010	0.0	40.0
Gen_0006	PV	1.070	-6.0	24.0
Gen_0008	PV	1.090	-6.0	24.0

Table 4: Data of lines given based on 100MVA

From Bus	To Bus	r in p.u.	x in p.u.	$q_c/2$ in p.u.	b in p.u.
1	2	0.01938	0.05917	0.0264	0.0528
1	5	0.05403	0.22304	0.0246	0.0492
2	3	0.04699	0.19797	0.0219	0.0438
2	4	0.05811	0.17632	0.0187	0.0374
2	5	0.05695	0.17388	0.0170	0.0340
3	4	0.06701	0.17103	0.0173	0.0346
4	5	0.01335	0.04211	0.0064	0.0128
6	11	0.09498	0.19890	0.0000	0.0000
6	12	0.12291	0.25581	0.0000	0.0000
6	13	0.06615	0.13027	0.0000	0.0000
9	10	0.03181	0.08450	0.0000	0.0000
9	14	0.12711	0.27038	0.0000	0.0000
10	11	0.08205	0.19207	0.0000	0.0000
12	13	0.22092	0.19988	0.0000	0.0000
13	14	0.17093	0.34802	0.0000	0.0000

Table B-5: Data of lines in the PowerFactory model

Line	From Bus	To Bus	Un in kV	R in $\Omega$	X in $\Omega$	B in $\mu S$
Line_0001_0002/1	1	2	132.0	6.753542	20.619560	151.5152
Line_0001_0002/2	1	2	132.0	6.753542	20.619560	151.5152
Line_0001_0005	1	5	132.0	9.414187	38.862490	282.3691
Line_0002_0003	2	3	132.0	8.187537	34.494280	251.3774
Line_0002_0004	2	4	132.0	10.125090	30.722000	214.6465
Line_0002_0005	2	5	132.0	9.922968	30.296850	195.1331
Line_0003_0004	3	4	132.0	11.675820	29.800270	198.5767
Line_0004_0005	4	5	132.0	2.326104	7.337246	73.4619
Line_0006_0011	6	11	33.0	1.034332	2.166021	0.0000
Line_0006_0012	6	12	33.0	1.338490	2.785771	0.0000
Line_0006_0013	6	13	33.0	0.720374	1.418640	0.0000
Line_0009_0010	9	10	33.0	0.346411	0.920205	0.0000
Line_0009_0014	9	14	33.0	1.384228	2.944439	0.0000
Line_0010_0011	10	11	33.0	0.893524	2.091643	0.0000
Line_0012_0013	12	13	33.0	2.405819	2.176693	0.0000
Line_0013_0014	13	14	33.0	1.861428	3.789938	0.0000

Table B-6: Data of transformers given based on 100MVA, with rated voltages added in the PowerFactory model

Trans-former	From Bus	To Bus	Ur HV in kV	Ur LV in kV	r in p.u.	x in p.u.	Transformer final turns ratio
Trf_0004_0007	4	7	132.0	1.0	0.0	0.20912	0.978
Trf_0004_0009	4	9	132.0	33.0	0.0	0.55618	0.969
Trf_0005_0006	5	6	132.0	33.0	0.0	0.25202	0.932
Trf_0007_0008	7	8	11.0	1.0	0.0	0.17615	0.000
Trf_0007_0009	7	9	33.0	1.0	0.0	0.11001	0.000